UNIVERSITY OF CAMBRIDGE

Analysis of PINK1/Parkin-related mitochondrial quality control in *Drosophila*

This dissertation is submitted for the degree of Doctor of Philosophy

by

Juliette Lee

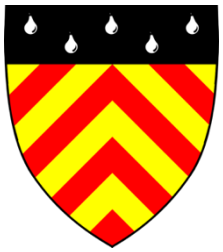

Clare Hall College

September 2020

Thesis Declaration

This thesis is the result of my own work and includes nothing which is the outcome of work done in collaboration except as declared in the Preface and specified in the text. It is not substantially the same as any that I have submitted, or, is being concurrently submitted for a degree or diploma or other qualification at the University of Cambridge or any other University or similar institution except as declared in the Preface and specified in the text. I further state that no substantial part of my thesis has already been submitted, or, is being concurrently submitted for any such degree, diploma or other qualification at the University of Cambridge or any other University or similar institution except as declared in the Preface and specified in the text. It does not exceed the prescribed word limit for the relevant Degree Committee.

Preface

Part of this project was a collaborative work with other members of the Whitworth lab, A. Sanchez-Martinez and S. Andreazza, and collaborators from the University of Liverpool, M. J. Clague and the University of the Basque Country, A. Martinez Zarate and U. Mayor.

Summary

Juliette Lee

Analysis of PINK1/Parkin-related mitochondrial quality control in *Drosophila*

Mitochondria are essential organelles that perform many critical metabolic functions but are also a major source of damaging reactive oxygen species (ROS) and harbour pro-apoptotic factors. Multiple homeostatic processes operate to maintain mitochondrial integrity; however, terminally damaged organelles are degraded through the process of targeted mitochondrial autophagy (mitophagy) to prevent potentially catastrophic consequences. Such homeostatic mechanisms are particularly important for post-mitotic, energetically demanding tissues such as nerves and muscles. There is increasing evidence that failure of this mechanism is linked to normal ageing and some neurodegenerative disorders. Interestingly, two proteins linked to Parkinson's Disease (PD), Parkin, a cytosolic ubiquitin ligase, and PINK1, a mitochondrially targeted kinase, have been shown to play key roles in this mitophagy. However, little is known about their impact on basal mitophagy *in vivo*. Moreover, while the consequences of mitophagy defects and the mechanisms that lead to neuronal cell death are currently unclear, aberrant induction of inflammatory signalling is becoming recognised as a key pathogenic mechanism in PD. The work conducted for this thesis aimed to explore the activation of the innate immune system, in the context of PD, using in *Drosophila* as an *in vivo* model.

First, to analyse mitophagy events *in vivo*, I developed and characterised transgenic *Drosophila* expressing the fluorescent mitophagy reporters, the mt-Keima and the mito-QC, were generated to evaluate the impact of *Pink1/parkin* mutations on basal mitophagy under physiological conditions. My results show that mitophagy is readily detectable and abundant in many tissues including the PD-relevant dopaminergic neurons. However, mitolysosomes were almost completely absent in flight muscles.

mechanism associated with the PINK1/Parkin pathway. My work provides evidence that Pink1 and parkin are not essential for bulk basal mitophagy in *Drosophila*. They also emphasize that mechanisms underpinning basal mitophagy remain largely obscure.

Recently, aberrant activation of immune signalling triggered by the DNA-sensing receptor cyclic GMP–AMP synthase (cGAS) and its downstream signalling effector stimulator of interferon genes (STING) has been implicated in PINK1/Parkin pathology. In order to determine whether the role of Sting in the Pink1/parkin pathology is conserved in *Drosophila*, I analysed loss of Sting coupled with *Pink1/parkin* mutants. My work demonstrates that loss of *Sting*, or the downstream effector *Relish*, is not sufficient to rescue the behavioural defects or the disruption of the mitochondrial integrity of *Pink1/parkin* mutant flight muscles, indicating that these phenotypes are not due to aberrant activation of the cGAS-STING pathway in *Drosophila*.

In a broader effort to understand the involvement of the immune system in the Pink1/parkin pathology, I knocked down key components involved in various other immune pathways, in combination with *Pink1* and *parkin* mutants. Like the Sting axis, most of the immune pathways investigated did not seem to modify *Pink1* and *parkin* mutant phenotypes; however, my data revealed that knockdown of key players of the Janus kinase (JAK)-signal transducer and activator of transcription (STAT) pathway significantly improved *Pink1* mutant phenotypes. Interestingly, this genetic interaction seems to be restricted to *Pink1* as loss of JAK/STAT components failed to modify the *parkin* mutant phenotypes. Although further work needs to be carried out to in order to understand the mechanism behind the interaction between *Pink1* and the JAK/STAT pathway, these findings suggest that downregulation of the particular pathway could be considered as a new therapeutic intervention for PD.

Acknowledgements

Firstly, I want to thank my supervisor Alex Whitworth, for his support and guidance during these four years.

Secondly, I want to thank my lab, the ‘fly lovers’: Wings, Aitor, Leo, Alvaro, Natalie, Ana, Tom (we already miss you!). Thank you for the help, the advice, the banter and all the good memories we have made over the years. My PhD would not have been the same without all of you. I am particularly thankful to Simo and Victoria who have been my two supportive pillars throughout this PhD. But also, Ana, who has been a true mentor and has helped me a lot with the second part of this project.

Thirdly, I want to thank the PhD students from the MBU, Dan, Margherita, Lisa and Anja. We powered through the PhD together and had a lot of fun along the way.

Fourthly, I will always be indebted to my parents. Without their love and support, I would not be where I am today.

Finally, to Filip, for everything. Without you I would probably not be currently writing/finishing this thesis. Thanks for the all the positivity, on a daily basis, the meals, the laughs, the trips and all the constant love and support.

List of abbreviations

6-OHDA	6-hydroxydopamine
A-T	Ataxia-Telangiectasia
AAA proteases	ATPase associated with various cellular activities
AAV	adeno-associated virus
AD	autosomal dominant
AMBRA1	activating molecule in Beclin1-regulated autophagy
AMP	antimicrobial peptide
AMPs	adult midgut precursors
APOBEC1	apolipoprotein B (apoB) mRNA editing catalytic polypeptide 1
AR	autosomal recessive
ARIH1	ariadne RBR E3 ubiquitin protein ligase 1
arm	armadillo
ASC	apoptosis-associated speck-like protein containing a caspase recruit domain
Atg5	autophagy-related gene 5
Atg7	autophagy-related gene 7
Aβ	Amyloid-β
bak	Bcl-2 antagonist killer 1
bax	Bcl-2- associated X protein
BCA	Bicinchoninic acid assay
bcl-2	B-cell lymphoma 2
BDSC	Bloomington Drosophila Stock Center
BNIP	Bcl-2 Interacting Protein 3
BNIP3L	BNIP3-like/NIX
BSA	Bovine serum albumin
bsk	basket
Ca^{2+}	calcium
CCCP	carbonyl cyanide *m*-chlorophenylhydrazone
CDNs	cyclic dinucleotides
cGAMP	cyclic guanosine monophosphate (GMP)-adenosine

	monophosphate (AMP)
cGAS	cyclic GMP-AMP synthase
CHOP	CCAAT/enhancer-binding protein (C/EBP)-homologous protein
CI	confidence interval
CNS	central nervous system
CTT	C-terminal tail
DA	dopaminergic
da	daughterless
DAMPs	damage-associated molecular patterns
DAPI	4,6-diamidino-2-phenylindole
DAT	dopamine transporter
dFADD	*Drosophila* Fas-associated protein with death Domain
DNM2	dynamin 2
dnr1	defense repressor 1
dome	domeless
dPIAS	protein inhibitor of activated STAT
DREDD	death-related ced-3/Nedd2-like protein caspase
Drp1	dynamin-related protein 1
EB	enteroblast
EC	enterocyte
ee	enteroendocrine cell
EM	electron microscopy
ER	endoplasmic reticulum
ERAD	ER-associated degradation
ETC	electron transport chain
FIS1	mitochondrial fission 1
FOXO	Forkhead Box O transcription factor
FRET	fluorescence resonance energy transfer
FUNDC1	FUN14 domain-containing protein 1
GFP	green fluorescent protein
GPx	Glutathione peroxidase
GWAS	genome wide association study
hep	hemipterous

hop	hopscotch
HRP	horse radish peroxidase
hsp	heat shock protein
IBR	in-between RING
IFM	indirect flight muscle
IFN	Interferon
IFNAR1	Interferon alpha and beta receptor subunit 1
IKK-β/IKK2	inhibitor of nuclear factor kappa beta
IL	interleukine
IMD	Immune deficiency
IMM	Inner mitochondrial membrane
IMS	intermembrane space
IP3	inositol 1,4,5-triphosphate
IP3R	inositol 1,4,5-triphosphate receptor
IRAK	IL-1 receptor-associated kinase
IRD5	Immune response deficient 5
IRF3	Interferon regulatory factor 3
ISC	intestinal stem cell
IκB	inhibitor of kappa B
JAK/STAT	Janus kinase (JAK)/signal transducers and activators of transcription (STAT)
JNK	c-Jun N-terminal kinase
KD	Kinase dead
KO	knockout
L-Dopa	Levodopa
LB	Lewy body
LC3	microtubule-associated protein 1A/1B light chain 3A
lic	licorne
LIR	LC3-interacing region
LN	Lewy neurite
LPS	lipopolysaccharide
LRRK2	Leucine rich repeat kinase 2
MAPK	mitogen-activated protein kinase

MAPKK	MAPK kinase
MAPKKK	MAPKK kinase
MARCH5	membrane-associated RING finger protein 5
MCU	mitochondria calcium uniporter
MDV	mitochondria-derived vesicle
mef2	myocyte enhancer factor 2
Mff	mitochondrial fission factor
MFN1/2	mitofusin 1/2
MHC	major histocompatibility complex
MiD 49 and 51	mitochondrial dynamics proteins 49 and 51
MitAP	mitochondrial antigen presentation
Mn(SOD)	manganese-dependent superoxide dismutase
MPP	mitochondrial processing peptidase
MPP+	1-methyl-4-phenylpyridinium
MPTP	1-methyl-4-phenyl-1,2,3,4-tetrahydropyridine
mPTP	mitochondrial permeability transition pore
MQC	mitochondria quality control
mt-KR	mitochondrial Killer-Red
mtDNA	mitochondrial DNA
MTS	mitochondrial targeting sequence
mtUPR	mitochondrial unfolded protein response
MUL1	mitochondrial ubiquitin ligase 1
MyD88	myeloid differentiation primary response 88
NDP52	nuclear dot protein 52
NF-κB	nuclear factor kappa beta
NIPSNAP 1/2	4-nitrophenylphosphatase domain and non-neuronal SNAP25-like protein homolog 1/2
NLR	NOD-like receptor
NLRP3/NALP3	nucleotide binding domain and leucine-rich repeat pyrin 3 domain
nsyb	n-synaptobrevin
OMAD	OMM associated degradation
OMM	outer mitochondrial membrane
OPA1	optic atrophy gene 1

OPTN	Optineurin
OXPHOS	oxidative phosphorylation
PAMPs	pathogen-associated molecular patterns
PARIS	Parkin interacting substrate protein
PARL	presenilin-associated rhomboid-like protease
PBS	phosphate-buffered saline
PBS-T	phosphate-buffered saline with 0.3% Triton X-100
PC	peripheral cell
PD	Parkinson's disease
PDH	pyruvate dehydrogenase
PGC-1α	peroxisome proliferator-activated receptor gamma co-activator 1 alpha
PGRPs	peptidoglycan recognition receptors
PHB	prohibitins
PI(4)P	phosphatidylinositol 4-phosphate
PINK1	PTEN-induced kinase 1
POLGγ	DNA polymerase gamma
PPL1	protocerebral posterior lateral
PRR	pattern recognition receptor
Prx	peroxiredoxin
Ptp61F	protein tyrosine phosphatase 61F
RBR	RING in between RING
REP	repressor element
RGC	retinal ganglion cell
RIPA	radioimmunoprecipitation assay
ROS	reactive oxygen species
rRNA	ribosomal RNA
RT	room temperature
RyRs	ryanodine receptors
Ser65	Serine 65
SNP	single nucleotide polymorphism
Snx9	sortin nexing 9
Socs	suppressor cytokine signalling

SOD	Superoxide dismutase
STING	Stimulator of interferon genes
Stx17	syntaxin17
SUMO	small ubiquitin-like modifier
TBS	Tris-buffered saline
TBS-T	Tris-buffered saline with 0.1% Tween-20
TCA	tricarboxylic acid cycle
TFAM	mitochondrial transcription factor A
TH	tyrosine hydroxylase
TIM	translocase of the inner membrane
TLR	Toll-like receptor
TNF	tumour necrosis factor
TNFR	tumor necrosis factor receptor
TOLLES	tolerance of lysosomal environments
TOM	translocase outer membrane
tRNA	transfer RNA
tub	tubulin
Ub	ubiquitin
Ubl	ubiquitin like
ULK1	Unc-51 like autophagy activating kinase 1
UPD	Unique parkin domain
upd	unpaired
UPS	ubiquitin proteasome system
UTR	untranslated region
VDAC	voltage dependent anion channel
VDRC	Vienna Drosophila Reference Center
vps35	vacuolar protein sorting 35
WT	wild-type
XO/X	xanthine oxidase/xanthine
YFP	yellow fluorescent protein
ΔOTC	mutant ornithine transcarbamylase

Table of contents

Chapter 1. Introduction 1

1.1. Parkinson's disease 2

1.1.1. Epidemiology 2

1.1.2. Clinical symptoms and pathology 2

1.1.3. Aetiology of PD 4

1.1.4. Monogenic forms of PD 5

1.1.4.1. Autosomal dominant PD: *SNCA* and *LRRK2* 6

1.1.4.2. Autosomal recessive PD: *PRKN*, *PINK1* and *DJ1* 7

1.1.4.3. Toxin-induced animal models of PD 9

1.2. Mitochondria: structure and functions 12

1.2.1. Mitochondria structure 13

1.2.2. Mitochondrial respiration and ATP synthesis 15

1.2.3. Mitochondrial dynamics 16

1.2.4. Other mitochondrial functions 19

1.2.5. Mitochondria quality control (MQC) 21

1.2.5.1. ATP-dependent proteases 21

1.2.5.2. Ubiquitin proteasome system 23

1.2.5.3. Mitochondrial unfolded protein response (mtUPR) 23

1.2.5.4. Mitophagy 24

1.2.5.4.1. PINK1/Parkin-mediated mitophagy 27

1.2.5.4.1.1. PINK1 and Parkin 27

1.2.5.4.1.2. Mechanism of PINK1/Parkin-mediated mitophagy 29

1.2.5.4.2. PINK1/Parkin-independent mitophagy 32

1.2.5.4.2.1. Receptor-mediated mitophagy 33

1.2.5.4.2.2. Cardiolipin-mediated mitophagy 35

1.2.5.4.2.3. Other E3 ligases 35

1.2.5.4.3. Investigating mitophagy *in vitro* 37

1.2.5.4.4. Investigating mitophagy *in vivo* 38

1.2.5.4.4.1. Tools to visualise mitophagy *in vivo* 41

1.2.5.5. Mitochondria-derived vesicles (MDVs) 46

1.3. Inflammation and PD 49

1.3.1. Mitochondria: key players in inflammation 50

1.3.1.1. Lessons from toxin-induced PD models 50

1.3.1.2. mtDNA and the c-GAS/STING pathway: a source of inflammation 52
1.3.1.3. Mitochondrial content and activation of the inflammasome 53
1.3.1.4. Lipopolysaccharides, inflammation and PD 55
1.3.1.5. Intestinal dysbiosis and gut-derived inflammation 56

1.4. *Drosophila* immune system 58
1.4.1. Humoral response and antimicrobial peptides 58
1.4.2. *Drosophila* Sting-IMD pathway 59
1.4.3. *Drosophila* Toll pathway 62
1.4.4. *Drosophila* JAK/STAT pathway 64
1.4.5. Other pathways 67
1.4.6. Implication of the immune system in Drosophila models of neurodegeneration ... 69

Chapter 2. Material and methods 73

2.1. *Drosophila* husbandry 74

2.2. Behavioural assays 77
2.2.1. Climbing assay 77
2.2.2. Flight assay 77
2.2.3. Lifespan assay 77

2.3. Immunohistochemistry 79
2.3.1. Sample preparation 79
2.3.2. Deferiprone treatment 81
2.3.3. LysoTracker live imaging 81

2.4. Microscopy 82
2.4.1. Imaging 82
2.4.2. Quantification of the mito-QC mitolysosomes 82
2.4.3. Quantification of thoracic mitochondrial morphology 85

2.5. Molecular biology 86
2.5.1. Immunoblotting 86

2.6. Antibodies 87

2.7. Statistical analysis 88

Chapter 3. Investigating Pink1/parkin-mediated mitophagy in *Drosophila* 89

3.1. Introduction 90

3.2. Chapter aims 92

3.3. Results 93

3.3.1. Validation of the mito-QC mitophagy reporter 93

3.3.2. Mito-QC reveals widespread mitophagy in adult and larval *Drosophila* tissues 99

3.3.3. Validation of the mt-Keima mitophagy reporter 106

3.3.4. Mt-Keima confirms abundant mitophagy in adult and larval *Drosophila* tissues 110

3.3.5. Basal mitophagy is minimally affected by loss of Pink1 114

3.3.5.1. Analysis of larval epidermis and CNS of *Pink1* mutants 114

3.3.5.2. Analysis of adult IFMs and CNS of *Pink1* mutants 116

3.3.6. Basal mitophagy is minimally affected by loss of parkin 120

3.3.6.1. Analysis of larval epidermis and CNS of *parkin* mutants 120

3.3.6.2. Analysis of adult IFMs and CNS of *parkin* mutants 121

3.3.7. Mitophagy is slightly increased in flies expressing mito-APOBEC1 124

3.3.7.1. Analysis of larval epidermis and CNS of mito-APOBEC1 flies 124

3.3.7.2. Analysis of adult brains and IFMs of mito-APOBEC1 flies 126

3.3.8. Mitophagy is increased in mito-APOBEC1 flies combined with Pink1 or parkin overexpression 129

3.4. Discussion 132

Chapter 4. Understanding the role of the innate immune system in *Pink1/parkin* mutants 141

4.1. Introduction 142

4.2. Chapter aims 145

4.3. Results 146

4.3.1. The Sting-IMD pathway does not contribute to *Pink1*/*parkin* or mtDNA mutator phenotypes 146

4.3.2. Loss of key regulators of the JNK pathway does not modify *Pink1/parkin* phenotypes 161

4.3.3. Loss of key components of the p38 MAPK pathway does not modify *Pink1/parkin* phenotypes 169

4.4. Discussion 176

Chapter 5. Investigating the role of the JAK/STAT pathway in *Pink1*/*parkin* mutants 181

5.1. Introduction 182

5.2. Chapter aims 188

5.3. Results 189

5.3.1. Loss of *Stat92E* partially rescues *Pink1* phenotypes 189

5.3.2. Loss of *Stat92E* does not rescue *parkin* phenotypes 197

5.3.3. *upd1* knockdown does not rescue *Pink1* or *parkin* phenotypes 199

5.3.4. Simultaneous loss of *upd2* and *upd3* partially rescue *Pink1*, but not *parkin* phenotypes 202

5.3.5. Loss of *dome* is beneficial in *Pink1* mutant flies 206

5.3.6. Loss of *hop* rescues *Pink1* climbing phenotype 208

5.3.7. Loss of *TotA* and *TotM* rescue *Pink1* mutants climbing deficits 210

5.3.8. The gut homeostasis seems perturbed in *Pink1* mutants 212

5.4. Discussion 214

Chapter 6. General discussion and future work 221

6.1. *In vivo* mitophagy: a controversial issue 222

6.2. Potential triggers of PINK1/Parkin-mediated mitophagy 225

6.3. Beyond mitophagy 229

6.4. Inflammation and PD 231

6.5. Relevance of genetic models of PD to sporadic PD 234

References 237

Publications arising from this work 309

Chapter 1. Introduction

1.1. Parkinson's disease

1.1.1. Epidemiology

Parkinson's disease (PD) is the second most frequent neurodegenerative disease after Alzheimer's Disease (de Lau & Breteler, 2006). About 1% of the population develops PD at 65 years old and this number increases up to 4-5% at 85, making age one of the main risk factor (Schapira & Jenner, 2011; Wood-Kaczmar et al., 2006). Although the disease's aetiology is not fully understood, the majority of PD cases are sporadic (95%) and seem to arise from a combination of environmental and genetic factors (Trinh & Farrer, 2013). The remaining 5% account for familial cases and can be traced to monogenic mutations, with both recessive and dominant modes of inheritance (Wood-Kaczmar et al., 2006).

1.1.2. Clinical symptoms and pathology

PD is characterised by a motor-symptom tetrad including resting tremor, rigidity, brady/akinesia and postural instability (Figure 1.1) (Polymeropoulos et al., 1997). By the time patients are diagnosed with PD, up to 50-60% of their dopaminergic (DA) neurons are lost, resulting in the depletion of 70% of the dopamine levels in the dorsal striatum (Lang & Lozano, 1998). Non-motor symptoms, that often manifest before the motor disabilities, have also been associated with PD; these include depression, sensory loss, sleep disturbance and hallucinations (Langston, 2006; Trinh & Farrer, 2013). From a histopathological point of view, PD is characterised by a progressive loss of dopaminergic neurons in the substantia nigra *pars compacta* (Figure 1.1) (Dickson, 2012; Spillantini et al., 1997). Examination of PD post-mortem brains revealed the presence of rounded eosinophilic inclusions, so-called Lewy bodies (LB), and Lewy neurites (LN) in the cellular processes of the remaining neurons (Braak et al., 1999; Schapira & Jenner, 2011; Spillantini et al., 1997). It has been shown that the amount of LB within the neurons directly correlates with the severity of the clinical symptoms and cognitive impairments (Braak et al., 1999; Mattila et al., 2000). Phosphorylated α-synuclein aggregates appear to be the major component of these

intraneuronal inclusions (Fujiwara et al., 2002; Lees et al., 2009; Wood-Kaczmar et al., 2006).

There is currently no treatment that can prevent the disease progression, only drugs that can alleviate the symptoms are available. One of the first line and most common treatments is Levodopa (L-Dopa), the precursor to dopamine, which results in a 20-30% improvement of the motor symptoms (Lees et al., 2009). Although patients respond initially well to the L-Dopa treatment, its long-term use often induces motor complications such as involuntary movements (dyskinesia) due to excessive dopamine levels within the motor system (Poewe et al., 2010).

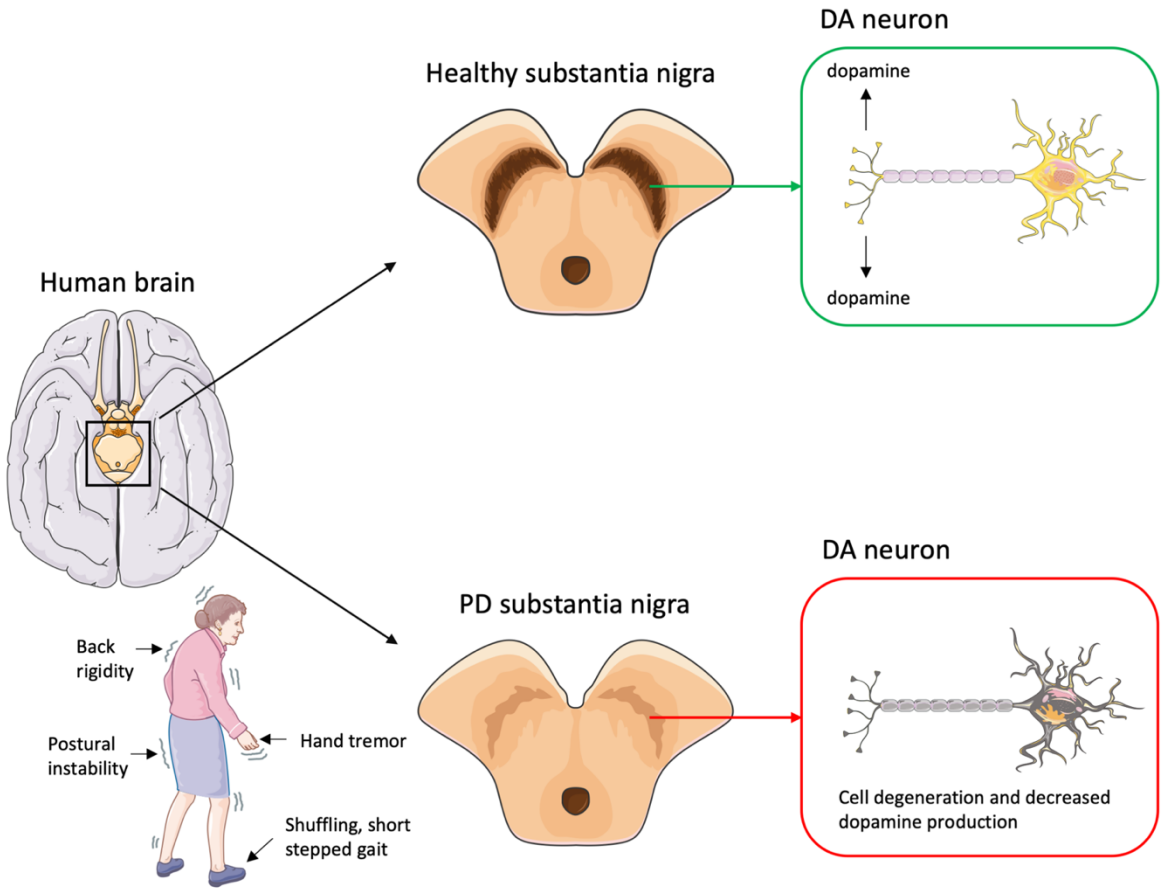

Figure 1.1. Symptoms and pathology of PD

PD is characterised by a loss of the DA neurons in the substantia nigra and a significant decrease in the dopamine levels by the time motor symptoms appear. The clinical symptoms include tremors, shuffling gait, rigidity and postural instability in addition to non-motor symptoms.

1.1.3. Aetiology of PD

Insights into PD aetiopathology were gained from the accidental exposure of drug abusers to 1-methyl-4-phenyl-1,2,3,4-tetrahydropyridine (MPTP), inducing a parkinsonian syndrome indistinguishable from PD (Davis et al., 1979; Langston et al., 1983). MPTP is the precursor of the neurotoxic 1-methyl-4-phenylpyridinium (MPP+), a compound that blocks the mitochondrial respiratory chain at the level of complex I (Ramsay et al., 1986a; Ramsay et al., 1986b). This blockade in turn results in a reduction in ATP levels, release of reactive oxygen species (ROS) the subsequent bioenergetic failure of the brain regions most sensitive to MPTP, particularly in the striatum (Chan et al., 1991; Fabre et al., 1999; Perier & Vila, 2012). Although MPP+ is produced in the glial cells, it is the uptake into the DA neurons via the dopamine transporter (DAT) within the substantia nigra that leads to the degeneration of this particular cell type (Bezard et al., 1999; Javitch et al., 1985; Kopin & Markey, 1988). Indeed, MPTP-induced neuronal cell death was suppressed in mice lacking DAT (Bezard et al., 1999). These findings established a link between PD and impaired mitochondrial function, leading the way to further investigations on mitochondrial respiration in PD patients. Post-mortem analysis of PD brains revealed a significant reduction in the mitochondrial respiratory activity, particularly due to a decrease in complex I function (Bindoff et al., 1989; Schapira et al., 1989, 1990). Observations of post-mortem frontal cortexes from PD patients revealed that complex I auto-oxidative damage to its catalytic subunit resulted in the mis-assembly and malfunction of the complex (Keeney et al., 2006; Perier & Vila, 2012). These findings led to the assumption that deficient complex I and oxidative stress were key to PD pathogenesis, although this is still under debate (Area-Gomez et al., 2019). Additionally, oxidative damage to proteins, lipids, nuclear DNA and mitochondrial DNA (mtDNA) have been observed in post-mortem brain samples from PD patients (Perier & Vila, 2012).

1.1.4. Monogenic forms of PD

Several genetic loci associated with PD have been classified from *PARK1-23* (Table 1.1) and include autosomal dominant (AD) and autosomal recessive (AR) forms of PD.

Table 1.1. Summary of *PARK* loci and genes associated with PD (Adapted from Del Rey et al., 2018 and Blauwendraat et al., 2020)

Locus	Gene	Year of discovery	Onset	Inheritance
PARK1/4	*SNCA*	1997/2003	Early onset PD	AD
PARK2	*PRKN*	1998	Early onset PD	AR
PARK3	Unknown	1998	Classical PD	AD
PARK5	*UCHL1*	1998	Classical PD	AD
PARK6	*PINK1*	2004	Early onset PD	AR
PARK7	*DJ-1*	2003	Early onset PD	AR
PARK8	*LRRK2*	2004	Classical PD	AD
PARK9	*ATP13A2*	2004	Atypical PD	AR
PARK10	Unknown	2002	Classical PD	Risk factor
PARK11	*GIGYF2*	2003	Late onset PD	AD
PARK12	Unknown	2003	Classical PD	Risk factor
PARK13	*HTRA2*	2005	Classical PD	AD
PARK14	*PLA2G6*	2009	Early onset PD	AR
PARK15	*FBXO7*	2008	Early onset parkinsonism	AR
PARK16	Unknown	2009	Classical PD	Risk factor
PARK17	*VPS35*	2011	Classical PD	AD
PARK18	*EIF4G1*	2011	Classical PD	AD
PARK19	*DNAJC6*	2012	Early onset PD	AR
PARK20	*SYNJ1*	2013	Atypical PD	AR
PARK21	*DNAJCL3*	2014	Late onset PD	AD
PARK22	*CHCHD2*	2016	Late/early onset PD	AD
PARK23	*VPS13C*	2016	Early onset PD	AR
-	*LRP10*	2018	-	AD
-	*GBA*	2009	-	AD, AR, risk factor
-	*MAPT*	-	-	Sporadic, risk factor

1.1.4.1. Autosomal dominant PD: *SNCA* and *LRRK2*

Mutations in the *SNCA* gene, encoding the α-synuclein protein, were the first familial mutations found to associate with dominantly inherited PD (Polymeropoulos et al., 1997). α-Synuclein is a protein widely expressed in the nervous system and highly enriched in neurons where it accounts for up to 0.5-1% of the total proteins (Bodner et al., 2009; Kamp et al., 2010; Spillantini et al., 1997). Although the protein shares sequence homology with two other members of the synuclein family, β- and γ-synuclein, only the α-synuclein is present in the LB (Giasson et al., 2001). While the physiological functions of α-synuclein remain elusive, interest for this protein has not stopped growing. At least five distinct mutations in the *SNCA* gene have been described so far (A53T, A30P, E46K, H50Q, G51D), all resulting in an early disease onset, often before the age of 60 (Appel-Cresswell et al., 2013; Kiely et al., 2013; Krüger et al., 1998; Polymeropoulos et al., 1997; Proukakis et al., 2013; Zarranz et al., 2004). In addition, some familial PD cases are caused by triplication or duplication of the *SNCA* gene. The age of onset and the severity of the symptoms seem to correlate with the number of *SNCA* copies, with triplication carriers developing PD at an earlier age (40 years old) than patients with duplication (50 years old) and exhibiting more disabling deficits (Chartier-Harlin et al., 2004; Ibáñez et al., 2004; Miller et al., 2004; Muenter et al., 1998; Singleton et al., 2003). Recently, the implication of α-synuclein's expression in PD became even more important as the *SNCA* locus appeared to be a significant susceptibility gene for sporadic PD, suggesting some common pathogenic mechanisms with inherited PD (Nalls et al., 2011; Stefanis, 2012). Several genome wide association studies (GWAS) have linked single nucleotide polymorphisms (SNPs) present in the 3'UTR (untranslated region) of *SNCA* with an increase in the risk of developing PD (Nalls et al., 2011; Stefanis, 2012).

Nine pathogenic mutations in the *Leucine rich repeat kinase 2 (LRRK2)* gene, encoding the dardarin protein have been associated with PD. This large protein contains multiple domains and belongs to the RAS GTPase superfamily (Khan et al., 2005; Paisán-Ruíz et al., 2004; Wood-Kaczmar et al., 2006; Zimprich et al., 2004). The G2019S mutation which lies within the kinase domain of the protein is by far the most common mutation accounting for 5% of familial PD and 1% of the sporadic cases (Gilks et al., 2005; Wood-Kaczmar et al., 2006). Although the function of LRRK2 and the

effect of its pathogenic mutations remain unclear, several mutations, including G2019S, seem to result in an increase in the kinase activity of the protein (Gloeckner et al., 2006; West et al., 2005). However, patients with *LRRK2* mutations exhibit diverse neuropathological features ranging from no LB to LB aggregates and neurofibrillary tau-positive tangles (Paisán-Ruíz et al., 2004; Zimprich et al., 2004).

1.1.4.2. Autosomal recessive PD: *PRKN*, *PINK1* and *DJ1*

Several autosomal recessive mutations have been identified. They mainly result in an early-onset PD (<45 years old at age of diagnosis) and a slower disease progression (Trinh & Farrer, 2013). Mutations in genes such as *DJ-1*, *PINK1* and *PRKN* are among the most characterised AR mutations (Abbas et al., 1999; Bonifati et al., 2003; Kitada et al., 1998; Valente et al., 2004; Van De Warrenburg et al., 2001).

Mutations in the *PRKN* gene are the major cause of autosomal recessive and early-onset PD, representing 70% of AR cases with an age of onset before 20 years old and suggesting that Parkin may play an important role in the pathophysiology of both familial and sporadic PD (Lill & Klein, 2017; Lücking et al., 2000). Patients carrying *PRKN* mutations suffer from neuronal loss in the substantia nigra often without LB pathology, suggesting that multiple distinct pathways can lead to PD, without α-synuclein as the main causative agent (Corti et al., 2011; Koros et al., 2017). Over 100 mutations in *PRKN* have been associated to familial forms of PD, this includes deletions, multiplications, insertions as well as missense mutations (Corti et al., 2011). Although some genetic alterations of the *PRKN* gene seem to associate with a higher risk of developing the disease, the involvement of heterozygous mutations as a susceptibility factor in the development of PD, remains controversial (Klein et al., 2007). *PRKN* encodes for Parkin an E3 ubiquitin ligase that regulates the ubiquitination of specific substrates and their subsequent degradation by the ubiquitin-proteasome system (UPS) (Shimura et al., 2000).

After *PRKN*, mutations in the *PTEN-induced putative kinase 1* (*PINK1*) gene are the second most common cause of autosomal recessive early-onset PD representing 1 to 5% of cases (Nuytemans et al., 2010). Patients carrying *PINK1* mutations clinically highly resemble those with mutations in the *PRKN* gene (Ibáñez et al., 2006). Although

patients with *PINK1* mutations present a pathology similar to those with idiopathic PD, including parkinsonism and motor dysfunction, the clinical symptoms appear at an earlier age (30-40 years old) and the disease progression is slower (Valente et al., 2002). *PINK1* encodes an ubiquitously expressed protein that comprises a C-terminal kinase domain facing the cytoplasm and an N-terminal mitochondrial targeting sequence (MTS) (Zhou et al., 2008). The presence of the MTS and evidence from *in vitro* work demonstrated the mitochondrial localisation of PINK1, further supporting the involvement of mitochondrial dysfunction in PD pathology (Gandhi et al., 2006; Valente et al., 2004). Around 90 pathogenic mutations in the *PINK1* gene have been identified so far (King & Plun-Favreau, 2017). Most of the mutations sit within the kinase domain of the protein and result in a dampening of its kinase activity, suggesting that PINK1 kinase activity plays a key role in the pathogenesis of PD (Deas et al., 2009; King & Plun-Favreau, 2017). While homozygous mutations invariably lead to the development of PD, heterozygous *PINK1* mutations seem to be a susceptibility factor for the development of sporadic PD (Kawajiri et al., 2011; Klein et al., 2007). This strengthens the existence of potential overlapping mechanisms between sporadic and familial PD.

Rare mutations in the DJ-1 protein have been linked to autosomal recessive early-onset PD (Bonifati et al., 2003; Van De Warrenburg et al., 2001). While the precise function of the protein still remains unclear, cytosolic DJ-1 was found to translocate to mitochondria in response to oxidative stress, suggesting a protective effect against cell damage and antioxidant properties (Canet-Avilés et al., 2004; Taira et al., 2004; Yokota et al., 2003). Small deletions and missense mutations have been identified, but they remain exceedingly rare and only account for 1% of early-onset PD cases (Koros et al., 2017).

1.1.4.3. Toxin-induced animal models of PD

In 1982, the discovery of MPTP led to the establishment of the first link between mitochondrial dysfunction and PD (Langston et al., 1983). Later on, a search for other environmental neurotoxic compounds was initiated and led to the discovery of similar compounds including paraquat, rotenone and 6-hydroxydopamine (6-OHDA) (Gorell et al., 1998; Parker et al., 1989; Senoh et al., 1959; Tanner, 1992; Ungerstedt, 1968). Altogether, these have reinforced the relevance of mitochondrial dysfunction in PD aetiology (King & Plun-Favreau, 2017).

MPTP is the toxin the most frequently used in animal models of PD. Animal ranging from cats, mice and monkeys in association with MPTP treatment have been useful to the understanding of the disease's pathology as they replicate the majority of the PD hallmarks (Blesa et al., 2012). MPTP intoxication in human and animal models produces the characteristic tetrad of PD symptoms, tremor, rigidity, slowness of movement and posture instability (Langston et al., 1984). However, although these animal models exhibit a selective loss of DA neurons in the substantia nigra and respond well to L-Dopa treatment, mice generally lack the classical LB-like formation, suggesting that this model only partially replicates PD pathology (Aryal & Lee, 2019; Fredriksson & Archer, 1994; Ogawa et al., 1985). Although the mouse model is the most popular, some variations in the phenotypes have been observed between different mouse strains (Blesa et al., 2012). Additionally, rats have proven to be resistant to MPTP treatment (Chiue et al., 1984; Blesa et al., 2012). Nevertheless, MPTP mouse models have been extremely valuable to better understand the molecular mechanisms occurring in PD. They represent the gold standard model and are often used as an initial tool to test and assess new potential therapeutic compounds for PD treatment (Blesa et al., 2012).

The herbicide paraquat has been commonly used in agriculture. Its structural resemblance to MPP+ led to the reasoning that paraquat should behave in a similar fashion, however unlike MPTP, paraquat is able to penetrate the blood-brain barrier. (Blesa et al., 2012; Snyder & D'Amato, 1985). Epidemiologic studies have reported an increase risk of developing PD upon paraquat exposure (Hertzman et al., 1990; Kamel et al., 2007; Lin et al., 2019; Ritz et al., 2009; Tanner et al., 2011; Tieu, 2011). In animal

models, exposure to paraquat induces deleterious effects including oxidative stress through excessive complex I-dependent superoxide production (Day et al., 1999; Tieu, 2011). Mice injected with paraquat display locomotor defects and nigral DA neuron degeneration in a dose and age dependent manner (Brooks et al., 1999; McCormack et al., 2002; Thiruchelvam et al., 2003). However, the true relevance of this toxin-induced animal model comes from its ability to replicate the α-synuclein aggregation and LB-like inclusions observed in DA neurons, therefore giving a more complete pathological picture of PD (Fernagut et al., 2007; Manning-Bog et al., 2002; Sherer et al., 2003).

Rotenone is a broad-spectrum pesticide and insecticide, that is naturally found in plants (Blesa et al., 2012; Hisata, 2002). Similar to MPTP and paraquat, rotenone blocks the mitochondrial electron transport chain at the level of complex I (Betarbet et al., 2000). Like paraquat, rotenone-intoxicated animals replicate most PD features, including the behavioural deficits, oxidative stress, synuclein aggregation and LB-like inclusions (Cannon et al., 2009; Inden et al., 2011; Pan-Montojo et al., 2010a; Pan-Montojo & Funk, 2010b; Takeuchi et al., 2009). Despite its advantages, rotenone has not been widely adopted by researchers. This is due to an apparent variability in animal sensitivity towards the toxin and several phenotypes observed by some researchers could not be reproduced by others (Fleming et al., 2004; Lapointe et al., 2004; Tieu, 2011; Zhu et al., 2004). Moreover, rotenone treatment is often associated with a high mortality rate, especially in rats, making this a difficult model to work with (Fleming et al., 2004; Jagmag et al., 2016). Finally, no examples of rotenone-induced PD in humans have been documented so far, thus some debate remains regarding the advantages that rotenone-based models offer over other toxin-induced models such as MPTP (Blesa et al., 2012).

6-OHDA is one of the first PD models associated with nigral DA neuronal death and still remains a classic PD model (Ungerstedt, 1968). The compound is a hydroxylated analogue of dopamine that was identified in the 1960s (Senoh et al., 1959). 6-OHDA was shown to predominantly enter DA neurons due to its high affinity for DAT (Luthman et al., 1989; Ungerstedt, 1968). Its accumulation and oxidation within the cytosol results in the production of ROS and the subsequent cytotoxicity related to oxidative stress (Blum et al., 2001; Saner & Thoenen, 1971; Tieu, 2011). 6-OHDA administration

in mouse models has been shown to nicely phenocopy the main PD features including loss of DA neurons in the substantia nigra, locomotor deficits and also some of the nonmotor symptoms such as psychiatric and cognitive dysfunctions (Branchi et al., 2008; Faull & Laverty, 1969; Jeon et al., 1995; Przedbroski et al., 1995; Sauer & Oertel, 1994; Tadaiesky et al., 2008). Unilateral 6-OHDA rat models have been extensively used to assess the potency of new therapeutics (Tieu, 2011). However, despite all these benefits, 6-OHDA, like several other neurotoxic models of PD, does not replicate the progressive and age-dependent characteristics of PD (Tieu, 2011). Moreover, as MPTP, 6-OHDA does not induce LB-like inclusions (Jackson-Lewis et al., 2012).

In summary, these toxin-induced animal models of PD have been incredibly useful to better understand the disease pathology and evaluate potential therapeutic treatments. However, most of them do not mimic all the pathological features of human PD, such as the formation of LB, a key hallmark of the PD histopathology.

1.2. Mitochondria: structure and functions

Mitochondria are essential organelles for eukaryotic cells, performing fundamental functions ranging from the generation of ATP, to calcium (Ca^{2+}) handling, lipid synthesis, apoptosis and more recently inflammation. Most eukaryotic cells harbour a plethora of mitochondria, ranging from a hundred to several thousands of these organelles per cell (Gray, 2012). Their number varies among tissues and over time to match the bioenergetic demands of each cell type. Mitochondria are thought to originate from an α-proteobacteria, although the exact mechanism is still under debate. There are currently two different views regarding the endosymbiotic event: archezoan or symbiogenesis scenarios (Gray, 2012; Lane & Martin, 2010; Roger et al., 2017). The first one relies on the engulfment of a α-proteobacteria by an amitochondriate eukaryotic host cell nucleus (Gray, 2012; Lane & Martin, 2010). The second scenario is based on the subsequent compartmentalisation and the establishment of a nucleus (Gray, 2012; Lane & Martin, 2010). This endosymbiotic event and the following development of the mitochondrion led to the transfer of genes to the host genome thus increasing the nuclear complexity and abrogating organelle autonomy (Gray, 2012; Lane & Martin, 2010; Roger et al., 2017). One of the major advantages of this endosymbiotic relationship is probably the mitochondrial genome, as it enables a rapid and controlled sensing for ATP demand, with the benefit of being able to modulate gene expression according to the metabolic needs of the cell (Lane & Martin, 2010). As a result, eukaryotes mainly rely on functional mitochondria to provide the ATP necessary for basal or high metabolic demands (Gray, 2012; Lane & Martin, 2010; Roger et al., 2017).

The existence of mitochondria was discovered in the late 1800s, with Richard Altmann's observation of some filaments that resembled strings of granules within nearly all cell types (Altmann, 1890). Altmann's work paved the way for others, including Warburg, to uncover the 'particular' nature of respiration (Ernster & Schatz, 1981). Since then, the knowledge of mitochondrial function has kept growing exponentially with the understanding of mitochondrial bioenergetics from the work of Peter Mitchell and others (Chance & Williams, 1955; Mitchell, 1966; Mitchell, 1961). These discoveries have shaped our current definition of mitochondria: a key player of

cellular metabolism and a dynamic organellar network that divides, fuses and mediates a plethora of functions (Pagliarini & Rutter, 2013). Despite tremendous work highlighting the critical role of mitochondria in providing energy for the cell, much effort remains to understand the contribution of mitochondria to several diseases such as type 2 diabetes, cancer, neurodegenerative disorders or the aging process (Corral-Debrinski et al., 1992; Cortopassi & Arnheim, 1990; Nunomura et al., 2001; Reddy et al., 2004; Sherer et al., 2003; Szendroedi et al., 2012; Wallace, 2012).

1.2.1. Mitochondria structure

Mitochondria are composed of two phospholipid bilayer membranes, the outer mitochondrial membrane (OMM) facing the cytosol and the inner mitochondrial membrane (IMM) enclosing the mitochondrial matrix. The space separating the two membranes is referred to as the inter-membrane space (IMS) (Figure 1.2) (Frey & Mannella, 2000; Perkins et al., 1997; Perkins & Frey, 2000). The highly permeable OMM allows free passage of ions and small uncharged molecules into the IMS through membrane protein pores (porins), such as voltage-dependent anion channel (VDAC) (Bayrhuber et al., 2008). This results in IMS ion concentrations roughly similar to the cytoplasm. Any larger molecules, need to be imported by a special importing machinery, such as the translocase of the OMM complex (TOM) (Gold et al., 2014; Kühlbrandt, 2015). Due to its porosity, there is no membrane potential across the OMM.

In contrast, movements across the IMM are tightly regulated and depend on specific membrane transport proteins that are selective for a particular ion or molecule, such as the translocase complex of the IMM (TIM) or carrier proteins such as the ATP/ADP carriers (Kühlbrandt, 2015; Pebay-Peyroula et al., 2003; Robinson et al., 2008). As a consequence, this ion selectivity results in an electrochemical membrane potential of ~180 mV across the IMM (Kühlbrandt, 2015). The IMM is where critical enzymes involved in oxidative phosphorylation (OXPHOS) and ATP production reside (complexes I, II, III, IV and the ATP synthase) (Barbot & Meinecke, 2016; Buzhynsky et al., 2007). The multiple invaginations of the IMM create mitochondrial cristae, extending deep into the matrix and increasing the membrane surface area (Frey & Mannella, 2000). These cristae accommodate the fully assembled complexes of the

electron transport chain (ETC) as well as the ATP synthase (Kühlbrandt, 2015).

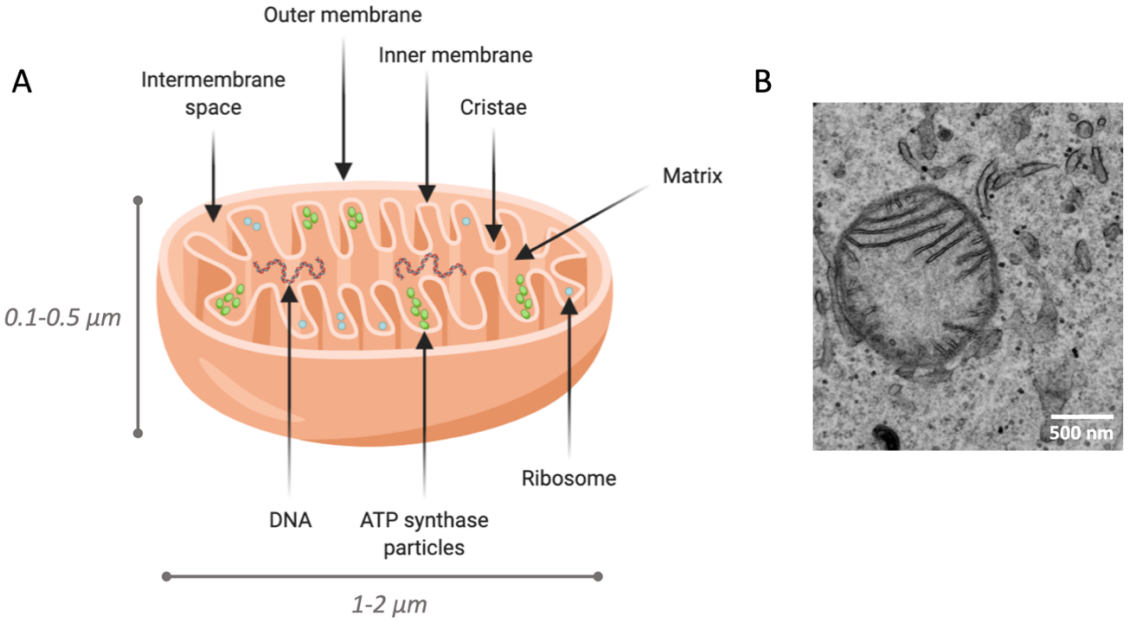

Figure 1.2. Structure of mitochondria

(A) Schematic representation of a mitochondrion and (B) electron microscopy (EM) of a mitochondrion in a neuroblastoma SH-SY5Y cell (EM image courtesy of Sébastien Paillusson).

Finally, enclosed by the IMM, is the mitochondrial matrix, which hosts enzymes of intermediary metabolism as well as hundreds of copies of mtDNA (Robin & Wong, 1988). Though with evolution most of the mitochondrial genetic information has been transferred to the nucleus, mitochondria have retained a vestigial genome (Gammage & Frezza, 2019). The human mitochondrial genome is made of a circular and double-stranded DNA molecule of 16.5 kilobase pair, encoding 13 subunits of the respiratory chain and ATP synthase, along with 22 transfer RNAs (tRNA) and 2 ribosomal RNAs (rRNAs) necessary for their translation (Andrews et al., 1999; Attardi & Schatz, 1988; Gammage & Frezza, 2019). Due to its proximity to the major source of ROS, mtDNA is considered to be particularly vulnerable to oxidative damage, resulting in the accumulation of spontaneous mutations, although this has been contradicted by other studies (Itsara et al., 2014; Kazak et al., 2012; Kennedy et al., 2013). Considering that mitochondria contain ~1500 proteins, a synergistic relationship between the nuclear and mitochondrial genomes is critical for the formation of the respiratory complexes as

well as maintaining mitochondria functions and integrity (Chinnery & Hudson, 2013; Gilkerson et al., 2008).

1.2.2. Mitochondrial respiration and ATP synthesis

One of the main functions of mitochondria is the production of energy which is performed by the four complexes of the respiratory chain (complexes I-IV) and the ATP synthase (complex V). Together, these complexes participate to the generation of ATP by OXPHOS, by coupling the oxidation of reduced cofactors that were obtained through the catabolism of nutrients (Sazanov, 2015). The ETC includes complex I (reduced nicotinamide adenine dinucleotide (NADH)-ubiquinone oxidoreductase), complex II (succinate ubiquinone oxidoreductase), complex III (cytochrome bc_1 oxidoreductase), complex IV (cytochrome c oxidase) and complex V (ATP synthase) (Figure 1.3). Complex I, complex III and complex IV contain multiple redox cofactors that store electrons and allow intra-protein electron transfer (Sazanov, 2015). Additionally, the ETC accommodates two mobile electron carriers: the membrane-embedded ubiquinone/coenzyme Q and the soluble cytochrome c that enable electron transport between the complexes (Sazanov, 2015). The catabolic processes of glycolysis, tricarboxylic acid cycle (TCA) and fatty acid oxidation reactions generate electrons that enter the ETC in the IMM. Complex I and complex II receive electrons from intermediary metabolism. Coenzyme Q, the electron shuttling protein then transfers the electrons to complex III. Finally, those electrons are delivered to cytochrome c and eventually transferred to complex IV, the final step of the ETC, whereby molecular oxygen is reduced to water, the ultimate electron acceptor (Perier & Vila, 2012; Sazanov, 2015). This movement of electrons is coupled to proton pumping across the IMM, from the matrix to the IMS, by complexes I, III and IV. The resulting electrochemical gradient (proton motive force Δp) across the IMM drives the generation of ATP by the ATP synthase (Letts et al., 2016; Perier & Vila, 2012; Watt et al., 2010). Reduction of this electrochemical potential is often used as a readout to assess the general functional status of mitochondria. Indeed, changes of this central parameter have been associated with activation of pathways to either repair or eliminate defective mitochondria, that will be discussed later.

The ATP synthesis within the mitochondria has been associated with the production of superoxide anion radial (O_2•−), which can further dismutate to generate hydrogen

peroxide (H_2O_2), which can itself form hydroxyl radical (•OH). It is well established that excessive ROS production from the mitochondria can damage mitochondrial compartments and induce further detrimental processes (Murphy, 2009).

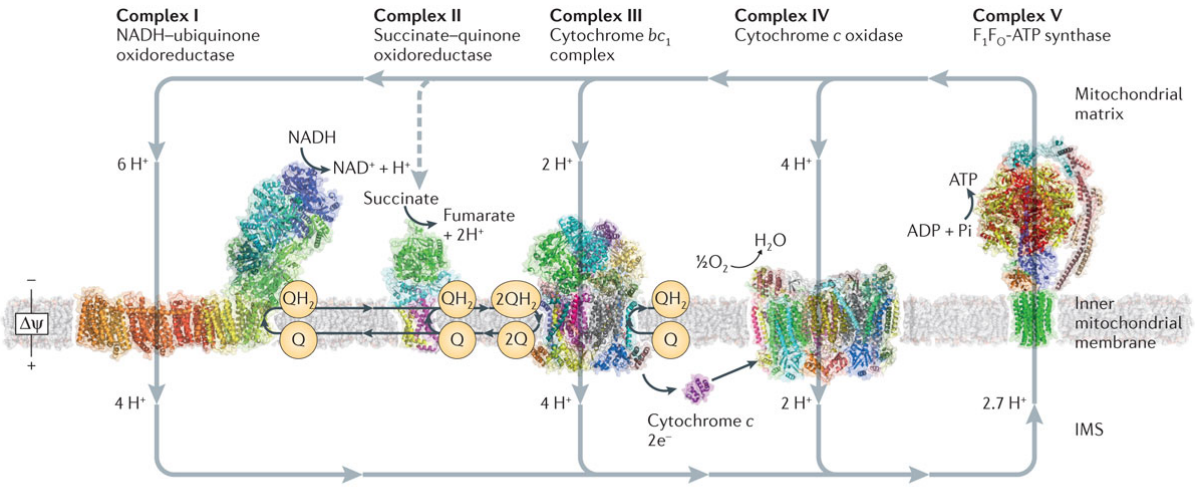

Figure 1.3 The electron transport chain

Electrons from NADH enter complex I and are used to reduce ubiquinone (Q) to ubiquinol (QH_2). Complex III uses QH_2 to reduce cytochrome c, which is subsequently used by complex IV to reduce molecular oxygen, the final electron acceptor. Complex II is an additional entry point for electrons. The electron transfer enables the proton pumping by complexes I, III and IV, which in turn generates the Δp across the IMM. This Δp is then used by the ATP synthase to generate ATP. (Figure from Sazanov, 2015).

1.2.3. Mitochondrial dynamics

As highly dynamic organelles, the mitochondrial tubular network is regulated by the fine-tuned balance between cycles of mitochondrial fusion and fission, referred to as ‘mitochondrial dynamics’. This adaptive system is crucial for many cellular processes such as apoptosis, calcium homeostasis, mitochondrial quality control or cell cycle (Mishra & Chan, 2014; Otera et al., 2013; Tilokani et al., 2018). Indeed, mutations in key components of the core machinery have been associated with various human diseases and are often the result of defective mitochondrial dynamics (Tilokani et al., 2018). Additionally, both mechanisms enable communication between two mitochondria as well as exchange of lipid membranes and intramitochondrial content, which is fundamental for complementing any mtDNA damage and maintaining a

healthy pool of mitochondria (Gilkerson et al., 2008). Beside ensuring the regulation of such processes, mitochondrial dynamics allow rapid response to bioenergetic demands by modulating the mitochondrial network to nutrient availability or cellular metabolic state (Molina et al., 2009; Quirós et al., 2012; Sebastián et al., 2012). The morphology of mitochondria influences the ability of cells to maintain their bioenergetic demands through the redistribution and concentration of their mitochondria to particular regions (Detmer & Chan, 2007). This is particularly important for highly polarised cells like neurons, which are heavily dependent on the transport of mitochondria to pre-and postsynaptic sites (Detmer & Chan, 2007). Mitochondrial elongation has been shown to provide a protective role against autophagosomal degradation during autophagy and is often associated with cell survival, especially during starvation events (Rambold et al., 2011; Tilokani et al., 2018). Mitochondrial fragmentation mainly correlates with stressful events or cell death, although it is also required for mtDNA inheritance, mitochondrial motility and quality control mechanisms (Tilokani et al., 2018).

The well characterised fusion machinery comprises three large GTPases: dynamin-related Mitofusin 1 and 2 (Mfn1 and Mfn2) and optic atrophy gene 1 (OPA1) which all act in a GTP hydrolysis-dependent manner (Tilokani et al., 2018). In addition to its role in mitochondrial fusion, Mfn2 is also a key regulator of the tethering occurring at mitochondria-endoplasmic reticulum (ER) contact sites (De Brito & Scorrano, 2008; Filadi et al., 2015). Mitochondrial fusion begins with the tethering of the OMM of two adjacent mitochondria allowing the formation of homo- (Mfn2/Mfn2) or heterotypic interactions of Mfn1/Mfn2 (Hoppins et al., 2011). GTP hydrolysis allows the conformational change of the Mfns further docking the two mitochondria together (Cao et al., 2017; Qi et al., 2016). Finally, the GTP-dependent oligomerization mediates the OMM fusion (Qi et al., 2016). The IMM fusion is ensured by OPA1 (Hoppins & Nunnari, 2009). Interestingly, the presence of OPA1 on one of the two ‘fusing’ mitochondria is enough to drive the fusion of the two IMM (Song et al., 2009). The interaction between OPA1 and the phospholipid cardiolipin allows the tethering of the two IMM, which subsequently fuse via GTP hydrolysis of OPA1 (Ban et al., 2017). After fusion of the OMM and IMM, Mfn2 and OPA1 disassemble (Figure 1.4) (Tilokani et al., 2018).
The initial step of the mitochondrial fission requires the ER. 3D images reconstructed from EM and tomography images have shown the ER wrapping around the

mitochondrion in order to mark the future mitochondrial fission site (Friedman et al., 2011). This marking of the constriction site induces a reduction of the mitochondrial diameter, that allows the formation of Drp1-oligomeric rings (Friedman et al., 2011; Phillips & Voeltz, 2016). Beside the ER, mitochondrial fission is mediated by the core component dynamin-related protein 1 (Drp1). Upon recruitment and oligomerisation, Drp1 has been shown to drive the constriction of mitochondrial and peroxisomal membrane in a GTP-dependent manner (Ishihara et al., 2009; Koch et al., 2003). Drp1 is recruited from the cytosol to the OMM where it assembles into ring-like structures that constrict the OMM (Fröhlich et al., 2013; Ingerman et al., 2005; Smirnova et al., 2001). The membrane constriction is further enhanced by GTP hydrolysis, thus marking the future fission site (Mears et al., 2011). Recent studies have reported that the mitochondrial fission 1 protein (Fis1) may not be involved in the fission event in basal conditions (Otera et al., 2016). Instead, mitochondrial dynamics proteins 49 and 51 (MiD49 and MiD51) as well as mitochondrial fission factor (Mff) have been suggested to act as Drp1 receptors (Gandre-Babbe & Van Der Bliek, 2008; Losón et al., 2013; Palmer et al., 2011). Mff and MiDs are believed to exert complementary functions in mitochondrial fission, such that MiDs recruit GTP-bound state of Drp1 to promote oligomerization and Mff recruits Drp1 in a oligomeric and active form (Losón et al., 2013; Osellame et al., 2016; Palmer et al., 2011). Finally, the GTPase dynamin-2 (DNM2) has been proposed to act in the end step of the scission event (Lee et al., 2016). By assembling in ring-like structures at the constriction site, DNM2 is thought to terminate the fission event, resulting in two daughter mitochondria with differing properties (Figure 1.4) (Ferguson & De Camilli, 2012; Lee et al., 2016; Tilokani et al., 2018). Recently, phosphatidylinositol 4-phosphate (PI(4)P) on trans-Golgi network vesicles was shown to be recruited at mitochondria-ER contact sites to regulate the final events of mitochondrial fission, downstream of Drp1 (Nagashima et al., 2020).

Altogether, the balance between fusion and fission events governs the maintenance of a functioning pool of mitochondria and the overall health of the cell (Twig et al., 2008). A failure to do so has been implicated in various neurological disorders, such as PD and Alzheimer's Disease, further emphasising the importance of mitochondrial dynamics.

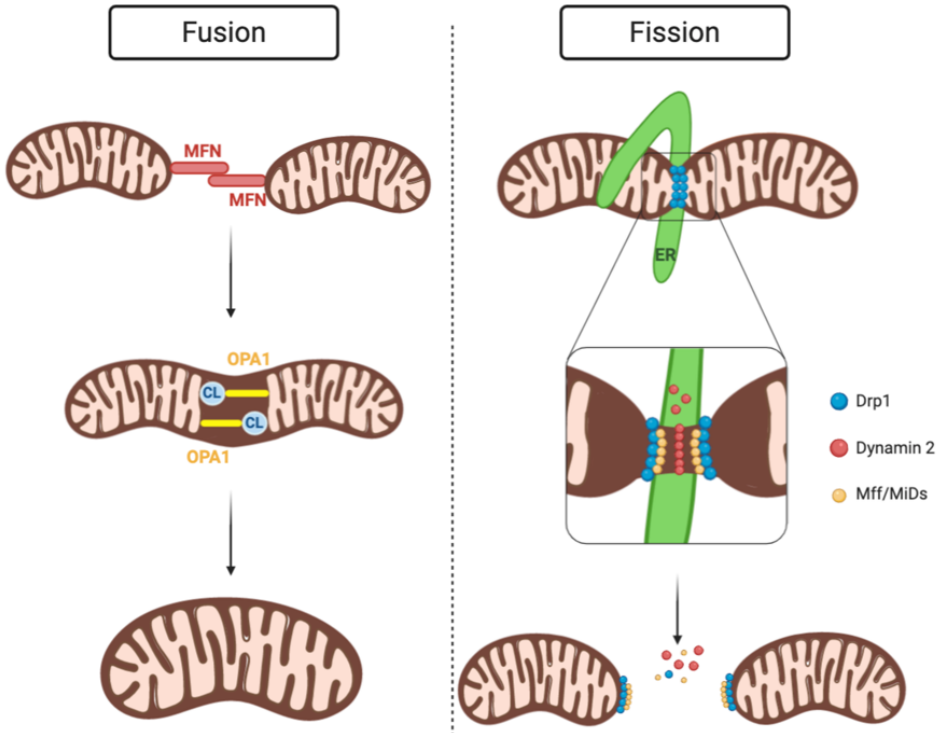

Figure 1.4. Schematic representation of mitochondrial fusion/fission.
(Fusion) OMM fusion is driven by Mfn1/2 interaction. The IMM fusion is ensured by OPA1 interactions and cardiolipins. (Fission) The ER (green) marks the future mitochondrial fission site by wrapping around the mitochondrion. Drp1 (blue) is recruited to the OMM and accumulates at mitochondria-contact sites where it assembles into ring-like structures that constrict the OMM. Mff and MiD49/MiD59 (yellow) act as Drp1 receptors. DNM2 (red) has been proposed to terminate the fission event, resulting in two daughter mitochondria with differing properties. (Adapted from Tilokani et al., 2018).

1.2.4. Other mitochondrial functions

Beyond their primary role in ATP production, mitochondria regulate many other cellular processes. Mitochondria are highly connected to the ER, and it is now well established that physical and biochemical interactions occur between them. It has been estimated that 2-5% of the OMM participate in the formation of contact sites with the ER (Cosson et al., 2012; Murley et al., 2013). This tightly coordinated cross-talk regulates many important functions of the cell, such as lipid synthesis/metabolism, apoptosis, Ca^{2+} trafficking, and mitochondrial dynamics (Phillips & Voeltz, 2016).

The phospholipid synthesis relies on the constant trafficking of the lipids between the ER and the mitochondria. Although the synthesis starts in the ER, the lipids need to be modified by enzymes present in the mitochondrial matrix. For instance, while

phosphatidylserine is produced in the ER, it shuttles to the mitochondria to be modified by mitochondrial enzymes to generate phosphatidylethanolamine, which can further be transported back to the ER and converted to phosphatidylcholine by ER-enzymes (Dennis & Kennedy, 1972; Osman et al., 2011).

The tight relationship between mitochondria and the ER at specific contact sites is also essential for the regulation of Ca^{2+} flux. Several mechanisms regulate Ca^{2+} concentrations in order to ensure the maintenance of low cytosolic Ca^{2+} levels and micromolar Ca^{2+} levels within the mitochondria (Phillips & Voeltz, 2016). Ca^{2+} is mainly stored in the ER lumen and its release into the cytosol is mediated by two main effectors: the inositol 1,4,5-triphosphate (IP3) receptors (IP3R) and ryanodine receptors (RyRs) present throughout the ER membrane (Marks, 1997). The binding of the second messenger IP3 to the IP3Rs stimulates the Ca^{2+} release from the ER and its subsequent uptake by mitochondria. Ca^{2+} is then taken up by the mitochondria via VDAC on the OMM and the mitochondria calcium uniporter (MCU), which transports Ca^{2+} across the IMM (Baughman et al., 2011; De Stefani et al., 2012; De Stefani et al., 2011). Due to the low affinity of MCU for Ca^{2+}, the basal Ca^{2+} levels in the cytosol are not sufficient to enable mitochondrial uptake (Csordás et al., 2010; Giacomello et al., 2010). Therefore, the release of Ca^{2+} occurs at specific ER-mitochondria contact sites that generate highly localised and concentrated Ca^{2+} microdomains, thus allowing Ca^{2+} transport into the mitochondria (Paupe & Prudent, 2018; Rizzuto et al., 1993). These ER-mitochondria Ca^{2+} exchanges are crucial for cellular bioenergetics as some matrix-localised enzymes of the TCA cycle are Ca^{2+}-dependent (Denton, 2009). Additionally, changes in mitochondrial Ca^{2+} levels play a role in cell death, such that the release of Ca^{2+} from the ER can trigger apoptosis by opening the mitochondrial permeability transition pore (mPTP) (Rizzuto et al., 2012; Scorrano et al., 2003; Zong et al., 2003).

Apoptosis is regulated by members of the B-cell lymphoma 2 (Bcl-2) family that comprises three subfamilies: pro-apoptotic BH3 members, pro-apoptotic effector molecules, such as cytosolic Bcl-2- associated X protein (Bax) and Bcl-2 antagonist killer 1 (Bak) and anti-apoptotic Bcl-2 family proteins (Wang & Youle, 2009). Upon apoptotic stimulus, activated pro-apoptotic BH3-only proteins act on the pro-apoptotic effectors, Bak and Bax or inhibit the members of the anti-apoptotic Bcl-2 family. Bax and Bak then translocate to the mitochondria, where they oligomerise and induce the

OMM permeabilization (Wang & Youle, 2009). This in turn leads to the release of cytochrome c from the IMS, and the subsequent formation of the apoptosome, the caspase cascade activation and cell apoptosis (Nagata, 2018).

1.2.5. Mitochondria quality control (MQC)

ROS, in particular O_2•−, •OH, H_2O_2 are toxic by-products of OXPHOS produced in the mitochondrial matrix and contribute to damage to mitochondrial lipids, DNA and proteins (Wallace, 2005). In turn, dysfunctional mitochondria can trigger Ca^{2+} and cytochrome c release in the cytosol, leading to the subsequent activation of apoptosis (Ashrafi & Schwarz, 2013). Therefore, besides being essential organelles, mitochondria are prone to the release of toxic and damaging components, especially when their homeostasis has been compromised. Such oxidative damage has been extensively linked to aging and a range of neurodegenerative diseases, including PD (Ashrafi & Schwarz, 2013; Balaban et al., 2005; Murphy, 2009). The cells are equipped with several mechanisms to quench free radicals in order to minimise the oxidative damage. These include the mitochondrial manganese-dependent superoxide dismutase (MnSOD) and SOD1 that promote the dismutation of O_2•− to H_2O_2, a catalase and members of the glutathione peroxidase (GPx) and peroxiredoxin (Prx) families that participate to the reduction and elimination of H_2O_2 (Handy & Loscalzo, 2012; Murphy, 2009). However, these mechanisms can rapidly become insufficient (Taylor & Rutter, 2011). Thus, in order to counteract continuous accumulation of damaging components that can negatively influence mitostasis and the overall cellular homeostasis, mitochondria have developed multiple mechanisms of quality control (Pickles et al., 2018). These processes lead to the elimination of dysfunctional mitochondrial components or eventually the entire mitochondrion, by mitophagy, in order to preserve a healthy pool (Ashrafi & Schwarz, 2013; Lemasters, 2005). An overview of the different types of MQC is given in Figure 1.5 and discussed in more details below.

1.2.5.1. ATP-dependent proteases

Mitochondria host over 20 proteases which participate in various functions, such as the quality control of misfolded, unfolded or damaged proteins (Figure 1.5) (Anand et al., 2013; Pickles et al., 2018). The main class of proteases involved in MQC comprises

the ATP-dependent proteases that reside in the IMM and matrix space (Koppen & Langer, 2007; Leonhard et al., 1996). When damage is still localised within the mitochondrion, the organelle uses its own proteolytic system which allows the degradation of misfolded membrane proteins that could interfere with mitochondrial function (Ni et al., 2015). The ATP-hydrolysis provides the energy necessary to unfold specific proteins and transport them into the proteolytic cavity (Koppen & Langer, 2007). The mitochondrial ATP-dependent proteases can be divided into three groups according to their localisation: (i) the Lon proteases in the matrix; (ii) the ClpXP complex also in the matrix and (iii) the AAA (ATPase associated with various cellular activities) proteases within the IMM (De Sagarra et al., 1999; Koppen & Langer, 2007; Langer, 2000; Santagata et al., 1999; Suzuki et al., 1994; Van Dyck et al., 1994). The Lon proteases seem to be particularly relevant under stress conditions when oxidatively damaged proteins accumulate in the mitochondrial matrix (Bota & Davies, 2002). After having recognised misfolded or damaged proteins, they mediate their proteolysis (Bota & Davies, 2002). The precise biological role of the ClpXP complex is currently not fully understood, although they have recently been implicated in the maintenance of mitochondrial metabolic pathways as well as in the degradation of misfolded proteins upstream of the mitochondrial unfolded protein response signalling pathway (Fischer et al., 2015). Finally, within the IMM are two AAA-proteases, the *i*-AAA and *m*-AAA which are oriented towards the IMS and the matrix, respectively (Fischer et al., 2012). Their function is to induce conformational changes in damaged proteins and promote their unfolding and disassembly (Fischer et al., 2012; Leonhard et al., 2000). Mutations in some of these proteases have been implicated in neurodegenerative conditions such as a form of hereditary spastic paraplegia due to mutations in the *m*-AAA protease (Atorino et al., 2003; Casari et al., 1998; Guha et al., 2011; Leonhard et al., 2000; Nolden et al., 2005). Additionally, impairment or dysregulation of the function of these enzymes has been linked to numerous pathologies, from neurodegenerative diseases to metabolic conditions and cancer (Bernstein et al., 2012; Ngo & Davies, 2009; Zhu et al., 2002). Moreover, mitochondrial proteases are crucial for the processing of PINK1, which suggests some cross-talk and interdependence between different MQC pathways (Greene et al., 2012; Sugiura et al., 2014).

1.2.5.2. Ubiquitin proteasome system

The cytosolic UPS is another quality control mechanism that mainly regulates OMM proteostasis (Figure 1.5). Among the known OMM-associated UPS substrates are many proteins involved in the regulation of either apoptosis or mitochondrial dynamics, such as Bcl-2 family proteins or Mfn 1 and 2 (Breitschopf et al., 2000; Cohen et al., 2008; Karbowski & Youle, 2011). Some intramitochondrial proteins such as the IMM-associated prohibitins (PHBs) or some subunits of ATP synthase have been reported as proteasomal substrates through their translocation to the OMM (Karbowski & Youle, 2011; Margineantu et al., 2007; Thompson et al., 2003). In fact, proteasome inhibition results in the accumulation of IMM proteins, suggesting that in addition to OMM-localised proteins, the UPS also frequently regulates IMM proteins (Margineantu et al., 2007). OMM ubiquitin-marked proteins are extracted from the mitochondrial membrane and released in the cytosol via a retro-translocation process, that is dependent on the AAA+ ATPase, p97, a membrane protein-extracting factor (Tanaka et al., 2010; Xu et al., 2011). The ubiquitination process is mediated by E3 ubiquitin ligases, such as Parkin, that tag lysine residues with the small protein modifier ubiquitin (Ub), which can further form polyubiquitin chains (Chau et al., 1989; Kirisako et al., 2006; Tanaka et al., 2010; Thrower et al., 2000). Finally, the tagged proteins are then targeted to and recognised by the 26S proteasome where they are subsequently degraded, in a similar manner to the ER-associated degradation (ERAD) pathway (Xu et al., 2011).

1.2.5.3. Mitochondrial unfolded protein response (mtUPR)

It is well-documented that unfolded or misfolded proteins can trigger ER-stress signalling pathways, such as the UPR (Ron & Walter, 2007). Accumulating evidence points towards the existence of a conceptually similar mechanism in mitochondria, although it remains less characterised (Haynes & Ron, 2010). While the mtUPR was first discovered in mammals, studies in *Caenorhabditis elegans* have shown that mitochondria have the ability to adapt to and deal with increased quantity of unfolded or misfolded proteins (Haynes & Ron, 2010; Yoneda et al., 2004; Zhao et al., 2002). During times of stress, the mtUPR enables mitochondria to maintain proteins in a proper folding state, thus preventing the potential and deleterious aggregation of proteins (Haynes & Ron, 2010). The mtUPR relies on a complex relationship between

the mitochondria and the nucleus which results in the activation of mitochondrial protective genes such as chaperones and proteases in order to regain mitochondrial homeostasis (Figure 1.5) (Pellegrino et al., 2013; Zhao et al., 2002). Activation of the mtUPR involves the expression of the nuclear encoded mitochondrial chaperone heat shock protein (hsp)60, the transcription factor CHOP (CCAAT/enhancer-binding protein (C/EBP)-homologous protein) and the protease ClpXP (Aldridge et al., 2007; Kang et al., 1990; Ostermann et al., 1990; Zhao et al., 2002). Briefly, accumulation of unfolded proteins within the mitochondrial matrix activates CHOP which triggers the transcription of several genes, such as hsp60 and ClpXP which digest protein aggregates into shorter peptides (Aldridge et al., 2007; Choi & Licht, 2005; Horibe & Hoogenraad, 2007; Pellegrino et al., 2013; Zhao et al., 2002). These small peptides are then pumped out of the mitochondria and contribute to the downstream signalling in the mtUPR (Haynes & Ron, 2010). The mtUPR has been implicated in response to several insults, including elevated ROS levels, mtDNA depletion, paraquat or the accumulation of aggregation-prone proteins in mitochondrial matrix (Cochemé & Murphy, 2008; Haynes & Ron, 2010; Lin et al., 2016; Zhao et al., 2002). More recently, mtUPR activation has been shown to correlate with prolonged lifespan in *C. elegans* and mouse models, suggesting that mtUPR upregulation, triggered by different mitochondrial stressors, could be the underlying process for increased longevity (Houtkooper et al., 2013).

1.2.5.4. Mitophagy

Since the first observation of mitochondria engulfed in an autophagosome structure in 1957, the interest for mitophagy has expanded far beyond (Clark, 1957). Extensively damaged mitochondria are removed by a selective form of autophagy, mitophagy, resulting in the degradation of the whole organelle (Figure 1.5). Mitophagy has proven to be a protective mechanism that prevents the accumulation of toxic mitochondrial products but also a way to regulate mitochondria number to match metabolic requirements (Kiššová et al., 2004; Youle & Narendra, 2011). The clearance of defective mitochondria is particularly relevant in the context of long-lived cells that do not regenerate such as neurons, cardiomyocytes or renal tubular cells (McWilliams & Muqit, 2017). In mammals, mitophagy has been implicated in diverse cellular events such as cell differentiation, the elimination of paternal mtDNA following fertilisation as

well as in the event of oxygen deprivation (Kundu et al., 2008; Rojansky et al., 2016; Schweers et al., 2007).

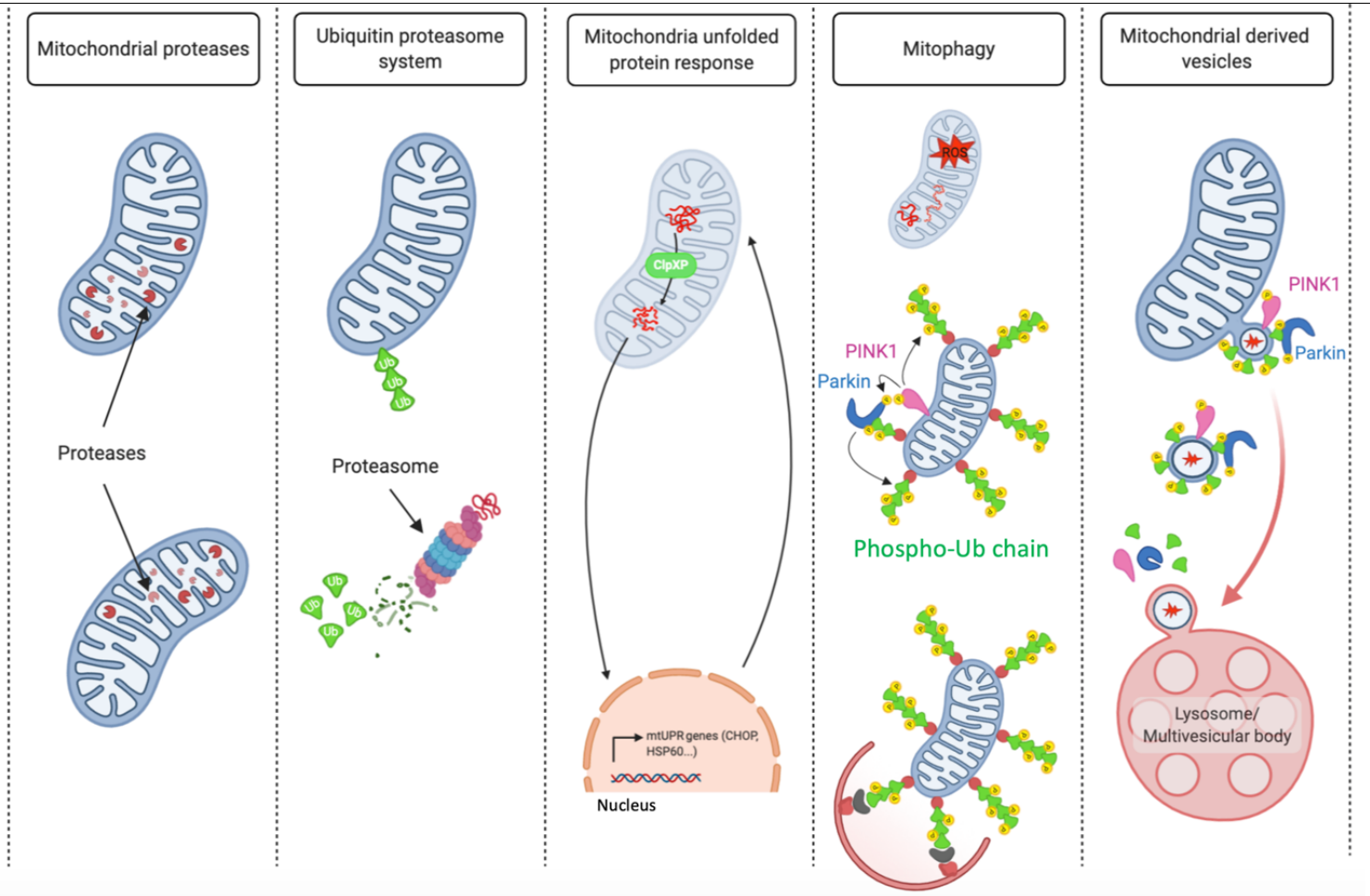

Figure 1.5. Schematic overview of the mitochondrial quality control

The mitochondrial proteases are likely to be the first defence mechanism. The UPS removes OMM proteins from the mitochondria for degradation by the proteasome. The mtUPR deals with unfolded protein via signalling with the nucleus. When the mitochondrial damage is too extensive, mitochondria are targeted to PINK1/Parkin mitophagy. Finally, MDVs, or piecemeal mitophagy, allow the removal of a portion of the mitochondrion leaving the rest intact.

1.2.5.4.1. PINK1/Parkin-mediated mitophagy

Since their discovery PINK1 and Parkin were known to play a role in mitochondrial homeostasis, but in recent years a large body of research has placed them as key regulators of stress-induced mitophagy. Consequently, this has become a major focus as a therapeutic target for PD. However, although mitophagy has been extensively studied *in vitro*, little is known about this process *in vivo* under basal conditions and in response to toxic insults.

1.2.5.4.1.1. PINK1 and Parkin

PINK1 is a 581 amino acid kinase protein encoded by the *PARK6* gene, and Parkin is a 465 amino acid E3 ubiquitin ligase encoded by the *PARK2* gene (King & Plun-Favreau, 2017). Both proteins are expressed in a wide variety of tissues, with higher transcript levels correlating with high-energy demanding tissues such as the heart, brain, skeletal muscles, liver and testis (King & Plun-Favreau, 2017; Kitada et al., 1998; Shimura et al., 2000). While PINK1 localises both at the OMM and IMM in mitochondrial fractions, Parkin localisation is mainly cytosolic (Kasap et al., 2009; Pridgeon et al., 2007; Shimura et al., 2000; Silvestri et al., 2005).

The C-terminus of PINK1 comprises the serine/threonine catalytic domain which contains three insertional loops. The N-terminus includes the MTS for PINK1 import to the mitochondria (Beilina et al., 2005; King & Plun-Favreau, 2017). Under basal conditions, PINK1 is imported into the mitochondria via TOM/TIM complexes (Lazarou et al., 2012). Once in the IMM, PINK1 undergoes a series of cleavages (Deas et al., 2011; Greene et al., 2012; Meissner et al., 2011; Narendra et al., 2010). The first cleavage involves the MTS removal from the 64 kDa full length PINK1 by the mitochondrial processing peptidase (MPP), resulting in a 60 kDa fragment. This is followed by a second cleavage by presenilin-associated rhomboid-like protease (PARL), producing a shorter fragment of 52 kDa (Deas et al., 2011; Jin et al., 2010; Kato et al., 2013; Kondapalli et al., 2012). This 52 kDa fragment is then externalised to the cytosol and degraded by the UPS through the N-end rule pathway (Greene et al., 2012; Lin & Kang, 2008; Narendra et al., 2010). This constant PINK1 import and degradation allows the maintenance of almost undetectable protein levels of PINK1 on healthy mitochondria (Figure 1.6) (Lin & Kang, 2008; Narendra et al., 2010).

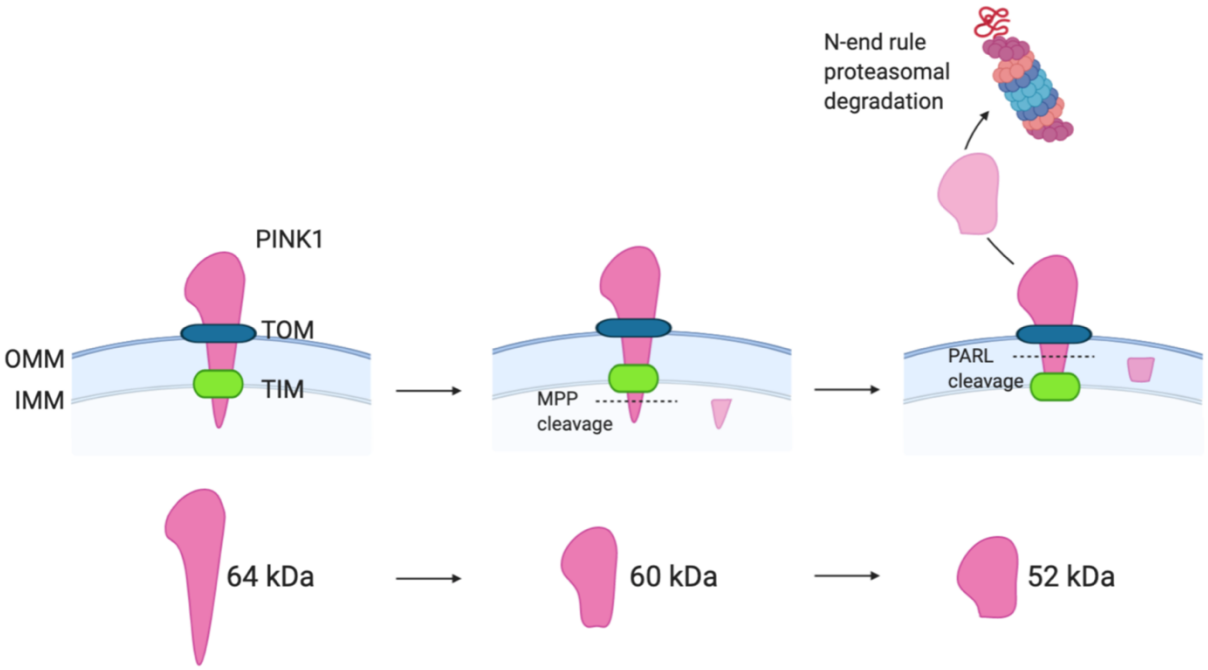

Figure 1.6. PINK1 turnover

Schematic representation of PINK1 turnover under basal conditions. In healthy mitochondria, when the membrane potential is intact, PINK1 is targeted to the mitochondria and imported via the TOM/TIM complexes. PINK1 is first cleaved by MPP in the matrix, followed by a second cleavage by PARL in the IMS. The remaining PINK1 fragment is released in the cytosol and targeted to the N-end rule degradation by the proteasome.

Parkin is an E3 ligase that belongs to the RING in between RING (RBR) domain family and catalyses the transfer of ubiquitin from an E2 ubiquitin-conjugating enzyme to a protein substrate. Thus, Parkin is responsible for the formation of mono- and poly-ubiquitin chains of different topologies and on various substrates (Chen et al., 2010; Chung et al., 2001; Matsuda et al., 2006). The protein comprises an ubiquitin-like (Ubl) domain at the N-terminus, a cysteine-rich RING0 domain, also known as unique Parkin domain (UPD), and a C-terminus composed of a RBR domain (Hristova et al., 2009; Trempe et al., 2013; Wauer & Komander, 2013). The RBR contains two RING domains, namely RING1 and RING2, separated by an in-between RING (IBR) domain (Trempe et al., 2013). In basal conditions, Parkin resides in the cytosol and in an inactive state due its autoinhibited conformation (Wauer & Komander, 2013). The inhibition occurs when the Ubl and the repressor element (REP) block the RING1 domain where the E2-ligase binding site sits and the RING0 domain blocks the catalytic cysteine in the RING2 domain (Chaugule et al., 2011; Nguyen et al., 2016;

Trempe et al., 2013; Wauer & Komander, 2013). Besides its role in mitophagy, Parkin has been implicated in mitochondrial biogenesis, in the regulation of cell death and in cancer (Kuroda et al., 2006; Shires et al., 2017; Veeriah et al., 2010).

1.2.5.4.1.2. Mechanism of PINK1/Parkin-mediated mitophagy

Upon mitochondrial membrane depolarisation, such as with the use of carbonyl cyanide 3-chlorophenylhydrazone (CCCP), the loss of the mitochondrial membrane potential leads to the blockade of PINK1 import through the TIM complex (Jin et al., 2010; Jin & Youle, 2013). As a result, PINK1 can no longer be cleaved and the unprocessed protein accumulates on the OMM, flagging mitochondria for degradation (Lazarou et al., 2012; Narendra et al., 2008). As PINK1 remains bound to the OMM through the TOM complex, it dimerizes and autophosphorylates, resulting in the activation of its kinase activity and Parkin recruitment (Matsuda et al., 2010; Okatsu et al., 2012). Basally ubiquitinated proteins present on the OMM act as initial substrates that PINK1 phosphorylates at the serine 65 (Ser65). Several studies have shown that Parkin has a particular affinity for phospho-Ser65-Ub (pSer65-Ub) which is responsible for Parkin stabilisation at the OMM (Kane et al., 2014; Kazlauskaite et al., 2014; Kondapalli et al., 2012; Shiba-Fukushima et al., 2012). pSer65-Ub binds to Parkin RING1 and RING0 domains which induces a shift from a closed to open conformation of Parkin and releases the autoinhibitory interaction from the Ubl and REP domains (Kane et al., 2014; Kazlauskaite & Muqit, 2015; Wauer et al., 2015; Yamano et al., 2015). Once in an open conformation, the particular Ser65 that sits in the Ubl domain of Parkin becomes more readily available to PINK1 phosphorylation, which further stabilises Parkin's active state. After activation of Parkin, the whole process enters a 'feed-forward' amplification loop whereby Parkin ubiquitylates several proteins on the OMM (such as Mfn1 and 2), generating more ubiquitin chains on the mitochondria, providing further substrates for PINK1 phosphorylation and recruiting more Parkin molecules (Okatsu et al., 2015). The ubiquitin coat generated by PINK1 and Parkin on the OMM leads to the recruitment of the classical autophagy machinery and the subsequent engulfment of the mitochondria by an autophagosome (Lazarou et al., 2015). Once the mitochondria are fully engulfed, the autophagosome fuses with a lysosome forming an autolysosome which will result in the degradation of the autosomal contents (Figure 1.7) (Nguyen et al., 2016). Evidence has suggested that

ER-mitochondria contact sites, through Mfn2 tethering, regulate the initiation of mitophagy (McLelland et al., 2018). Indeed, a reduction of ER-mitochondria contact sites results in an increase of mitochondria turnover via PINK1/Parkin mitophagy (McLelland et al., 2018). Mechanistically, phospho-ubiquitination of Mfn2 by PINK1/Parkin triggers the disassembly of Mfn2 complexes from the OMM and the dissociation of contact sites between the two organelles, allowing mitophagy to proceed (McLelland et al., 2018).

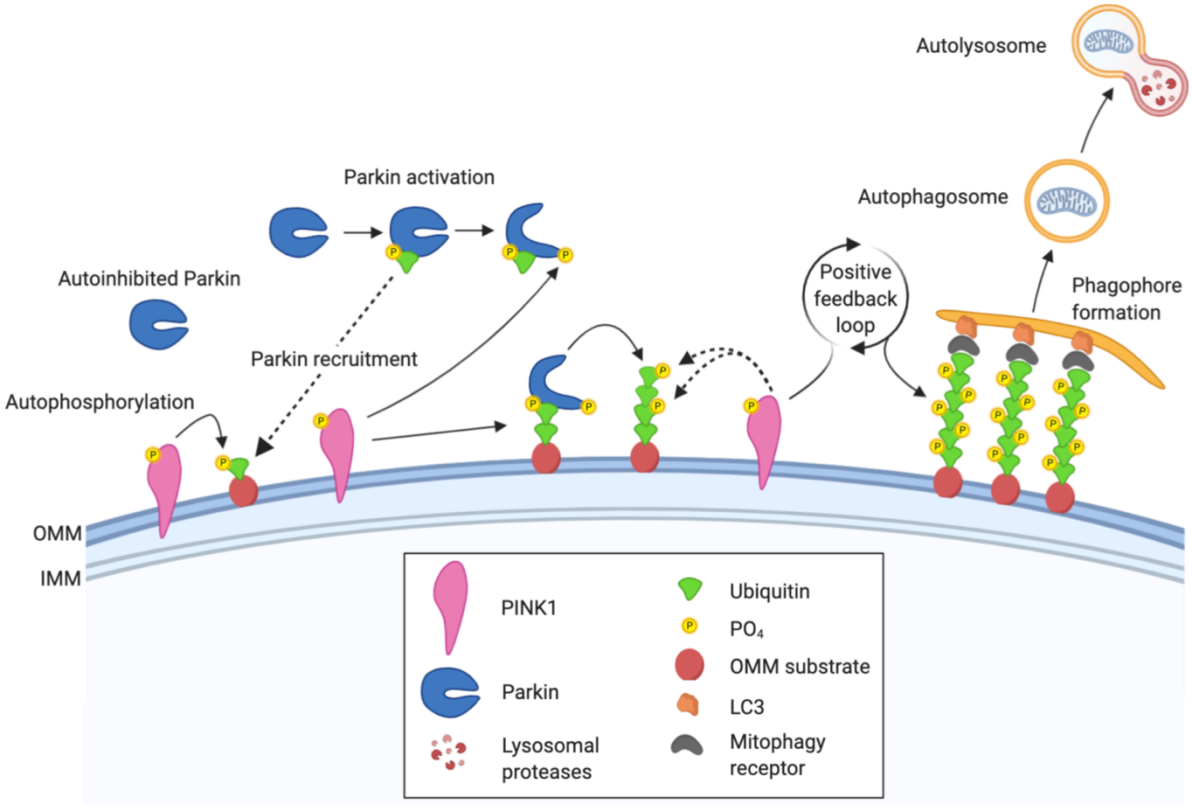

Figure 1.7. PINK1/Parkin-mediated mitophagy

PINK1 is stabilised at the OMM and undergoes auto-phosphorylation, which results in its activation. PINK1 phosphorylates the Ser65 of Ub attached to OMM proteins and of the Ubl domain of Parkin, leading to Parkin activation. Binding of phospho-Ub to Parkin induces conformational changes in Parkin which enable the phosphorylation of the Ubl domain of Parkin by PINK1. Parkin ubiquitinates OMM proteins which provides additional substrates for PINK1 to phosphorylate. This leads to more Parkin recruitment, resulting in a positive feedback loop.

Optineurin (OPTN), nuclear dot protein 52 (NDP52) and p62 are some of the several autophagy receptors that have been shown to translocate to the mitochondria during PINK1/Parkin mitophagy (Heo et al., 2015; Lazarou et al., 2015; Wong & Holzbaur, 2014). These receptors play a key role in the recruitment of the microtubule-associated protein 1A/1B light chain 3A (LC3) to the mitochondria. Additionally, OPTN and NDP52 have been shown to be required for the initiation of the autophagosome formation during mitophagy (Lazarou et al., 2015; Nguyen et al., 2016). These receptor proteins comprise a linear LC3-interacing region (LIR) domain allowing their interaction with LC3 proteins on the autophagosome membrane. The LIR motif is a composed of the consensus amino acid sequence (W/F/Y)XX(L/I/V), where the X can be any residue (Rodger et al., 2018; Svenning & Johansen, 2013). So far, multiple autophagy receptors containing LIR motifs have been identified and implicated in the degradation of various cargoes, in addition to mitochondria, through the autophagy process (Heo et al., 2015; Lazarou et al., 2015; Rodger et al., 2018).

OPTN and NDP52 have been shown to work in a similar fashion, but seem to be expressed in different tissues, suggesting that their function may vary depending on the tissue (Lazarou et al., 2015). The recruitment of these two receptors to the OMM relies on their binding to the pSer65-Ub generated by PINK1 phosphorylation (Lazarou et al., 2015). Interestingly, mitochondrial depolarisation can induce the recruitment of a small subset of OPTN and NDP52, independently of Parkin (Nguyen et al., 2016). Moreover, expression of a kinase dead form of PINK1 inhibits the recruitment of OPTN and NDP52, suggesting that although these autophagy receptors can be recruited in the absence of Parkin, it seems to be PINK1-dependent (Heo et al., 2015; Lazarou et al., 2015).

The Levine group identified an IMM protein, prohibitin 2 (PHB2), as a receptor required for Parkin-mediated mitophagy, in particular for the degradation of paternal mitochondria after embryonic fertilisation in *C. elegans* (Wei et al., 2017). In cells overexpressing Parkin in combination with mitochondrial insult, Parkin mediates the proteosomal degradation of OMM proteins, revealing the IMM and allowing PHB2 to directly binds to LC3, via its LIR domain (Wei et al., 2017). Following this study, Yan et al. showed that in addition to being a mitophagy receptor, PHB2 can also induce PINK1/Parkin-mediated mitophagy (Yan et al., 2019). By regulating PINK1 processing

by PARL, PHB2 stabilises PINK1, thus enhancing Parkin recruitment to the mitochondria (Yan et al., 2019).

More recently, Pincely Abudu et al., have shown the relevance of two matrix proteins 4-nitrophenylphosphatase domain and non-neuronal SNAP25-like protein homolog 1 and 2 (NIPSNAP1 and 2) proteins in promoting mitophagy following mitochondrial depolarisation (Princely Abudu et al., 2019). While NIPSNAP1 and 2 appear to exert redundant functions, they were shown to stabilise at the OMM in response to CCCP treatment. Additionally, evidence from Pincely Abudu et al., indicate that both proteins are capable of interacting with LC3 as well as p62, OPTN and NPD52, indicating that NIPSNAP1 and 2 may play a role in the recruitment of these autophagy receptors (Princely Abudu et al., 2019). Interestingly, while CCCP treatment induced mitochondrial depolarisation followed by Parkin recruitment and ubiquitination of OMM substrates, the recruitment of autophagy receptors was significantly reduced in mice lacking NIPSNAP1 and 2 (Princely Abudu et al., 2019). This latter observation suggests that NIPSNAP1 and 2 are necessary for the recruitment of these autophagy receptors and the subsequent mitophagy (Princely Abudu et al., 2019). Previous work from Nautiyal et al., reported that NIPSNAP1 and 2 are exclusively expressed in the nervous system and high expression levels were detected in DA neurons (Nautiyal et al., 2010). Interestingly, zebrafish lacking NIPSNAP1 exhibit elevated ROS levels, which correlated with locomotor deficits and a loss of DA neurons (Princely Abudu et al., 2019).

1.2.5.4.2. PINK1/Parkin-independent mitophagy

Over the last years, a significant number of PINK1 and/or Parkin-independent mitophagy pathways have been documented. For instance, loss of iron has been shown to trigger mitophagy in cells lacking *parkin* expression, thus suggesting the activation of PINK1/Parkin independent pathways (Allen et al., 2013). Moreover, recent *in vivo* work in *Drosophila* and mice revealed that PINK1 and Parkin are dispensable for basal mitophagy, indicating that other pathways may compensate for the PINK1/Parkin mitophagy pathway under physiological mitophagy (Lee et al., 2018; McWilliams et al., 2018b). Furthermore, mice lacking PINK1 or Parkin display extremely mild to almost no phenotypes, suggesting that PINK1/Parkin may not be

responsible for all mitophagic processes (Gispert et al., 2009; Perez & Palmiter, 2005). In sharp contrast to the requirement of Parkin translocation and the feed-forward ubiquitination loop, several OMM proteins have been shown to directly interact with the autophagosome through their LC3 domain and thereby linking these two components in a Parkin-independent fashion (Villa et al., 2018).

1.2.5.4.2.1. Receptor-mediated mitophagy

Bcl-2 Interacting Protein 3 (BNIP3) and its related homolog BNIP3-like (BNIP3L) also called NIX, are two well described receptors involved in PINK1/Parkin-independent mitophagy. These two OMM proteins belong to pro-apoptotic Bcl-2 family and interact with the LC3 present on the autophagosome through their LIR domain (Hanna et al., 2012; Rogov et al., 2017). BNIP3 and NIX share 50% homology and are both transcriptionally unregulated during hypoxia, and thus are believed to play a role in hypoxia-induced mitophagy (Matsushima et al., 1998; Sowter et al., 2001). Mitochondria of erythrocytes lacking NIX are clustered and unable to be engulfed in autophagosomes suggesting that NIX is essential for the targeting of mitochondria to the autophagosome (Rodger et al., 2018; Sandoval et al., 2008; Schweers et al., 2007). NIX-mediated mitophagy has been linked to mitochondrial degradation at the terminal stage of the erythroid maturation (Sandoval et al., 2008). The process is of particular relevance as defects in mitophagy at this particular maturation event has been linked to human anaemia (Sandoval et al., 2008). NIX has also been implicated in the differentiation of retinal ganglion cells (RGCs) (Esteban-Martínez et al., 2017). Local hypoxia is induced during RGCs development which triggers the transcriptional activation of NIX and elimination of mitochondria (Esteban-Martínez et al., 2017). This degradation process drives a metabolic shift towards an increase in glycolysis that is essential for cell differentiation (Esteban-Martínez et al., 2017). Finally, work from Melser et al., revealed that NIX-dependent mitophagy can also occur when the mitochondrial energetic activity from OXPHOS is high (Melser et al., 2013). BNIP3 and mitophagy have been linked to the development of cancer, where loss of this protein leads to a reduction of mitophagy, accumulation of damaged mitochondria and elevated ROS, altogether promoting metastasis and cancer propagation (Chourasia et al., 2015).

The OMM-spanning FUN14 domain-containing protein 1 (FUNDC1) is another mitophagy receptor that also contains a LIR motif (Liu et al., 2012). FUNDC1 functions independently of PINK1/Parkin and is involved in mitophagy in response to hypoxia or mitochondrial uncoupling (Liu et al., 2012). The phosphorylation status of FUNDC1 regulates its activity, by blocking its interaction with LC3 (Chen et al., 2014; Liu et al., 2012). In addition to this, Unc-51 like autophagy activating kinase 1 (ULK1) can also phosphorylate FUNDC1, increasing its ability to associate with LC3 and therefore promoting mitophagy (Villa et al., 2018; W. Wu et al., 2014). Finally, in addition to phosphorylation, the membrane-associated RING finger protein 5 (MARCH5), an OMM E3 ligase has been shown to ubiquitinate FUNDC1, resulting in its degradation by the proteasome, preventing excessive and improper mitochondrial degradation (Chen et al., 2017; W. Wu et al., 2014). It is worth mentioning that all these receptors require post-translational modifications in order to regulate their association with LC3 and trigger mitophagy (Di Rita et al., 2018b).

More recently, the activating molecule in Beclin1-regulated autophagy (AMBRA1) was shown to induce both Parkin-dependent and -independent mitophagy (Di Rita, et al., 2018a; Strappazzon et al., 2015). The LIR domain of AMBRA1 can directly interact with LC3 thus bringing damaged mitochondria into autophagosomes and induce mitophagy independently of PINK1 or Parkin (Di Rita et al., 2018a; Strappazzon et al., 2015). However, AMBRA1 has been shown to interact with Parkin and amplify the PINK1/Parkin-mediated mitochondrial clearance during prolonged mitochondrial depolarisation (Strappazzon et al., 2015; Van Humbeeck et al., 2011). While AMBRA1 is not required for Parkin translocation, AMBRA1/Parkin interaction is necessary for the downstream signalling event that triggers the phagophore formation around the depolarised mitochondria (Fimia et al., 2007; Van Humbeeck et al., 2011). The association of the two proteins seems to be crucial for the subsequent mitochondrial clearance (Van Humbeeck et al., 2011). Finally, AMBRA1 overexpression has been shown to trigger and restore mitophagy in fibroblasts from PD patients carrying *PINK1* or *PRKN* mutations (Strappazzon et al., 2015).

1.2.5.4.2.2. Cardiolipin-mediated mitophagy

In addition to the receptors mentioned above, cardiolipin, a phospholipid normally localised on the IMM has been shown to trigger mitophagy. Upon mitochondrial damage, mitochondrial cardiolipin is externalised on the OMM and directly interacts with LC3, resulting in mitochondrial clearance (Chu et al., 2013). These findings illustrate the ability of components of the IMM to directly participate in mitophagy. Like receptor-mediated mitophagy, cardiolipin-induced mitophagy is a PINK1/Parkin-independent mechanism that does not require PINK1 accumulation or the recruitment of Parkin to the OMM (Chu, 2019; Chu et al., 2013).

1.2.5.4.2.3. Other E3 ligases

For a long time, Parkin was thought to be the primary E3 ligase involved in mitophagy. Recently, evidence from three new players has pointed towards additional Parkin-independent mitophagy processes. The mitochondrial E3 ubiquitin protein ligase 1 (MUL1), an E3 ligase located on the OMM, has been shown to be involved in apoptosis, mitochondrial dynamics and to act in parallel to the PINK1/Parkin pathway (Jung et al., 2011; Prudent et al., 2015; Rojansky et al., 2016; Yun et al., 2014). A *Drosophila* study revealed that MUL1 overexpression is able to rescue the strong *Pink1* and *parkin* mutant phenotypes (Yun et al., 2014). Additionally, the removal of *MUL1* in the context of a loss of *Pink1* or *Parkin* enhanced the phenotypes compared with the single mutants, reinforcing the idea that the two pathways act in parallel (Yun et al., 2014). As SUMOylation of Drp1 by MUL1 has been shown to regulate mitochondrial fission, and given that increase fission tends to rescue *Drosophila Pink1/parkin* mutant defects, it is likely that the protective effect of MUL1 on *Pink1/parkin* mutants is the result of MUL1's implication in the regulation of mitochondrial dynamics (Li et al., 2015; Prudent et al., 2015; Yun et al., 2014). Two other studies have linked MUL1, Parkin and PINK1. One study has shown that MUL1 and Parkin act redundantly as downstream targets of PINK1 allowing the elimination of paternal mitochondria in mouse embryos (Rojansky et al., 2016). The other study, recently published, proposed that MUL1 functions upstream of PINK1 in a Parkin-independent fashion (Igarashi et al., 2020). In the latter, Igarashi et al., found that an anticancer drug was able to induce PINK1 stabilization and the subsequent mitophagy, in the absence of mitochondrial depolarization and independently of parkin. This PINK1 stabilization was MUL1-

mediated. The authors suggest that PINK1 stabilization might be related to MUL1 preventing PINK1 import into the IMM, probably due to the positive role of MUL1 in mitochondrial fission (Igarashi et al., 2020). More recently, identification of Ariadne RBR E3 ubiquitin protein ligase 1 (ARIH1), revealed a new PINK1-dependent but Parkin-independent mitophagy pathway, which protects cancer cells against chemotherapy-induced death (Villa et al., 2017). While Parkin is mostly expressed in neurons and absent in cancer cells, ARIH1 seems to be predominantly present in various cancer cells, suggesting different expression patterns and therefore some kind of tissue-specific mitophagy (Villa et al., 2017). Although ARIH1 and Parkin share common substrates, none of the classical Parkin substrates, such as Mfn, appear to be required for ARIH1-mediated mitophagy, suggesting that the type of mitophagy (Parkin or ARIH1-dependent) might be substrate specific (Villa et al., 2017, 2018). Finally, the F-box family protein FBXO7 is another E3 ligase that has been involved in PINK1-Parkin-dependent mitophagy (Burchell et al., 2013). Interestingly, FBXO7 directly interacts with PINK1 and Parkin, and lack of FBXO7 has been shown to prevent Parkin translocation to the OMM upon membrane depolarisation (Burchell et al., 2013). Human FBXO7 overexpression has been shown to rescue *parkin,* but not *Pink1*, mutant phenotypes in *Drosophila*, suggesting that FBXO7 acts downstream of the PINK/Parkin pathway (Clark et al., 2006; Park et al., 2006). Although FBXO7 activity seems to rely on PINK1 activity in flies, FBXO7 was not found to be a PINK1 substrate, highlighting an indirect activation mechanism (Kondapalli et al., 2012). Nutcracker (ntc) has been suggested as the fly ortholog of mammalian FBXO7. However, flies lacking ntc do not resemble *parkin* null mutants, although, like *parkin* mutants, they do display male sterility (Bader et al., 2011). This suggests some differences between ntc and FBXO7.

Altogether evidence from the literature indicate that multiple E3 ligases can act in different forms of mitophagy, but they may differ in their specificity (tissue, stimulus…). However, it is also likely that several E3 ligases may act as a cooperative network to perform mitophagy.

1.2.5.4.3. Investigating mitophagy *in vitro*

Most of the studies aiming to investigate PINK1/Parkin mitophagy have used immortalised cell lines treated with mitochondrial uncouplers or inhibitor of the respiratory chain. However, mitochondrial uncouplers such as CCCP have been shown to depolarise other cellular membranes such as lysosomal membranes and interfere with autophagosomal degradation (Padman et al., 2013). Moreover, neuronal cell cultures treated with CCCP have been shown to undergo apoptosis before Parkin recruitment to the mitochondria occurs, suggesting that results obtained with mitochondrial uncoupler should be interpreted with extra care (Cai et al., 2012). These mitochondrial toxins are also often used at concentrations higher than the ones necessary for mitochondrial membrane depolarisation. The global depolarisation of the entire mitochondrial network that such compounds induce is therefore unlikely to occur in physiological conditions. It is easy to believe that such event would result in more dramatic cellular events. To address this issue, alternative spatiotemporally-controlled insults such as photobleaching with the ROS-mediated mitochondrial Killer-Red (mt-KR) have been developed to increase ROS production in the matrix of a small subset of mitochondria (Wang et al., 2012). Significant induction of mitophagy *in vitro* often requires PINK1 or Parkin overexpression. Indeed, in several cell types used, endogenous levels of Parkin are not sufficient to trigger mitophagy on timescales that are tractable by standard methods of monitoring, even when depolarisation agents are used. In fact, several studies performed in neurons and other cell lines have reported the dispensable role of Parkin for basal mitophagy (Lee et al., 2018; McWilliams et al., 2018b). Therefore, it is presently unclear how these current mitophagy models can translate to more physiological conditions.

1.2.5.4.4. Investigating mitophagy *in vivo*

Despite the tremendous advances accomplished over the last decade, whether PINK1 and Parkin play a major role in mitophagy under physiological conditions and during ageing, and whether defective mitophagy plays a major role in pathogenesis remains under debate. This has been challenged by the discrepancies between PD patients and mouse models, as *Pink1*$^{-/-}$ or *Prkn*$^{-/-}$ mice do not exhibit any locomotor or neurodegeneration phenotypes.

In contrast to mouse models, *Drosophila Pink1* and *parkin* mutants exhibit robust phenotypes, including locomotor defects and DA neuronal loss (Greene et al., 2003; Park et al., 2006). In addition to the neurodegeneration, *Pink1*/*parkin* flies display severe disruption of the flight muscle mitochondrial integrity, affecting their flight ability (Clark et al., 2006; Greene et al., 2003; Park et al., 2006). This muscle degeneration is a development defect already present at adult hatching (Greene et al., 2003; Park et al., 2006). While EM analysis of *parkin* mutant flight muscles revealed no signs of muscle degeneration 96-120h after the puparium formation, 1-day-old *parkin* mutant flight muscles display decreased myofibril density, shorter sarcomere length as well as several TUNEL-positive nuclei, indicating cell death through an apoptotic process (Greene et al., 2003; Park et al., 2006). Similar findings were obtained in *Pink1* mutants. Swollen mitochondria were observed in both *Pink1* and *parkin* mutant flies, accompanied with a severe disintegration of the cristae structure as well as loss of the outer membrane (Greene et al., 2003; Park et al., 2006). Interestingly, Marf knockdown, the Mfn fly ortholog, or Drp1 overexpression are able to rescue the mitochondria swelling, broken cristae and the cell death observed in *Pink1/parkin* mutants. As Parkin directly regulates Marf levels, this flight muscle phenotype may be the result of alterations in mitochondrial dynamics during development of this particular tissue (Deng et al., 2008; Ziviani et al., 2010).

Although there is substantial evidence supporting the role of mammalian PINK1 and Parkin in mitophagy, it remains unclear how the strong phenotypes in flies relate to defects in the mitophagy process. A proteomic assay conducted in *Drosophila* by Vincow et al., provided new evidence on Pink1/parkin mitochondrial degradation and informed on turnover rate *in vivo* (Vincow et al., 2013). By feeding deuterated leucine

to adult flies, the half-lives of several mitochondrial and non-mitochondrial proteins were simultaneously monitored using mass spectrometry analysis (Vincow et al., 2013). *parkin* null mutants displayed prolonged half-lives for many mitochondrial proteins, in particular the ones related to mitochondrial respiratory chain subunits (Vincow et al., 2013). This work provided compelling evidence for a role of parkin and Pink1 in mitophagy *in vivo*. Although similar results were obtained with *Pink1* and *Atg7* mutants, the turnover of respiratory chain components was more affected in *Pink1* and *Parkin* null than *Atg7* mutants (Vincow et al., 2013). This suggests that the degradation of these specific proteins may be Pink1/parkin-dependent but -independent of the autophagy machinery (Corti, 2019).

Other groups have tried to investigate the existence of PINK1/Parkin-mediated mitophagy *in vivo*. As *Pink1* and *Prkn* knockout (KO) mice do not display any behavioural deficits or signs of neurodegeneration, efforts have been put towards stimulating the pathway using mitochondrial stressors, such as the mtDNA mutator mouse. The rational came from the observation that DA neurons of PD patients and aged individuals are highly prone to accumulation of mtDNA deletions (Bender et al., 2006; Kraytsberg et al., 2006). The mtDNA mutator mouse carries a mutation in the proofreading domain of the DNA polymerase-γ responsible for mtDNA replication (Kujoth et al., 2005; Pickrell et al., 2015). Despite lacking any signs of neurodegeneration, these mice exhibit a progressive accumulation of mtDNA mutations, leading to a premature ageing and shorter lifespan (Kujoth et al., 2005). Interestingly, *mutator:Prkn*$^{-/-}$ combination results in a significant loss of DA neurons in the midbrain and motor phenotypes, suggesting that Parkin may prevent degeneration of these neuronal cells bearing highly dysfunctional mitochondria (Pickrell et al., 2015). Mass spectrometry analysis of cortical brain tissues revealed higher levels of pSer65-Ub in the mutator mouse and *mutator:Prkn* KO samples compared to wild-type (WT), consistent with Parkin functioning downstream of PINK1 (Pickrell et al., 2015). Although this work reinforced the involvement of PINK1/Parkin in the mitophagy process, these findings may be the result of a synthetic phenotype due to the strongly-induced mitochondrial dysfunction occurring in *mutator:Prkn* KO mice (Pickrell et al., 2015). Others have addressed the relevance of PINK1/Parkin-mediated mitophagy using similar approaches. *Prkn*$^{-/-}$ mice have been crossed with different transgenic models, including the MitoPark mouse, that lacks the mitochondrial transcription factor

A (TFAM) gene resulting in mtDNA depletion (Sterky et al., 2011). While, MitoPark mice develop PD-like phenotypes, including DA neuron loss and locomotor deficits, *Prkn* deficiency does not worsen this phenotype (Sterky et al., 2011). In contrast, and consistent with the mutator mouse, the combination of *Prkn* loss with a mouse carrying a mutated version of Twinkle, a helicase involved in mtDNA replication, exacerbated the existing PD-like phenotype of the Twinkle mutated mice (Song et al., 2017). Work in adult *Drosophila* muscle suggested that activation of the Pink1/Parkin pathway results in a decrease in mtDNA deletion (mtDNAΔ) (Kandul et al., 2016). Despite suggesting that Parkin may be important for the clearance of mitochondria harbouring high levels of mtDNA, none of these studies provided direct evidence of the implication of the PINK1/ Parkin axis in mitophagy and some other functions or processes could account for the synthetic phenotypes observed.

1.2.5.4.4.1. Tools to visualise mitophagy *in vivo*

For many years, one of the main limitations to studying mitophagy *in vivo* has been the lack of suitable reporters. Therefore, extensive effort has been put towards establishing new systems that could be easily adapted to animal models to visualize mitophagy *in vivo*.

Based on the pre-existing and widely used autophagy reporter, the mCherry-GFP-LC3 system, mtRosella was originally developed in yeast and later adapted to *C. elegans* and *Drosophila* to follow mitophagy *in vivo* (Dan et al., 2020; Edenharter et al., 2018; Rosado et al., 2008; Schiavi et al., 2015). The mtRosella reporter is targeted to the IMM and combines the properties of DsRed fused to a pH-sensitive GFP, named pHluorin (Rosado et al., 2008). Under normal conditions, the signal from both fluorophores is visualised whereas during mitophagy, the acidic pH of the autolysosome/lysosome compartments results in the quenching of the pHluorin, leaving only the signal from the DsRed (Figure 1.8) (Edenharter et al., 2018; Rosado et al., 2008).

Another model named MitoTimer, was also developed by Terskikh et al, as a mutant of DsRed (DsRed-E5) targeted to the mitochondrial matrix (Terskikh et al., 2000). Mitochondria expressing the MitoTimer reporter transition from a green to red fluorescence over a period of 48h, allowing time-dependent tracking of mitochondrial content (Figure 1.8) (Terskikh et al., 2000). Mitophagy is monitored by measuring the rate of disappearance of the MitoTimer red signal (Gottlieb & Stotland, 2015). In addition to being extensively used in cultured cells, the reporter has been adapted to *Drosophila*, *C. elegans* and mouse models to assess mitochondrial turnover, protein import or just investigating mitochondrial biology (Ferree et al., 2013; Laker et al., 2014).

The mito-QC reporter was developed by Allen et al. (Allen et al., 2013). It uses a tandem-tagged mCherry-GFP fusion protein targeted to the OMM via the C-terminus of FIS1 (residues 101-152). At steady state, the neutral pH of the cytosol allows the fluorescence of both GFP and mCherry, giving a yellow signal when both channels are merged (Allen et al., 2013). Upon mitophagy, mitochondria are targeted to the

lysosomes where the GFP is quenched by their acidic pH (Figure 1.8). As mitochondria are being degraded within the lysosomes, these mCherry-positive, GFP-negative entities are labelled in the form of 'red-only puncta', called mitolysosomes, which act as a proxy end-point readout (Allen et al., 2013). The mito-QC has been adapted to many models, including *Drosophila* and mice (Lee et al., 2018; McWilliams et al., 2016).

Katayama et al., have developed the mt-Keima reporter that exploits the properties of the Keima protein, a coral-derived acid-stable and pH-sensitive fluorescent molecule, which is targeted to the mitochondrial matrix using a COX VIII MTS (Katayama et al., 2011). At steady state conditions (pH 7), the excitation of the shorter wavelength (458 nm, green) predominates and mitochondria fluoresce green. However, at the lysosomal acidic pH (pH 4), mainly the longer excitation wavelength (561 nm, red) dominates, allowing qualitative assessment of mitochondria delivery to lysosomes (Figure 1.8) (Sun et al., 2015). *Drosophila* and mouse models expressing the mt-Keima reporter have later been developed to monitor mitophagy *in vivo* (Cornelissen et al., 2018; Lee et al., 2018; Sun et al., 2017).

More recently, a new mitophagy reporter termed, mito-SRAI (signal-retaining autophagy indicator) was developed by Katayama et al. Similar to the mt-Keima, the reporter is targeted to the mitochondrial matrix using a COX VIII MTS (Katayama et al., 2020). The reporter comprises a yellow-fluorescent protein (YFP), YPet, fused to a protein named Tolerance of Lysosomal Environments (TOLLES), that is resistant to lysosomal proteases (Katayama et al., 2020). The reporter relies on the fluorescence resonance energy transfer (FRET) mechanism whereby TOLLES act as the FRET donor and YPet the FRET acceptor. Therefore, in the acidic environment of the lysosomes, the yellow fluorescence disappears as YPet is protease-sensitive, while the signal of the TOLLES protein remains intact (Figure 1.8) (Katayama et al., 2020). Like the mt-Keima, the mito-SRAI is also a ratiometric sensor of mitophagy, however the advantage of this new reporter is its compatibility with fixation procedures (Katayama et al., 2020). By using the adeno-associated virus (AAV) system, the mito-SRAI was expressed in neurons of mouse midbrains to follow mitophagy (Katayama et al., 2020).

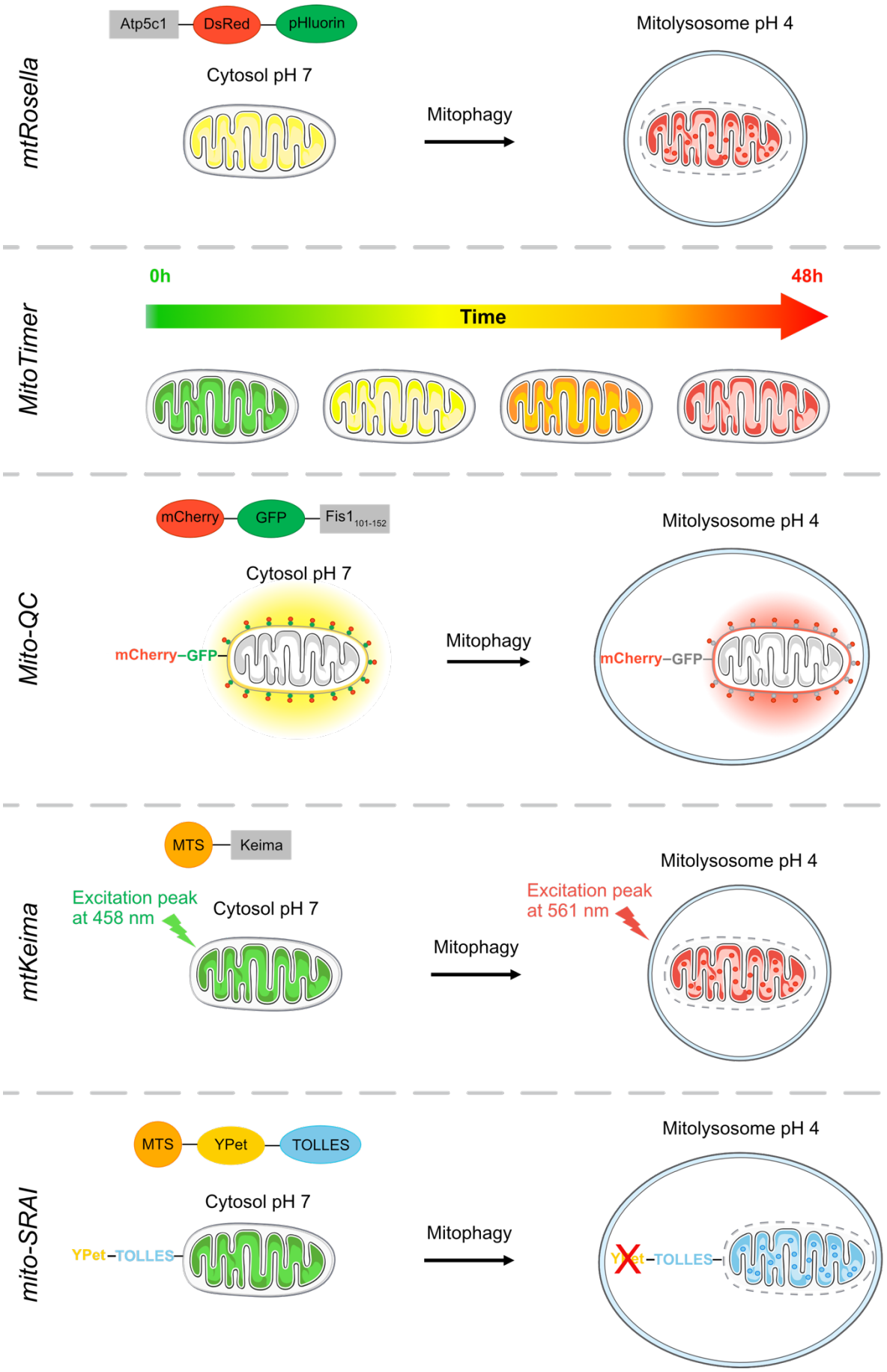
mtRosella
Atp5c1
DsRed
pHluorin
Cytosol pH 7
Mitophagy
Mitolysosome pH 4
MitoTimer
0h
48h
Time
Mito-QC
mCherry
GFP
Fis1 101-152
Cytosol pH 7
mCherry–GFP
Mitophagy
Mitolysosome pH 4
mCherry–GFP
mtKeima
MTS
Keima
Excitation peak at 458 nm
Cytosol pH 7
Mitophagy
Mitolysosome pH 4
Excitation peak at 561 nm
mito-SRAI
MTS
YPet
TOLLES
Cytosol pH 7
YPet–TOLLES
Mitophagy
Mitolysosome pH 4
YPet–TOLLES

Figure 1.8. Schematic representation of the reporters used to monitor mitophagy
The mtRosella reporter is targeted to the IMM and uses the properties of DsRed fused to pHluorin. Under normal conditions, the signal from DsRed and pHluorin can be visualised whereas during mitophagy, the lysosomal acidic pH results in the quenching of the pHluorin, leaving only the signal from the DsRed. MitoTimer relies on a modified version of DsRed (DsRed-E5) targeted to the mitochondrial matrix, and allows the monitoring of mitochondria over a period of 48h. Over this period, the fluorescence shifts from green to red. The mito-QC consists of a mCherry-GFP tag targeted to the OMM. At steady state, cytosolic mitochondria fluorescence green and red. However, when damaged mitochondria are engulfed in lysosomes, the acidic pH quenches the GFP, leading to a red signal only in the form of 'red-only puncta' called mitolysosomes. The mt-Keima is targeted to the mitochondrial matrix. In the cytosol (pH 7), excitation of the 458 nm wavelength predominates, however, when mitochondria are delivered to the lysosomes (pH 4), the Keima protein is mainly excited by light peaking at 561nm. Mito-SRAI is a tandem fusion of YPet and TOLLES targeted to the mitochondrial matrix. The acidic pH of the lysosomes results in the degradation of the YPet leaving only the TOLLES signal.

The investigation of mitophagy *in vivo* quickly escalated with the generation of animal models expressing the mito-QC and the mt-Keima (Cornelissen et al., 2018; Lee et al., 2018; McWilliams et al., 2018b; Sun et al., 2015). The transgenic expression of these reporters in mice and *Drosophila* revealed widespread mitophagy under basal conditions during development and in adulthood, with some tissues including the brain exhibiting higher mitochondrial turnover than others, such as muscles (Cornelissen et al., 2018; Lee et al., 2018; Sun et al., 2015). Significant decrease of the mitophagy signal was observed following deletion of key autophagy genes, such as *Atg5*, suggesting that these reporters are likely to report autophagy-dependent events such as PINK1/Parkin-mediated mitophagy (Lee et al., 2018). When combining *Pink1* and *parkin* mutant flies with the mito-QC reporter, Lee et al., found no change in mitophagy levels, even in the two most disrupted tissues, flight muscles and DA neurons, suggesting that Pink1/parkin are not required for basal mitophagy in *Drosophila* (Lee et al., 2018). However, a similar study from the Vandenberghe group, performed with the mt-Keima, revealed an age-dependent increase in mitophagy, that was Pink1/parkin-dependent, indicating that the two proteins may be required for mitophagy during aging (Cornelissen et al., 2018). Whether or not mitophagy is an age-dependent process still remains elusive as some groups have reported increased levels of mitophagy with age, while other have found opposite results (Cornelissen et al., 2018; McWilliams et al., 2018b; Sun et al., 2015). Similar work was performed in mito-QC

and mt-Keima mouse models. Combination of the mito-QC mouse with loss of *Prkn* or *PINK1* led to similar results to the *Drosophila*, supporting the idea that the two proteins are dispensable for basal mitophagy (McWilliams et al., 2018a, 2018b). Additionally, these findings suggest that other MQC pathways may be upregulated in the absence of PINK1 or Parkin and compensate for the loss of these proteins (McWilliams et al., 2018a, 2018b). More recently, an increase in mitophagy was observed in mice expressing the mt-Keima reporter following exhaustive exercise, and this was accompanied by an increase in the pSer65-Ub detected by mass-spectrometry analysis in heart samples (Sliter et al., 2018). Interestingly, no increase in the mt-Keima signal or pSer65-Ub levels were visible in the absence of *PINK1*, suggesting that activation of PINK1/Parkin mitophagy may occur only under specific stimuli (Sliter et al., 2018). Further work from Sliter et al., also revealed that multiple inflammatory cytokines were upregulated in *Pink1*$^{-/-}$ and *Prkn*$^{-/-}$ mice following exhaustive exercise, which correlated with fever in these animals, illustrating some activation of the immune system (Sliter et al., 2018). This will be discussed later in more details.

Despite tremendous work trying to better understand the mitophagy process, many unanswered questions still remain. It will be interesting to know how much mitophagy contributes to the general MQC, especially in tissues highly affected in PD, such as DA neurons. Furthermore, although exhaustive exercise seems to be a physiological trigger for mitophagy in heart tissues, it will be relevant to understand if different stimuli differently impact mitophagy depending on the tissues – are neurons more sensitive to decreased levels of mitophagy? Finally investigating the mechanisms that regulate basal versus triggered PINK1/Parkin-mediated mitophagy will help understanding the contribution of the pathway to PD pathophysiology.

1.2.5.5. Mitochondria-derived vesicles (MDVs)

MDVs were discovered in 2008 and proposed as an alternative MQC, that allows the removal of small portions of a mitochondrion in the form of vesicles, thus leaving the rest of the organelle intact (Neuspiel et al., 2008). They rely on a tightly controlled vesicular budding process, independent of the fission machinery, where parts of the mitochondrion are ejected from the organelle. Electron microscopy of standard immunogold staining of one of the cargo proteins revealed small and rounded vesicles of around 100 nm of diameter, pinching off the mitochondrion (Neuspiel et al., 2008; Soubannier et al., 2012a; Sugiura et al., 2014). These isolated mitochondrial vesicles later fuse with various other organelles, such as peroxisomes or lysosomes, depending on the stimulus (Neuspiel et al., 2008). The formation of MDVs is independent of the autophagy machinery as they are distinct from the classical autophagic engulfment and occur in the absence of Atg5 or LC3 proteins (McLelland et al., 2014; Soubannier et al., 2012a). An important feature of MDVs is their cargo selectivity which is highly dependent on the mitochondrial stressor. MDVs were first identified as a mechanism to transport vesicles budding off the mitochondria to the peroxisomes. Immunogold staining of one of the main cargo protein MUL1, revealed the presence of double-membraned vesicles (Braschi et al., 2010). While the main function of the vacuolar protein sorting 35 (Vps35) is to be part of the retromer complex that participates in the recycling of proteins from endosomes to the *trans*-Golgi complex or back to the plasma membrane, the protein has been shown to participate in the MDVs formation and their targeting to the peroxisomes (Braschi et al., 2010). Interestingly, mutations in *Vps35* have been linked with some forms of PD, although as yet, its implication in the disease has not been fully understood yet (Sugiura et al., 2014; Zimprich et al., 2011). To further reinforce the idea of cargo selectivity, different stimuli were proven to trigger the formation of MDVs with contrasting content. For instance, antimycin A treatment, a complex III inhibitor that generates high level of ROS within the mitochondria, induces the formation of double-membraned MDVs enriched in mitochondrial matrix proteins but deprived of the OMM protein TOM20 (McLelland et al., 2014). In contrast, xanthine oxidase/xanthine (XO/X) treatment leads to the generation of TOM20 positive single-membraned vesicles that lack matrix or IMM markers (Neuspiel et al., 2008; Soubannier et al., 2012b). These vesicles transport highly oxidised mitochondrial proteins to lysosomes for their degradation (Soubannier et al., 2012a, 2012b).

Although these particular MDVs seem to be upregulated under oxidative stress, they can also be observed under basal conditions, suggesting that MDVs also allow the removal of proteins from actively respiring mitochondria (Sugiura et al., 2014). Work from Soubannier et al., has shown that MDVs can incorporate proteins from the ETC, including complex II, III and IV, while others such as complex I, V or mtDNA nucleoids seem to be excluded probably due to size limitations (Soubannier et al., 2012b). These findings indicate that MDVs can form without the requirement of mitochondrial depolarisation or other stimuli, suggesting that their formation sits upstream of other MQC, such as mitophagy (Soubannier et al., 2012b). Moreover, the formation of MDVs targeted to the lysosomes appears to be on a scale of tens of minutes to an hour, whereas mitophagic clearance of mitochondria is a considerably lengthier process occurring over 12-24h (McLelland et al., 2014). The formation of MDVs destined for lysosomes requires the presence of PINK1 and Parkin (McLelland et al., 2014). These double-membrane MDVs can be formed in response to antimycin A treatment and contain mitochondrial matrix proteins such as pyruvate dehydrogenase (PDH) but are devoid of the OMM cargo protein TOM20 (McLelland et al., 2014). While this process is Drp1-independent, the recruitment of the syntaxin17 (Stx17) protein is necessary for the fusion of the MDV with lysosomes (McLelland et al., 2014). Although it is unlikely that Syntaxin17 directly interacts with PINK1 or Parkin, Syntaxin17 may be recruited to the sites of MDVs formation through pSer65-Ub, the main substrate that PINK1 phosphorylates upon mitochondrial depolarisation (Kazlauskaite et al., 2014; McLelland et al., 2016). MDV formation mechanism is described as follow: (1) excessive ROS production or protein misfolding leads to aggregation of unfolded/highly oxidised proteins in the mitochondrial matrix, (2) the oxidation of cardiolipin generates phosphatic acid which allows the mitochondrial membrane to enter a curvature process, (3) aggregation of damaged proteins at the membrane induces a localised failure of the import machinery, which is aggravated by cardiolipin oxidation, (4) the blockade of the import machinery results in PINK1 accumulation, phosphorylation of free Ub and Parkin Ubl domain, leading to recruitment and activation of Parkin, (5) finally, a small vesicle engulfing the oxidised/aggregated proteins is formed and released from the mitochondria into the cytoplasm. Although still unidentified, several proteins are probably involved in this last step (Sugiura et al., 2014).

More recently, MDVs have been implicated in mitochondrial antigen presentation (MitAP) (Matheoud et al., 2016). Under cellular stress, such as exposure to lipopolysaccharides (LPS), antigens can be extracted from the mitochondria, transported in MDVs to lysosomes, processed to peptides and presented on major histocompatibility complex (MHC) class I molecules at the cell surface of macrophages and dendritic cells, which inevitably results in the activation of adaptive immune responses (Matheoud et al., 2016). However, in normal conditions, PINK1 and Parkin induce the proteasomal degradation of sorting nexing 9 (Snx9), a protein required for the formation of this particular type of MDVs, thus inhibiting any potential immune response (Matheoud et al., 2016; Roberts et al., 2016). Interestingly, while only immune cells only present MHC class II molecules, all nucleated cells can engage with the MHC class I pathway, suggesting that this MHC class I peptide presentation could occur in DA neurons (Matheoud et al., 2016). The findings from Matheoud et al., suggest that loss of PINK1 or Parkin can result in overactivation of MitAP, which in turn could trigger auto-immune mechanisms in PD (Roberts & Fon, 2016). In addition, it is tempting to extrapolate that upon Parkin loss, MitAP activation may be responsible for the cytotoxic T cells activation which would eventually result in neuronal cell death (Grünewald et al., 2019). The identification of MitAP and the implication of PINK1/Parkin in the repression of this mechanism has opened new perspectives on the role of immunity and auto-immune responses in PD.

1.3. Inflammation and PD

Multiple lines of evidence have indicated that a potential dysfunction of the immune system may be linked to PD. However, whether this aberrant phenomenon contributes to or is a consequence of the disease, and in particular to the neuronal loss, remains to be elucidated. Individuals with autoimmune disorders, such as multiple sclerosis, have been shown to have a higher risk of developing PD, suggesting that autoimmunity may be involved in PD pathogenesis (Li et al., 2012). GWAS studies revealed that PD-associated variants in genes such as *LRRK2* and *MAPT* can predispose to autoimmune diseases such as Crohn's disease, an inflammatory bowel disorder (Raj et al., 2014; Witoelar et al., 2017). The latter illustrates that there may be some overlapping genetic variations associated with both PD and autoimmune diseases, affecting the overall immune function in both disorders (Raj et al., 2014). Interestingly, genetic polymorphisms in the *PARK2* human gene have been associated with an increase susceptibility to intracellular pathogens such as *Salmonella enterica* and *Mycobacterium tuberculosis*, (Manzanillo et al., 2013). Work from Manzanillo et al., demonstrated that *parkin*-deficient flies exhibit a significantly shortened lifespan following pathogen infection, due to their inability of getting rid of the intracellular pathogens through autophagic clearance. The group revealed similar findings in *Prkn*$^{-/-}$ mice, suggesting a role of Parkin in innate immunity (Manzanillo et al., 2013). Several examples illustrate that activation of immune responses correlates with the downregulation of *PINK1*/*PRKN*. Firstly, in the absence of *Pink1* or *Prkn*, MitAP is no longer suppressed, which results in the activation of mitochondria-specific cytotoxic CD8+ T cells in the brain, driving the DA neuronal loss (Matheoud et al., 2019). Secondly, elevated levels of pro-inflammatory cytokines, including IL-6 and IL-1β, have been confirmed by analysis of post-mortem brains and blood cytokine concentrations of PD patients (Maitra et al., 2019; Qin et al., 2016). Furthermore, elevated blood levels of IL-6 have been associated with an increased risk of developing PD (Chen et al., 2008). In addition, work by Scalzo et al., has shown that IL-6 serum levels also correlated with the physical and cognitive decline observed in PD patients (Scalzo et al., 2010). Finally, several immune-related genes are upregulated when observed by transcriptional profiling in *Drosophila Pink1*/parkin mutants and in mouse models of PD following MPTP treatment (Greene et al., 2005; Shen et al., 2020; Tufi et al., 2014).

These studies highlight the upregulation of several immune-related genes in animal models of PD and PD patients. Thirdly, microglia activation, the local macrophages of the brain, has been reported in post-mortem brains of PD patients and toxin-based animal models of PD (Arimoto & Bing, 2003; Cicchetti et al., 2002; Gao et al., 2003c; Langston et al., 1999; McGeer et al., 1988; Zhao et al., 2007). While their primary function is the clearance of debris through phagocytic activity, overactivation of microglia can exert toxic effects on DA neurons resulting in their subsequent loss, by production of interferons (IFNs), nitric oxide and tumour necrosis factor (TNF) (Harms et al., 2017; Mount et al., 2007; Sun et al., 2018). Fourthly, infiltration of lymphocyte T-cells across the blood brain barrier have been reported in post-mortem studies of PD patients and animal models of PD, including MPTP and 6-OHDA, but whether or not this invasion is responsible for PD pathogenesis remains unknown, although it does seem to correlate with DA neuronal loss (Brochard et al., 2009; Carvey et al., 2005; Liu et al., 2017; Sommer et al., 2018; Zhao et al., 2007). Finally, increasing amount of evidence suggests a link between PD and the gastrointestinal tract. In fact, chronic constipation is a common feature of PD patients and often appears decades prior to the motor symptoms (Edwards et al., 1992). Post-mortem studies have shown that aggregates of α-synuclein are often found in the myenteric plexus of the enteric nervous system, which led Braak and his team to hypothesise that the gastrointestinal tract may be the starting point of the PD pathology, that would later propagate to the brain (Braak et al., 2003, 2006; Gelpi et al., 2014; Wakabayashi et al., 1988). Gastrointestinal infections, bacterial or viral, have been shown to increase the risk of developing PD later in life (Nerius et al., 2019; Sun & Shen, 2018). In addition, analysis of stool samples from PD patients revealed a significant alteration in their gut microbiota composition (Lin et al., 2019).

Altogether, these studies, along with a plethora of literature, suggest a role of inflammation, in the brain or in the periphery in the PD pathogenesis. However, whether this is a cause or a consequence of the disease remains to be elucidated.

1.3.1. Mitochondria: key players in inflammation

1.3.1.1. Lessons from toxin-induced PD models

Inflammation has been reported in many mitochondrial toxin-induced PD models,

suggesting that mitochondrial dysfunction may be involved in the aberrant immune response observed in PD. Mitochondrial stresses can induce the release of damaged-associated molecular patterns (DAMPs), such as ROS and oxidised or mutated mtDNA, which activate the inflammatory cytokines and downstream immune signalling cascades (Newman & Shadel, 2018; Wilkins et al., 2016). In fact, rotenone has been shown to activate microglia and the subsequent secretion of pro-inflammatory cytokines, resulting in the loss of DA neurons (Main et al., 2017; Mount et al., 2007). Work by Main and colleagues have further demonstrated that blockade of interferon alpha and beta receptor subunit 1 (IFNAR1), and downstream JAK/STAT signalling, abrogate the locomotor deficits, DA loss, microglia activation and decrease the pro-inflammatory cytokine levels occurring in MPTP mouse models of PD (Main et al., 2017). More recently, transcriptomic profiling of *Drosophila* samples revealed the upregulation of genes involved in innate immune responses following paraquat treatment (Maitra et al., 2019). The expression of several of these genes is regulated by the transcription factor Relish, an ortholog of the nuclear factor kappa beta (NF-κB). Interestingly, DA neuron specific knockdown of *Relish* rescues DA neuron loss, shorter lifespan and the climbing defects observed in flies treated with paraquat (Maitra et al., 2019). Consistent with these findings, NF-κB inhibition was shown to abrogate microglia activation, locomotor deficits and DA neuronal loss observed in mice exposed to MPTP treatment (Ghosh et al., 2007). Interestingly, the pro-inflammatory cytokine TNF-α, which is predominantly synthetised by microglia, was also found elevated in PD patients, MPTP and 6-OHDA animal models (Barcia et al., 2005; McCoy et al., 2006; Mogi et al., 1999; Shen et al., 2020; Sriram et al., 2002). Finally, pharmacological blockade of TNF-α or loss of TNF-α receptor (TNFR) in mice was shown to protect DA neurons against 6-OHDA and MPTP toxicity (McCoy et al., 2006).

These results illustrate that the inflammatory processes observed in PD patients are also present in the toxin-induced animal models of PD, further reinforcing the role of pro-inflammatory cytokines, and general inflammation, in PD pathogenesis (Shen et al., 2020).

1.3.1.2. mtDNA and the c-GAS/STING pathway: a source of inflammation

Mitochondrial stress induced by viral infection and depletion of TFAM, the key mediator of mitochondrial transcription, promotes mtDNA release in the cytosol which in turn activates the c-GAS/STING pathway and induces the production of type I IFNs (West et al., 2015). The c-GAS/STING pathway mediates innate immune signalling in response to cytosolic bacterial or viral DNA derived from pathogens (West et al., 2015). In brief, exogenous DNA binds to and activates c-GAS, which then produces cyclic guanosine monophosphate-adenosine monophosphate (2', 3'-cGAMP) dinucleotides that directly interact with STING and activate a downstream signalling cascade, ultimately culminating in the induction of IFNs and cytokines (Ishikawa & Barber, 2008; Xiao & Fitzgerald, 2013). Besides mtDNA depletion, TFAM heterozygous KO induces altered mtDNA organisation as well as impaired mtDNA damage repair capacity, which altogether provide a robust model for mtDNA stress (West et al., 2015). Work by West et al., suggested that mtDNA can act as an intrinsic signal that can trigger an innate immune response and potentiate type I IFN gene expression (West et al., 2015). A recent study from Wilkins and colleagues further reinforced the idea that mitochondrial content can act as DAMPs and trigger neuroinflammation (Wilkins et al., 2016). They showed that injections of either isolated mitochondria or mtDNA in mouse brains, increased some markers of inflammation, including NF-κB (Wilkins et al., 2016). Additionally, injection of whole mitochondria in mouse brains was also shown to increase biomarkers associated with AD, such as Amyloid-β(Aβ)-42 and amyloid precursor protein levels, suggesting that other mitochondrial content, beside mtDNA, can induce brain inflammation (Wilkins et al., 2016).

These results strongly reinforce the role of inflammation in PD pathogenesis and are consistent with the observation that anti-inflammatory treatments reduce the risk of developing PD (Tan et al., 2020). Overall, these results suggest that elevated levels of inflammation can be detrimental, rather than protective, in the context of PD. However, the relationship between increased levels of circulating mtDNA and defective mitophagy remains unclear and the mechanisms underlying the escape of mtDNA from the mitochondria are still poorly understood.

1.3.1.3. Mitochondrial content and activation of the inflammasome

Nucleotide binding domain and leucine-rich repeat pyrin 3 domain (NLRP3) (also known as NALP3) is one the best characterised inflammasomes. NLRP3 is a cytosolic pattern recognition receptor (PRR) involved in the recognition of pathogen-associated molecular patterns (PAMPs) and DAMPs, that results from intracellular or extracellular insults (Gross et al., 2011; Karin & Clevers, 2016; Zhong et al., 2018). NLPR3 inflammasome activation occurs in a two-step mechanism. In the initial step, named 'priming': PAMPs/DAMPs bind to specific receptors, including those of the NOD-like receptor (NLR) family and Toll-like receptor (TLR). For instance, LPS can be recognised by the receptor protein TLR4 present on the macrophage surface (Gross et al., 2011; Karin & Clevers, 2016; Zhong et al., 2018). This results in the activation of the NF-κB, which regulates the expression of NLRP3, pro-IL-1β and pro-IL-18 (Gross et al., 2011; Karin & Clevers, 2016; Zhong et al., 2018). On the second step, additional agonists, such as damaged mitochondria, display signals, including mtROS, mtDNA, and cardiolipin, which activate the NLRP3 complex formation at the interphase between the ER and mitochondria. NLRP3 then recruits the apoptosis-associated speck-like protein containing C-terminal caspase recruitment domain (CARD) (ASC) and pro-caspase-1 (Zhong et al., 2018). Assembly of the complex results in the auto-cleavage and activation of caspase-1 which leads to the maturation and secretion of the pro-inflammatory cytokines IL-1β and IL-18, both participating in tissue damage repair (Martinon et al., 2002). There is now strong evidence that a close relationship exists between NLRP3 and mitochondria. Indeed, ROS and the presence of oxidised mtDNA in the cytosol have been shown to activate NLRP3 (Nakahira et al., 2011; Zhou et al., 2011). Several studies have reported that mitophagy/autophagy blockade results in increased ROS levels due to the accumulation of damaged mitochondria and translocation of mtDNA into the cytosol, which in turn boosts NLRP3 activation and the downstream maturation of pro-inflammatory cytokines (Nakahira et al., 2011; Saitoh et al., 2008; Zhou et al., 2011). The assumption is that non-specific damage to the mitochondria somehow results in aberrant ROS production (Murphy, 2018). Additionally, blockade of complex I and complex III with rotenone and antimycin A, respectively, was reported to increase ROS levels and activation of the NLRP3 inflammasome, further reinforcing the pivotal role of mitochondria in NLRP3-mediated inflammation (Zhou et al., 2011). Furthermore, specific inhibition of mitochondrial ROS

with chemical scavengers suppressed the inflammasome response, further illustrating the role of elevated ROS levels in the inflammasome activation (Pétrilli et al., 2007). Shimada et al., have shown that ROS production results in the oxidation of mtDNA, which are subsequently released in the cytosol and act as an NLRP3 agonist (Shimada et al., 2012). More recently, Zhong et al., have demonstrated that the mtDNA responsible for the inflammasome activation is in fact newly synthesised, and then oxidised by ROS within the mitochondria, prior to its release into the cytosol (Zhong et al., 2018). Lack of TFAM specifically in mouse immune cells results in loss of mtDNA and defective activation of the inflammasome, supporting the idea that mtDNA is essential for NLRP3 activation (Zhong et al., 2018). Zhong and colleagues' work suggests that this newly synthesised mtDNA is produced by conventional mtDNA synthesis, however, why this newly-formed mtDNA is more susceptible to oxidative damage remains unknown (Zhong et al., 2018). The authors suggest the formation of a pore within the IMM, while others have proposed the implication of the mPTP, that has been shown to open upon elevated ROS (Zhong et al., 2018). Release of mtDNA could also occur through MDVs as these have been shown to carry oxidised proteins to the lysosomes (Murphy, 2018; Soubannier et al., 2012b). Interestingly, inflammasome activation has been shown to be negatively regulated by Parkin-dependent mitophagy (Zhong et al., 2016). Indeed, NF-κB seems to not only regulate NLRP3 and pro-IL-1 expression, but also the mitophagy receptor p62 (Zhong et al., 2016). Furthermore, *Prkn* knockdown in mice results in upregulated levels of NLRP3 associated with the downregulation of the inflammasome negative regulator, A20 (Mouton-Liger et al., 2018). Finally, it is important to mention that the *Drosophila* genome lacks *NLR* genes, only Caspase-1 is conserved. Consequently, the implication of the NLRP3 inflammasome in PD pathogenesis cannot be investigated in *Drosophila*.

1.3.1.4. Lipopolysaccharides, inflammation and PD

Multiple lines of evidence from the literature support that LPS treatment can induce a PD-like pathology, in particular the vulnerability of DA neurons (Arimoto & Bing, 2003; Frank-Cannon et al., 2008; Gao et al., 2003a, 2003b, 2003c; Sharma & Nehru, 2015). Evidence from rodent models suggest that LPS injections in the substantia nigra result in motor deficits, reduced dopamine levels, microglial inflammation and increased pro-inflammatory cytokine levels (Sharma & Nehru, 2015). Indeed, chronic low-dose LPS treatment in the substantia nigra of rat brains, has been shown to induce microglia activation followed by progressive and selective loss of DA neurons (Gao et al., 2002). Similar results were observed in MPTP and rotenone rodent models. While low levels of MPTP or rotenone induce minimal neurotoxicity, the combination of these toxins with LPS injections triggers microglia stimulation, leading to ROS release and subsequent death of DA neurons (Gao et al., 2003a, 2003c). Interestingly, while *Pink1*$^{-/-}$ or *Prkn*$^{-/-}$ mice do not display any of neurodegeneration or locomotor deficits, intraperitoneal LPS injections over a prolonged period of 3 months in *Prkn* mutant mice have been reported to induce DA neuronal loss as well as slight locomotor deficits (Frank-Cannon et al., 2008). This was associated with increased levels of TNF in the midbrain and cortex of LPS injected *Prkn*$^{-/-}$ mice (Frank-Cannon et al., 2008). Although the exact mechanism by which Parkin regulates pro-inflammatory cytokines and inflammation in general remains unknown, this elegant study from Frank-Cannon and colleagues strongly suggests a specific role of Parkin in neuroprotection, especially in response to inflammatory agents such as LPS (Frank-Cannon et al., 2008). Similar findings were obtained from LPS injections in *Pink1* null-mice (Akundi et al., 2011). *Pink1*$^{-/-}$ mice challenged with LPS treatment exhibit lower levels of DA and increased expression of pro-inflammatory cytokine genes, such as TNF-α and IL-1β (Akundi et al., 2011).

1.3.1.5. Intestinal dysbiosis and gut-derived inflammation

It is now well-established that in addition to neurological symptoms, PD patients also exhibit alterations in their intestinal microbiome, dysbiosis, as well as intestinal inflammation (Lin et al., 2019). Interestingly, gastrointestinal abnormalities often precede the locomotor deficits by many years (Sampson et al., 2016). In addition, analysis of the stool samples from PD patients revealed a significant alteration in their gut microbiota composition, which correlated with a change in circulating cytokine profiles, including IL-6 and TNF-α (Devos et al., 2013; Lin et al., 2019). Further evidence linking gut inflammation to PD come from an elegant study by Villarán et al., where they showed that LPS injection in the substantia nigra of rats with ulcerative colitis, further enhanced the increased IL-6 and TNF-α and DA neuronal loss seen with LPS treatment alone (Villarán et al., 2010). Interestingly, infections from specific genera of gut microbiota, such as *Helicobacter pylori*, are more likely to occur in PD patients and often result in the worsening of the motor symptoms (Dardiotis et al., 2018; McGee et al., 2018). Mice treated with rotenone have been shown to exhibit a PD-like phenotype, as well as intestinal and brain inflammation (Perez-Pardo et al., 2018). TLR4 levels, were found to be elevated in stool samples of PD patients (Perez-Pardo et al., 2018). Interestingly, loss of TLR4 prevented the development of PD-like symptoms, such as DA neuron loss, locomotor defects and intestinal inflammation in mice treated with rotenone (Perez-Pardo et al., 2018). Collectively, these results strongly support the role of enteric inflammation in PD pathophysiology. Beside LPS or toxin-induced animal models of PD, altered gut microbiota has also been reported in mice overexpressing α-synuclein (Sampson et al., 2016). The resulting phenotypes, such as the motor deficits or microglia activation were suppressed by antibiotic treatment, reinforcing the intricate relationship between the gut microbiome and the brain, and suggesting that alterations of the human microbiota may participate in the development of PD pathology (Sampson et al., 2016).

More recent work from Matheoud and colleagues, provided further insights into the MitAP mechanism, where they showed that intestinal infection in *Pink1*$^{-/-}$ mice activates MitAP and is accompanied by the brain infiltration of mitochondria-specific immune cytotoxic T cells, which can in turn attack the DA neurons of the substantia nigra (Matheoud et al., 2019). Interestingly, while neither loss of PINK1 or Parkin in mouse

leads to PD-like phenotypes, intestinal infection of *Pink1*$^{-/-}$ mice induces DA neuron degeneration which correlates with strong behavioural defects that can be reversed by Levodopa treatment (Matheoud et al., 2019). This breakthrough discovery amounts to a significant contribution to the evidence implicating the gut-brain axis as a key player in PD pathology.

Altogether, the immune system is playing a central role in PD. However, whether it is the cause or a consequence of the disease remains a fundamental question to answer, although it is likely to be a mixture of both. What is clear is that a complex interplay between the various different players, such as the gut and the brain, is driving the disease progression and subsequent outcomes. It is important to understand the interaction of immune pathways, with key PD proteins, such as PINK1, Parkin or LRRK2. Furthermore, there is a need for a better understanding of the early phases of neurodegeneration and how key immune factors, such as the pro-inflammatory cytokines are involved in this early stage of the disease progression. This will allow the development of better therapeutics, which will be more likely successful.

1.4. *Drosophila* immune system

The *Drosophila* has been heavily used as a model to investigate the innate immunity and has led to many breakthroughs in the immunity field (Lemaitre & Hoffmann, 2007). Although it was thought for a long time that *Drosophila* do not possess an adaptive/acquired immunity, immune priming resulting in a stronger immune response following a second infection, has been described (Pham et al., 2007). More recently, flies were shown to acquire immunity against viral RNA, resulting in the engulfment of virus-infected cells and subsequent immune memory, similar to the mammalian adaptive immunity (Flemming, 2017; Tassetto et al., 2017). The robust innate immune system comprises both humoral and cellular defence mechanisms that are mediated by a plethora of conserved immune signalling cascades (Hoffmann, 2003). The humoral innate immune system relies on signalling pathways that control the production of local effector molecules called antimicrobial peptides (AMPs) (Hoffmann, 2003; Lemaitre & Hoffmann, 2007). This is mainly driven by the Immune deficiency (IMD) and Toll pathways that respond to bacterial and fungi insults (Tanji et al., 2007). Other pathways, such as the JAK/STAT are activated upon viral infection and septic injury (Dostert et al., 2005). The *Drosophila* cellular defence mechanism involves only three types of specialised blood cells, called the haemocytes. Plasmatocytes, macrophage-like cells, represent 90% of the haemocyte population and are responsible for the phagocytosis of pathogens and cellular debris; crystal cells are necessary for wound healing; and lamellocytes engulf large wasp eggs that parasite the larvae (Gold & Brückner, 2015; Tepass et al., 1994). It is worth noting that these immune signalling pathways are not individual entities but rather often overlap and cross-regulate each other.

1.4.1. Humoral response and antimicrobial peptides

The immune response against external pathogens involves the activation of PRRs that specifically recognise components of the microbes' cell wall. There are two families of PRRs: the peptidoglycan recognition receptors (PGRPs) and the gram-negative binding proteins (GNBPs). Upon ligand binding, two immune signalling pathways are activated, the Toll and the IMD pathways, which induce the transcriptional expression

of AMPs and other immune-related genes (Lemaitre et al., 1997). As for mammals, flies can trigger a timely controlled and specific immune response depending on the type of infectious agents. While the Toll pathway mediates a response to gram-positive bacteria and fungi, the IMD pathway is activated by gram-negative bacteria (Agaisse & Perrimon, 2004).

AMPs are small, positively charged peptides that attack and destabilise microbial cell envelopes, resulting in the death of pathogens (Joo et al., 2016). 21 AMP genes, categorised in seven families have been identified so far: Drosomycin and Metchnikowin (antifungal activity), Cecropins and Defensin (antifungal and antibacterial activity) and Drosocin, Attacins and Diptericins (antibacterial activity) (Hanson & Lemaitre, 2020). Their classification depends on the type of pathogen they react against, such as bacteria or fungi. These AMPs are secreted either locally, at the epithelium in contact with the pathogens, or by the fat body, the equivalent of the mammalian liver, and accumulate in the haemolymph, the invertebrate open blood system (Lemaitre & Hoffmann, 2007). Their antimicrobial activity can persist days after infection (Boman et al., 1972).

Additionally, other signalling cascades such as JAK/STAT and c-Jun N-terminal kinase (JNK) pathways, can induce expression of AMP genes, reinforcing the existence of a crosstalk between all these signalling pathways in order to allow a broad-spectrum host response.

1.4.2. *Drosophila* Sting-IMD pathway

The IMD pathway is involved in the immune response against gram-negative bacteria (Kleino & Silverman, 2014; Stokes et al., 2015). The pathway relies on the activity of the *Drosophila* NF-κB protein, Relish which regulates the expression of several AMPs (Myllymäki et al., 2014). The IMD pathway is activated by the recognition of peptidoglycans present in the cell wall of gram-negative bacteria and some gram-positive bacteria (Kaneko et al., 2006). The binding of peptidoglycans to PGRP-LC transmembrane receptors or PGRP-LE intracellular receptors induces the recruitment of the adaptor protein IMD (Kaneko et al., 2006). IMD recruits the *Drosophila* Fas-associated protein with death Domain (dFADD) and the death-related ced-3/Nedd2-

like protein caspase (DREDD/caspase 8) that cleaves IMD, which is then activated by ubiquitination (Kleino & Silverman, 2014). Relish is activated through its cleavage by DREDD and its phosphorylation by the Immune Response Deficient 5 (IRD5; homolog of inhibitor of nuclear factor kappa beta (IKK-β)) and Kenny (IKK-ɣ mammalian homolog). While the 49 kDa fragment resulting from Relish cleavage stays in the cytosol, the resultant 68 kDa fragment translocates to the nucleus, triggering the expression of various immune-related genes such as AMPs, including *diptericin* and *cecropin* (Kleino & Silverman, 2014; Lemaitre & Hoffmann, 2007). Although the recognition receptors of the *Drosophila* IMD pathway and the mammalian TNF signalling cascade are not inherently homologous, the intracellular mechanisms of the two pathways are very similar (Lemaitre & Hoffmann, 2007).

Recently, the *Drosophila* Sting pathway has been shown to signal through the IMD pathway (Figure 1.9). Pathogen DNA that abnormally localise in the cytosol, represent key PAMPs that can initiate a host's defence mechanism and trigger downstream immune signalling cascades such as the cGAS-STING pathway (Cheng et al., 2020; Paludan & Bowie, 2013). Mammalian STING has been shown to play a pivotal role in innate immunity in response to invading pathogen by recognising their nucleic acids. Cytosolic DNA can be detected by the cGAS that generates 2',3'-cGAMP which activates STING (Li et al., 2013; Sun et al., 2013). Activation of mammalian STING results in the NF-κB and Interferon regulatory factor 3 (IRF3) activation and the subsequent production of IFN-β (Ishikawa & Barber, 2008). Bacterial cyclic dinucleotides (CDNs), such as c-di-AMP, c-di-GMP or 3',3'-cGAMP can also be directly recognised by STING (Burdette et al., 2011; Cheng et al., 2020; Whiteley et al., 2019). In flies, following bacterial infection, Sting can directly detect the CDNs derived by the pathogen and induce the production of AMPs through the IMD-Relish pathway (Goto et al., 2018; Martin et al., 2018). While a homolog of the mammalian cGAS has been identified in *Drosophila*, the presence or absence of cGAS does not interfere with the ability of the flies to fight *Listeria monocytogenes* infection (Goto et al., 2018; Martin et al., 2018). In fact, *Drosophila* cGAS lacks the zinc-ribbon domain and the positively charged N-terminal that are both required for DNA binding, further suggesting that the cGAS function is not conserved in *Drosophila* (Figure 1.9) (X. Wu et al., 2014; Martin et al., 2018).

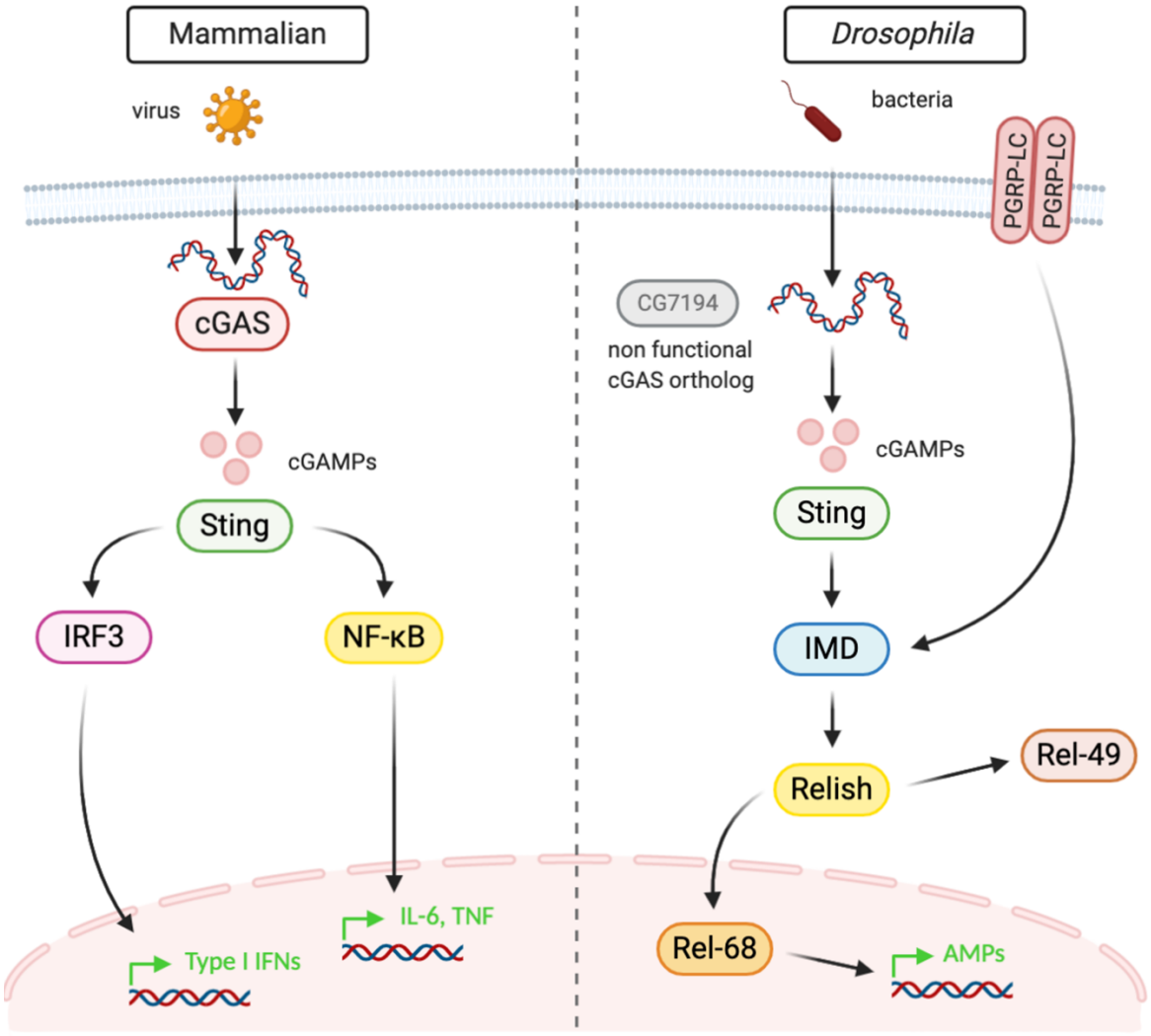

Figure 1.9. Simplified schematic representation of the STING signalling cascade in mammals and *Drosophila*

In mammals, DNA from pathogens is released in the cytosol and recognised by the cGAS that generates 2',3'-cGAMP which activates STING. This results in the activation NF-κB and IRF3 and the subsequent production of type I IFN, IL-6 or TNF. In *Drosophila*, following bacterial infection, CDNs from pathogens are directly recognised by Sting. Activation of Sting results in the production of AMPs through the IMD-Relish pathway.

1.4.3. *Drosophila* Toll pathway

The Toll pathway is similar to the mammalian TLR signalling cascade and is implicated in the immune response against gram-positive bacterial and fungal infections (Valanne et al., 2011). Toll receptors receive signals from recognition proteins that circulate in the haemolymph and signal the presence of pathogens to the cytokine-like ligand Spaetzle (Weber et al., 2003). The Toll pathway requires proteolytic cascades that result in the cleavage and activation of Spätzle (Stokes et al., 2015). The activated form of Spätzle binds as a dimer to its Toll receptor inducing conformational change and dimerization of the Toll receptor (Stokes et al., 2015). Once activated, the Toll receptor forms a complex with three adaptor proteins, myeloid differentiation primary response 88 (MyD88), Tube – the IL-1 receptor-associated kinase 4 (IRAK4) ortholog – and Pelle – the IRAK1 ortholog –, which mediates the phosphorylation of the inhibitory protein Cactus – the inhibitor of kappa B (IκB) ortholog –, and its subsequent proteasomal degradation (Stokes et al., 2015). As a consequence, the NF-κB-like transcription factors Dorsal (during larval stages and adulthood) and Dif (during adulthood) translocate from the cytosol to the nucleus where they activate the expression of immune-effectors, such as the AMP Drosomycin (Figure 1.10) (Lemaitre & Hoffmann, 2007; Manfruelli et al., 1999; Meng et al., 1999).

Mammalian TLRs highly resemble the *Drosophila* Toll receptors, and the downstream cytoplasmic signalling of the pathway is highly conserved between the two species (Rock et al., 1998). While the Toll pathway leads to the production of AMPs, the mammalian cascade results in the induction of pro-inflammatory cytokines. Importantly, endosomal TLR 3, 7, 8, and 9 are sensors of double and single RNA. Their activation results in the expression of pro-inflammatory cytokines and INFs (Crowl et al., 2017). The endpoint of the respective cascades is to fight the pathogen invasion and promote its clearance. The *Drosophila* genome encodes for 10 TLR (Anthoney et al., 2018). The most studied one, Toll shares a high degree of structural homology with the mammalian TLR4 and is also localised at the plasma membrane. The only main difference is that TLR4 directly binds to pathogens, while Toll relies on the signalling from extracellular proteins, which illustrates that mammals have adapted to provide faster immune responses (Stokes et al., 2015). TLR4 have been associated to PD, they are activated in microglia upon α-synuclein aggregation, and their depletion has

been shown to be beneficial to mice treated with rotenone (Perez-Pardo et al., 2018).

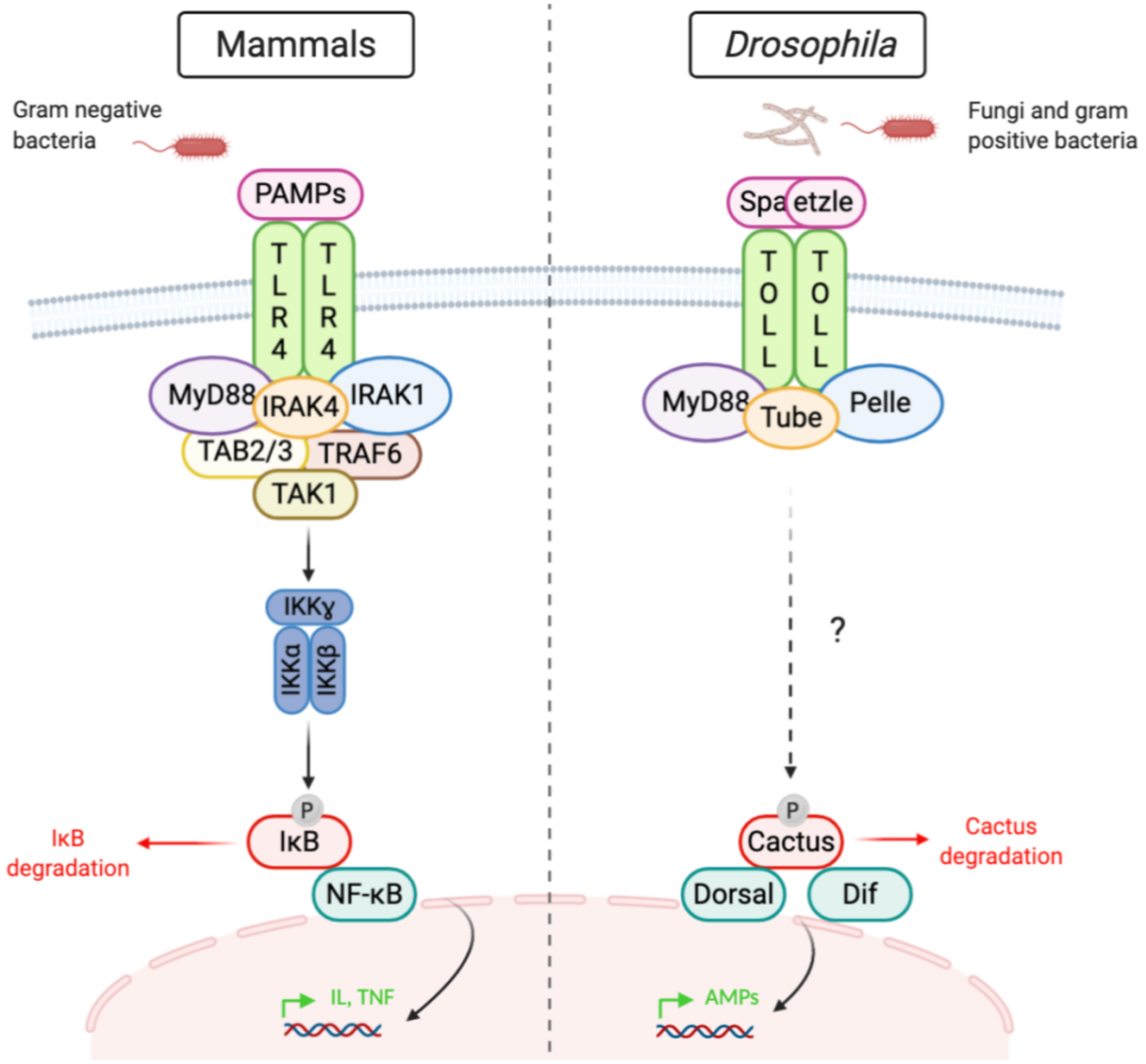

Figure 1.10. Simplified schematic representation of the Toll pathway in mammals and *Drosophila*

Drosophila Toll resembles the mammalian TLR4. In mammals, TLRs directly recognise components of gram-negative bacteria, such as LPS. This triggers the formation of a complex composed of MyD88, IRAK1/4, TAB2/3, TRAF6 and TAK1, which phosphorylates IκB, resulting in its proteasomal degradation. NF-κB then translocates to the nucleus to activate pro-inflammatory cytokines and INFs. In *Drosophila*, the Toll pathway is similar but involves less components than in mammals. Fungi and gram-positive bacteria activate Toll receptors after cleavage and activation of Spätzle. Spaetzle dimer binds to Toll receptors, which induces the dimerization and activation of the receptors. Toll receptors form a complex with MyD88, Tube and Pelle which leads to Cactus phosphorylation and degradation. Dorsal and Dif then translocate to the nucleus to activate expression of AMPs.

1.4.4. *Drosophila* JAK/STAT pathway

Extensive work on various different models led to the observation that the JAK/STAT pathway has been conserved throughout evolution. *Drosophila* possess a simpler JAK/STAT pathway with significantly less components (Stokes et al., 2015; Zeidler et al., 2000). The mammalian JAK/STAT pathway is composed of more than 40 different cytokines, including ILs and IFNs, but *Drosophila* only comprise three cytokine-like proteins, unpaired (upd) 1-3 (H. Myllymäki & Rämet, 2014). All three ligands bind to a single receptor Domeless (Dome), which shares similarities with mammalian class I cytokine receptors such as IL-6 receptor (Brown et al., 2001; Hombría et al., 2005). The diversity of ligands and receptors reflects how the inflammatory response has evolved in mammals in order to develop a specific immunity. Additionally, *Drosophila* have a single JAK, hopscotch (Hop) and a unique STAT, Stat92E (Hou et al., 1996). The activation of the pathway is similar to the mammalian system. The binding of Upd ligands to the Dome receptors induces the dimerization of the receptor and brings two Hop proteins in close proximity. The juxtaposition of Hop molecules leads to their mutual phosphorylation and subsequent activation (Rawlings et al., 2004; Zeidler et al., 2000). They also phosphorylate the cytoplasmic tail of Dome, which provides a docking site for Stat92E (Agaisse & Perrimon, 2004). Once Stat92E proteins are bound to Dome, they are phosphorylated by hop which result in their dissociation from the receptor, dimerization and translocation to the nucleus to induce transcription of several immune-related genes (Figure 1.11) (Kisseleva et al., 2002; Zeidler et al., 2000).

To ensure tight control of the immune response, the pathway is regulated at various levels of the signalling cascade. These negative regulators have been conserved during evolution and therefore homologs exist between *Drosophila* and mammals. The *Drosophila* genome encodes for a single protein inhibitor of activated STAT (*dPIAS*) gene. *Drosophila* dPIAS behaves in a similar way to its mammalian homolog, by targeting activated Stat92E for degradation (Betz et al., 2001; Hari et al., 2001). In addition, a family of activity of suppressor cytokine signalling (*Socs*) genes was also identified in *Drosophila*, with *Socs36E* being the homolog of the mammalian *SOCS-5* (Zeidler et al., 2000). Socs36E is able to directly interact with Dome and prevent the tyrosine phosphorylation by Hop (Hou et al., 2002; Stec et al., 2013). Finally, genome-

wide RNAi screens led to the identification of the protein tyrosine phosphatase 61F (Ptp61F), which targets activated Hop and possibly nuclear-localised Stat92E for deactivation (Figure 1.11) (Baeg et al., 2005). Furthermore, in mammals unphosphorylated-STAT has been found to regulate a different set of genes than phosphorylated-STAT, when it cooperates with NF-κB (Liu et al., 2011; Yang et al., 2007).

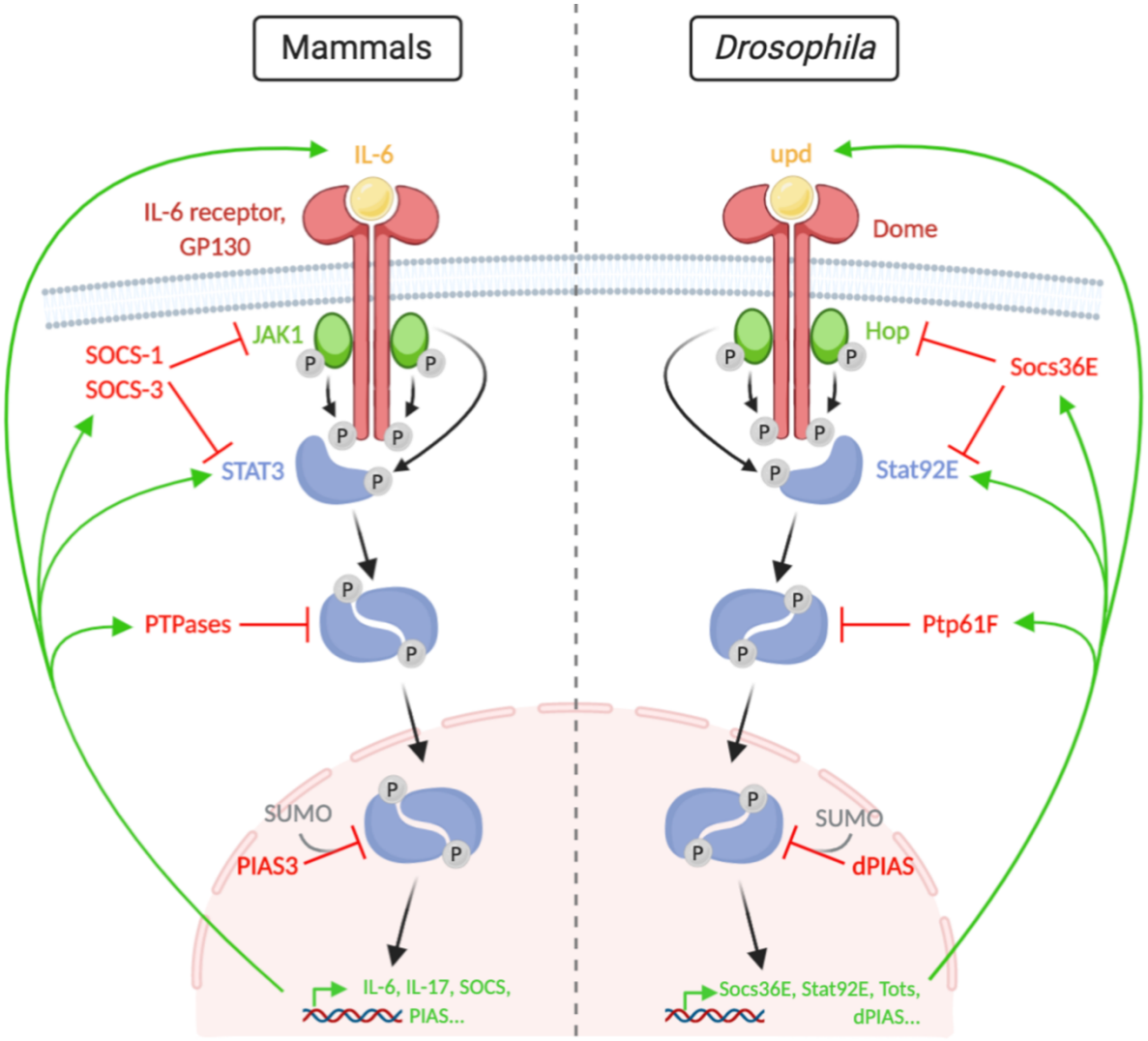

Figure 1.11. Simplified schematic representation of the JAK/STAT pathway in mammals and *Drosophila*

The mammalian cascade is similar to the *Drosophila* one. Binding of the ligand IL-6/Upd to its transmembrane receptor results in the dimerization of the receptor IL6-R/Dome, which in turn brings two JAK/Hop proteins in close proximity. The juxtaposition of the JAK/Hop molecules allow their mutual phosphorylation and subsequent activation. Activated JAK/Hop phosphorylate the tyrosine residues of the cytosolic part of their associated receptors, thus providing a docking site for the normally cytosolic STAT/Stat92E molecules. Once recruited, STAT/Stat92E proteins are phosphorylated by JAK/Hop, resulting in their dissociation from the receptor and their dimerization prior to their nuclear translocation. Once in the nucleus, activated STAT/Stat92E bind specific regulatory sequences that can either results in activation or repression of target genes. The pathway is negatively regulated by PIAS/dPIAS, PTPases/Ptp61F and SOCS/Socs36E proteins.

1.4.5. Other pathways

Beside the Toll, IMD and JAK/STAT pathways, other signalling cascades, such as the JNK and p38 mitogen-activated protein kinase (MAPK) pathways, are involved in the *Drosophila* immune response. The MAPK signalling cascade comprises three components: MAPK, MAPK kinase (MAPKK) and MAPKK kinase (MAPKKK) (Ip & Davis, 1998; Kyriakis & Avruch, 1996; Pearson et al., 2001). In the MAPK signalling cascades, MAPKKKs phosphorylate MAPKKs, which results in their activation and the phosphorylation of MAPKs (Ip & Davis, 1998; Kyriakis & Avruch, 1996; Pearson et al., 2001). Eleven MAPKKKs have been identified upstream of JNK/p38 MAPK pathways, which illustrate their ability to respond to a variety of stimuli (Hayakawa et al., 2006). In addition to cellular stresses, mammalian JNKs, and p38 MAPKs, can be activated by inflammatory cytokines (Inoue et al., 2001). The mammalian MAPKK superfamily comprises several members including MAPK-kinase (MKK) 4 that can activate JNKs and p38 MAPK, MKK7 that is specific to the JNKs and MKK3 and MKK6 that only activate p38 MAPKs (Figure 1.12) (Inoue et al., 2001). In addition to having a role in cell proliferation and many developmental processes, the JNK signalling pathway is also induced in response to many intrinsic and environmental insults such as ROS, DNA damage, inflammatory cytokines and pathogens (Chen et al., 2010; Tafesh-Edwards & Eleftherianos, 2020; Yoshida et al., 2005; Zeke et al., 2016). The pathway has also been shown to be crucial for wound healing as well as AMP production through its interaction with the IMD pathway (Myers et al., 2018; Tafesh-Edwards & Eleftherianos, 2020). Similar to the other pathways presented above, the *Drosophila* JNK cascade comprises most of the mammalian components of the pathway, but with less redundancy. *Drosophila* only contains a single *JNK* gene, encoded by *basket* (*bsk)*; *hemipterous* (*hep*), ortholog of human *MKK7*; *MKK4* which has not been fully characterised and *DJun/DFos* (Figure 1.12) (Glise et al., 1995; Riesgo-Escovar et al., 1996; Sluss et al., 1996; Tafesh-Edwards & Eleftherianos, 2020). The pathway is primarily activated by a wide range of extrinsic and intrinsic insults that result in the phosphorylation and activation of Bsk (Tafesh-Edwards & Eleftherianos, 2020). Hep, activates Bsk, which in turn phosphorylates the transcription factor AP-1 (Jun/Fos heterodimers) and the Forkhead Box O transcription factor (FOXO) which lead to activation of many cellular responses in a tissue- and context-specific manner (Figure 1.12) (Tafesh-Edwards & Eleftherianos, 2020).

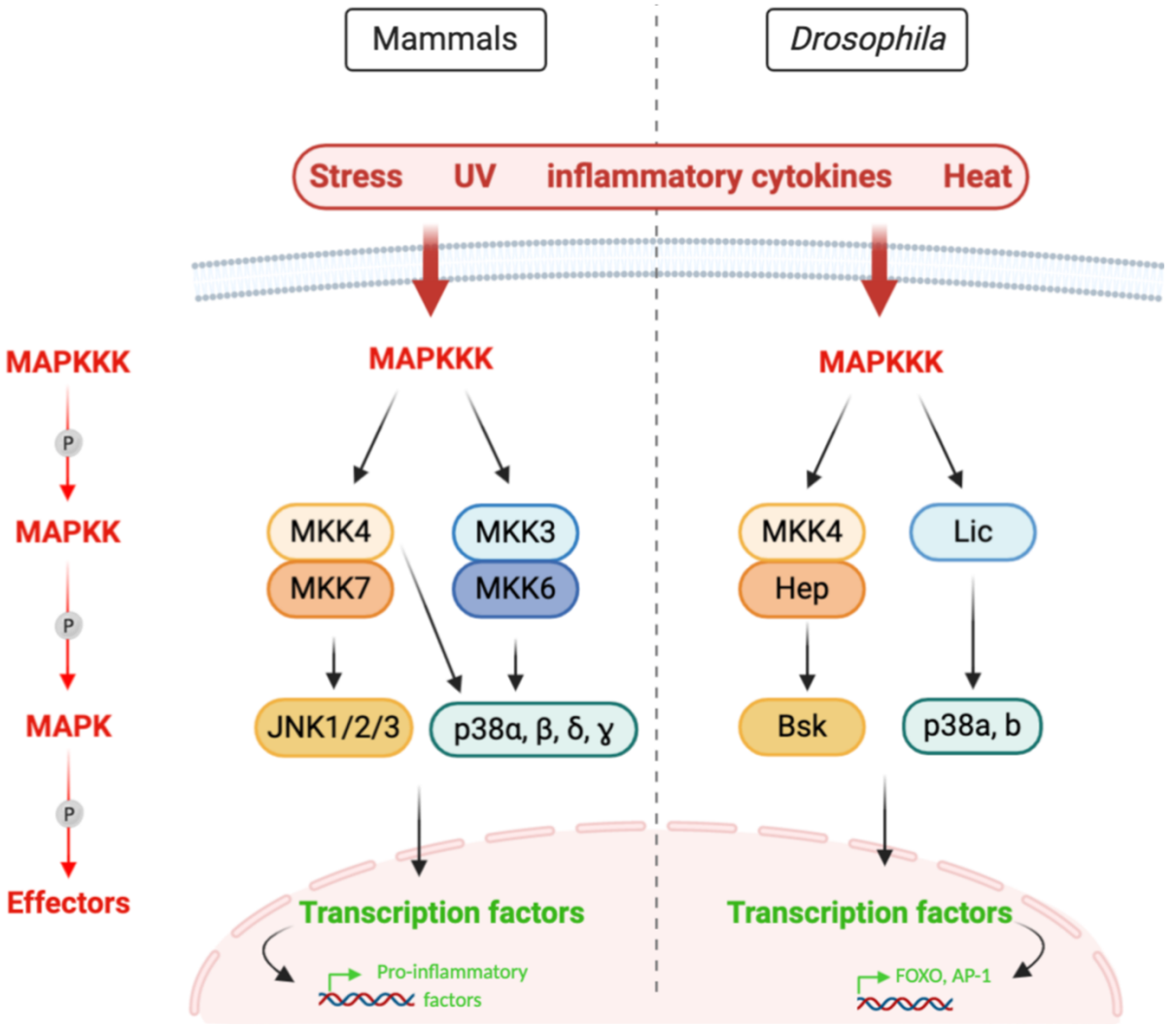

Figure 1.12. Simplified schematic representation of the JNK/p38 MAPK pathways in mammals and *Drosophila*

Several MAPKKKs that phosphorylate MAPKKs have been identified in mammals and *Drosophila*. MKK4 activates JNKs and p38 MAPKs, MKK7/Hep only activates JNKs/Bsk; MKK3/Lic and MKK6 activate p38 MAPKs. Activation of the MAPKs results in the activation of several transcription factors.

Drosophila p38 MAPK cascade is a conserved pathway induced in response to stress factors or immune threats, such as LPS, heat shock or UV irradiation. It regulates cell cycle arrest and apoptosis, as well as the secretion of cytokines (Han et al., 1998). *Drosophila* comprises three key members p38a, p38b and p38c. p38a and p38b share similarities with the mammalian p38α, p38β, p38δ and p38ɣ. However, p38c is unique to fly and lacks a TGY site phosphorylated by MKK3/MKK6; it is mainly expressed in the intestine (Craig et al., 2004). Both p38a and p38b have redundant functions and

can be activated upon bacterial infections (Craig et al., 2004). Several MAPKKKs can activate Licorne (Lic) the ortholog of the mammalian MKK3, resulting in the activation of the p38a and p38b MAPKs (Adachi-Yamada et al., 1999; Han et al., 1998; Inoue et al., 2001; Suzanne et al., 1999).

1.4.6. Implication of the immune system in Drosophila models of neurodegeneration

In addition to the aberrant activation of the STING signalling cascade in *Pink1* and *Prkn* KO mice, inappropriate regulation of other immune pathways has shown in several *Drosophila* and mammalian models of neurodegenerative disorders. Primary evidence came from transcriptional profiling of *Pink1* and *parkin* mutants revealing the upregulation of many immune-related genes, such as AMPs and *Tots* (Greene et al., 2005; Tufi et al., 2014). Furthermore, elevated levels of *TotA*, *TotM* and *TotX*, downstream targets of the JAK/STAT pathway, were also reported in flies exposed to the PD-toxin, paraquat (Ekengren & Hultmark, 2001; Maitra et al., 2019).

The downregulation of genes encoding key regulators of the *Drosophila* Toll pathway has shown to rescue the neurotoxicity induced by the overexpression Aβ-42 (Tan et al., 2008). More recently, aberrant activation of the IMD pathway has been linked to neurodegeneration and shortened lifespan in *Drosophila* (Kounatidis et al., 2017). Earlier studies have shown that flies lacking a repressor of the IMD pathway, named defence repressor 1 (dnr1) exhibit neurodegeneration due to elevated expression levels of AMPs (Cao et al., 2013). Additionally, in a fly model of Ataxia-Telangiectasia, Petersen et al., reported that high levels of AMPs in glial cells directly correlated with the level of neurodegeneration observed in these mutants, suggesting that Relish participates to the disease pathogenesis (Petersen et al., 2012, 2013). Maitra et al., have shown that loss of Relish specifically in the DA neurons confers resistance to paraquat treatment and abrogates the locomotor deficits as well as the loss of DA neurons usually observed following exposure to this PD toxin (Maitra et al., 2019). Reduced JAK/STAT signalling has been observed in *Drosophila* glial cells overexpressing human Tau, resulting in decreased lifespan and formation of glial fibrillary tangles (Colodner & Feany, 2010). Finally, in a study investigating the immune response in *parkin* mutants, Cha et al., revealed that activation of the JNK signalling

cascade specifically occurs in DA neurons as seen by the localization of activated phospho-JNK in this particular cell population (Cha et al., 2005). This correlated with a perturbed morphology of the DA neurons and a decrease in their tyrosine hydroxylase (TH) levels which were both rescued by loss of *hep* (Cha et al., 2005). Although the mechanism remains unknown, this suggests that downregulation of the JNK pathway is beneficial to *parkin* mutants.

Together, these studies suggest that dysregulation of the *Drosophila* immune system may contribute to neurodegenerative disorders, as seen in mammals. However, how immunity and its dysregulation can affect the whole-body pathophysiology, as seen in PD, remains unclear.

Thesis aims

As summarised above, PINK1/Parkin-mediated mitophagy is a key MQC pathway that enables the maintenance of a healthy pool of mitochondria. While this mechanism has been extensively studied in cultured cells exposed to depolarisation agents such as CCCP, little is known about the implication of these two proteins under basal conditions *in vivo*. Therefore, this project aimed to provide an extensive analysis of Pink1/parkin role in mitophagy in *Drosophila*; first, by developing *in vivo* mitophagy reporters, and second, by subsequently assessing the role of immune signalling pathways as a cause of the mutant phenotypes.

Chapter 3 provides a thorough analysis of mitophagy *in vivo* using two mitophagy reporters that have been adapted to the *Drosophila* system, the mito-QC and the mtKeima. Mitophagy was examined in several tissues from larvae to adult and aged animals. In addition, this chapter provides some comparison of the two reporters which may be relevant to the mitophagy field and other *Drosophila* labs. To address the role of Pink1/parkin in basal mitophagy, *Pink1* and *parkin* mutants were combined with the mito-QC or mtKeima reporters to quantify mitophagy levels in several tissues. These results provide further information on the function of PINK1/Parkin in basal versus induced mitophagy and challenge the current view of their role in mitophagy.

Chapter 4 addresses whether or not some key *Drosophila* immune pathways are implicated in PD pathology, and more particularly in *Pink1* and *parkin* mutants. In this chapter, loss of key players of the Sting-IMD, JNK and p38-MAPK pathways were analysed in *Pink1* or *parkin* mutant background. As climbing defects and aberrant mitochondria morphology are key features of these two mutants, these phenotypes were used as a readout to assess any potential genetic interactions. How this may relate to the mammalian system is further discussed in this chapter.

Finally, similar experiments were performed in Chapter 5, which focuses on the JAK/STAT pathway. Individual loss of six components of the pathway were combined with *Pink1* or *parkin* mutants. Additionally, as JAK/STAT plays a pivotal role in gut homeostasis, which is altered in PD, the overall gut architecture was investigated in

Pink1 mutants. Uncovering a strong interaction between JAK/STAT and *Pink1* mutants suggests that downregulation of the JAK/STAT pathway could be considered for therapeutic targeting in the treatment of PD.

Chapter 2. Material and methods

2.1. *Drosophila* husbandry

Flies were maintained on a 12:12 hour light/dark cycle in Sanyo incubators (MIR-254), on food containing cornmeal, agar, molasses, yeast, and propionic acid. Expanded short-term stocks, genetic crosses and experimental crosses were kept at 25°C to shorten generation time to ten days, whereas long-term fly storage was maintained at 18°C. Unless specified, flies were immobilised via CO_2-induced anaesthesia. Anaesthesia was minimised as much as possible, and behavioural assays were performed the next day at the earliest. A list of fly lines used in this study is given in Table 2.1, with their source and identifier code.

Table 2.1. Fly lines used with source and ID. BDSC = Bloomington Drosophila Stock Center (RRID:SCR_006457). FlyORF = Zurich ORFeome Project (Bischof et al., 2013), VDRC = Vienna Drosophila Reference Center (RRID:SCR_013805).

Genotype	Source	ID
GAL4 drivers		
arm-GAL4	BDSC	RRID:BDSC_1560
da-GAL4	BDSC	RRID:BDSC_55850
TH-GAL4	BDSC	RRID:BDSC_8848
nSyb-GAL4	BDSC	RRID:BDSC_51635
$nSyb_{ZH\text{-}86FB}$-GAL4	BDSC	RRID:BDSC_68222
(new) *Mef2*-GAL4	BDSC	RRID:BDSC_27390
(original) *Mef2*-GAL4	Ordway via Pallanck	
repo-GAL4	Matthias Landgraf	
Controls		
w^{1118}	BDSC	RRID:BDSC_6326
UAS-lacZ$_{ZH\text{-}86Fb}$	FlyORF	RRID:FlyBase_FBst0503118
UAS-lacZ RNAi	VDRC	v51446
UAS-mito.HA.GFP	BDSC	RRID:BDSC_8443

Mitophagy reporters		
UAS-mito-QC (attP16)	(Lee et al., 2018)	
UAS-mito-QC (attP2)	(Lee et al., 2018)	
UAS-mt-Keima (II)	(Lee et al., 2018)	
UAS-mt-Keima (III)	(Lee et al., 2018)	
p38 MAPK pathway		
UAS-p38b RNAi^{KK}; UAS-p38b RNAi^{GD}	Marco Milan	
UAS-p38b^{KD}	Marco Milan	
p38a^{1}	BDSC	RRID:BDSC_8822
UAS-lic RNAi^{TRIP} (attP40)	BDSC	RRID:BDSC_60010
UAS-lic RNAi^{TRIP}(attP2)	BDSC	RRID:BDSC_35154
JNK pathway		
UAS-bsk RNAi^{TRIP} (attP2)	BDSC	RRID:BDSC_331476
bsk^{LL}	Oren Schuldiner	
UAS-egr RNAi^{TRIP} (attP40)	BDSC	RRID:BDSC_55276
egr^{3}	Masayuki Miura	
Relish pathway		
UAS-Rel RNAi^{TRIP} (attP2)	BDSC	RRID:BDSC_33661
UAS-Rel RNAi^{GD} (II)	VDRC	v49413
Rel^{E20}	BDSC	RRID:BDSC_55714
Sting pathway		
UAS-Sting RNAi^{TRIP} (attP2)	BDSC	RRID:BDSC_31565
UAS- Sting RNAi^{GD} (II)	VDRC	v4031
Sting$^{\Delta RG5}$	(Martin et al., 2018)	
JAK/Stat pathway		
UAS-upd1 RNAi^{TRIP} (attP2)	BDSC	RRID:BDSC_28722
upd2Δ, upd3Δ	BDSC	RRID:BDSC_55729
dome^{G0441}	BDSC	RRID:BDSC_12030

hop^{2}	BDSC	RRID:BDSC_6032
UAS-Stat92E RNAi^{KK}	VDRC	v100519
Stat92E^{06346}	BDSC	RRID:BDSC_11681
Stat92E^{85C9}	Marco Milan	
10XStat92E-GFP (II)	Martin Zeidler	
UAS-totA RNAi^{TRIP} (attP2)	BDSC	RRID:BDSC_55378
UAS-totA RNAi^{TRIP} (attP40)	BDSC	RRID:BDSC_58257
UAS-totM RNAi^{TRIP} (attP40)	BDSC	RRID:BDSC_6004
Other lines		
Pink1^{B9}	(Park et al., 2006)	
park^{25}	(Greene et al., 2003)	
UAS-mito-APOBEC1	(Andreazza et al., 2019)	
UAS-TcPink1	(Woodroof et al., 2011)	
UAS-parkin$_{C2}$	(Greene et al., 2003)	

2.2. Behavioural assays

2.2.1. Climbing assay

Unless specified, 1 to 3-day-old adult males were collected the day preceding the assay, up to a maximum of 22 flies per group. On the day of the experiment, flies were moved to the ~23°C climbing room to acclimatize for 30 min, then transferred in test tubes for 30 min. Flies were then placed in a counter-current apparatus as previously described (Greene et al., 2003). Flies were tapped to the bottom of the test tube, and then given 10 s to climb to the upper part of the apparatus (10 cm), where they were shifted to the neighbouring chamber. After five trials, the average score was expressed as a climbing index.

Because X chromosome nondisjunction is present in multiple balanced *Pink1*^{B9} mutant stocks, correct genotypes were determined by either combining paternal animals with X chromosome markers (yellow) or by PCR-based genotyping the discarded tissue after dissection.

2.2.2. Flight assay

Up to a maximum of 22 adult males, 1-3 days post-eclosion, were placed into vials the day before performing the experiment. To execute the assay, the vials containing the flies were tapped into a funnel placed on top of a 1 L graduated cylinder containing a vacuum grease-coated acetate sheet. The flies become stuck onto the sheet where they landed. The sheet was removed from the cylinder, and the immobilised flies in each of four equally divided sections were counted. A score of zero was given to the flies that did not adhere to the sheet; any flies that escaped the cylinder were not scored.

2.2.3. Lifespan assay

For lifespan experiments, flies were grown at 25°C under identical conditions at low-density. Progenies were collected under minimal anaesthesia and placed in tubes of 20 males each, to approximately 100 in total. Flies were transferred onto fresh food

every 2-3 days and the number of dead flies was recorded on each flip. At the end of the experiment, the percent survival was calculated after correcting for any escaper.

2.3. Immunohistochemistry

2.3.1. Sample preparation

For larval brains and epidermal cells, larvae were pinned and stretched dorsal side up on a Sylgard plate and cut along the midline in order to open the larvae longitudinally. For epidermis imaging, the guts, other internal organs and muscles were removed in order to fully expose the cells. For flight muscles, thoraces were divided along the midline into two halves. For adult brains, male heads were removed from the rest of the body. The head cuticle was opened to expose the brain. Trachea and any remaining connective tissue were removed for better imaging purposes. An overview of the different tissues dissected is giving in Figure 2.2

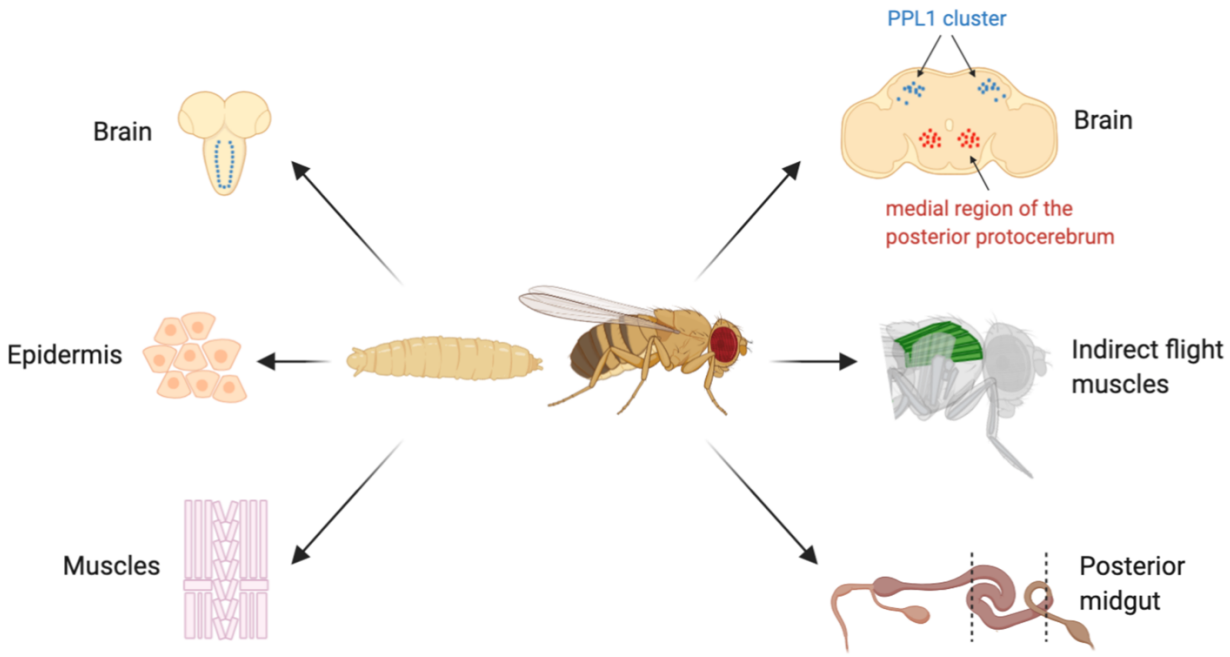

Figure 2.1 schematic of the *Drosophila* tissues dissected and analysed in this study.
(Left) Larval brain, epidermis and muscles were analysed in this study as well as (Right) adult brains (DA neurons of the PPL1 cluster and neurons from the medial region of the posterior protocerebrum), indirect flight muscles and posterior midgut.

Unless otherwise stated, the dissections of adult tissues were performed on 2-day-old animals. All tissues were dissected in Phosphate-buffered-saline (PBS) at pH 7.4. The samples were then were fixed in 4% formaldehyde (ThermoFisher Scientific) for 20 min (larval tissues) or 30 min at room temperature (RT) (adult tissues). For mitolysosome analysis of mito-QC, tissues were fixed in 4% formaldehyde adjusted at pH 7.0. For larval tissues, adult thoraces and non-stained adult brains, tissues were permeabilized in PBS-T (PBS with 0.3% Triton X-100) for 30 min, and blocked with PBS-T plus 1% bovine serum albumin (BSA) for 1 h at RT. Tissues were incubated with the primary antibody, diluted in PBS-T plus 1% BSA overnight at 4°C, then rinsed 3 times 10 min with PBS-T, and incubated with the appropriate fluorescent secondary antibodies for 2 h at RT (larval tissues) or overnight at 4°C (adult thoraces). Once antibody incubations were complete, tissues were washed 2 times in PBS and mounted on slides using Prolong Diamond Antifade mounting medium (ThermoFisher Scientific).

For the mito-QC experiments, the samples were imaged on the same day or the day after being mounted at the latest.

For gut dissections, the guts were fixed and mounted on poly-L-lysine hydrobromide (Sigma) coated slides for better adherence of the tissue on the slide. Prolong Diamond Antifade mounting medium with 4,6-diamidino-2-phenylindole (DAPI) (ThermoFisher Scientific) was used as a mounting media.

For the immunostaining of DA neurons, 30-day-old fly brains were dissected in PBS, fixed in 4% formaldehyde for 30 min at RT and washed with PBS-T, 3 times 20 min. The tissues were then blocked for 4 hours with PBS-T plus 1% BSA on a shaker at RT, before incubation with the anti-TH antibody diluted in the blocking solution for 4 days at 4°C. The brains were then washed with PBS-T, 3 times 20 min. The secondary antibody was diluted in the blocking solution and incubated with the brains for 4 hours at RT. After incubations, the tissues were washed 2 times in PBS and mounted on slides using Prolong Diamond Antifade mounting medium (ThermoFisher Scientific).

A list of the primary and secondary antibodies used in this study is given in Table 2.2.

2.3.2. Deferiprone treatment

Mito-QC or mt-Keima expressing animals were raised on normal food dosed with deferiprone (LKT Laboratories) to a final concentration of 65 µM dissolved in water.

2.3.3. LysoTracker live imaging

Larval epidermal cells were dissected in PBS and stained for 2 min with LysoTracker™ Deep Red (Invitrogen) diluted to a final concentration of 500 nM in PBS. Samples were mounted in PBS immediately visualized by confocal microscopy.

2.4. Microscopy

2.4.1. Imaging

Fluorescence imaging was conducted with a Zeiss LSM 880 (Carl Zeiss MicroImaging) equipped with Nikon Plan-Apochromat 40x/1.3 NA, 63x/1.4 NA and 100x/1.4 NA oil immersion objectives. For the mito-QC experiments, the imaging was performed with an Andor Dragonfly spinning disk confocal microscope equipped with a Nikon Plan-Apochromat 100x/1.45 NA oil immersion objective. Z-stacks were acquired at 0.2 µm steps.

For the mt-Keima, live images were acquired via sequential excitations (458 nm, green; 561 nm, red) being captured at 578 to 638 nm emission range.

For the dopaminergic neuron counting, z-stacks of brain tissues were acquired at 2 µm steps.

For thoracic indentations, images were acquired using a Leica DFC490 camera mounted on a Leica MZ6 stereomicroscope. Images were prepared using Fiji software (Fiji, RRID:SCR_002285).

2.4.2. Quantification of the mito-QC mitolysosomes

For quantification of mitolysosomes, z-stack images were acquired from the Andor Dragonfly spinning disk confocal microscope (Figure 2.2 A). An average of 3 images per animal were taken and processed using Imaris analysis software (BitPlane version 9.0.2) (RRID:SCR_007370) to identify and count individual ‘red-only’ puncta. The GFP signal was adjusted to only retain the distinct mitochondrial network (Figure 2.2 B). This step was essential to obtain a sharp and detailed structure of the mitochondrial network. In a similar process, the mCherry signal was altered to dampen the signal from the mitochondrial network and highlight the red puncta. Then, a 3D rendered surface matching the mitochondria network was generated using the GFP channel (Figure 2.2 B). Finally, this volume was subtracted from the red channel to only collect the mCherry signal that did not co-localize with the GFP-labelled mitochondrial network

(Figure 2.2 C). The ‘red-only’ puncta, called mitolysosomes, were then selected according to their fluorescence intensity and an estimated size of 0.5 µm diameter that was previously measured with Imaris (Figure 2.2 D and E).

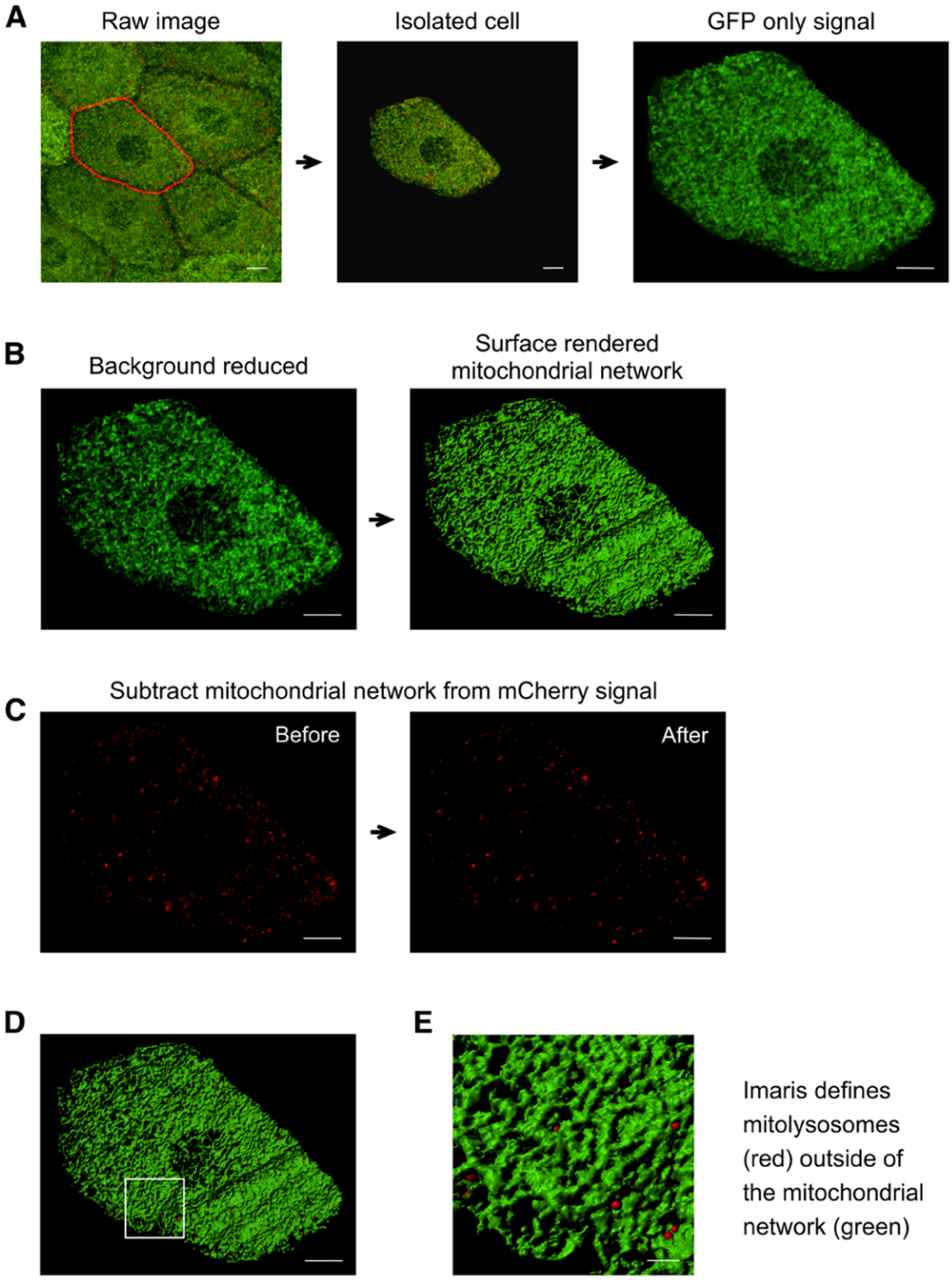

Figure 2.2. Image analysis and quantification of the mito-QC mitolysosomes

(A) Z-stack images were acquired, and individual cells were isolated using Imaris analysis software. (B) The background of the GFP signal was adjusted to only retain the mitochondria network and a 3D surface rendered was applied to the mitochondrial network. (C) Finally, this volume was subtracted from the red channel to only collect the mCherry signal that did not co-localize with the GFP-labelled mitochondria network. (D) 'red-only' puncta corresponding to mitolysosomes were then quantified. (E) zoom of (D).

Cells from the larval epidermis and central nervous system (CNS) were analysed individually as these cell types could easily be distinguished from one another. For DA neurons and adult CNS soma, several cells were analysed together, and an average score was calculated per cell.

The average number of mitolysosomes per cell was then calculated per animal to account for animal variability. The quantification charts show data points corresponding to the average number of mitolysosomes per cell for individual animals, where n ≥ 6 animals for each condition.

For the quantification of mitolysosomes in adult thoracic muscles: 8 animals per genotype were dissected at 2 days and 20 days. 2 images per thorax were acquired. Before being analysed, images were blinded for genotype and age. Using the Fiji software, each image was defined by one random region of interest (ROI) of 6400 μm^2 for further analysis. Finally, the number of red puncta present in the ROI was counted manually. The number of mitolysosomes display in the graph corresponds to the number of red puncta within this 6400 μm^2 ROI.

2.4.3. Quantification of thoracic mitochondrial morphology

8 animals per genotype were dissected. 3 images were obtained per thorax and analysed by 3 investigators blinded to genotypes. The images were scored by the level of disorganisation of mitochondria based on the control genotype w^{1118}.

2.5. Molecular biology

2.5.1. Immunoblotting

Proteins were isolated from whole adult flies using a RIPA lysis buffer (50 mM Tris-HCl, 150 mM NaCl, 10% (vol/vol) glycerol, 1% Triton X-100, 10 mM N-ethylmaleimide, 2 mM EGTA, 1 mM, $MgCl_2$, 50 µM MG-132) supplemented with cOmplete mini EDTA-free protease inhibitors (Roche). After protein quantification using the bicinchoninic acid assay (BCA) (ThermoFisher), 4X Laemmli buffer (Bio-Rad) containing 1:10 β-mercaptoethanol (Sigma) was added to 20 ug of protein samples. The samples were then resolved by SDS-PAGE using 4-20% gradient precast gels (Bio-Rad) and transferred onto nitrocellulose membrane (Bio-Rad) using a semi-dry Bio-Rad TransBlot system. Membranes were blocked with 5% (w/v) dried skimmed milk powder in TBS-T (Tris-buffered saline with 0.1% Tween-20) for 1 h at RT and probed with the appropriate primary antibodies diluted in the blocking solution overnight at 4°C. After several washes with TBS-T, the membranes were incubated with the appropriate horse radish peroxidase (HRP)-conjugated secondary antibodies (Dako) for 1 h at RT. Detection was achieved with ECL-Prime detection kit (Amersham). As a loading control, membranes were incubated with anti-α-Tubulin or anti-Actin antibodies for 1 h at RT.

2.6. Antibodies

A list of the primary and secondary antibodies used in this study is given in Table 2.2 with their source, identifier code and dilution.

Table 2.2. Primary and secondary antibodies used for this study

Antibody	Species	Source	ID	Dilution
Primary				
ATP5A	mouse	Abcam	RRID:AB_301447	1:5 000 (WB) 1:300 (IF)
GFP	rabbit	Abcam	RRID:AB_303395	1:2 000 (WB) 1:300 (IF)
DsRed	rabbit	Clontech Laboratories, Inc.	RRID:AB_10013483	1:1 000
Keima-Red	mouse	MBL International	RRID:AB_10210643	1:1 000
TH	mouse	Immunostar	RRID:AB_572268	1:200
α-Tubulin	mouse	Sigma-Aldrich	RRID:AB_477585	1:5 000
Actin	mouse	Millipore	RRID:AB_2223041	1:5 000
Secondary				
anti-mouse HRP	goat	Abcam	RRID:AB_955439	1:10 000
anti-rabbit HRP	goat	ThermoFisher	RRID:AB_2536530	1:10 000
anti-mouse AF488	goat	ThermoFisher	RRID:AB_2534069	1:300
anti-mouse AF647	goat	ThermoFisher	RRID:AB_2535804	1:300

2.7. Statistical analysis

Data are reported as mean ±SD or 95% confidence interval (CI) as indicated in figure legends. Unless otherwise noted, n refers to the number of animals tested.

For climbing and flight analysis, Welch's *t*-test or Kruskal-Wallis non-parametric test with Dunn's post-hoc correction was used for multiple comparisons. For statistical analyses of lifespan experiments a Log-rank (Mantel-Cox) test was used. V. Hewitt and L. Garcia developed the algorithm to aid processing of the lifespan data. Analyses were performed using GraphPad Prism software (RRID:SCR_002798) versions 7 and 8. The number of mitolysosomes was analysed by Welch's *t*-test or one-way ANOVA with Sidak's post-hoc test.

For number of DA neurons analysis, one-way ANOVA with Bonferroni's post-hoc correction was used for multiple comparisons.

Any significance for the mitochondrial morphology in adult thoraces was obtained by via χ^2 test after multiple comparison.

Chapter 3. Investigating Pink1/parkin-mediated mitophagy in *Drosophila*

3.1. Introduction

In order to maintain a healthy pool of mitochondria, these organelles are constantly surveyed by quality control mechanisms, such as mitophagy, that allow relatively rapid clearance of any dysfunctional mitochondria. The PINK1/Parkin pathway remains the most studied and well-understood mitophagic mechanism. Briefly, mitochondrial depolarisation induces PINK1 stabilisation and accumulation at the OMM (Matsuda et al., 2010; Narendra et al., 2010). Ub is then phosphorylated at the OMM by stabilised PINK1, which results in Parkin recruitment of Parkin at the mitochondrial surface and the phosphorylation of its Ser65 residue by PINK1 (Kane et al., 2014; Kazlauskaite et al., 2014, 2015; Kondapalli et al., 2012). Parkin phosphorylation by PINK1 allows the full activation of the ligase (Wauer et al., 2015). Once Parkin is activated, the ligase drives the ubiquitination of several substrates located on the OMM, and creates a feed-forward loop by providing additional ubiquitin chains for PINK1 to phosphorylate (Lazarou et al., 2015; Okatsu et al., 2015; Ordureau et al., 2014). This process leads to the recruitment of the autophagy machinery and the engulfment of the mitochondrion by the autophagosome which then fuses with the lysosome for degradation (Montava-Garriga & Ganley, 2020). Over the past decades, mitochondrial dysfunction has been recognised as a common feature across many neurodegenerative disorders, including PD (Fang et al., 2019; Johnson et al., 2019). Additionally, the implication of defective mitophagy in the PD pathology has been reinforced by the fact that mutations in *PINK1* and *PRKN* genes result in familial forms of PD. Impairment of mitophagy in these PD mutants has been hypothesised to account for the mitochondrial defects observed in PD patients, such as high levels of mtDNA mutations and complex I deficiency, resulting from the accumulation of dysfunctional mitochondria (Bender et al., 2006; Kraytsberg et al., 2006; Schapira et al., 1990). A failure in mitophagy is highly relevant for post-mitotic neurons, such as the ones populating the substantia nigra. The constant pace-making activity and the extensive arborisation of these neurons heavily relies on the ability of their mitochondrial network to meet these high energy demands (Sulzer & Surmeier, 2013). As neurons are unable to dilute any mitochondrial damage through cell divisions, these particular cells are more likely to depend on mitophagy in order to maintain a constant pool of healthy mitochondria (Palikaras et al., 2018). Research in the mitophagy field has grown exponentially in the recent years, and it

became evident that the mitochondrial turnover relying on this process is a complex mechanism varying according to the tissues, energetic demand or stress contexts (Montava-Garriga & Ganley, 2020).

For many years, immortalized cultured cells overexpressing Parkin in conjunction with an acute mitochondrial depolarization, such as CCCP, have been the predominant method to study the molecular details of PINK1/Parkin-induced mitophagy (Pickrell & Youle, 2015; Yamano et al., 2016). However, as cells do not always fully replicate mechanisms occurring in a tissue *in vivo*, and there has been increasing discrepancies between *in vitro* and *in vivo* work, such as whether or not mitochondrial depolarization is the true physiological trigger for PINK1/Parkin pathway. In fact, little is known about the physiological stimuli activating PINK1/Parkin-mediated mitophagy and whether different stimuli might trigger different MQC pathways. *In vitro* experiments have thoroughly proven that CCCP induces depolarization of the mitochondrial membrane, Parkin recruitment and subsequent mitophagy. Nonetheless, CCCP is also known to depolarize other cellular membranes including lysosomal membranes, and is often used at concentrations higher than the ones necessary for mitochondrial membrane depolarization (Padman et al., 2013). This raises the concern that *in vitro* use of such compounds might induce a level of mitochondrial clearance somewhat different than *in vivo* physiological conditions.

While little was known about the physiological relevance of mitophagy *in vivo*, the development of mouse and *Drosophila* models of these two mitophagy reporters shed light on the physiological stressors impacting this recycling process and provided for the first time a new way of investigating and monitoring mitophagy *in vivo*. Although these reporters reveal widespread basal mitophagy, the contribution of PINK1 and Parkin remains to be addressed.

3.2. Chapter aims

In this chapter, I aimed to investigate Pink1/parkin-mediated mitophagy in *Drosophila,* using the newly generated mt-Keima and mito-QC mitophagy reporters. I first conducted a thorough validation of these reporters. These tools were then used to assess basal mitophagy in a variety of larval and adult tissues of WT animals and in the absence of any external stimuli. In the next step, and the true aim of this chapter, I combined the mitophagy reporters with the well-established *Drosophila Pink1* and *parkin* null mutants. This provided further insight on the role of these two proteins in mitophagy *in vivo*. In the second part of this chapter, I investigated the impact of an additional and physiologically relevant mitochondrial stressor, in order to potentially boost mitophagy. To this end, I combined the recently described mtDNA mutator, mito-APOBEC1, with the mito-QC to assess mitophagy in larvae, young and aged adult flies. Finally, in order to further interrogate the implication of PINK1 and parkin in mitophagy, I overexpressed these two proteins in a WT background or in combination with the additional stressor mito-APOBEC1 and assessed the level of mitophagy in larval brains.

3.3. Results

3.3.1. Validation of the mito-QC mitophagy reporter

The mito-QC generated by Allen et al., was adapted to the *Drosophila* system (Allen et al., 2013). Two *Drosophila* lines expressing the mito-QC reporter were generated by a previous lab member, UAS-mito-QC II and UAS-mito-QC III, on the 2nd and 3rd chromosome, respectively. The expression of these new transgenes was verified by western blot. A band was observed at ~70 kDa, corresponding to the expected molecular weight of the mito-QC, when probed with an antibody against GFP or DsRed (Figure 3.1 A). *w^{1118}* was used as a WT control genotype. Both lines evenly expressed the mito-QC when induced by the ubiquitous *daughterless* driver (*da*-GAL4). Although flies expressing the mito-QC flies appeared viable and healthy, behavioural assays, including climbing and flight were performed (Figure 3.1 B and C). No significant differences in the climbing ability were observed between control and transgenic flies expressing high levels of mito-QC, confirming that expression of these lines had no significant impact on the flies' fitness (Figure 3.1 B and C).

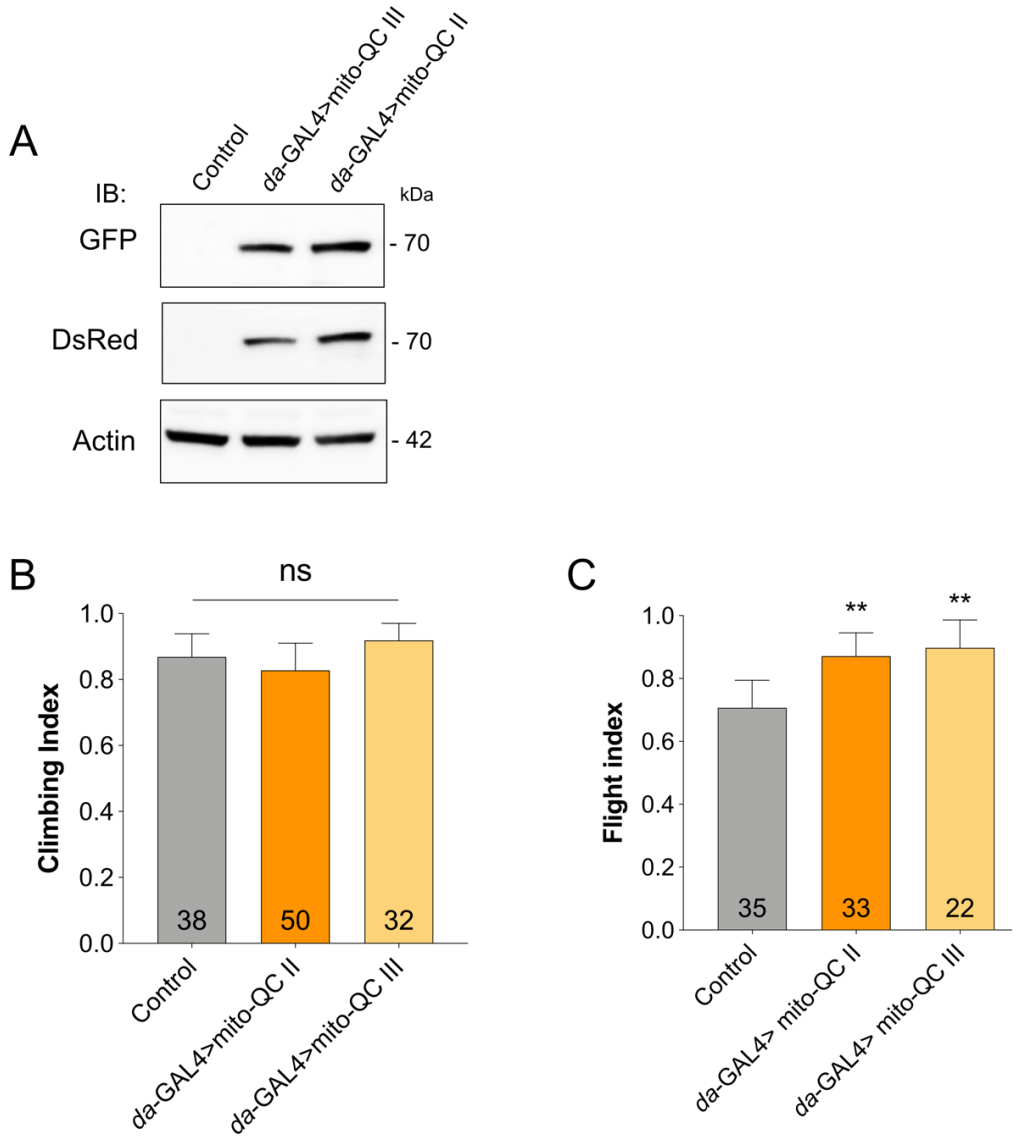

Figure 3.1. Expression of mito-QC is benign in *Drosophila*

(A) Immunoblotting of two transgenic lines expressing the mito-QC induced by the ubiquitous *da*-GAL4 driver. Immunoblot was probed with the indicated antibodies. Actin antibody was used as a loading control. Control genotype is non-transgenic w^{1118}. Locomotor assays for (B) climbing and (C) flight ability of the same genotypes analysed above. Charts show mean ± 95% CI. Number of animals analysed is shown in each bar. Statistical analysis was determined by Kruskal-Wallis non-parametric test with Dunn's post-hoc correction for multiple comparisons; ** $P < 0.001$; ** $P < 0.01$ and ns = non-significant. Control genotype for behaviour is *da-GAL4/+.*

Previous work in cultured cells and mice has confirmed the proper targeting of the mito-QC to mitochondria, as well as its 'spectral shift' under more acidic conditions and the co-localization of the red puncta with lysosomes (McWilliams et al., 2016). The first step was to validate the appropriate targeting of mito-QC to the mitochondria in these

new transgenic *Drosophila* lines. A co-localization experiment with the mitochondrial protein ATP5A was performed in the larval epidermis (Figure 3.2 A) and adult flight muscles (Figure 3.2 B) two tissues harbouring a defined mitochondrial network and thus highly suitable for fine microscopy imaging. A substantial co-localisation of mito-QC with ATP5A was observed, thus confirming the correct targeting of the mito-QC to mitochondria (Figure 3.2 A and B). It is worth mentioning that the OMM targeted mito-QC displayed a rather variable distribution across the mitochondrial network in the epidermal cells, emphasizing the dynamic and heterogeneity of this network. Additionally, as the ATP5A immunostaining marks the IMM, rather than the OMM, this resulted in an incomplete co-localisation.

As a second step, co-staining and live imaging with LysoTracker was performed in larval epidermis in order to confirm the localization of the ‘red-puncta’ with acidic compartments such as lysosomes. A striking co-localization of the mito-QC ‘red-puncta’ was observed with LysoTracker (Figure 3.2 C). As an initial step, these data demonstrated the appropriate targeting of the reporter to the OMM and the correct localisation of the ‘red-only’ puncta with acidic compartments.

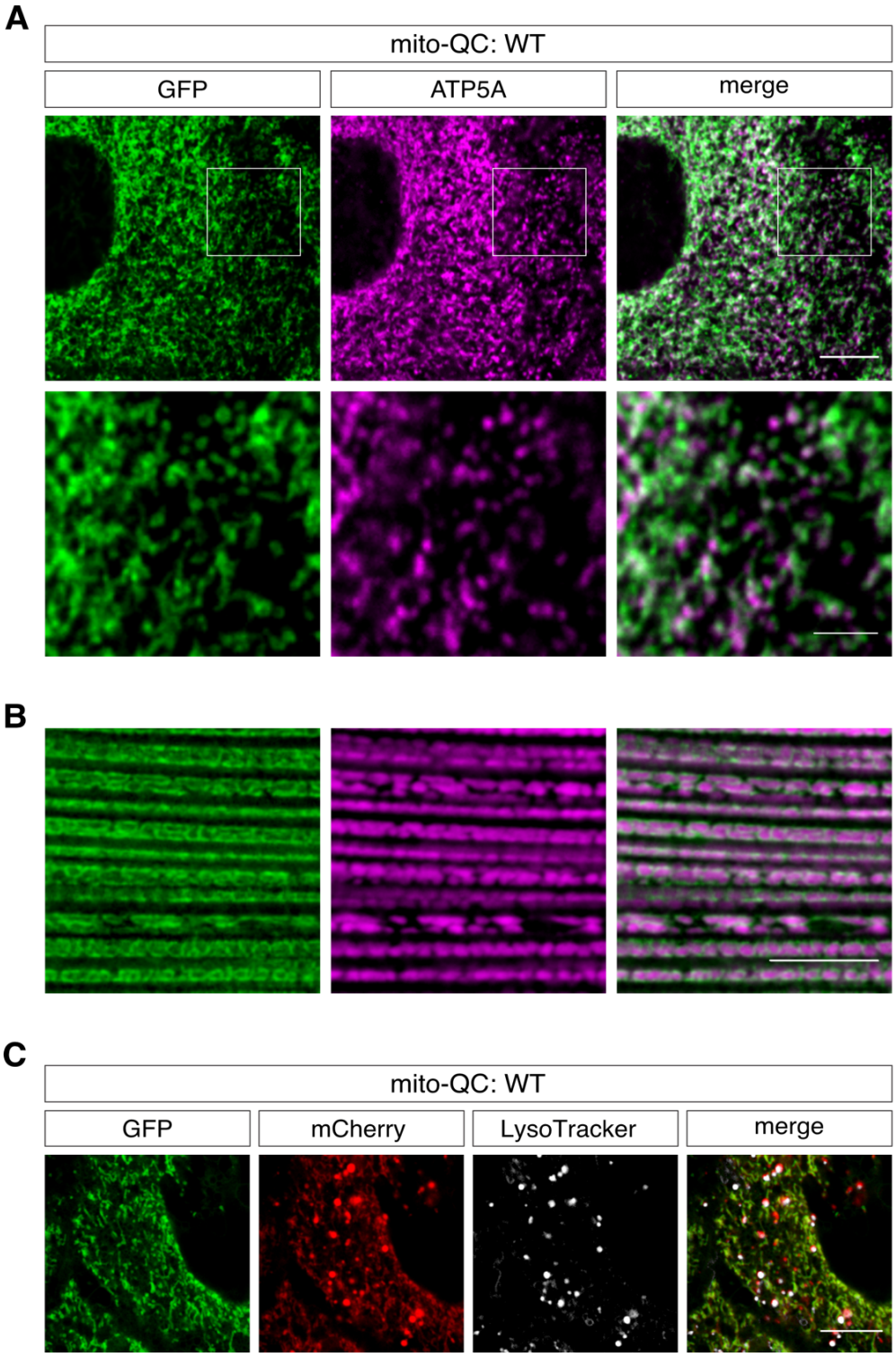

Figure 3.2. Validation of the mito-QC reporter

Immunohistochemical and confocal imaging analysis of (A) larval epidermal cells and (B) adult flight muscle. Mitochondrial localization of the mito-QC was assessed by immunostaining with anti-ATP5A (magenta). (C) Confocal live imaging analysis of larval epidermal cells for mito-QC co-stained for LysoTracker to mark lysosomes. Fluorescence spectra of neutral pH shown in green, acidic pH shown in red. LysoTracker is shown in white. Genotypes analysed are (A and C) *da-GAL4/UAS-mito-QC* and (B) *Mef2-GAL4/UAS-mito-QC*. Scale bars (A and C) = 10 µm, (A) bottom panel = 4 µm.

The next step was to confirm that the signal from the reporter could respond to different conditions, by either enhancing or inhibiting mitophagy. As sustained treatment with mitochondrial depolarizing agents, such as CCCP, was not feasible *in vivo*, the previously reported iron chelator, deferiprone, was used to induce mitophagy (Allen et al., 2013). By feeding animals deferiprone, a 40% increase in mitolysosomes reported by mito-QC was observed by confocal imaging of the larval epidermis (Figure 3.3 A and B). Finally, to further validate the reporter responsiveness, a knockdown of the key autophagy factor *Atg5* with an RNAi transgene was used to reduce the 'red-only' puncta in larval epidermal cells. The ubiquitous knockdown of *Atg5* with *da*-GAL4 driver, showed a 50% reduction in the number of mitolysosomes, confirming their formation during autophagic degradation (Figure 3.3 A and B). Interestingly, this highlights that not all red puncta account for mitophagy, suggesting that there may be other MQC mechanisms, different from mitophagy, that would result in mitochondria being engulfed in acidic compartments such as lysosomes. Alternatively, this 50% reduction in the mitophagy signal could also be the result of a partial knockdown of *Atg5* due to the use of a RNAi. The levels of *Atg5* knockdown were not assessed in the present study.

Taken altogether these results validated the reliability of the mito-QC reporter as well as its faithful role in monitoring mitochondria turnover in *Drosophila*.

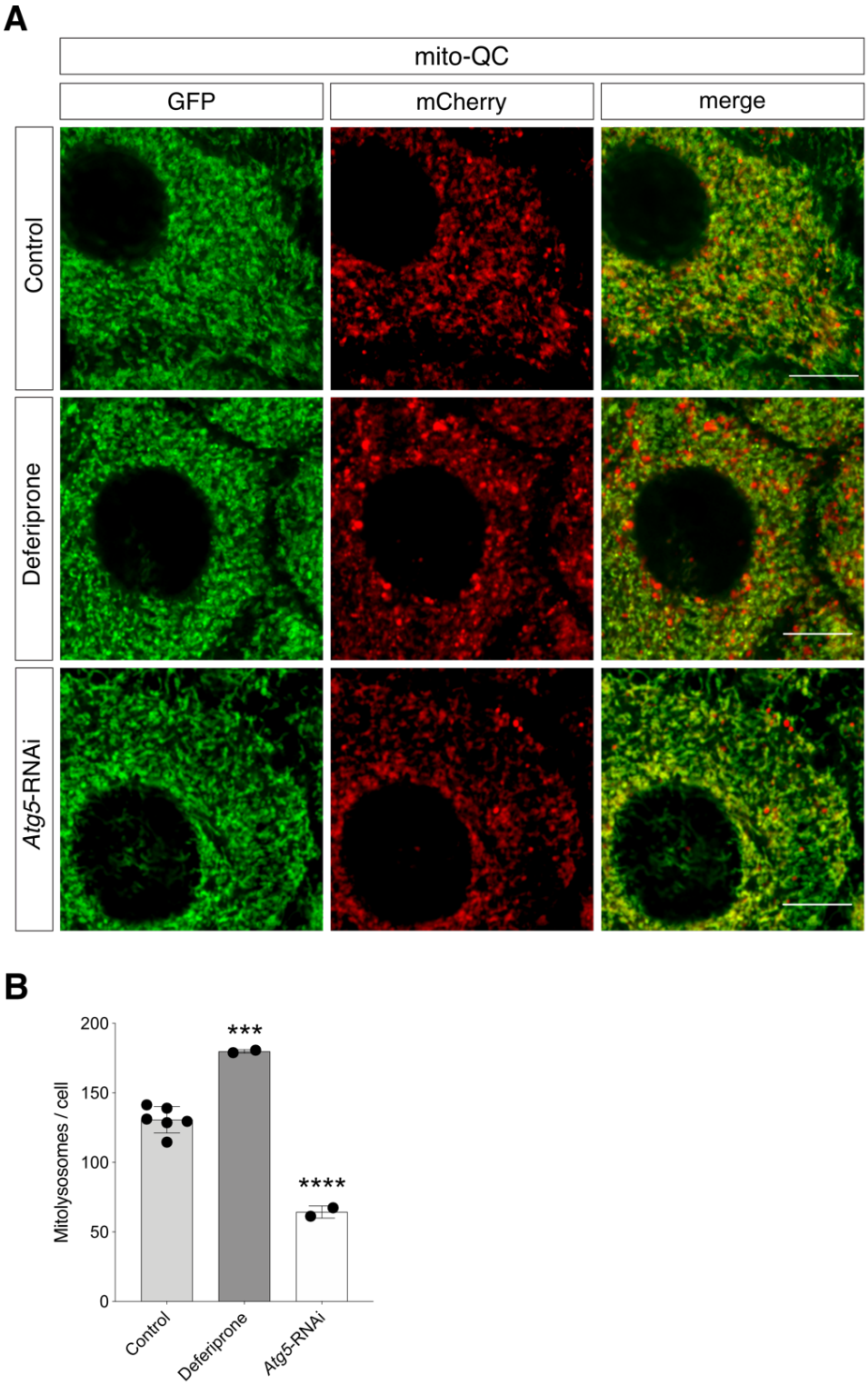

Figure 3.3. mito-QC is an inducible system

(A) Confocal imaging of larval epidermal cells for mito-QC upon expression of *Atg5*-RNAi, or exposure to the iron chelator deferiprone. (B) Quantification of mitolysosomes in mito-QC larval epidermal cells shown in (A). Chart shows mean ± SD of n = 6 animals for (WT) control, n = 2 animals for deferiprone and *Atg5*-RNAi expression. Statistical significance determined by one-way ANOVA with Sidak's post-hoc test; *** $P < 0.001$, **** $P < 0.0001$. Genotypes analysed are *da-GAL4/UAS-mito-QC* and *da-GAL4, UAS-mito-QC/UAS-Atg5*-RNAi. Scale bars = 10 μm.

3.3.2. Mito-QC reveals widespread mitophagy in adult and larval *Drosophila* tissues

After having carried out basic characterisation of the mito-QC, the next step was to evaluate the prevalence of mitolysosomes in various larval and adult tissues under basal conditions. Two larval tissues were first analysed, the epidermal cells, and the ventral ganglion, part of the CNS (Figure 3.4 A). Mitolysosomes were highly abundant in epidermal cells, with around 130 puncta/cell (Figure 3.4 B). Although the number of mitolysosomes in the larval CNS was considerably lower compare to the epidermis, 16 puncta/cell, mitophagy was still widespread in this tissue (Figure 3.4 B). The large difference in the mitolysosome numbers is probably due to the CNS having significantly smaller cells than the epidermis. In contrast, mitolysosomes were almost completely absent in larval muscles (Figure 3.4 A). While the mainstream idea is that mitophagy acts as a general housekeeping mechanism, these results suggest that mitophagy is a rather heterogenous process, that is highly variable across different tissues. After having assessed larval samples, adult fly tissues were dissected. The first tissue analysed was the indirect flight muscle (IFM). IFMs are characterized by a highly ordered arrangement of mitochondria in defined chain-like networks. As IFMs are crucial to power flight, it is believed that this tissue requires high energy demands, which are met by a great number of mitochondria and possibly a significant mitochondria turnover. Moreover, IFMs are the most affected tissues in *Pink1* and *parkin* mutants, exhibiting disorganised muscle fibres, swollen mitochondria and some signs of degeneration, suggesting a role of PINK1 and Parkin in the maintenance of mitochondrial homeostasis in this particular tissue (Park et al., 2006). This led to the hypothesis that IFMs may be a major site of mitophagy and a predominant tissue to analyse when combining the mito-QC with *Pink1/parkin* mutants.

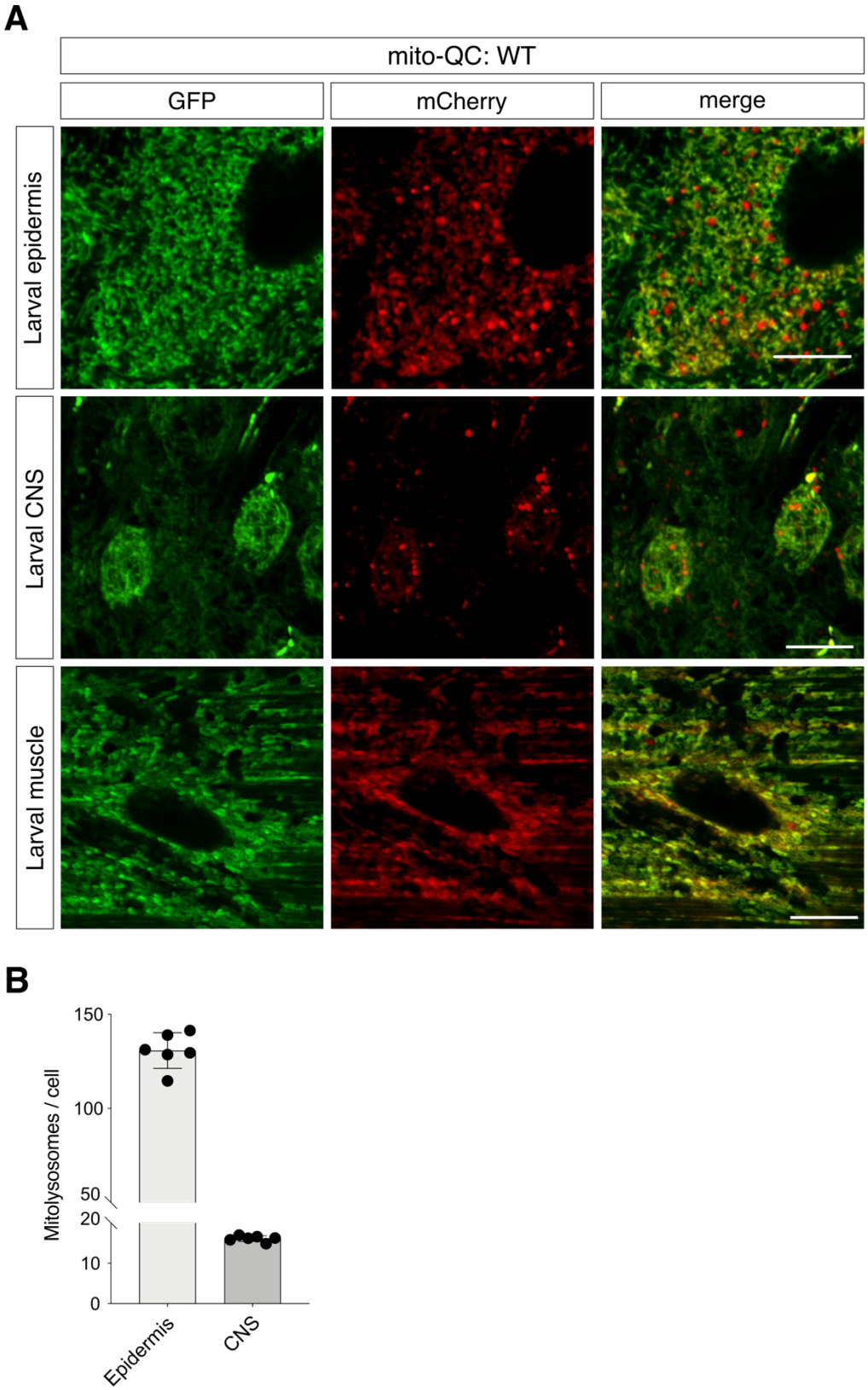

Figure 3.4. mito-QC reveals widespread mitophagy in WT larval tissues

(A) Confocal microscopy of (fixed) larval epidermal cells, CNS and muscles of larvae expressing the mito-QC. Mitolysosomes are evident as GFP-negative/mCherry-positive ('red-only') puncta. (B) Quantification of mitolysosomes shown in (A). Genotype analysed is *da-GAL4/UAS-mito-QC*. Scale bars = 10 μm.

As the mito-QC signal with *da*-GAL4 in the IFM was too weak to be properly imaged, the muscle driver myocyte enhancer factor 2 (*Mef2*)-GAL4 was used instead. Surprisingly, but consistent with observations in larvae, flies overexpressing the mito-QC specifically in the muscle, display a nearly undetectable number of mitolysosomes in pre-adult (late pupal) and 2-day-old adult IFMs (Figure 3.5). As the low amount of mitolysosomes observed in young flies was rather surprising and assuming that mitophagy increases with ageing, flies aged up to 20 days were dissected and imaged. Quantification of WT adult thoraces confirmed an increase in mitophagy with age, as the number of mitolysosomes was significantly higher at 20 days (70 mitolysosomes per mitochondria area) compare to 2 days (12 mitolysosomes per mitochondria area), suggesting an increase in mitochondria turnover over time in this particular tissue (Figure 3.5).

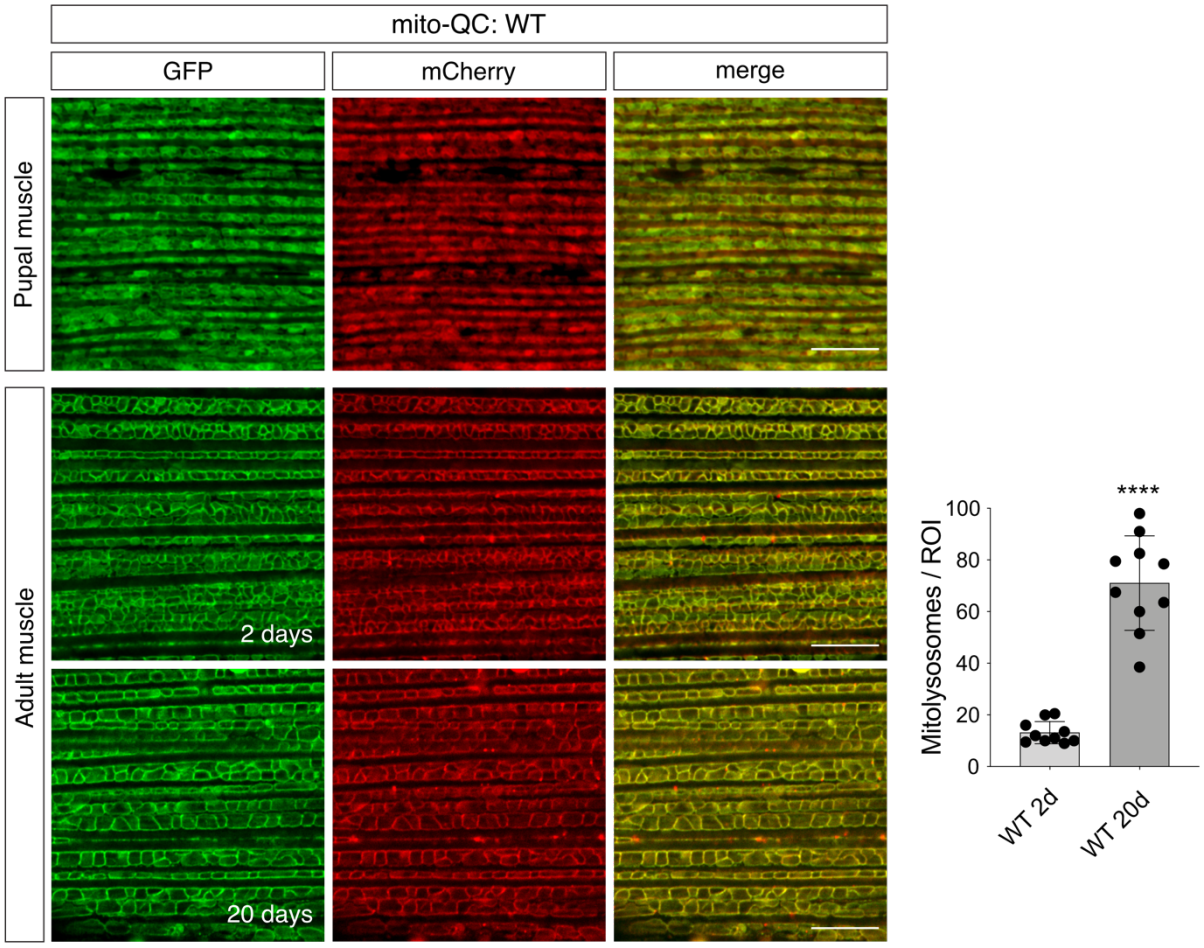

Figure 3.5. mito-QC is less abundant in WT pre-adult (pupal) and adult IFMs

Confocal imaging of IFMs of late pupae, 2- and 20-day-old WT flies using mito-QC. In each fly, 2 random 6400 μm^2 ROI were analysed. Statistical significance determined by Welch's t-test, *** $P < 0.001$. Genotype analysed is *Mef2-GAL4/UAS-mito-QC.* Scale bars = 10 μm.

Due to the low level of mitophagy signal in young and aged flies, another muscle specific driver, labelled 'new *Mef2*-GAL4' for the purpose of this study, was used to express mito-QC and compare the mitophagy signal to the 'original' *Mef2*-GAL4 (Figure 3.6 A, top panel). Although both *Mef2*-GAL4 are muscle specific drivers, expression of the mito-QC with the 'original' *Mef2*-GAL4 showed significantly lower levels of mitophagy compare to the 'new *Mef2'*GAL4*'* in young and aged flies (Figure 3.6 A). A simple explanation can be based on different expression levels between the two drivers, implying that one GAL4 drives a weaker expression of the mito-QC. Interestingly, western blot analysis of flies expressing the mito-QC using both drivers did not show any visible difference (Figure 3.6 B). A band was observed at ≃70 kDa when immunoblotting with an anti-DsRed antibody, corresponding to the mito-QC molecular weight as shown previously in Figure 3.1 A. This suggests that equivalent expression levels of the mito-QC were induced using these two *Mef2*-GAL4 (Figure 3.6 B). While expression of the mito-QC with these two muscle drivers led to some variations in the levels of mitophagy observed in adult IFMs, they both highlight significant lower levels of mitophagy in young animals, which seem to increase with aging (Figure 3.6 A, bottom panel). As the two GAL4 appear to drive similar expression levels of the mito-QC it remains unclear why variabilities in the number of mitolysosomes were observed. One potential explanation relies on the fact that the two driver lines were established in different genetic backgrounds which might introduce some degree of variability. Additionally, mitophagy is likely to be intrinsically variable between individuals.

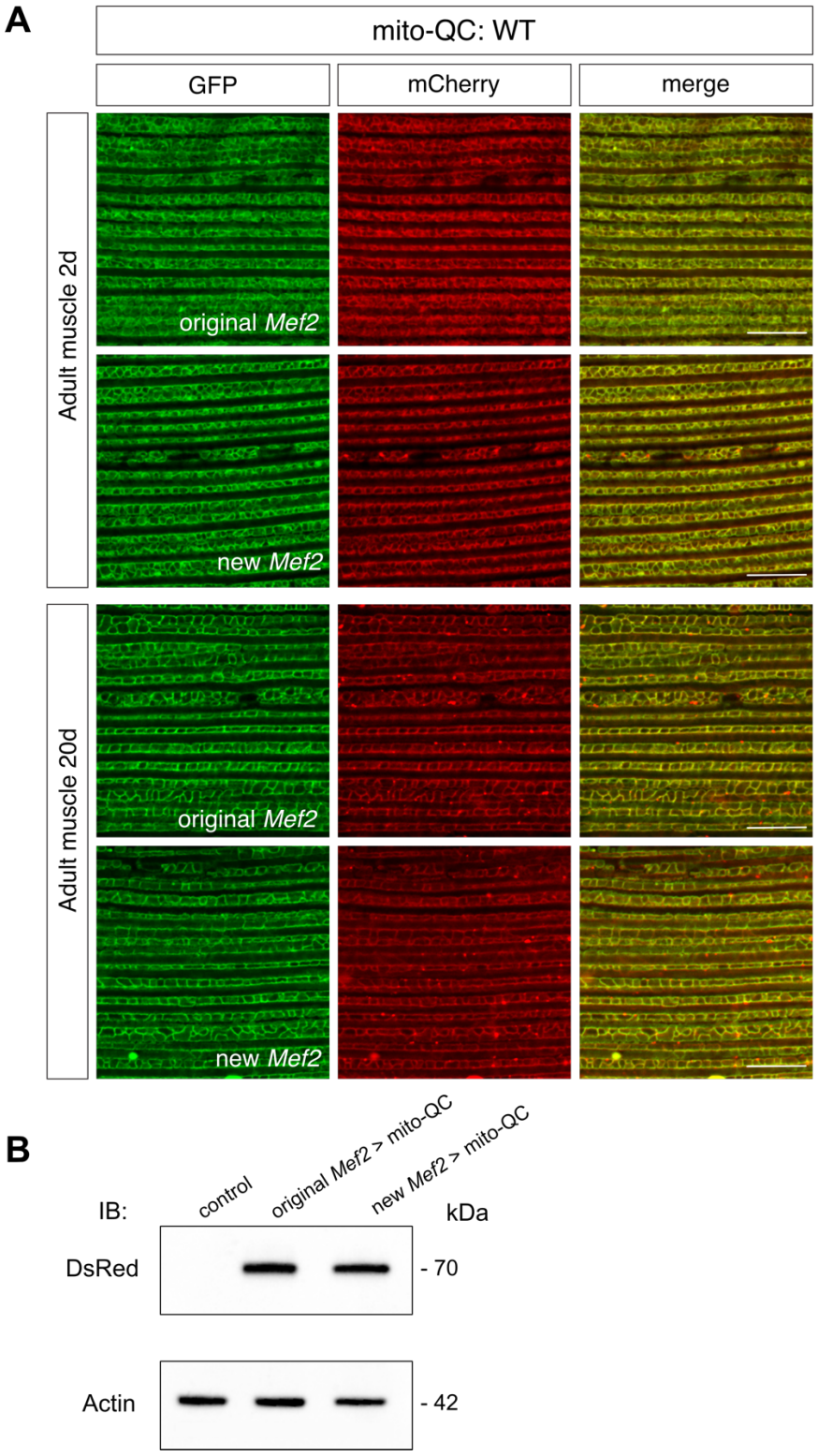

Figure 3.6. Variable mitophagy levels using different muscle drivers

(A) Confocal imaging of IFMs of 2- and 20-day-old WT flies using mito-QC. (B) Immunoblotting of 2-day-old flies expressing the mito-QC with two *Mef2*-GAL4 drivers 'original' and 'new'. Immunoblot was probed with the DsRed antibody. Actin antibody was used as a loading control. Control genotype is non-transgenic w^{1118}. Genotypes analysed are 'original' *Mef2-GAL4/UAS-mito-QC* and 'new' *Mef2-GAL4/UAS-mito-QC.* Scale bars = 10 μm.

The second adult tissue analysed was adult brain. These post-mitotic, highly energetic tissues would be expected to accumulate substantial mitochondrial damage over time and therefore more likely to undergo mitophagy. Mito-QC was expressed in the brain using the neuronal driver *nSyb*-GAL4 (neuronal Synaptobrevin), WT adult fly brains were dissected and the medial region of the posterior protocerebrum was imaged at 2 and 30 days (for location of this region see Figure 2.1). As for the larval tissues shown previously, mitolysosomes were widespread in this brain region, with around 3 mitolysosomes per cell (Figure 3.7 A). Similar to adult IFMs, the number of mitolysosomes in this particular brain region was slightly increased in flies aged to 30 days, rising up to 4 mitolysosomes per cell (Figure 3.7 A). Although these numbers are slightly lower than the ones obtained from larval CNS, it is worth mentioning that these neurons are smaller than the cells analysed in the larval brain. Finally, mito-QC was selectively expressed in dopaminergic neurons via the *TH*-GAL4 driver and mitolysosomes were quantified in the paired posterior lateral 1 (PPL1) cluster (for location of this region see Figure 2.1). This population of ~14 DA neurons was particularly assessed as aged *Drosophila Pink1* and *parkin* mutants exhibit a reduced number of DA neurons in this cluster. Analysis of the PPL1 cluster of 2-day-old flies, revealed an abundant number of mitolysosomes, with an average of 5 mitolysosomes per cell (Figure 3.7 B). Interestingly, a slight increase was observed at 10 days rising up to 6 mitolysosomes/cell, although it did not appear to increase beyond that in flies aged up to 30 days (Figure 3.7 B).

My results suggest that mitophagy is a widespread process happening from the larval to the adult stage of the fly. Observations from larval CNS and epidermis showed high levels of mitophagy that were maintained throughout adulthood, especially in adult brains. However, mitophagy signal was almost undetectable in adult IFMs, consistent with larval muscles. This strongly highlights the heterogeneity of mitophagy, whereby different tissues exhibit various degrees of mitochondria turnover, reflecting unique metabolic demands and cellular signalling pathways. Interestingly, results from adult IFMs and two different neuronal populations of aged adult brains suggest a slight increase of mitophagy with age, although further work is needed to determine how mitophagy levels are affected by the aging process.

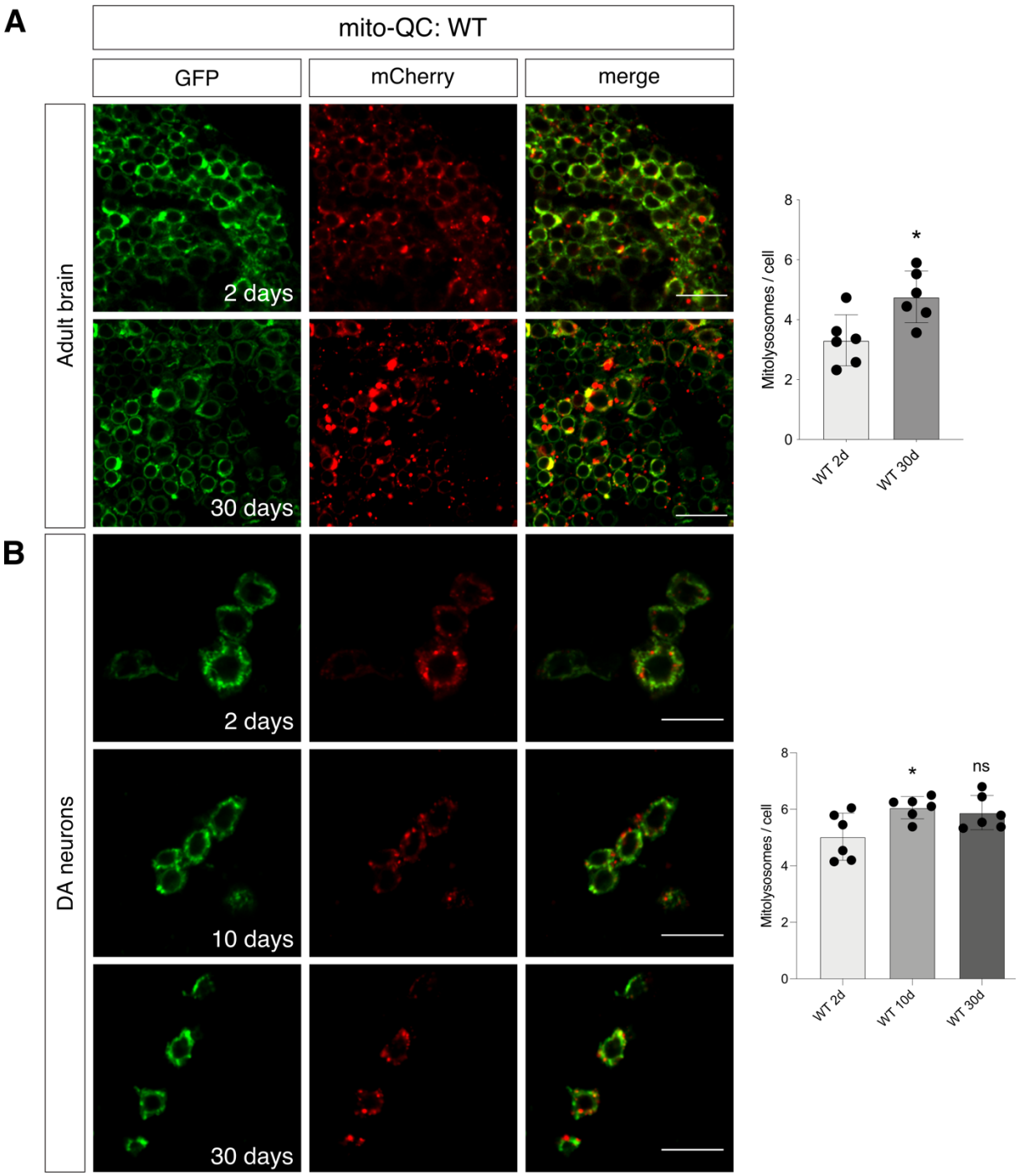

Figure 3.7. mito-QC shows high levels of mitophagy in WT adult brains

Confocal imaging of mito-QC reporter (fixed) in (A) adult brain of 2-day-old flies (medial region of the posterior protocerebrum) and (B) DA neurons (PPL1 cluster) at 2-, 10- and 30-days. Graphs show quantification of mitolysosomes from the images. Chart show mean ± SD of n = 6 animals for each condition. Number of cells analysed: WT brain 2 days = 220, WT brain 30 days = 240, WT DA neurons 2 days = 100, WT DA neurons 10 days = 77 and WT DA neurons 30 days = 78. Statistical significance determined by Welch's t-test and by one-way ANOVA with Sidak's post-hoc test for multiple comparison; * $P < 0.05$ and ns = non-significant. Genotypes analysed are (adult brain) *UAS-mito-QC/+; nSyb$_{ZH86FB}$-GAL4/+* and (DA neurons) *UAS-mito-QC/+; TH-GAL4/+*. Scale bars = 10 µm.

3.3.3. Validation of the mt-Keima mitophagy reporter

In order to obtain complementary data, a similar groundwork was conducted with the matrix-targeted mt-Keima reporter. Two constructs were generated by Prof. M Clague's group (University of Liverpool) and A. Martinez-Zarate and U. Mayor (University of the Basque Country): mt-Keima II and mt-Keima III, on the 2nd and 3rd chromosome, respectively. Additionally, a recombinant line with the ubiquitous driver tubulin (*tub*)-GAL4 was established in order to constitutively drive the expression of the reporter. As a first validation step, expression levels of the constructs driven by *da*-GAL4 were assessed by western blotting using an anti-Keima antibody. A band at 27 kDa, corresponding to the molecular weight of the Keima protein was observed in all the lysates expressing the reporter (Figure 3.8 A). Using *da*-GAL4, the expression levels of both mt-Keima lines were similar. However, it is worth mentionning that the mt-Keima expression appeared weaker with *da*-GAL4 compare to *tub*-GAL4 (Figure 3.8 A). For this reason, future work was performed using the recombinant line *tub*-GAL4, mt-Keima. In addition to immunoblotting experiments, flies' fitness was assessed by climbing and flight assays. No significant differences between the control and the mt-Keima flies were observed, thus confirming that the reporter expression was benign to the flies (Figure 3.8 B).

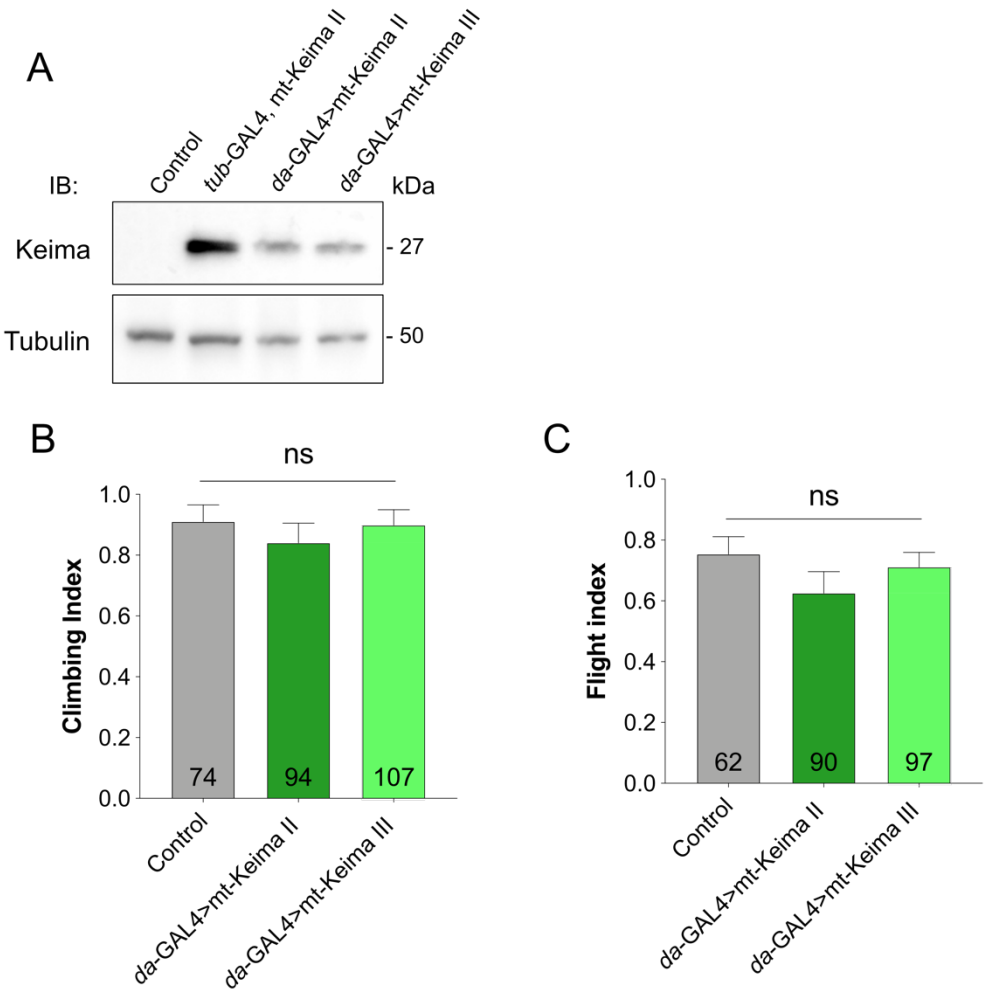

Figure 3.8. Expression of mt-Keima is benign in *Drosophila*

(A) Immunoblotting of three transgenic lines expressing the mt-Keima induced by the ubiquitous drivers, *tub*-GAL4 and *da*-GAL4. Immunoblot was probed with the indicated antibodies. Tubulin antibody was used as a loading control. Control genotype is non-transgenic w^{1118}. Locomotor assays for (B) climbing and (C) flight ability of flies expressing the mt-Keima with *da*-GAL4. Charts show mean ± 95% CI. Number of animals analysed is shown in each bar. Statistical analysis was determined by Kruskal-Wallis non-parametric test with Dunn's post-hoc correction for multiple comparisons; ns = non-significant. Control genotype for behaviour is *da-GAL4/UAS-mitoGFP*.

In order to validate the correct location of the mt-Keima to the mitochondria, co-localization of the Keima protein with the ATP5A protein was performed in larval epidermis. Unlike the mito-QC, which showed a less uniform distribution across the mitochondrial network, the mt-Keima precisely co-localized with the ATP5A immunostaining (Figure 3.9 A). Similar to the mito-QC, the mitolysosomes are marked by a fluorescence spectral shift of the Keima protein, with an increased signal from 561 nm excitation when under more acidic conditions. As for the mito-QC, a striking co-

localization of mt-Keima 'mitophagy' puncta was observed with acidic compartments, such as lysosomes when co-stained with LysoTracker (Figure 3.9 B).

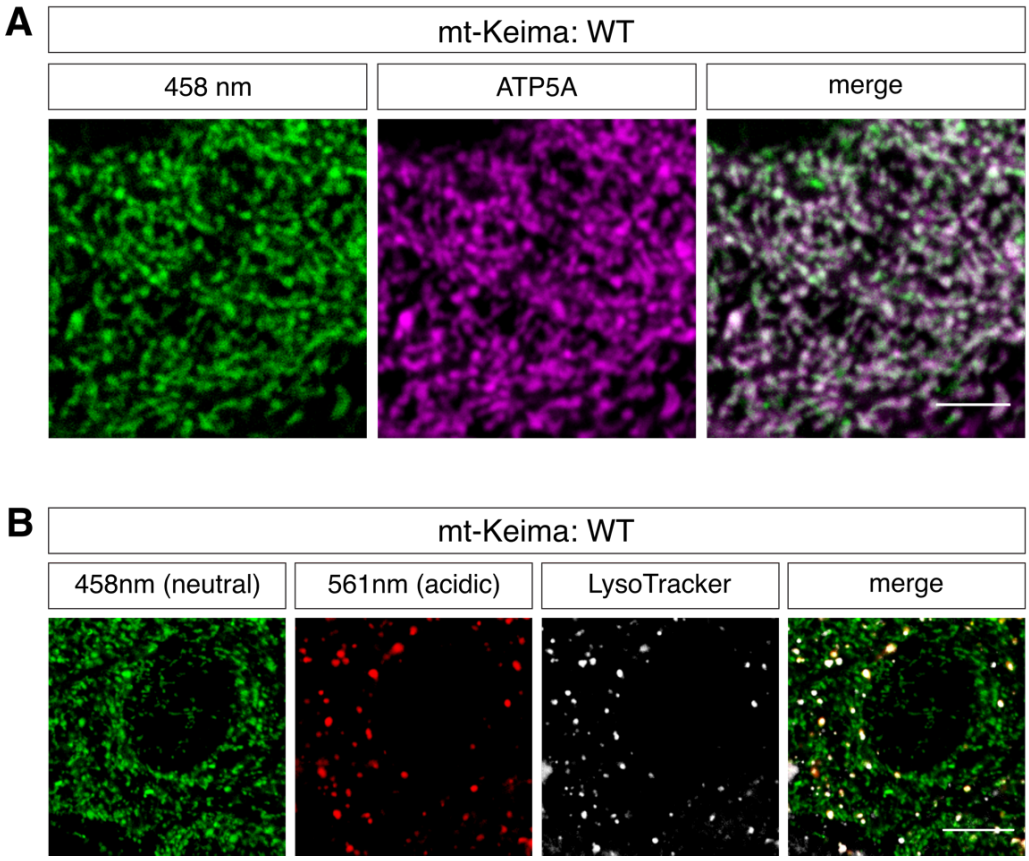

Figure 3.9. Validation of the mt-Keima reporter

(A) Immunohistochemical and confocal imaging of larval epidermal cells. The mitochondrial localisation of the mt-Keima (green) was assessed by immunostaining with anti-ATP5A (magenta). (B) Confocal live imaging analysis of larval epidermal cells for mt-Keima co-stained for LysoTracker to mark lysosomes. Fluorescence spectra of neutral pH shown in green, acidic pH shown in red. LysoTracker is shown in white. Genotype analysed is *tub-GAL4*, *UAS-mt-Keima/+*. Scale bars A = 4 µm and B = 10 µm.

Feeding flies with the iron chelator deferiprone resulted in a noticeable increase in the mitolysosome number in the larval epidermis. In contrast, when the mt-Keima reporter was combined with an *Atg5*-RNAi, mitolysosomes were almost entirely absent (Figure 3.10).

Altogether, these results were in line with the ones obtained with the mito-QC reporter.

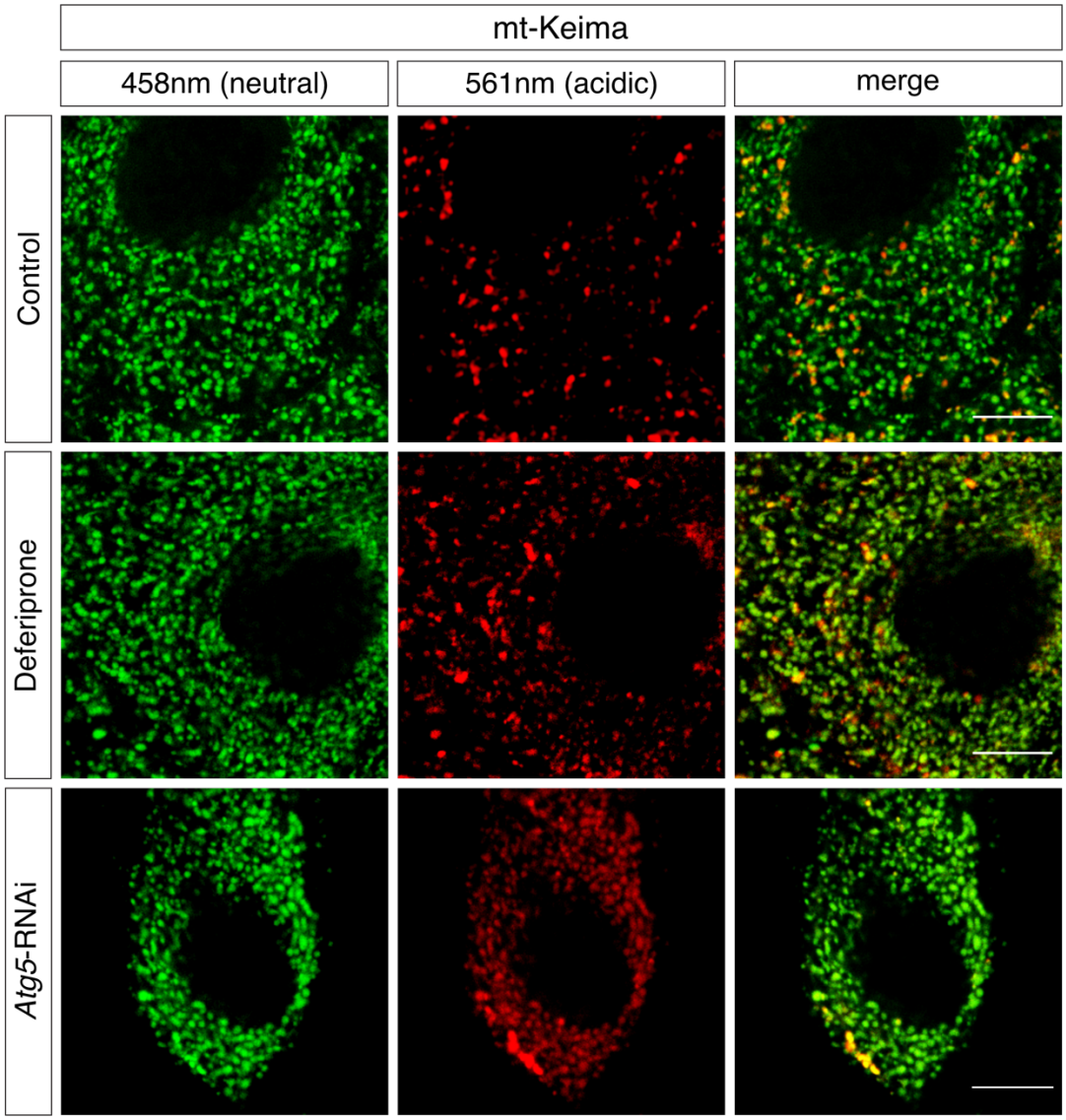

Figure 3.10. mt-Keima is an inducible reporter

Confocal live imaging of larval epidermal cells for mt-Keima upon expression of an *Atg5*-RNAi transgene to inhibit autophagy, or exposure to the iron chelator deferiprone to induce mitophagy. Genotypes analysed are (control) *tub-GAL4*, *UAS-mt-Keima/+* and *tub-GAL4*, *UAS-mt-Keima*/*UAS-Atg5*-RNAi. Scale bars = 10 μm

3.3.4. Mt-Keima confirms abundant mitophagy in adult and larval *Drosophila* tissues

The same previously described larval and adult tissues were analysed to assess mitophagy under basal conditions using the mt-Keima reporter. Larval epidermis, CNS and muscles were dissected. As the properties of the fluorophore are not compatible with fixation, the mt-Keima reporter can only be imaged using live microscopy. All tissues revealed abundant mitolysosomes, although slightly less puncta were visible in larval muscles compared to the other tissues (Figure 3.11).

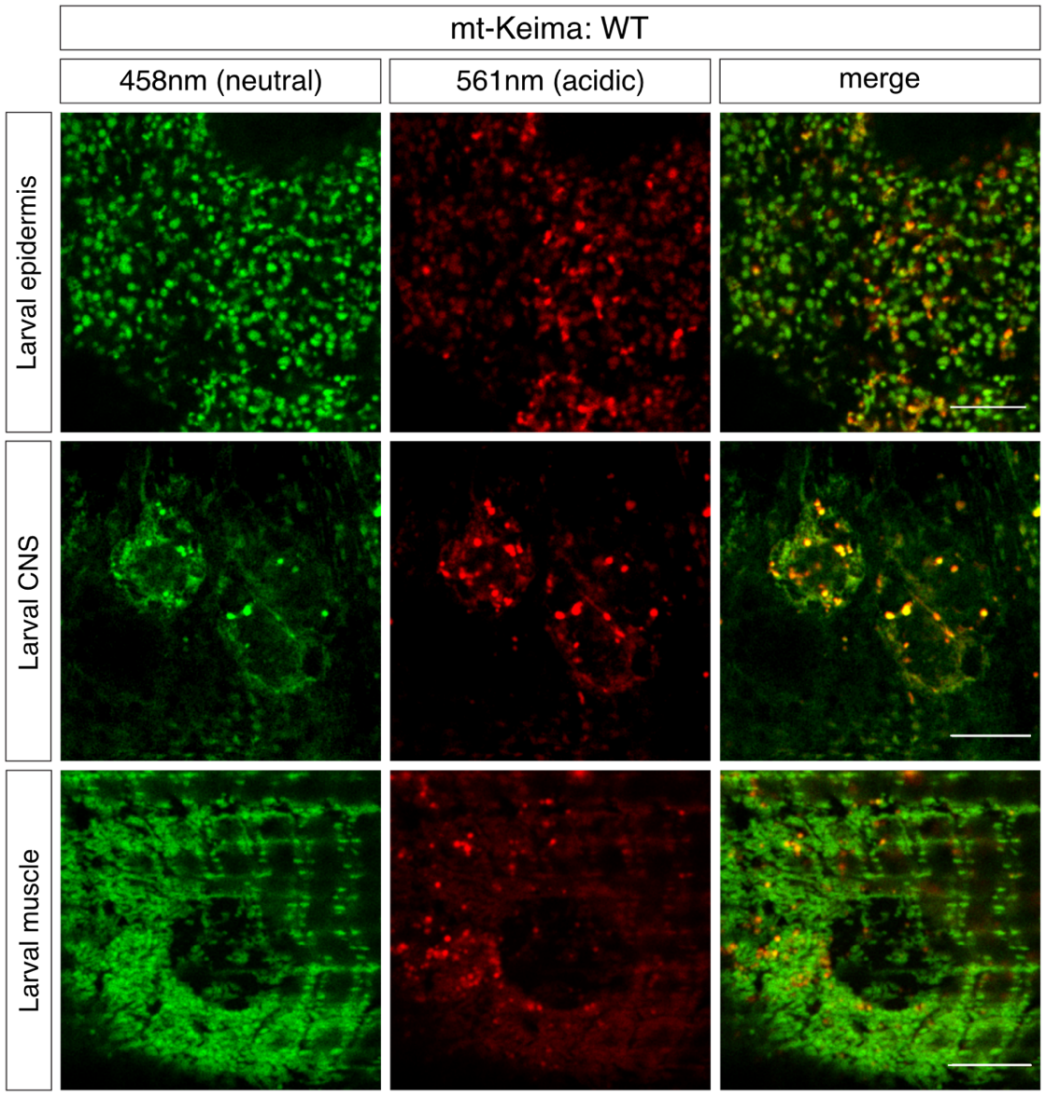

Figure 3.11. mt-Keima confirms widespread mitophagy in WT larval tissues

Confocal live microscopy imaging of WT larval epidermal cells, CNS and larval muscles visualising mt-Keima. Mitolysosomes are evident as red puncta. Genotype analysed is *tub-GAL4*, *UAS-mt-Keima/+*. Scale bars = 10 µm.

Finally, as previous results obtained with the mito-QC showed low levels of mitophagy in IFMs, it was interesting to compare this tissue with the mt-Keima reporter. In order to make sure that the lower signal observed in adult IFMs was not due to the fixation of the mito-QC, flies expressing the reporters under the *Mef2*-GAL4 driver were dissected side by side and imaged by live microscopy at the same time (Figure 3.12). When specifically expressed in adult IFMs, the mt-Keima revealed some levels of mitophagy, albeit much lower than in other tissues (Figure 3.12). Additionally, the fixation process did not to impact on the mitophagy levels in IFMs, suggesting that this particular tissue seem to undergo substantially less mitophagy compare to other tissues.

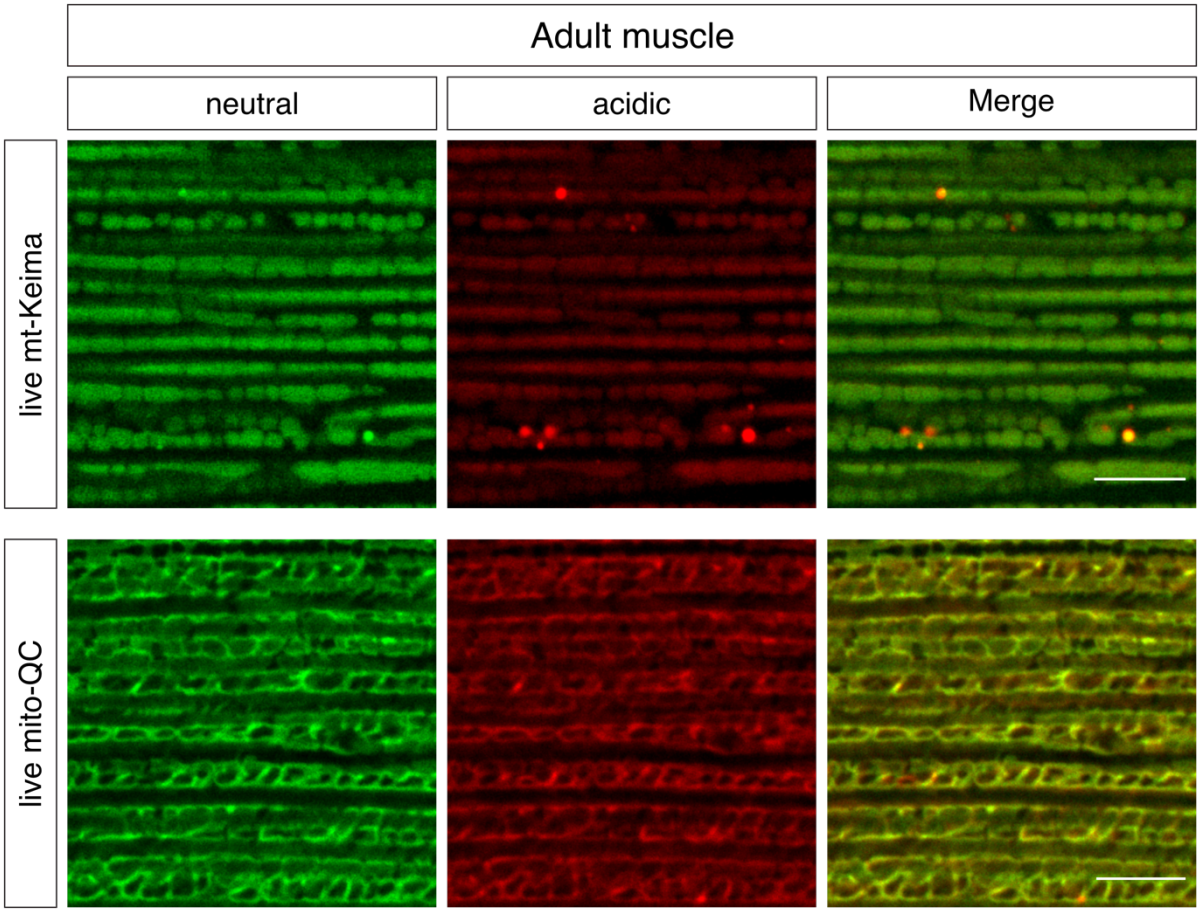

Figure 3.12. Live imaging of mt-Keima and mito-QC in the IFMs

Confocal live microscopy of WT adult IFMs visualising mt-Keima and mito-QC. Genotypes analysed are *Mef2-GAL4*/*UAS-mt-Keima* and *Mef2-GAL4*/*UAS-mito-QC.* Scale bars = 10 µm.

These results were similar to the mito-QC ones, suggesting that overall both tools report comparable levels of mitophagy. During this stage of analysis, it became apparent that the mt-Keima signal was markedly weaker than the mito-QC signal but was also rapidly bleaching upon extended exposure or repeated scanning, especially the acidic (561 nm excitation) spectrum (Figure 3.13). For this reason, the subsequent experiments were mostly conducted with the mito-QC. Additionally, the ability to fix the samples with the mito-QC makes it an easier reporter to work with.

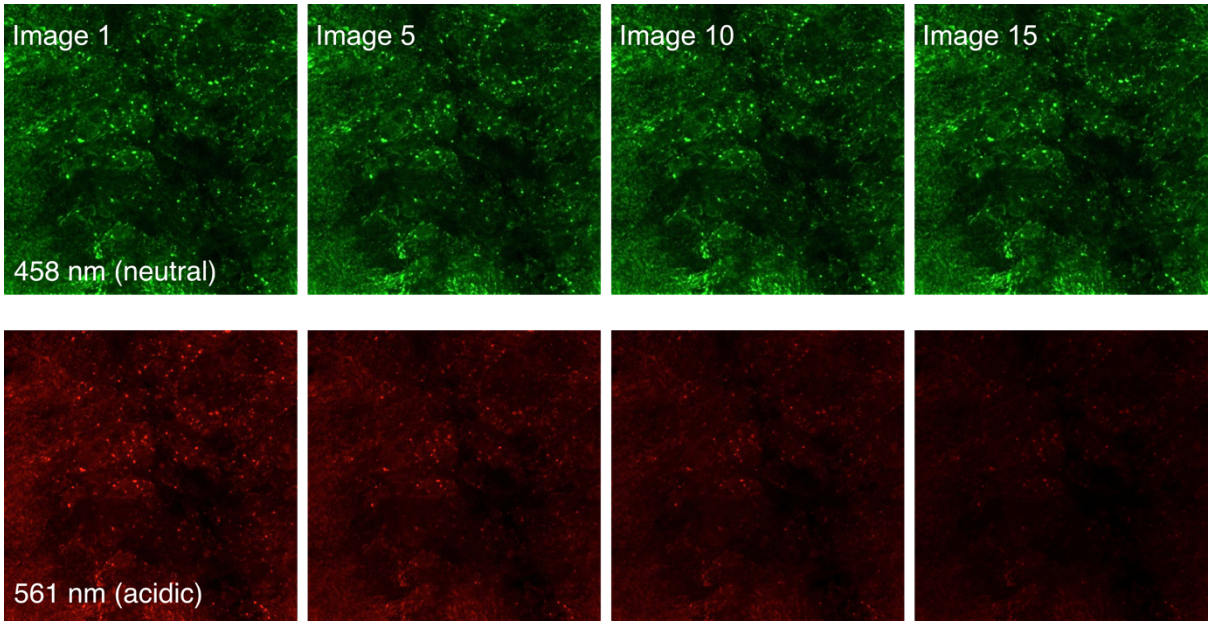

Figure 3.13. mt-Keima signal rapidly bleaches.

Confocal live imaging of larval CNS for mt-Keima results in rapid bleaching particularly of the acid-enhanced (561 nm excitation) spectrum. A series of 15 images of a single plane were collected. Genotype analysed is *tub-GAL4*, *UAS-mt-Keima/+*. Scale bar = 10 µm.

During the preparation of this study, a new mt-Keima *Drosophila* line established by another group in Leuven, was published (Cornelissen et al., 2018). Tom Cornelissen kindly shared these flies with us. In order to compare the fluorescent signal of their new reporter, which is named 'mt-Keima (Leuven)' for the purpose of this study, larval and adult tissues were dissected and imaged using live microscopy. Simultaneously, levels of mitophagy were qualitatively assessed in larval brain and adult IFMs of young and old flies (Figure 3.14). Although, the mt-Keima (Leuven) signal was too weak to provide high resolution images, the levels of mitophagy were similar to our two

reporters. However, unlike our reporters, the mt-Keima (Leuven) did not report any increase of mitophagy in aged IFMs (Figure 3.14).

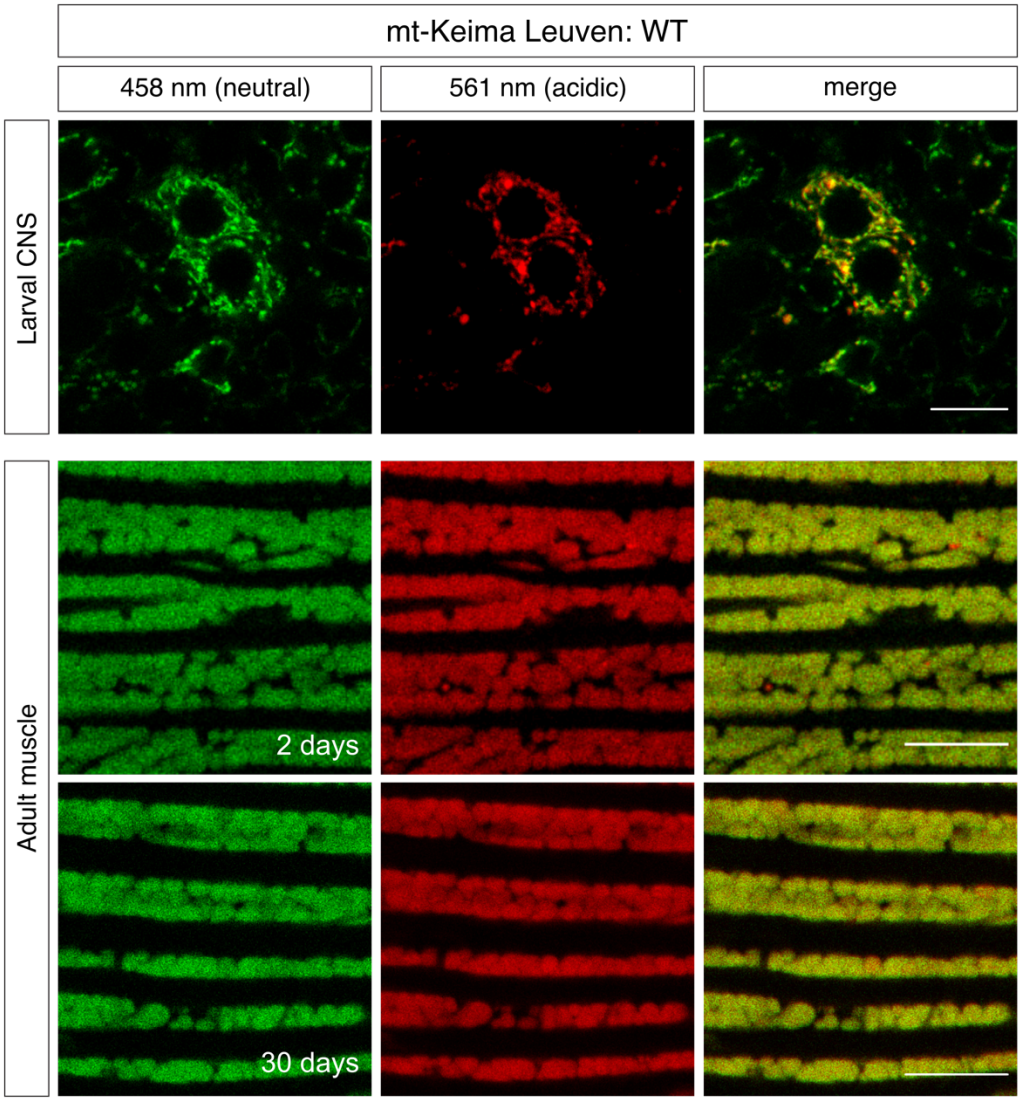

Figure 3.14. Analysis of the mt-Keima (Leuven) in larval CNS and adult IFMs

Confocal live microscopy analysis of larval CNS and adult IFMs visualising the mt-Keima (Leuven) in 2- and 30-day-old flies. Genotype analysed are *nSyb-GAL4/UAS-mt-Keima* (Leuven) and *Mef2-GAL4*/*UAS-mt-Keima* (Leuven). Scale bars = 10 µm.

3.3.5. Basal mitophagy is minimally affected by loss of Pink1

3.3.5.1. Analysis of larval epidermis and CNS of *Pink1* mutants

The mito-QC and mt-Keima mitophagy reporters were combined with the well-characterised *Pink1* (*Pink1*^{B9}) mutants. The same previously described larval tissues were analysed in a *Pink1* mutant background. Surprisingly, quantitative analysis revealed no differences in mitolysosome numbers between WT and *Pink1* null mutants in larval epidermal cells and muscles. A slight decrease in mitophagy, where the difference in *Pink1* mutants just reached significance, was observed in larval CNS (Figure 3.15). To further confirm these unexcepted results, *Pink1* mutants were combined with the mt-Keima and qualitatively assessed for mitophagy. Consistent with the mito-QC, larval epidermis and CNS of the mt-Keima in a *Pink1* mutant background did not show any differences in the mitophagy signal (Figure 3.16).

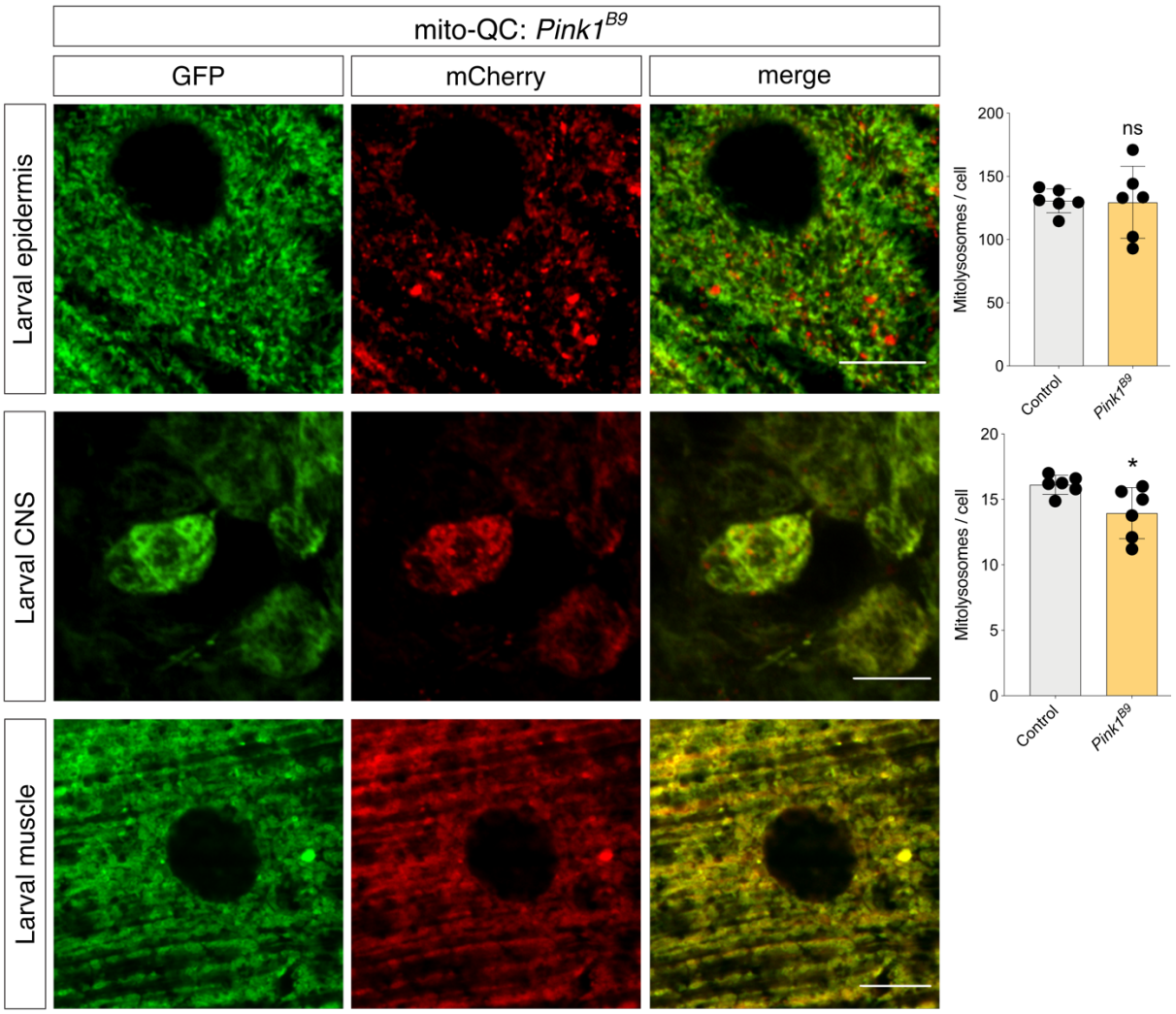

Figure 3.15. Basal mitophagy is minimally affected in larval tissues of *Pink1* mutants

Confocal microscopy analysis of mito-QC reporter in larval epidermis, CNS and muscle of *Pink1*^{B9} mutants. Charts show quantification of mitolysosomes, mean ± SD of n = 6 animals. Number of cells analysed: epidermis, control = 29, *Pink1*^{B9} = 29; CNS, control = 28 and *Pink1*^{B9} = 26.=. Statistical significance determined by Welch's *t*-test; * $P < 0.01$ and ns = non-significant. Control genotype is *da-GAL4/UAS-mito-QC* shown and used for quantification in Figure 3.4. Genotype analysed is *Pink*^{B9}*/Y; da-GAL4/UAS-mito-QC*. Scale bars = 10 μm.

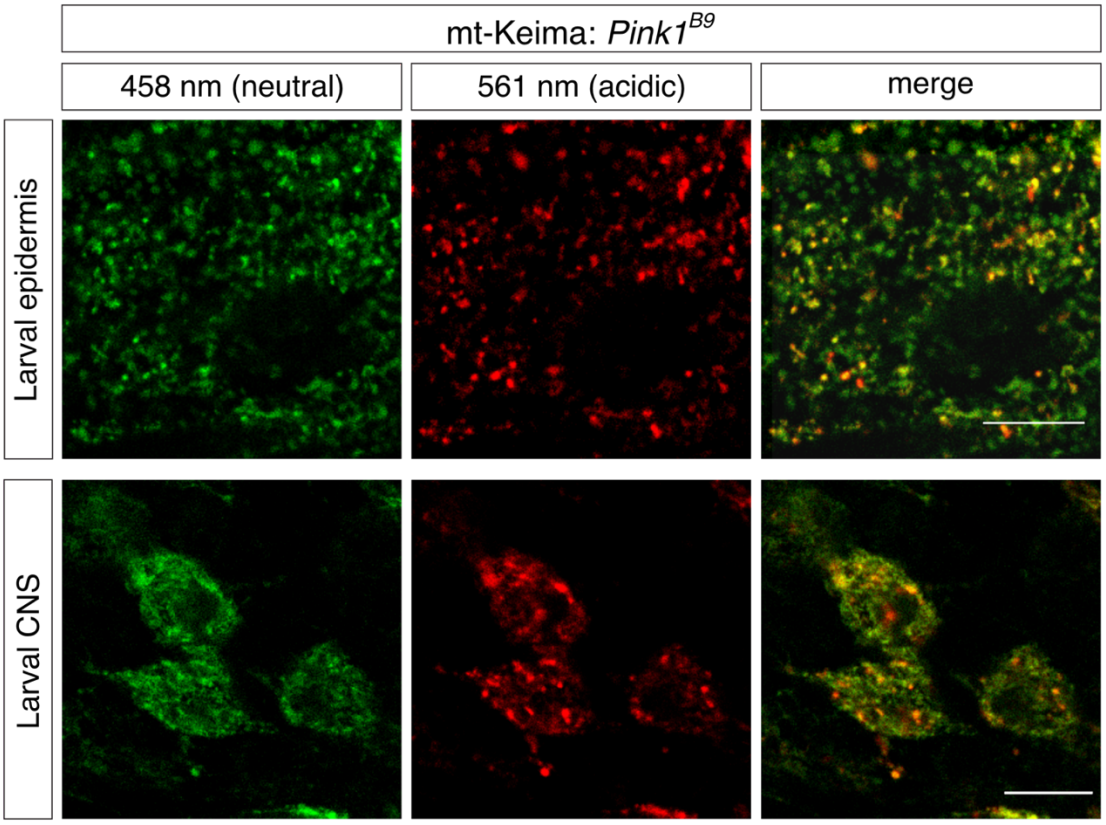

Figure 3.16. mt-Keima validates the mito-QC results in *Pink1* mutant larval tissues

Live confocal imaging of larval epidermis and CNS visualising the mt-Keima in *Pink1*^{B9} mutants. Genotype analysed is *Pink1*^{B9}*/Y; tub-GAL4*, *UAS-mt-Keima/+.* Control genotype is *tub-GAL4*, *UAS-mt-Keima/+* shown in Figure 3.11. Scale bars = 10 μm.

3.3.5.2. Analysis of adult IFMs and CNS of *Pink1* mutants

Considering the severe mitochondrial disruption and tissue degeneration occurring in adult flight muscles of *Pink1* mutants, this tissue appeared as the predominant tissue to look at when combining the mitophagy reporters with *Pink1* null mutants. Results presented earlier have shown fewer mitolysosomes in WT late-pupal and adult muscles at 2 days old, and this low level of mitophagy was maintained in *Pink1* mutant IFMs (Figure 3.17). When the flies were aged up to 30 days, two distinct mitophagy patterns were observed. First, although not quantified, an increase in the mitophagy signal was detected in the most 'intact bundles' of *Pink1* mutant IFMs, consistent with observations in WT animals (Figure 3.17 'intact bundle'). Second, in the most profoundly damaged bundles, mitolysosomes were absent, implying an absence of mitophagy (Figure 3.17 bottom panel 'degenerate bundle').

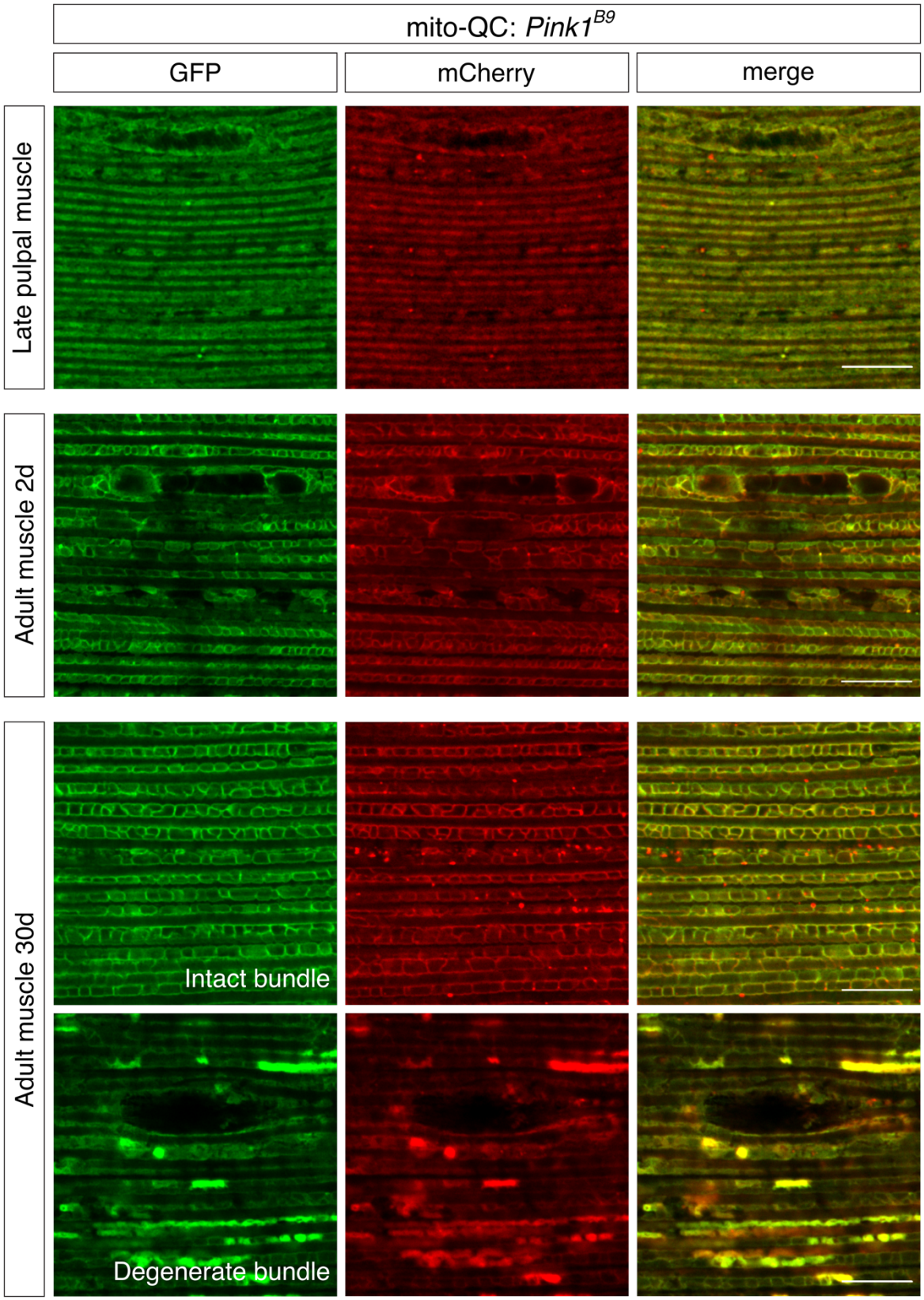

Figure 3.17. Basal mitophagy is minimally affected in late pupal and adult IFMs of *Pink1* mutants

Confocal microscopy analysis of mito-QC in IFMs of late pupal, 2- and 30-day-old *Pink1*^{B9} mutants. Genotype analysed is *Pink1*^{B9}*/Y;* 'original' *Mef2-GAL4/UAS-mito-QC.* Control genotype is original' *Mef2-GAL4/UAS-mito-QC* shown in Figure 3.5. Scale bars = 10 μm.

Finally, *Pink1* mutants were combined with mito-QC expressed in adult brains and more selectively in DA neurons, via *nSyb*-GAL4 and *TH*-GAL4 drivers respectively. Again, abundant mitolysosomes were observed in the adult brains of 2-day-old *Pink1* mutants (Figure 3.18 top panel). It is well-documented that *Drosophila* models of PD, such as *Pink1/parkin* recapitulate the preferential degeneration of DA neurons observed in human PD. It has remained an open question whether the loss of DA neurons is linked to an impaired mitophagy. To address this, *Pink1* mutant DA neurons of the PPL1 cluster were imaged and analysed at 2, 10 and 30 days. Somewhat surprising, but consistent with observations in other tissues, a substantial number of mitolysosomes were visible in these specific neurons and the amount of mitophagy signal did not markedly increase with age, similar to the results in the WT animals (Figure 3.18 bottom panel). Overall, these results strongly suggest that loss of Pink1 does not perturb basal mitophagy in larval and adult *Drosophila* tissues, including adult IFMs and DA neurons, two tissues particularly damaged in *Pink1* mutants.

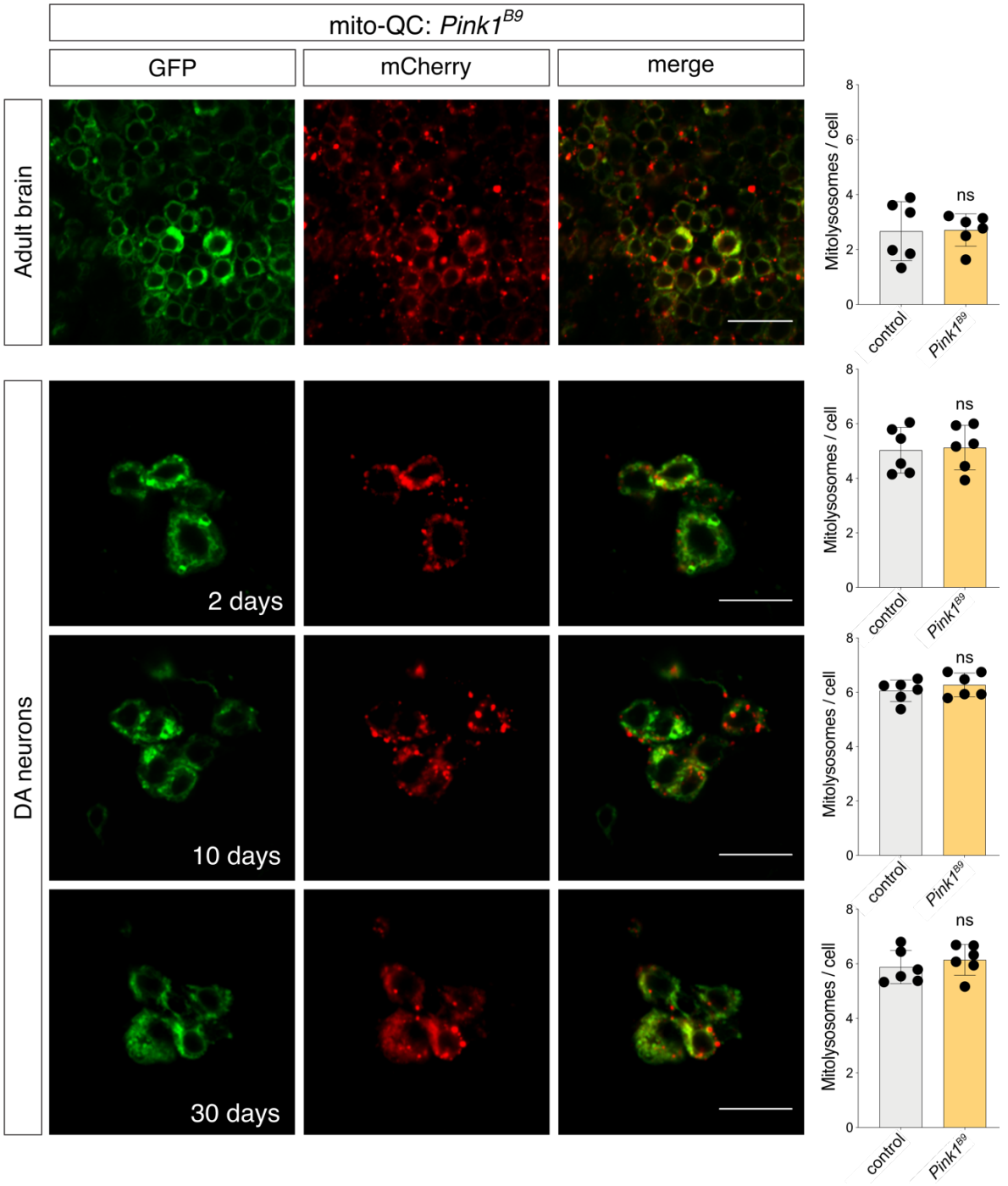

Figure 3.18. Basal mitophagy is minimally affected in adult brains of *Pink1* mutants

Confocal imaging of mito-QC reporter in *Pink1*^{B9} mutant adult brains (medial region of the posterior protocerebrum) at 2-day old and DA neurons of the PPL1 cluster at 2-, 10- and 30-day-old. Charts show quantification of mitolysosomes, mean ± SD of n = 6 animals. Number of cells analysed: adult brain, control = 74, *Pink1*^{B9} = 66; DA neurons 2 days, control = 100, *Pink1*^{B9} = 54; 10 days, control = 77, *Pink1*^{B9} = 80; 30 days, control = 78, *Pink1*^{B9} = 82. Control genotypes are (adult brain) *UAS-mito-QC/+; nSyb*$_{ZH86FB}$*-GAL4/+* and (DA neurons) *UAS-mito-QC/+; TH-GAL4/+* shown and used for quantification of WT control samples in Figure 3.7. Statistical significance determined by Welch's *t*-test; ns = non-significant. Genotypes analysed are (adult brain) *Pink*^{B9}*/Y; UAS-mito-QC/+;nSyb*$_{ZH86FB}$*-GAL4/+* and (DA neurons) *Pink*^{B9}*/Y; UAS-mito-QC/+; TH-GAL4/+*. Scale bars = 10 µm.

3.3.6. Basal mitophagy is minimally affected by loss of parkin

3.3.6.1. Analysis of larval epidermis and CNS of *parkin* mutants

Having analysed *Pink1* mutants, the mito-QC was visualized in larval tissues of *parkin* null mutants (*park*^{25}). Consistent with *Pink1* mutants, mitophagy was widespread in larval epidermis, CNS and muscles and no difference was observed when compared with the control animals (Figure 3.19).

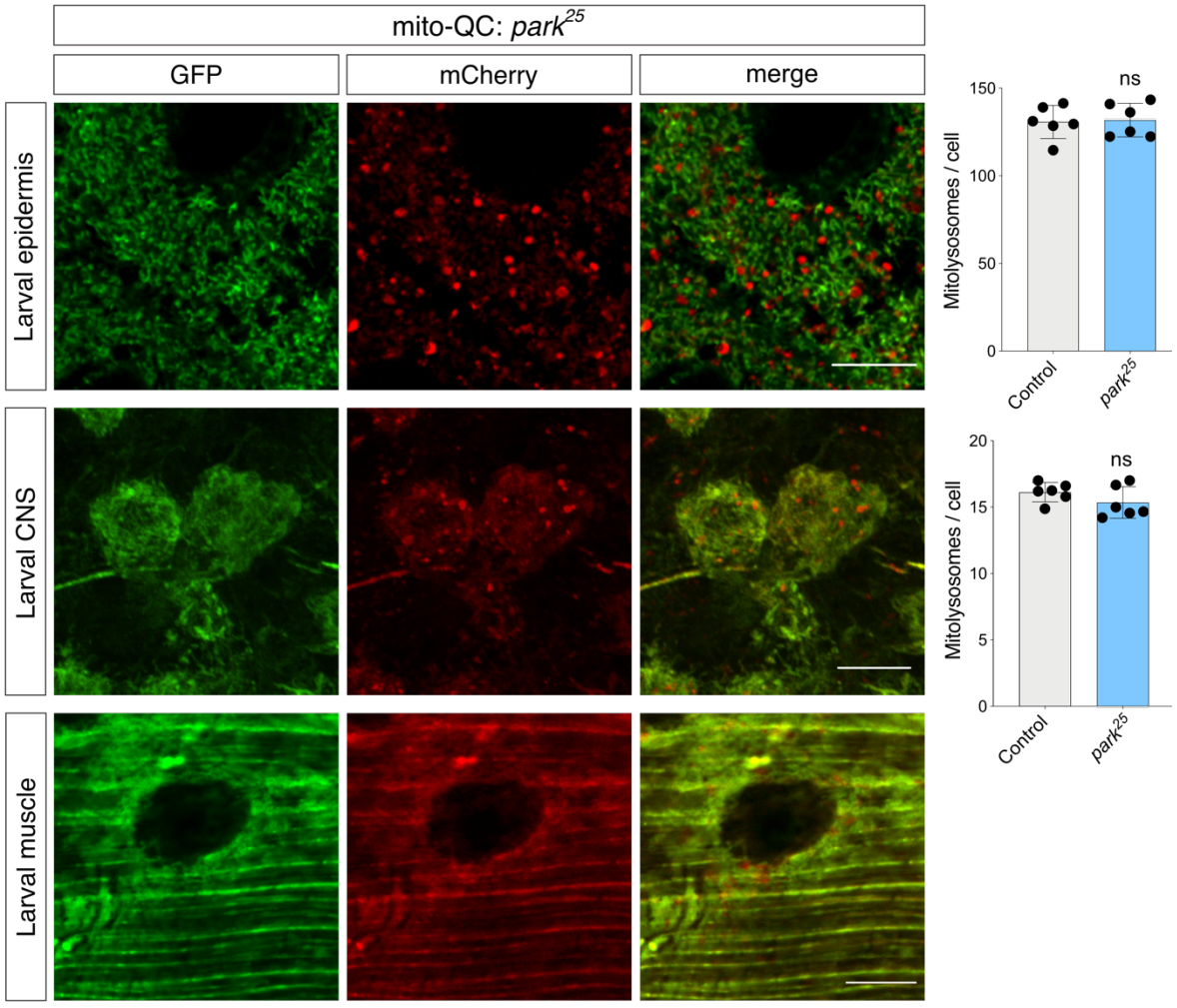

Figure 3.19. Basal mitophagy is minimally affected in larval tissues of *parkin* mutants

Confocal imaging of mito-QC reporter in *park*^{25} larval epidermis, CNS and muscle. Charts show quantification of mitolysosomes, mean ± SD of n = 6 animals. Number of cells analysed: epidermis, control = 29, *park*^{25} = 30; CNS, control = 28 and *park*^{25} = 31. Control genotype is *da-GAL4/UAS-mito-QC* shown in Figure 3.4 and quantification of WT control samples is the same as in Figure 3.15. Statistical significance determined by Welch's *t*-test; ns = non-significant. Genotype analysed is *park*^{25}*,da-GAL4/park*^{25}*,UAS-mito-QC*. Scale bars = 10 µm.

3.3.6.2. Analysis of adult IFMs and CNS of *parkin* mutants

As for *Pink1* mutants, *parkin* loss causes a strong degeneration of the IFMs as well as swollen/aggregated mitochondria. Consistent with the observations in *Pink1* mutants, mitolysosomes were abundant in adult IFMs of 2- and 30-day-old *parkin* null mutants. Similar to aged *Pink1* mutant thoraces, mitophagy was slightly increased in aged flies, although this was not quantified. This increase was more striking in intact muscle bundles (Figure 3.20 bottom panel 'intact bundle') compare to the profoundly damaged ones, as seen in *Pink1* mutants (Figure 3.20 bottom panel 'degenerate bundle').

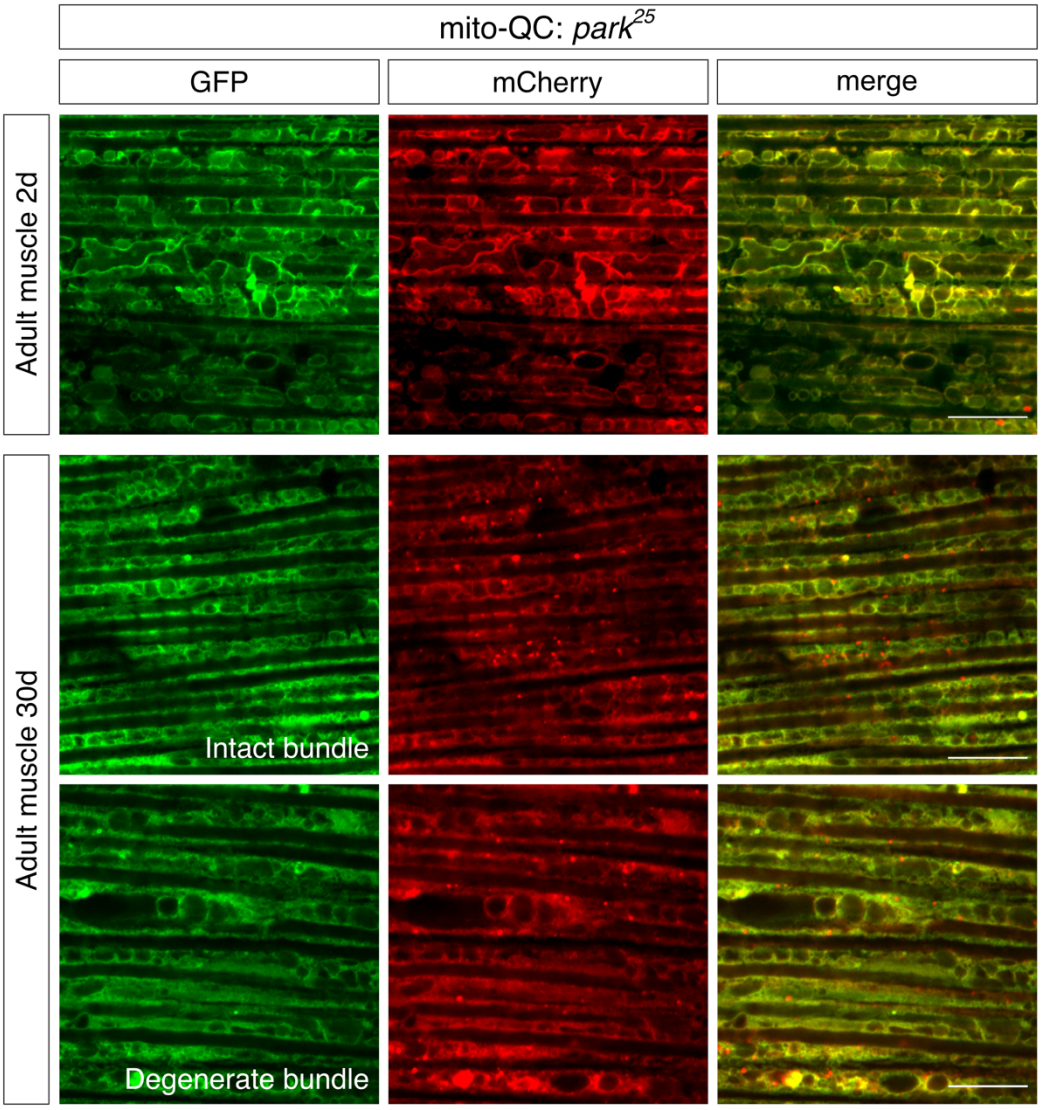

Figure 3.20. Basal mitophagy is minimally affected in adult IFMs of *parkin* mutants

Confocal imaging of mito-QC *park*^{25} mutants at 2 and 30 days IFMs. Control genotype is *Mef2-GAL4/UAS-mito-QC* shown in Figure 3.5. Genotype analysed is *park*^{25}*,Mef2-GAL4/park*^{25}*,UAS-mito-QC*. Scale bars = 10 μm.

Finally, adult brains and DA neurons of *parkin* mutants were imaged and quantified for mitolysosomes by confocal microscopy. Mitophagy was widespread in adult brains (Figure 3.21 top panel) and DA neurons (Figure 3.21 bottom panel). Interestingly, the quantification did not show any significant difference with the control animals. The number of mitolysosomes seem to slightly increase in DA neurons of aged animals, consistent with the findings in WT conditions (Figure 3.21).

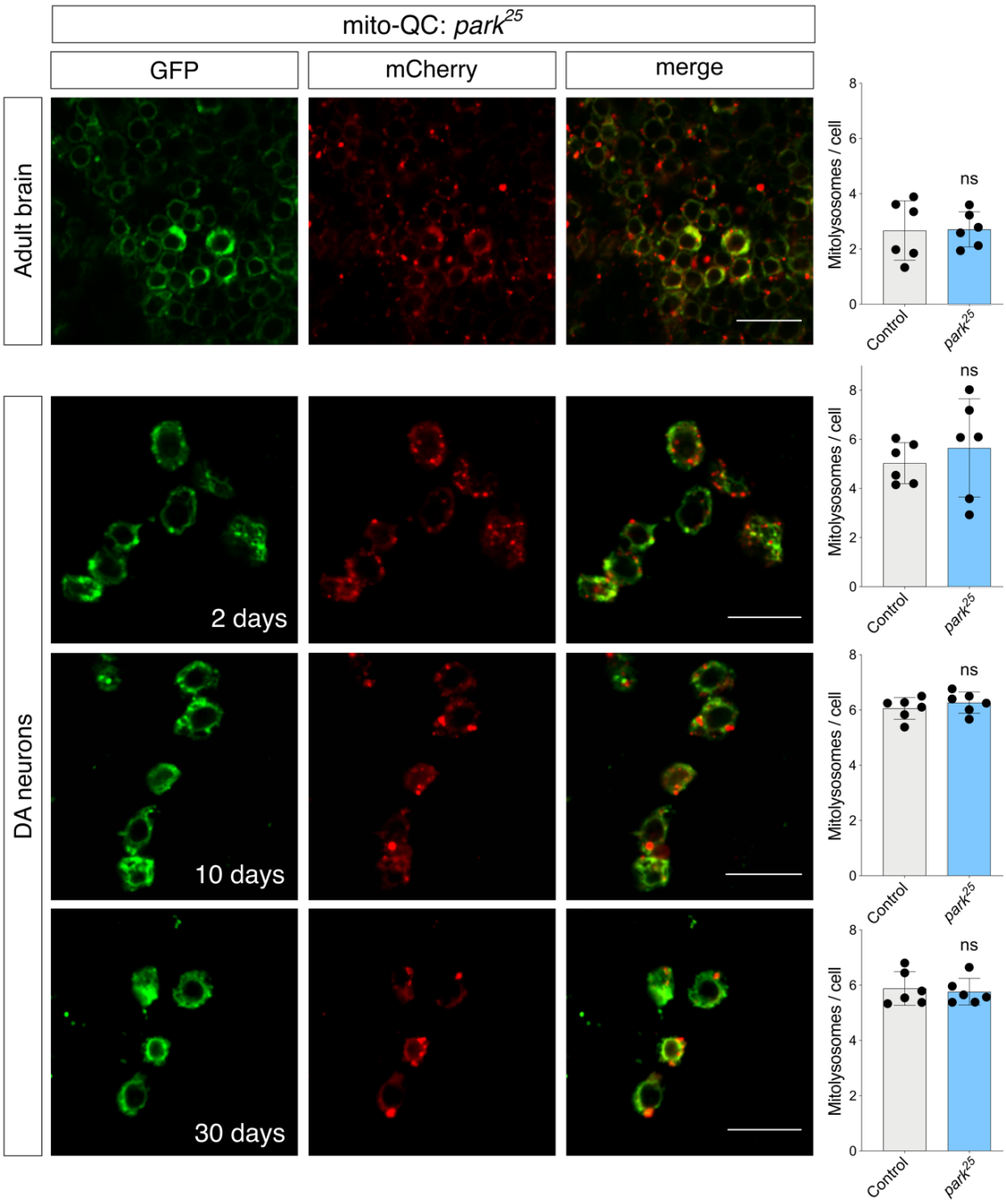

Figure 3.21. Basal mitophagy is minimally affected in adult brains of *parkin* mutants

Confocal imaging of mito-QC reporter in *park*^{25} adult brains (medial region of the posterior protocerebrum) and DA neurons of the PPL1 cluster at 2-, 10- and 30-day-old. Charts show quantification of mitolysosomes, mean ± SD of n = 6 animals. Number of cells analysed: adult brain, control = 74, *park*^{25} = 78; DA neurons 2 days, control = 100, *park*^{25} = 69, 10 days, control = 77, *park*^{25} = 74 and 30 days, control = 78, *park*^{25} = 83. Control genotypes are (adult brain) *UAS-mito-QC/+; nSyb*$_{ZH86FB}$*-GAL4/+* and (DA neurons) *UAS-mito-QC/+; TH-GAL4/+* shown in Figure 3.7 and quantification of WT control samples is the same as in Figure 3.7 and Figure 3.18. Statistical significance determined by Welch's *t*-test; ns = non-significant. Genotypes analysed are (adult brain) *UAS-mito-QC/+; park*^{25}*,nSyb*$_{ZH86FB}$*-GAL4/park*^{25} and (DA neurons) *UAS-mito-QC/+; park*^{25}*,TH-GAL4/park*^{25}. Scale bars = 10 µm.

Taken together, these results showed that basal mitophagy is present in a plethora of *Drosophila* tissues; however, they also surprisingly indicate the dispensable role of Pink1 and parkin in basal mitophagy in *Drosophila*. One evident explanation is that distinct types of stress or conditions may trigger different MQC pathways that can either be independent of Pink1/parkin or unrelated to mitophagy. Similar to the MDV generation, ROS or accumulation of mtDNA mutations may activate different MQC responses. In this case, Pink1/parkin mitophagy may be dispensable for basal mitophagy but essential in response to other stressors. To address this, and in line with the fact that *Parkin* KO combined with the mutator mouse induces DA neurodegeneration (Pickrell et al., 2015), mitophagy was assessed in *Pink1*/*parkin* mutants in combination with a mtDNA mutator model, mito-APOBEC1.

3.3.7. Mitophagy is slightly increased in flies expressing mito-APOBEC1

3.3.7.1. Analysis of larval epidermis and CNS of mito-APOBEC1 flies

Our lab recently described a novel mtDNA mutator model, named mito-APOBEC1 (Andreazza et al., 2019). APOBEC1(Apolipoprotein B (apoB) mRNA editing catalytic polypeptide 1) is cytosine deaminase that catalyses the conversion of cytosine to uracil (C>U). Andreazza et al. showed that mitochondrially targeted APOBEC1 induces a high level of C:G > T:A point mutations. Interestingly, this mutagenic profile has been associated with human ageing (Andreazza et al., 2019). Thus, we used mito-APOBEC1 mutator to chronically stress mitochondria and assess the impact on mitophagy using mito-QC. First, larval epidermis and CNS were imaged and analysed (Figure 3.22). A nearly 50% increase in the number of mitolysosomes was observed in the epidermal cells of mito-APOBEC1 larvae, however, there was no significant difference in the larval CNS (Figure 3.22).

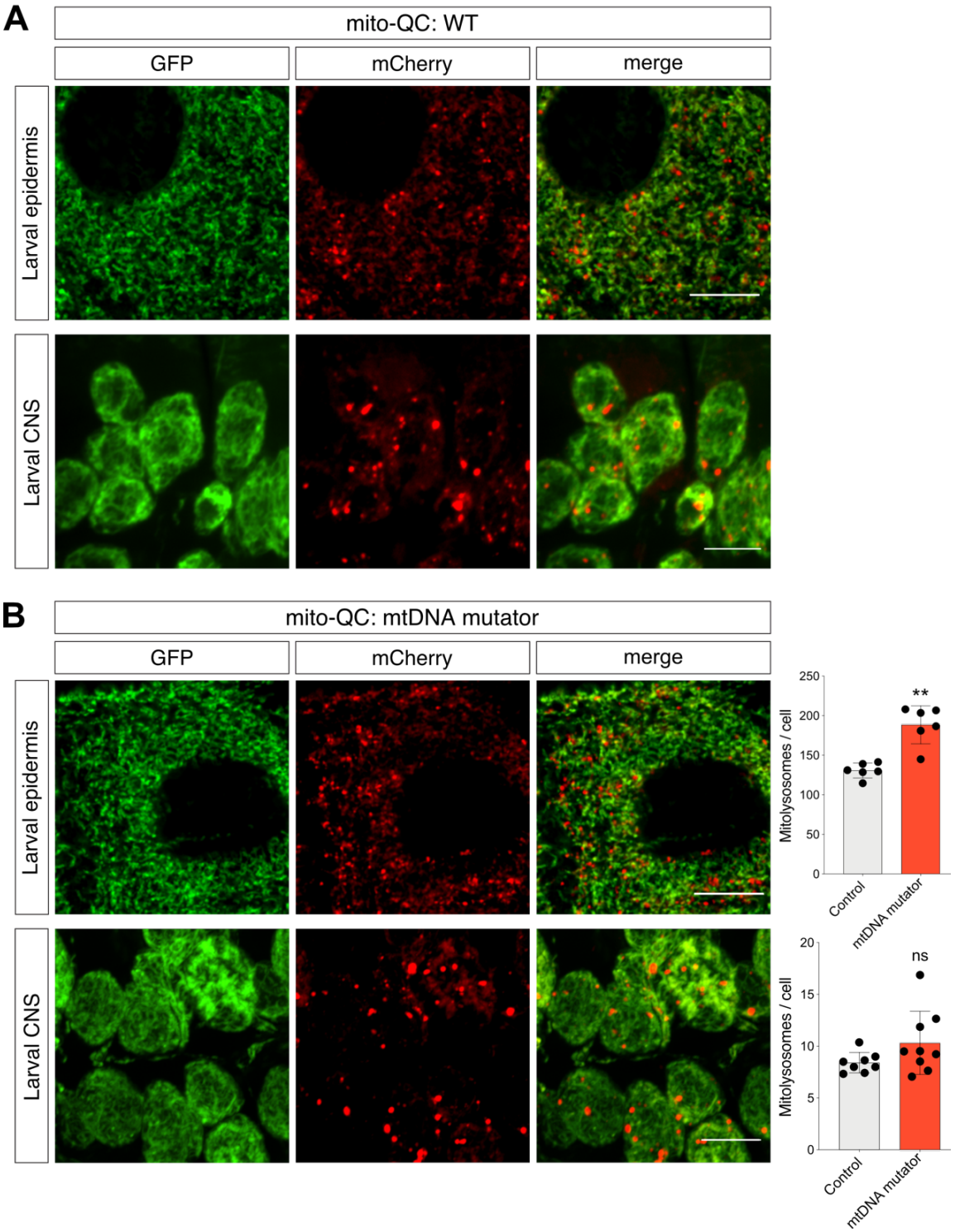

Figure 3.22. Mitophagy is increased in larval epidermis of mito-APOBEC1flies

Confocal imaging of mito-QC reporter in larval epidermis and CNS of (A) control and (B) mito-APOBEC1flies. Charts show quantification of mitolysosomes, mean ± SD of n = 6 animals. Number of cells analysed: larval epidermis, control = 29, mito-APOBEC1= 23; CNS, control = 119, mito-APOBEC1= 142. Control genotypes are (epidermis) *da-GAL4/UAS-mito-QC, UAS-lacZ* and (CNS) *UAS-mito-QC/+; nSyb-GAL4/UAS-lacZ*. Statistical significance determined by Welch's *t*-test; ** $P < 0.01$ and ns = non-significant. Genotypes analysed are (epidermis) *UAS- mito-APOBEC1/+; da-GAL4/UAS-mito-QC* and (CNS) *UAS-mito-QC/UAS-mito-APOBEC1; nSyb-GAL4/UAS-lacZ.* Scale bars = 10 μm.

3.3.7.2. Analysis of adult brains and IFMs of mito-APOBEC1 flies

As mitophagy was found to be increased in larval epidermis and as mito-APOBEC1 induces premature ageing, analysing adult and aged animals seemed an attractive experiment to conduct. To this end, mito-QC flies expressing mito-APOBEC1 were dissected and the adult brains were quantified for the mitophagy signal. Interestingly, the number of mitolysosomes was not increased in 2-day-old or 30-day-old brain of mito-APOBEC1 flies (Figure 3.23). However, the number of mitolysosomes significantly increased in IFMs of 2-day-old flies expressing mito-APOBEC1, although no differences were observed between control and mito-APOBEC1 flies at 20 days (Figure 3.24). These results indicate that accumulation of mtDNA mutations may only influence mitophagy in some particular tissues such as the IFMs.

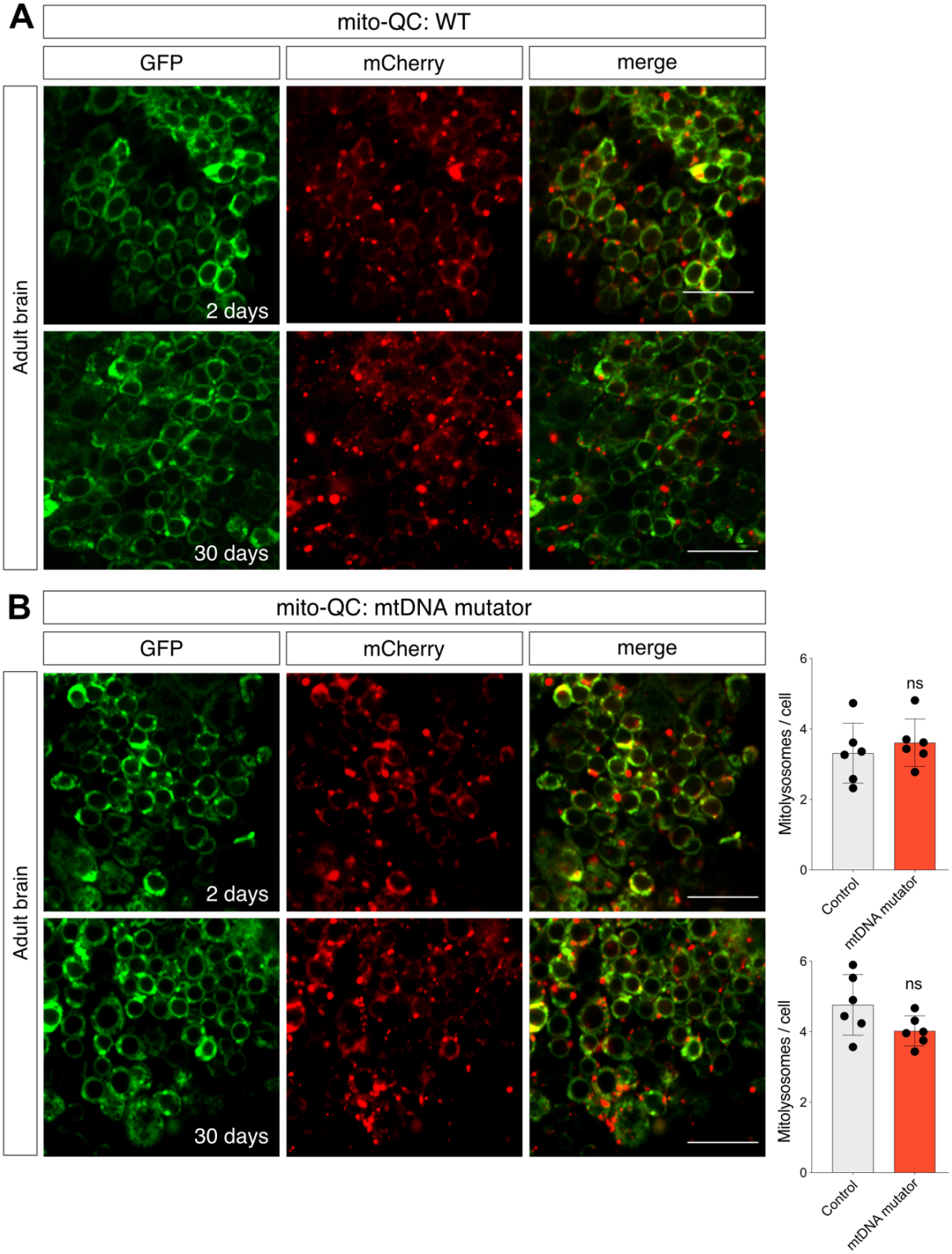

Figure 3.23. Mitophagy is not increased in adult brains of mito-APOBEC1flies

Confocal imaging of mito-QC reporter in adult brains of 2- and 30-day-old flies of (A) control and (B) expressing the mito-APOBEC1. Charts show quantification of mitolysosomes, mean ± SD of n = 6 animals. Number of cells analysed: adult brain 2 days, control = 220, mito-APOBEC1= 217; 30 days, control = 240, mito-APOBEC1= 219. Control genotype is *UAS-mito-QC/+; nSyb-GAL4/UAS-lacZ*. Statistical significance determined by Welch's *t*-test; ns = non-significant. Genotype analysed is *UAS-mito-APOBEC1/UAS-mito-QC; nSyb-GAL4 /+*. Scale bars = 10 μm.

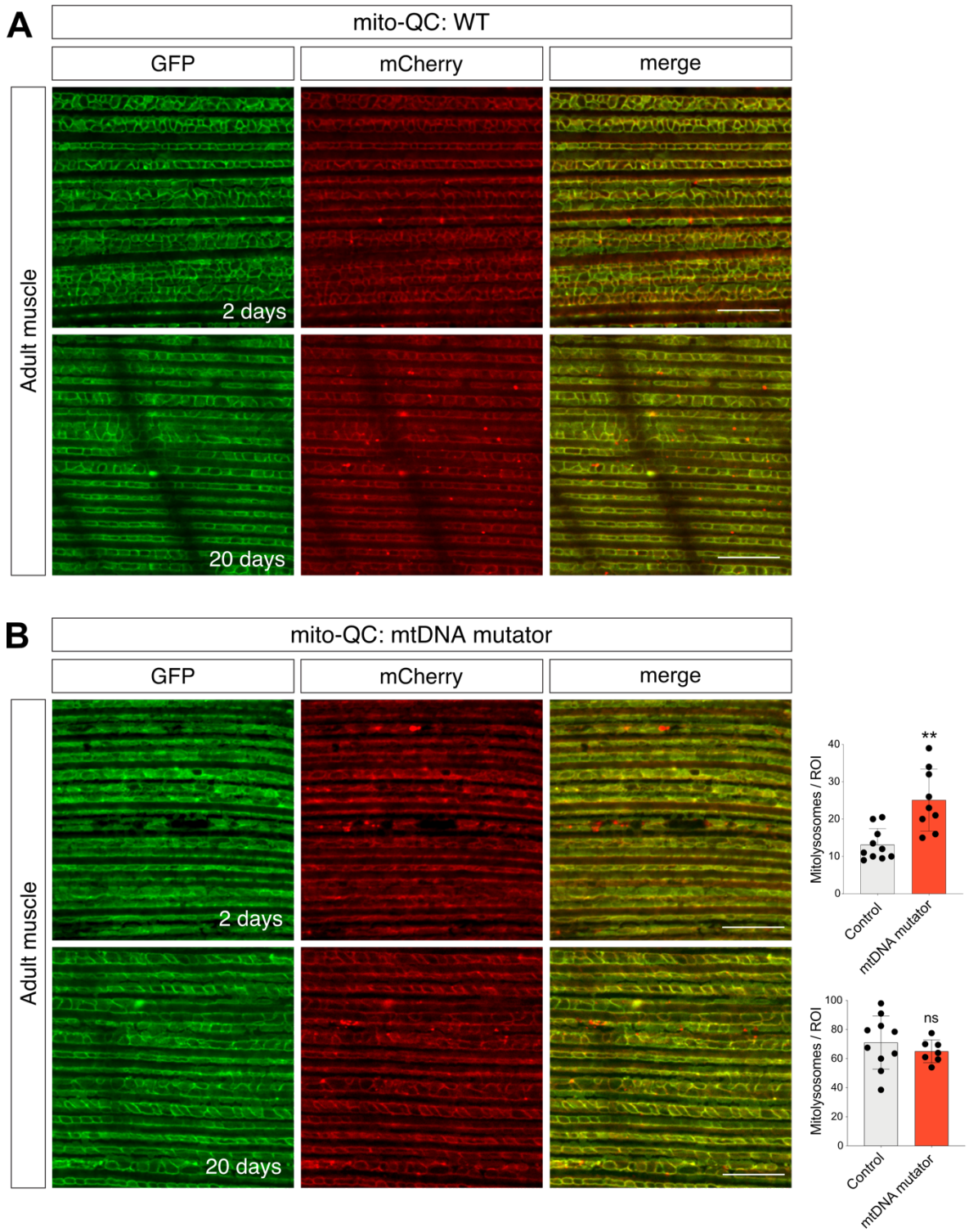

Figure 3.24. Mitophagy is not increased in IFMs of mito-APOBEC1 flies.

Confocal microscopy analysis of mito-QC reporter in adult IFMs of 2- and 30-day-old flies of (A) control and (B) expressing mito-APOBEC1. Charts show quantification of mitolysosomes, mean ± SD of n ≥ 7 animals. In each fly, 2 random 6400 μm^2 ROI were analysed. Control genotypes is *UAS-lacZ/+*; *UAS-mito-QC/ Mef-GAL4* and quantification of WT samples is the same as in Figure 3.5. Statistical significance determined by Welch's *t*-test; ns = non-significant. Genotype analysed is *UAS-mito-APOBEC1/+; Mef2-GAL4 /UAS-mito-QC.* Scale bars = 10 μm.

3.3.8. Mitophagy is increased in mito-APOBEC1 flies combined with Pink1 or parkin overexpression

As loss of *Pink1* or *parkin* did not affect basal mitophagy, analysing the reverse manipulation, i.e. overexpressing these two proteins, for their impact on mitophagy was an attractive idea. To address this, Pink1 was first overexpressed with *nSyb*-GAL4 in a WT background (Figure 3.25 A). Interestingly, Pink1 overexpression on its own did not change the mitophagy level, as the number of mitolysosomes remained unchanged in larval brains (around 8 mitolysosomes per cell). The quantification of the representative images is shown in Figure 3.25 B. However, when Pink1 and mito-APOBEC1 were co-expressed, the number of mitolysosomes almost doubled compared to control conditions (Figure 3.25 A). An analogous experiment was performed with parkin overexpression in a WT background and led to similar results (Figure 3.26 A). Indeed, parkin overexpression alone did not increase the mitophagy signal (Figure 3.26 B). However, overexpression of parkin in the mito-APOBEC1 background significantly increased the number of mitolysosomes, in a similar fashion to Pink1 and mito-APOBEC1 co-expression (Figure 3.26). Unfortunately, as the co-expression of Pink1 with mito-APOBEC1 is lethal at the late larval stage, mitophagy could not be further assessed in those genotypes at adult stage.

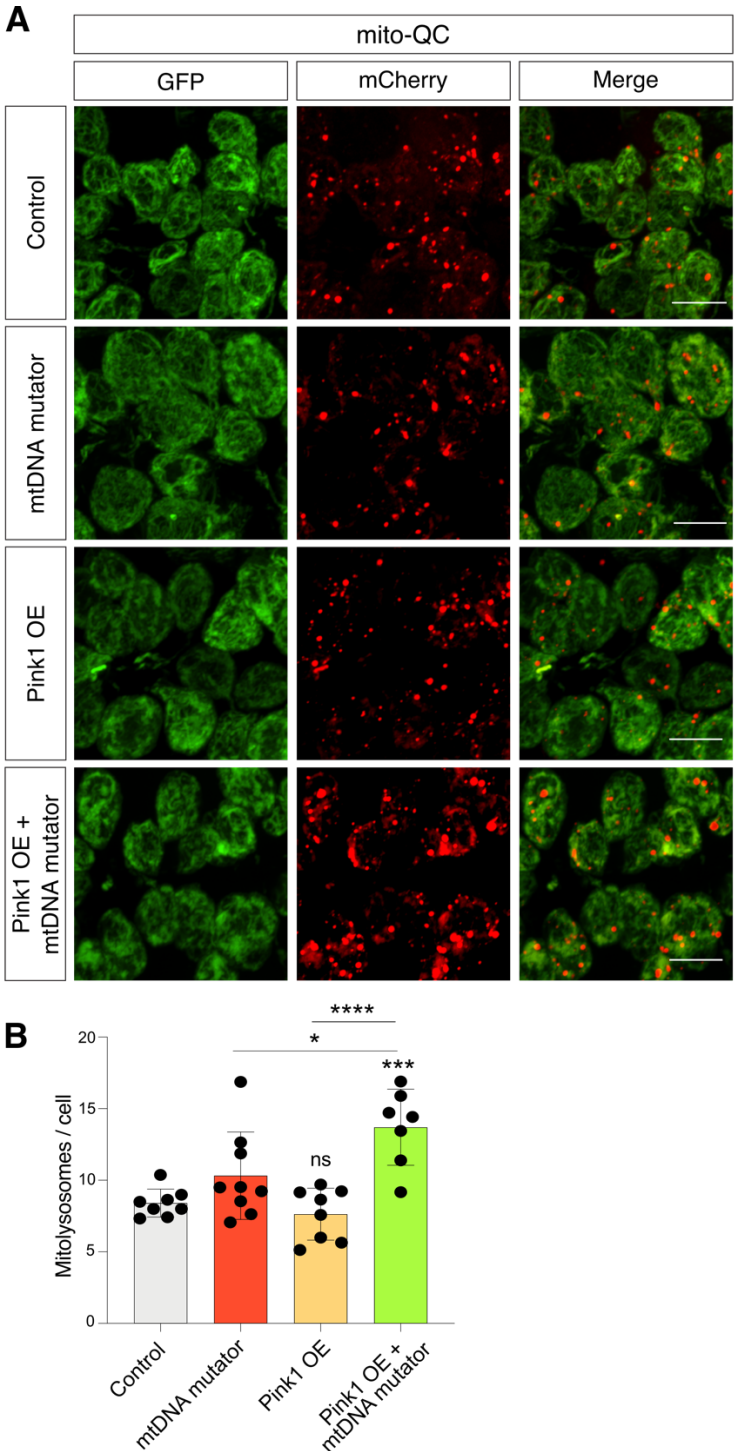

Figure 3.25. Mitophagy is increased in larval brain of mito-APOBEC1 flies overexpressing Pink1

(A) Confocal imaging of mito-QC reporter in larval CNS of WT; mito-APOBEC1; Pink1 OE and mito-APOBEC1 + Pink1 OE. (B) Chart shows quantification of mitolysosomes, mean ± SD of n > 7 animals. Number of cells analysed: control = 119; mito-APOBEC1= 142; Pink1 OE = 122 and mito-APOBEC1 + Pink1 OE= 91. Control genotype is *UAS-mito-QC/+; nSyb-GAL4/UAS-lacZ*. Statistical significance determined by Welch's *t*-test; **** $P < 0.0001$; *** $P < 0.001$; * $P < 0.05$, and ns = non-significant. Genotypes analysed are *UAS-mito-APOBEC1/UAS-mito-QC; nSyb-GAL4/+, UAS-TcPink1/UAS-mito-QC; nSyb-GAL4/+ and UAS-mito-APOBEC1, UAS-mito-QC/UAS-TcPink1; nSyb-GAL4/+*. OE = overexpression. Scale bars = 10 µm.

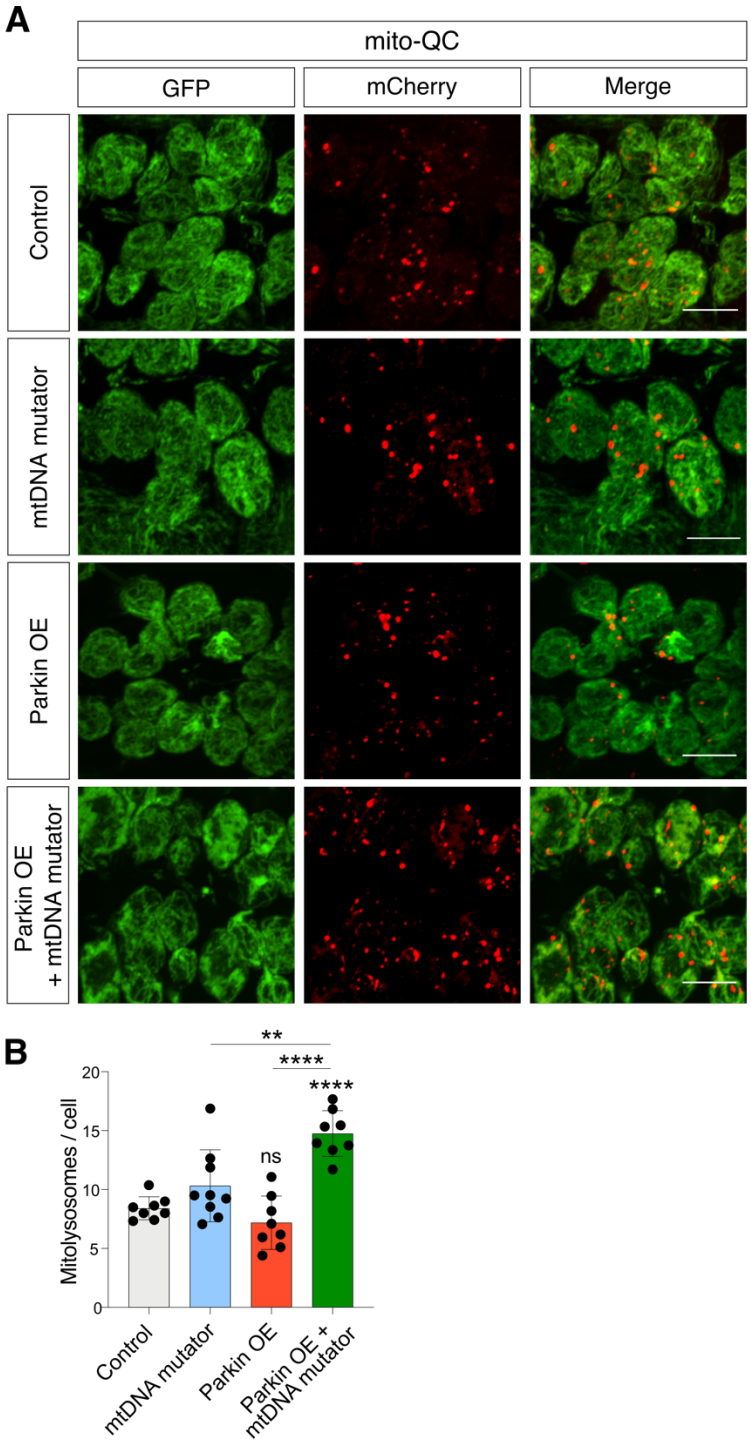

Figure 3.26. Mitophagy is increased in larval brain of mito-APOBEC1 flies overexpressing parkin

(A) Confocal imaging of mito-QC reporter in larval CNS of WT; mito-APOBEC1, parkin OE, mito-APOBEC1 + parkin OE. (B) Chart shows quantification of mitolysosomes, mean ± SD of n > 7 animals. Number of cells analysed: control = 119; mito-APOBEC1= 142; parkin OE = 143 and mito-APOBEC1 + parkin OE = 127. Control genotype is *UAS-mito-QC/+; nSyb-GAL4/UAS-lacZ* and quantification of WT is the same as in Figure 3.25. Statistical significance determined by Welch's *t*-test; **** $P < 0.0001$; ** $P < 0.01$, and ns = non-significant. Genotypes analysed are *UAS-mito-APOBEC1/ UAS-mito-QC; nSyb-GAL4 /+, UAS-Parkin$_{C2}$/UAS-mito-QC; nSyb-GAL4 /+ and UAS-mito-APOBEC1, UAS-mito-QC/ UAS-Parkin$_{C2}$; nSyb-GAL4 /+.* OE = overexpression. Scale bars = 10 µm.

3.4. Discussion

The PINK1/Parkin pathway has been dominating the mitophagy field over the last decade, and while it has been substantially studied *in vitro* using cultured cells and cytotoxic mitochondrial agents, little was known about the implication of these two proteins in mitophagy *in vivo.* Although *in vitro* work has been extremely informative regarding the molecular mechanism of stress-induced mitophagy, it remained difficult to investigate the physiological conditions under which mitophagy occurs *in vivo*, mainly due to the lack of rigorous detection methods of mitophagy.

In the present study, two previously established mitophagy reporter constructs have been adapted to the *Drosophila* system in order to visualise mitophagy *in vivo* for the first time. The possibility to work with both reporters, allowed a thorough comparison between the two systems. Although conceptually, mito-QC and mt-Keima appear similar, as they are both pH-sensitive biosensors, they present some advantages and disadvantages. The mt-Keima is targeted to the mitochondrial matrix via a COX VIII MTS, while the mito-QC is a tandem mCherry-GFP tag fused to the FIS1 MTS, which also happens to be a peroxisomal protein. Therefore, it remains a possibility that a small amount of the mito-QC goes to the peroxisomes, although the majority of the reporter signal seems to correctly localised at the mitochondria (Allen et al., 2013; McWilliams et al., 2016). Additionally, the mito-QC present on the OMM can be degraded by the proteasome by a mechanism called OMM associated degradation (OMMAD), a process equivalent to the ERAD (Pickles et al., 2018). As a result, some mitophagy signal may be missed due to prior degradation of the mito-QC. This may explain some discrepancies obtained between the two reporters, in particular in the context of the adult IFMs and aged DA neurons, which will be discussed in more detail later. While the Keima protein is resistant to lysosomal proteases, its fate within the lysosomes remains unclear. The signal from the expression of the Keima protein in cultured cells has been reported to survive at least 6 hours in lysosomal compartments (Katayama et al., 2011). However, the maximal amount of time this signal can survive *in vitro* or *in vivo* has not been measured yet. A recent paper on bioRxiv has determined that, in zebrafish, the mt-Keima reporter can report mitophagy events that have occurred in the past 5-7 days (Wrighton et al., 2020). This is an important property of the fluorophore to consider, especially now that the field is moving towards the use of

in vivo mitophagy reporters. One of the main differences between the two reporters is their compatibility with fixation and the subsequent labelling of additional proteins or specific cell populations of interest. The mito-QC can be fixed whereas the mt-Keima requires live imaging. However, as the mito-QC uses the properties of the GFP and the mCherry, the number of other fluorophores compatible with the reporter for immunostaining is rather limited, mainly remain blue (405 nm) and far red (633-647 nm). In my hands, the red puncta detected with the mito-QC were quite unstable over time, such that within couple of days, all the puncta would have disappeared, which makes imaging time-limited. Additionally, it seems that detergents or other reagents used for immunostaining procedures would also provoke the disappearance of the red puncta, thus making immunolabeling of these mitolysosomes not feasible. This illustrates that although immunostaining is technically compatible with the mito-QC, several other variables that may interfere with this procedure, need to be considered beforehand. While the mt-Keima allows the use of other fluorescent labels as well, the fluorophore is incompatible with fixation. It is therefore impossible to immunolabel proteins or other cellular compartments while keeping the signal of the mt-Keima intact (Sun et al., 2015). Indeed, when the mt-Keima is present in the lysosomes, the protein is predominantly excited by the red wavelength but still remains slightly excited by the green wavelength. In addition, while the mito-QC displays strong levels of fluorescence with common ubiquitous drivers, the fluorescence from the currently available mt-Keima lines was barely detectable, making this reporter a more difficult tool to work with. A summary of each reporter's advantages and disadvantages is given in Table 3.1.

Table 3.1. Comparison of the two mitophagy reporters: mito-QC and mt-Keima

	mito-QC	mt-Keima
Localisation	OMM (FIS1)	Matrix (COX VIII)
Excitation wavelength (nm)	488 (green) and 561 (red)	458 (green) and 561 (red)
Emission wavelength (nm)	509 (green) and 580 (red)	620
Imaging	Fixed or live	Live only
Immunostaining	Yes?	No
Intensity of signal	Strong	Weak

After having properly validated the mito-QC and mt-Keima reporters, mitochondrial turnover was assessed in a plethora of *Drosophila* tissues, from larval to adult stage. While mitophagy was detected in most of the tissues analysed, the reporters highlighted a high degree of heterogeneity and variability in their signal. Indeed, some tissues, such as larval epidermis and larval/adult CNS, displayed high levels of mitophagy, whereas mitolysosomes were barely detectable in others, such as larval muscles and adult IFMs. The finding that larval and adult muscles exhibit extremely low rate of mitophagy was rather surprising as muscles are believed to be high energy demanding tissues, implying that they would potentially undergo more mitophagy. Alternatively, the muscles may rely on a different mitochondrial turnover mechanism, that is not related to mitophagy. Similar results were observed in a study by Kim et al., where the authors also detected low levels of mitophagy in larval and adult flight muscles (Kim et al., 2019). Interestingly, contrasting results were obtained by another group using their own *Drosophila* mt-Keima line, referred to here as 'mt-Keima (Leuven)', where mitolysosomes were abundantly detected in IFMs of young flies (Cornelissen et al., 2018). One potential explanation that would explain these discrepancies is that the two reporters have different sensitivity, although the levels of mitophagy displayed by the mt-Keima and 'mt-Keima (Leuven)' were in my hands quite similar. It is also possible that these differences are just due to different experimental

techniques. Cornelissen et al. found that mitophagy levels were tremendously higher in the DA neurons compare to adult IFMs, further reinforcing the idea that IFMs exhibit very little amount of mitophagy (Cornelissen et al., 2018). The latter suggests that the low mitophagy rates occurring in the IFMs may be below the detection limit of the mito-QC. Indeed, slightly more mitophagy was appreciable with our mt-Keima construct, compared to the mito-QC in this particular tissue. Additionally, as the mito-QC is targeted the OMM, it may be subjected to degradation by the UPS, further dampening the amount of mitophagy observed.

Evidence from the literature has reported that ageing is accompanied by a rising number of dysfunctional and damage mitochondria which may drive increased levels of mitophagy (Balaban et al., 2005; López-Otín et al., 2013). Compelling evidence from this study point towards an increase in mitophagy with age. This was particularly apparent in some neuronal cell populations and the IFMs, which both exhibited higher rates of mitophagy at 20-30 days. Cornelissen et al., also reported higher levels of mitophagy in adult IFMs, aged up to 4 weeks, further reinforcing the notion that mitophagy may be an age-related phenomenon (Cornelissen et al., 2018). However, the levels of mitophagy in DA neurons of the PPL1 cluster were found to be stable during ageing. These results are in sharp contrast with the ones from Cornelissen et al. where mitophagy levels between 1-week-old and 4-week-old flies almost doubled in DA neurons (Cornelissen et al., 2018). While this increase remained lower than the one reported in adult IFMs, it remains unclear why these discrepancies were observed. Intriguingly, Cornelissen's results using the 'mt-Keima (Leuven)' line could not be reproduced in the present study. Contrasting with the *Drosophila* work, a mammalian study by Sun *et al.*, in which the authors assessed mitophagy using the mt-Keima mouse, reported a decline in mitophagy with age in the dendate gyrus region, suggesting that whether or not mitophagy is an age-related process remains to be determined (Sun et al., 2015). Interestingly, studies in *Drosophila* IFMs have reported accumulation of cytoplasmic p62-poly ubiquitin protein aggregates as well as a decrease in lysosome number and function in 2-month-old flies (Demontis & Perrimon, 2010). Additionally, EM analysis of old animals revealed accumulation of enlarged mitochondria with abnormal cristae organisation, leaning towards the idea of a potential defect in mitochondria turnover with ageing (Demontis et al., 2013; Demontis & Perrimon, 2010). As mitophagy rates seem highly heterogeneous, it is tempting to

speculate that distinct tissues may encounter variable amount of mitochondrial damage during ageing, which is reflected by different rates of mitophagy.

Although there is no doubt about the significant relevance of the PINK1/Parkin pathway, the results from the present study strongly indicate that Pink1 and parkin are not essential to basal mitophagy in *Drosophila*. At the same time, Cornelissen and his team found that loss of *Pink1* or *parkin* result in an age-dependent decrease in mitophagy in DA neurons and IFMs (Cornelissen et al., 2018). While an increase in mitophagy was still appreciable in IFMs of *Pink1* and *parkin* mutants at 30 days, we did not see any difference in 30-day-old DA neurons of WT animals compare to *Pink1* and *parkin* mutants. These discrepancies could be explained by differences in the imaging techniques or the IFM bundles chosen for quantification as some less intact bundles exhibit less mitophagy.

Importantly, while this work was ongoing, a complementary study from Ganley's group was published and reported similar effects on mitophagy in *Pink1* KO mice combined with the mito-QC reporter (McWilliams et al., 2018b). Work by McWilliams et al., has shown that loss of Pink1 did not affect the mitophagy levels in DA neurons as well as other non-neuronal tissues, such as microglia, heart and liver (McWilliams et al., 2018b). An additional publication from the same group reached similar results with a phosphorylation-deficient *Parkin*^{S65A} knock-in mouse model (McWilliams et al., 2018a). These mice did not exhibit any gross neurological or behavioural impairments during development, although, they did show a decrease in their beam performance at 12 and 18 months old (McWilliams et al., 2018a). By generating a *Parkin*$^{S65A/S65A}$ – mito-QC mice, McWilliams et al., analysed mitophagy in nigrostriatal DA cell bodies/projections and did not observe any differences between these mutant and WT mice, further strengthening the dispensable role of PINK1 and Parkin in basal mitophagy (McWilliams et al., 2018a).

It is important to mention that these results do not assert that PINK1 and Parkin are dispensable for all forms of mitophagy. Here, I offer several lines of explanations. These data indicate the existence of distinguishable pathways that may regulate basal versus stress-evoked mitophagy. One explanation is that if PINK1 and Parkin do not play a role in basal mitophagy, they are likely to be necessary in response to

physiological stimuli, such as accumulation of mtDNA or excessive ROS production. For instance, while *Prkn* KO mice do not exhibit any sign of neurodegeneration, loss of *Prkn* combined with the mitotoxicity of the mtDNA mutator leads to DA neuron loss and locomotor deficits, recapitulating some key features of PD (Pickrell et al., 2015). More recently, exhaustive exercise was shown to increase mitophagy in mt-Keima mice and this was suppressed in *Pink1*$^{-/-}$ mice, illustrating the idea that PINK1/Parkin-mediated mitophagy is triggered under specific stressors (Sliter et al., 2018). It is also possible that the mitochondrial damage that mice accumulate in their lifespan is not enough to trigger PINK1/Parkin mitophagy. In fact, Pickrell et al., reported that while the levels pSer65-Ub in the cerebral cortex of aged WT mice are rather low, they become significantly elevated in mutator mice, supporting the requirement of a 'second hit' in addition to aging, necessary to activate PINK1/Parkin mitophagy. While in our hands, overexpression of mito-APOBEC1 in larval and adult brains did not significantly increase mitophagy, the number of mitolysosomes almost doubled in adult IFMs, reinforcing the idea that some tissues may be more susceptible to accumulation of mtDNA mutations. When combining the mt-Keima with polymerase gamma (*POLGγ*) knock-in mice, containing a mutated proof-reading deficient form of the *POLGγ*, Sun et al., reported that accumulation of mtDNA mutations led to higher rates of mitophagy (Sun et al., 2015). These observations suggest that the age-dependent decline in mitophagy may be responsible for the mitochondrial dysfunction observed with aging. Therefore, rather than being the result of an increase in mitochondrial damage with age, the authors suggest that accumulation of mtDNA, ROS and other mitochondrial dysfunction may be the consequence of the inability of tissues to clear out these damaged mitochondria due to the age-dependent decline in mitophagy (Sun et al., 2015). I sought to investigate if Pink1 or parkin overexpression would lead to increased mitophagy levels. While none of these independent overexpressions led to any change in the mitophagy signal in the larval brains, the combination of the mito-APOBEC1 and Pink1 or parkin overexpression led to substantially higher levels of mitophagy. This supports the idea that PINK1/Parkin-dependent mitophagy may only act under specific conditions. Unfortunately, while the independent overexpressions of the mito-APOBEC1, Pink1 or parkin are viable, the combinations mito-APOBEC1:Pink1 or mito-APOBEC1:parkin overexpression seem to be larval lethal. The extensive accumulation of mtDNA may drive excessive Pink1/parkin-mediated mitophagy, as seen with the mito-QC signal, which in turn is detrimental to the fly. It may just be about finding the

right balance between too little and too much mitophagy.

Another plausible explanation relies on the fact that an increase in mitophagy occurs at the level of MDVs and therefore remains undetectable with the mito-QC. More recently, growing evidence has indicated that PINK1/Parkin-mediated mitochondria turnover can occur via MDVs. Due to the small size of these mitochondrial-cargo vesicles, this phenomenon may not be visualised with the mito-QC. Additionally, it seems that loss of *Pink1* or *parkin* does not completely abrogate mitophagy but rather slows down this process (Vincow et al., 2013). While, the resulting mitophagy kinetics of *Pink1* and *parkin* KO have not been assessed in this study, others have analysed mitochondrial protein turnover rates in *Pink1* and *parkin Drosophila* mutants using mass spectrometry (Vincow et al., 2013). Results in both mutants revealed a significantly slower turnover of a plethora of mitochondrial proteins, especially proteins composing the mitochondrial respiratory chain subunits (Vincow et al., 2013). Interestingly MDVs have been shown to carry complex IV subunits, reinforcing the idea that PINK1/parkin-dependent MDV generation may be impacted by loss of *PINK1* and *Parkin* but at a level undetectable by the mitophagy reporters (Neuspiel et al., 2008; Vincow et al., 2013). Unfortunately, as cell culture work suggests a 10-24h timescale, investigating mitophagy kinetics *in vivo* is not compatible with such long windows of live experiments. It is interesting to link these findings to human PD patients and how PINK1/parkin-mitophagy may relate to the PD pathology. Intriguingly, PD patients carrying *PINK1* or *Parkin* mutation, survive many years without symptoms and locomotor symptoms only manifest in the third or fourth decade of the patient's life. Thus, it is tempting to speculate that a complete loss of mitophagy would result in a more severe phenotype.

Finally, other mitochondrial quality controls can be triggered as a developmental or epistatic compensatory mechanism. In light of this, while Cornelissen et al., have used *parkin*-RNAi, this study was exclusively based on *Pink1* and *parkin* null mutants (Cornelissen et al., 2018). These mutants may have developed compensatory mechanisms over time and generations that may cover for any potential effect of *Pink1/parkin* loss on mitophagy. This is reinforced by the fact that *PINK1* KO mice do not exhibit any sign of neurodegeneration whereas conditional post-natal KO of *PINK1* or *Prkn* in mice results in the loss of DA neurons, thus suggesting that germline KO

can lead to the induction of compensatory mechanisms during development (Lee et al., 2017; Shin et al., 2011).

Altogether, the mitophagy reporters described in this study have been adapted to the *Drosophila* model and provide valuable new systems for investigating mitophagy *in vivo* under physiological conditions. These novel tools will be useful for screening of potential new regulators of mitochondrial turnover pathways that are also relevant to neurodegenerative diseases. Key questions still remain unanswered, especially regarding the stress-evoked PINK1/Parkin-mediated mitophagy. Understanding the particular conditions under which this pathway is activated will help determining the pathogenic causes of PD as well as developing much needed new therapies.

Chapter 4. Understanding the role of the innate immune system in *Pink1/parkin* mutants

4.1. Introduction

Although inflammation is a hallmark of many neurodegenerative disorders, including PD, what exactly causes this activation of the immune system remains a mystery. Several studies have demonstrated that some DAMPs originate in the mitochondria, such as succinate, ATP, ROS or mtDNA and can initiate an immune response (Grazioli & Pugin, 2018; Nakahira et al., 2015). Further understanding of the relationship between inflammation and PD came from a study performed by Sliter et al., where the authors have shown that in the absence of *Pink1* or *Prkn*, chronic (mtDNA mutator) and acute (exhaustive exercise) mitochondrial stresses result in inflammatory phenotypes, such as increased body temperature and cytokine levels (Sliter et al., 2018). Using the mt-Keima mouse, the authors observed that mitophagy was significantly increased in WT animals subjected to exhaustive exercise, however mitophagy levels remained the same in *Prkn* and *Pink1* KO mice with or without exercise (Sliter et al., 2018), further reinforcing the idea that PINK1/Parkin mitophagy may be triggered under specific conditions. In order to further investigate the link between inflammation and PINK1/Parkin mitophagy, Sliter et al., combined the mtDNA mutator, a chronic mitochondrial stressor, with *Pink1*/*Prkn* KO mice (Sliter et al., 2018). As for the exhaustive exercise, the *mutator:Prkn*$^{-/-}$ combination led to elevated body temperature, a sign of fever and hallmark of inflammation, as well as increased cytokine levels (Sliter et al., 2018). Interestingly, increased levels of circulating mtDNA were detected in the serum of *Prkn*$^{-/-}$ mice following exhaustive exercise and in *mutator:Prkn*$^{-/-}$ mice, suggesting that failure to remove mitochondrial disruptions via mitophagy may be responsible for the PD pathology (Sliter et al., 2018). The authors hypothesised that release and accumulation of mtDNA in the cytosol may activate the DNA-sensing cGAS-STING pathway and the subsequent inflammatory phenotypes. Interestingly, loss of STING completely suppressed the locomotor deficits and neuronal loss, as well as the associated inflammation (Sliter et al., 2018). For the first time, a direct connection between PINK1/parkin related-mitophagy and inflammation has been established. While it has long been thought that the primary role of mitophagy is to preserve cells from oxidative damage, these findings raise the question of whether the key function of mitophagy in the context of PD is to protect from the exposure of DAMPs that trigger inflammatory responses rather than ROS-mediated damage.

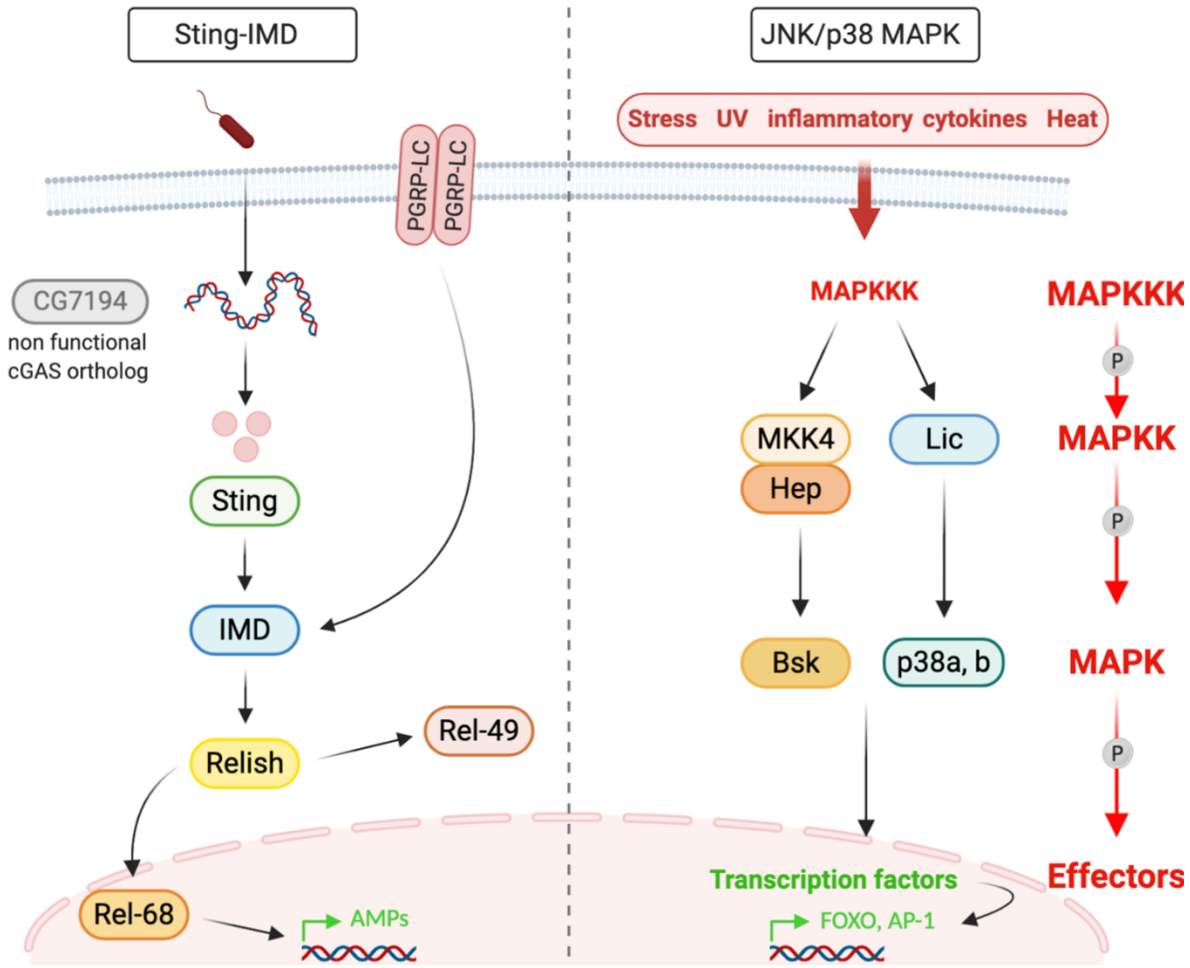

Figure 4.1. Simplified schematic representation of the *Drosophila* Sting-IMD and JNK/p38MAPK pathways

(Left) In *Drosophila*, following bacterial infection, CDNs from pathogens are directly recognised by Sting. Activation of Sting results in the production of AMPs through the IMD-Relish pathway. Although a cGAS ortholog (CG7194) has been identified in *Drosophila*, its function does not seem to be conserved in flies. Activation of the IMD pathway induces in the recruitment of the adaptor protein IMD and other components, resulting in the activation of Relish, NF-κB ortholog. Relish is then cleaved, resulting in a 49 kDa fragment that stays in the cytosol and a 68 kDa fragment that translocates to the nucleus to activate the expression of AMPs. (Right) Several MAPKKKs phosphorylate MAPKKs such as MKK4. MKK4 activates JNKs and p38 MAPKs, Hep only activates Bsk; Lic and MKK6 activate p38 MAPKs. Activation of the MAPKs results in the activation of several transcription factors.

As *Drosophila* better mimic some of the phenotypes occurring in human PD, this new role of STING should be tested in other models, such as flies. Although current evidence points towards the implication of STING-induced inflammation, other immune responses have been shown to play a role in PINK1/Parkin pathology, such as MitAP and the adaptive system. Therefore, it remains unclear which other immune pathways, such as Toll, JNK, JAK/STAT or p38 MAPK may be involved in the disease.
As all these pathways are conserved in *Drosophila*, flies provide a nice model organism for studying the role of the activation of innate immunity in *Pink1*/*parkin* mutants.

4.2. Chapter aims

The first aim of this chapter was to determine whether the implication of *Sting* in the *Pink1/parkin* pathology is conserved in *Drosophila*. To address this, loss of Sting was combined with *Pink1*/*parkin* mutants and any potential genetic interactions were assessed by behavioural assays and mitochondrial integrity evaluated in flight muscles. Furthermore, in order to recapitulate the experiments performed by Sliter et al., *parkin* mutants were combined with an additional mitochondrial stressor, the mtDNA mutator (mito-APOBEC1), in the absence of *Sting*. Finally, as Sting functions upstream in the IMD pathway, I sought to examine loss of *Relish*, a downstream effector, in the context of *Pink1/parkin* loss-of-function. As my results drastically differed from Sliter et al., I decided to investigate other immune system responses: the JNK and p38-MAPK pathways. Consequently, the second part of this chapter focussed on the analysis of RNAi and mutants of key regulators of these pathways combined with loss of *Pink1/parkin*. Climbing assay and microscopy analysis of mitochondrial integrity in IFMs were used as a read-out for potential genetic interactions. None of these pathways seemed to contribute to the *Pink1/parkin* pathology. In contrast, the JAK/STAT pathway did genetically interact with *Pink1* which is investigated in the following chapter.

4.3. Results

4.3.1. The Sting-IMD pathway does not contribute to *Pink1*/*parkin* or mtDNA mutator phenotypes

Mammalian STING plays a pivotal role in mediating an innate immune signalling cascade in response to nucleic acids derived from invading pathogens such as viruses and bacteria, that have been released into the cytosol of infected cells. Recently, the *Drosophila* ortholog *Sting* was found to trigger an innate immune response via Relish, a *Drosophila* NF-κB ortholog (Goto et al., 2018; Martin et al., 2018). A study published by Goodman's group has shown that upon *Listeria monocytogenes* infection, Sting is able to directly recognise bacterial CDNs and induce the production of AMPs through the IMD/NF-κB pathway (Martin et al., 2018). *Drosophila* also possess a cGAS ortholog, CG7194, although it does not activate Sting in this context (Figure 4.1) (Martin et al., 2018; Qiu & Zhou, 2018).

The function of *Drosophila Sting* has previously been characterised using *Sting*-RNAi lines as well as a genetic mutant, $Sting^{\Delta RG5}$ (Martin et al., 2018). However, as behavioural analysis of loss of *Sting* in the absence of pathogenic infection has not been reported before, climbing experiments were first performed. Two *Sting*-RNAi lines were expressed using the ubiquitous *da*-GAL4 driver and the flies were subjected to climbing assays at 2 and 20 days (Figure 4.2). A small impact on climbing ability was observed in 2-day-old flies expressing the $RNAi^{TRIP}$, but not the $RNAi^{GD}$ transgene which might be the result of different efficiencies between the two RNAi lines (Figure 4.2 A) This decrease was further enhanced in aged flies, probably due to an overall reduction of the flies' fitness and a lack of proper immune response (Figure 4.2 B).

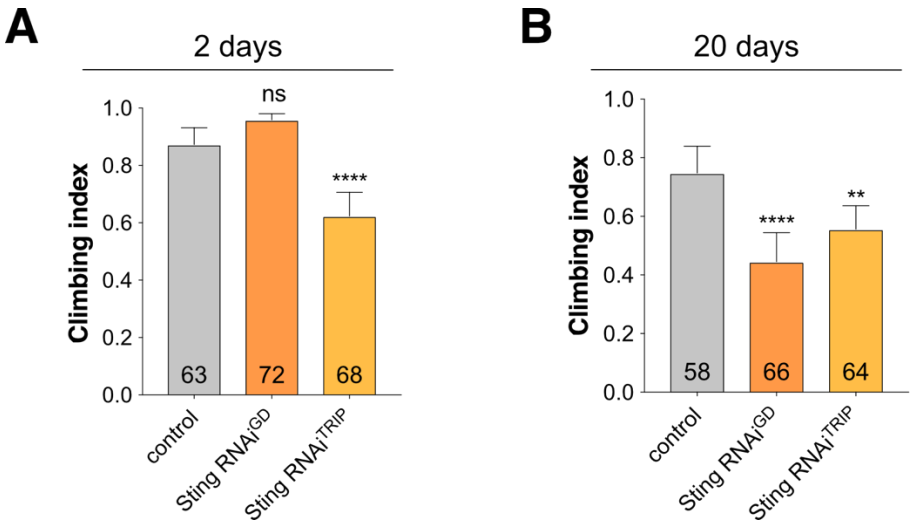

Figure 4.2. *Sting* knockdown leads to locomotor deficits

Locomotor assays analysing climbing ability in (A) 2-day- and (B) 20-day-old flies of control and two *Sting*-RNAi lines using the *da*-GAL4 driver. Charts show mean ± 95% CI. Number of animals analysed is shown in each bar. Statistical analysis was determined by Kruskal-Wallis non-parametric test with Dunn's post-hoc correction for multiple comparisons; **** P <0.0001; ** P < 0.01 and ns = non-significant. Control genotype is *UAS-lacZ* RNAi/+; *da-GAL4/+*.

In order to determine whether Sting plays a conserved role in the *Pink1/parkin* pathology, *Sting*-RNAi lines were combined with *Pink1* mutants. Behavioural analysis of these flies at 2 days old did not show any modification (suppression or enhancement) of the *Pink1* mutants climbing defect (Figure 4.3). The extensive muscle degeneration observed in *Pink1* and *parkin* mutants is often accompanied by thoracic indentations, due to the dorsal cuticle caving in the thorax (Greene et al., 2003; Park et al., 2006). These thoracic indentations were still present in the absence of *Sting* (Figure 4.3 B) and the mitochondrial integrity of the flight muscles remained largely disrupted (Figure 4.3 C). The contribution of Sting function towards *parkin* mutant phenotypes was assessed in an analogous approach. Similar to *Pink1* mutants, loss of *Sting* did not modify the climbing defect (Figure 4.4 A), thoracic indentations (Figure 4.4 B) or the disordered mitochondrial architecture (Figure 4.4 C) observed in *parkin* mutant flies.

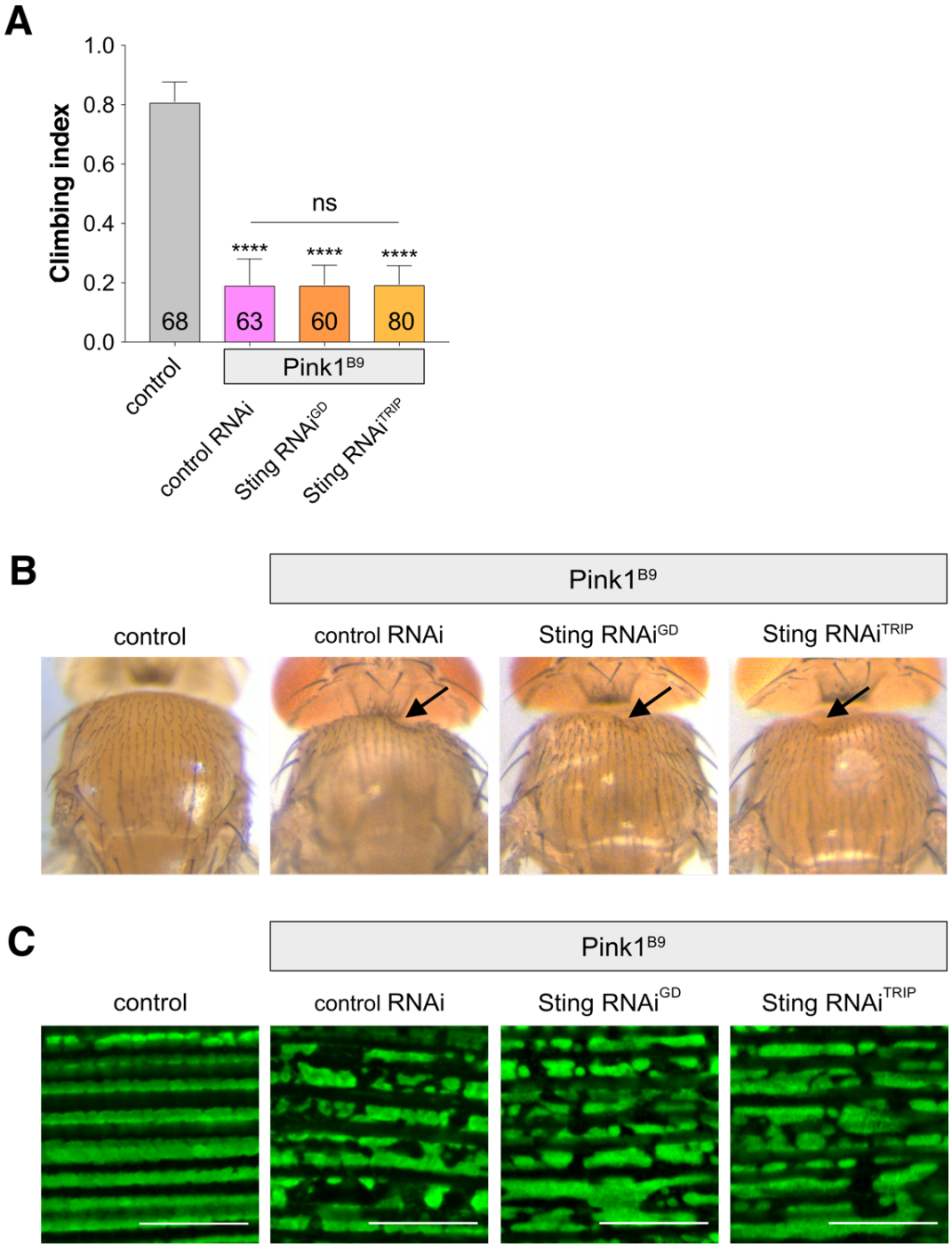

Figure 4.3. Sti*ng* knockdown does not modify *Pink1* mutant phenotypes

(A) Analysis of climbing ability, (B) thoracic indentations, and (C) mitochondrial morphology in *Pink1*^{B9} mutants combined with *Sting*-RNAi lines. Charts show mean ± 95% CI. Number of animals analysed is shown in each bar. Statistical analysis was determined by Kruskal-Wallis non-parametric test with Dunn's post-hoc correction for multiple comparisons; **** P <0.0001 and ns = non-significant. Confocal microscopy images show flight muscle mitochondria immunostained with anti-ATP5A. Scale bar = 10 µm. Control genotypes are *da-GAL4*/+ for climbing, and *w*^{1118} for thoracic indentation and microscopy. Genotypes analysed are (control RNAi) *Pink1*^{B9}*/Y; UAS-lacZ* RNAi*; da-GAL4, Pink1*^{B9}*/Y; UAS-Sting* RNAi^{GD}*/+; da-GAL4/+* and *Pink1*^{B9}*/Y;; da-GAL4*/*UAS-Sting* RNAi^{TRIP}.

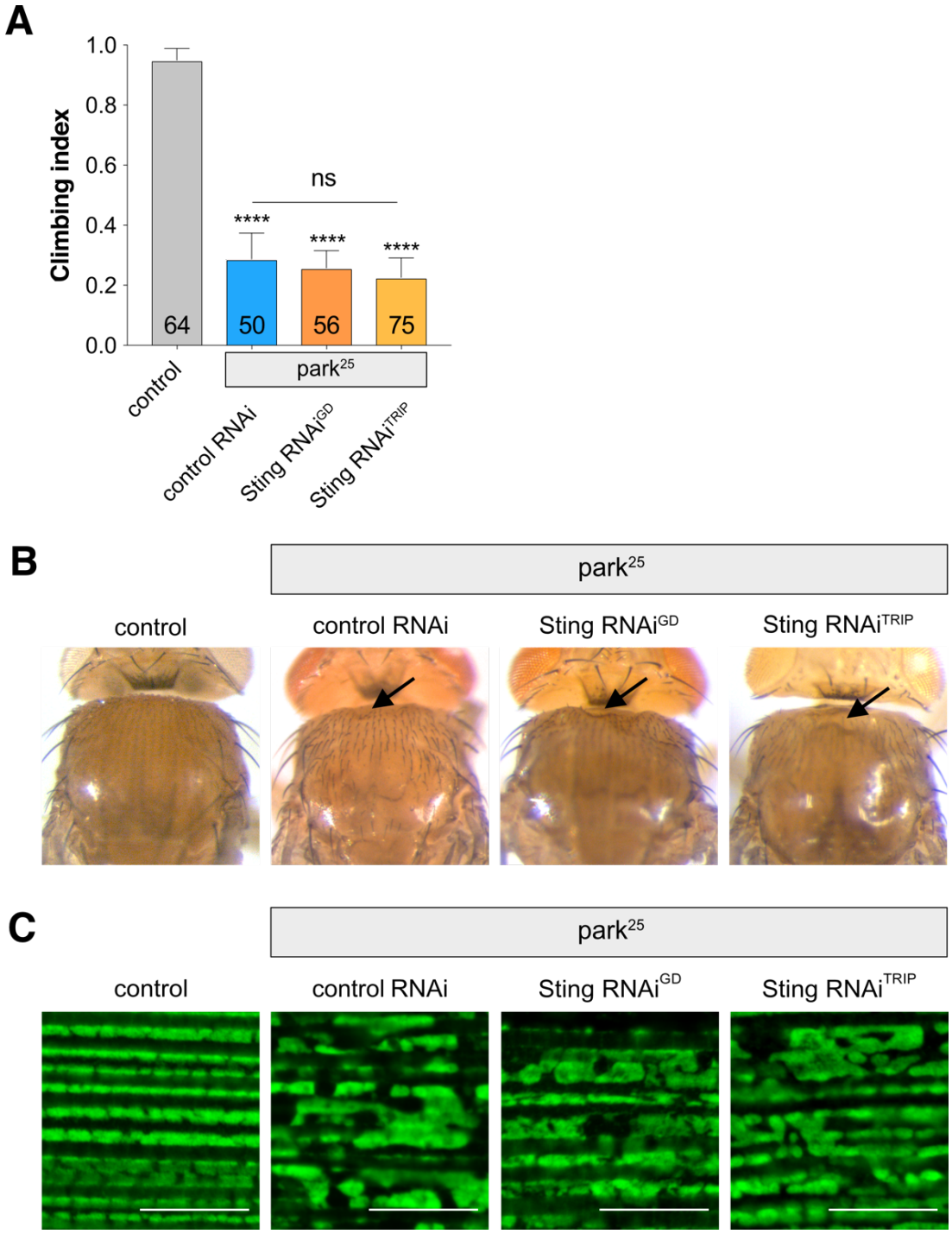

Figure 4.4. *Sting* knockdown does not modify *park*^{25} mutant phenotypes

(A) Analysis of climbing ability, (B) thoracic indentations, and (C) mitochondrial morphology in *park*^{25} mutants combined with *Sting*-RNAi lines. Charts show mean ± 95% CI. Number of animals analysed is shown in each bar. Statistical analysis was determined by Kruskal-Wallis non-parametric test with Dunn's post-hoc correction for multiple comparisons; **** P <0.0001 and ns = non-significant. Confocal microscopy images show flight muscle mitochondria immunostained with anti-ATP5A. Scale bar = 10 µm. Control genotypes are *da-GAL4*/+ for climbing, and *w*^{1118} for thoracic indentation and microscopy. Genotypes analysed are (control RNAi) *UAS-lacZ* RNAi/+; *da-GAL4, park*^{25}*/park*^{25}, *UAS-Sting* RNAi^{GD}/+; *da-GAL4, park*^{25}*/park*^{25} and *da-GAL4, park*^{25}*/UAS-Sting* RNAi^{TRIP}, *park*^{25}.

As RNAi do not always confer the complete loss-of-function that can occur with a genetic mutation, the previously established *Sting*$^{\Delta RG5}$ null mutant was used to complement the data obtained with the *Sting*-RNAi lines. Work from Martin et al., has shown that upon infection, these null mutants exhibit a significantly shorter lifespan and are unable to produce some key AMPs, highlighting their inability to fight the pathogen invasion and further validating the role of *Sting* as a key component of the *Drosophila* immune system (Martin et al., 2018). As no behavioural phenotypes were analysed prior to this study, heterozygous and homozygous *Sting*$^{\Delta RG5}$ mutants were tested for climbing at 2 and 20 days. A small decline in climbing ability was observed in young homozygous *Sting* mutants which was consistent with the *Sting*-RNAi results (Figure 4.5 A). Although aged *Sting*-RNAi flies showed a consistent decrease in their climbing ability, this was not evident in *Sting* mutants (Figure 4.5 B), reinforcing the usefulness of relying on two different tools to investigate loss-of-functions. Immunostaining and microscopy analysis of the indirect flight muscles did not reveal any obvious disruption of the mitochondrial integrity of the *Sting* mutants, suggesting that the decrease in climbing might be the result of an overall reduction in the flies' fitness in response to a lack of proper immune response (Figure 4.5 C).

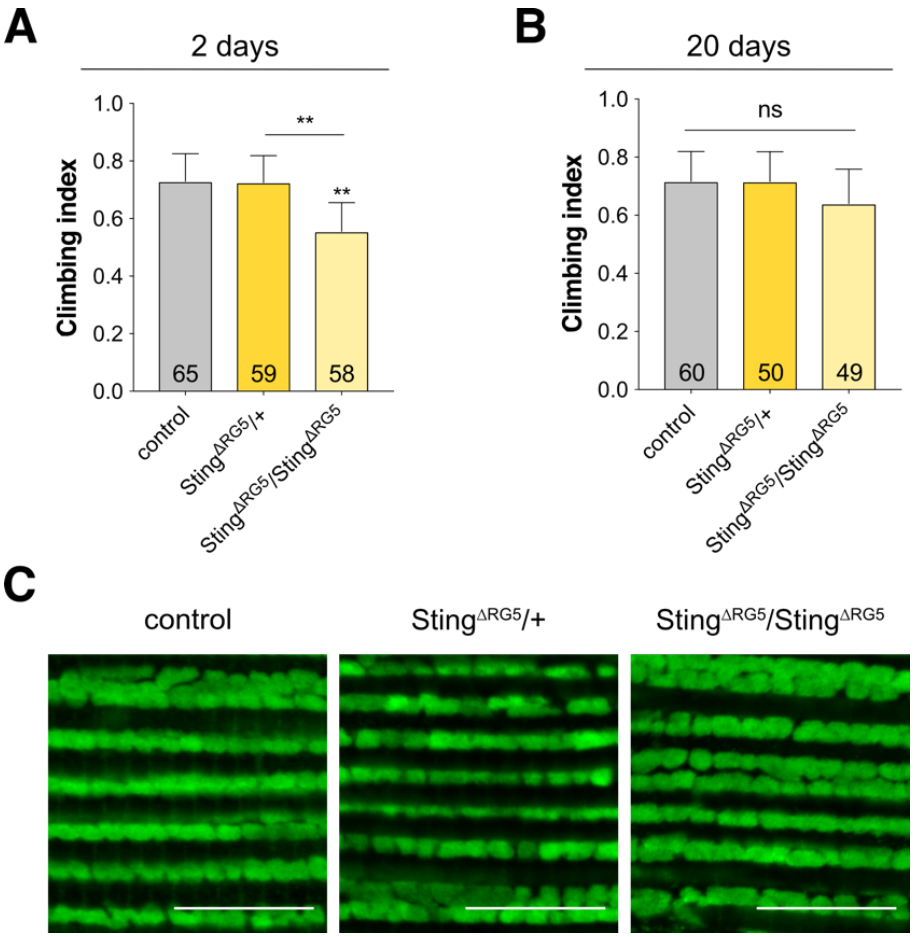

Figure 4.5. Loss of *Sting* leads to limited locomotor deficits

Locomotor assays analysing climbing ability in (A) 2-day- and (B) 20-day-old flies of control and *Sting* null mutant (*Sting*$^{\Delta RG5}$). Charts show mean ± 95% CI. Number of animals analysed is shown in each bar. Statistical analysis was determined by Kruskal-Wallis non-parametric test with Dunn's post-hoc correction for multiple comparisons; ** P <0.01 and ns = non-significant. Control genotype is w^{1118}. (C) Representative confocal microscopy analysis of mitochondria in flight muscles, immunostained with anti-ATP5A, in control (w^{1118}) and *Sting* heterozygous and homozygous mutants. Scale bar = 10 µm.

Consistent with the observations obtained with the RNAi lines, combination of heterozygous and homozygous *Sting*$^{\Delta RG5}$ with *Pink1* mutants did not modify the climbing defect (Figure 4.6 A), thoracic indentations (Figure 4.6 B) or the disorganisation of the mitochondrial architecture in the flight muscles (Figure 4.6 C).

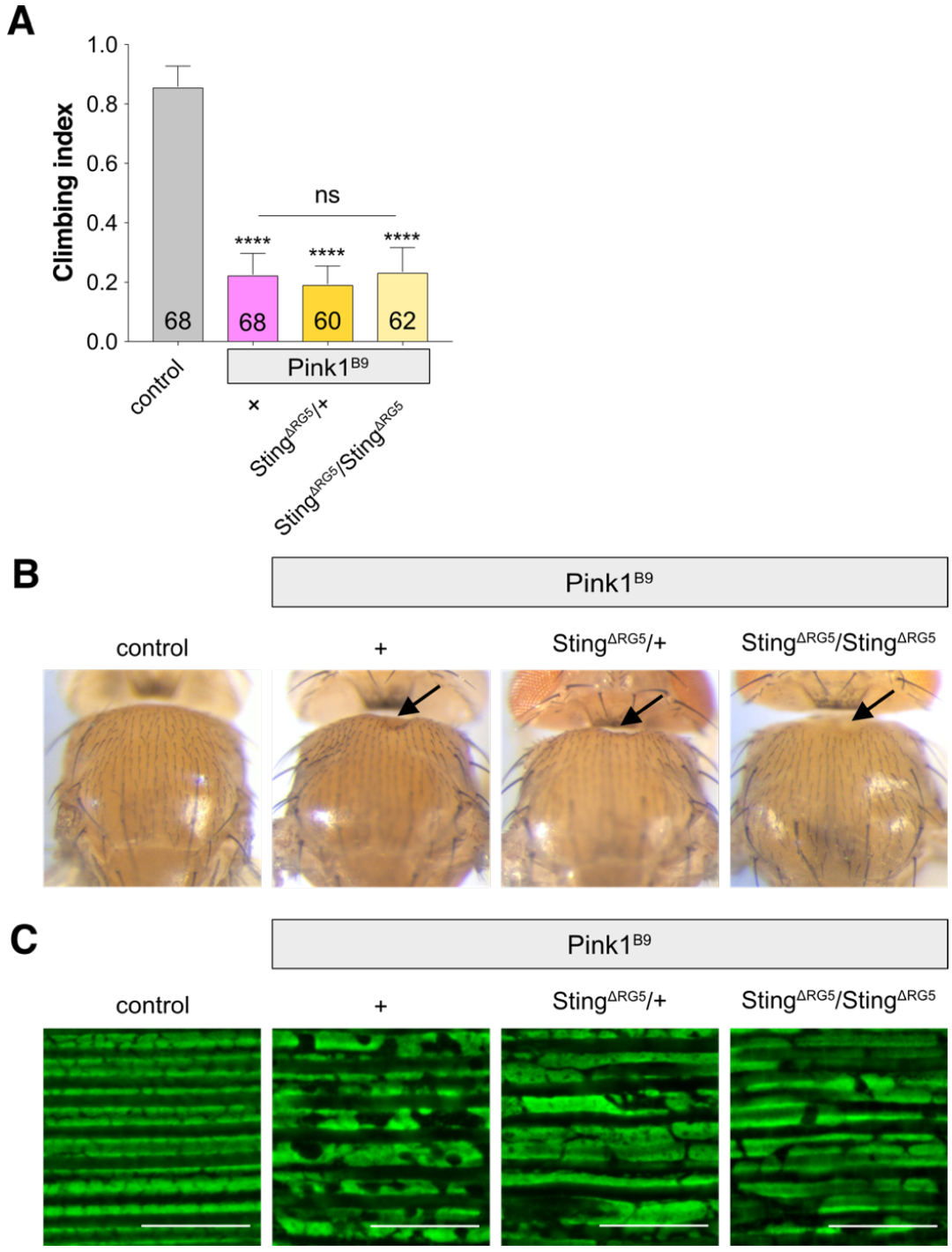

Figure 4.6. Loss of *Sting* does not rescue *Pink1* mutant phenotypes

(A) Analysis of climbing ability, (B) thoracic indentations, and (C) mitochondrial morphology in *Pink1*^{B9} mutants combined with *Sting*$^{\Delta RG5}$. Charts show mean ± 95% CI. Number of animals analysed is shown in each bar. Statistical analysis was determined by Kruskal-Wallis non-parametric test with Dunn's post-hoc correction for multiple comparisons; **** P <0.0001 and ns = non-significant. Confocal microscopy images show flight muscle mitochondria immunostained with anti-ATP5A. Scale bar = 10 µm. Control genotype is *w*^{1118}. Genotypes analysed are *Pink1*^{B9}/Y, *Pink1*^{B9}/Y; *Sting*$^{\Delta RG5}$/+ and *Pink1*^{B9}/Y; *Sting*$^{\Delta RG5}$/*Sting*$^{\Delta RG5}$.

Loss of *Sting* in a *parkin* mutant background led to similar results (Figure 4.7). Indeed, loss of *Sting* failed to rescue the decline in the climbing ability (Figure 4.7 A), the thoracic indentations (Figure 4.7 B) or the disrupted mitochondrial organisation of the IFMs (Figure 4.7 C) observed in *parkin* mutants. These data nicely complemented the observations from the *Sting*-RNAi, however, they significantly differed from the results derived from *Sting:Prkn* or *Sting:Pink1* double mutant mice from Sliter et al (Sliter et al., 2018). While the STING pathway was proposed to mediate the motor and neurodegenerative defects observed in *Pink1*/*Prkn* null mice and although DA neurodegeneration was not investigated in our study, the above data indicate that *Drosophila Sting* does not contribute to the behavioural or mitochondrial phenotypes observed in *Pink1/parkin* mutants.

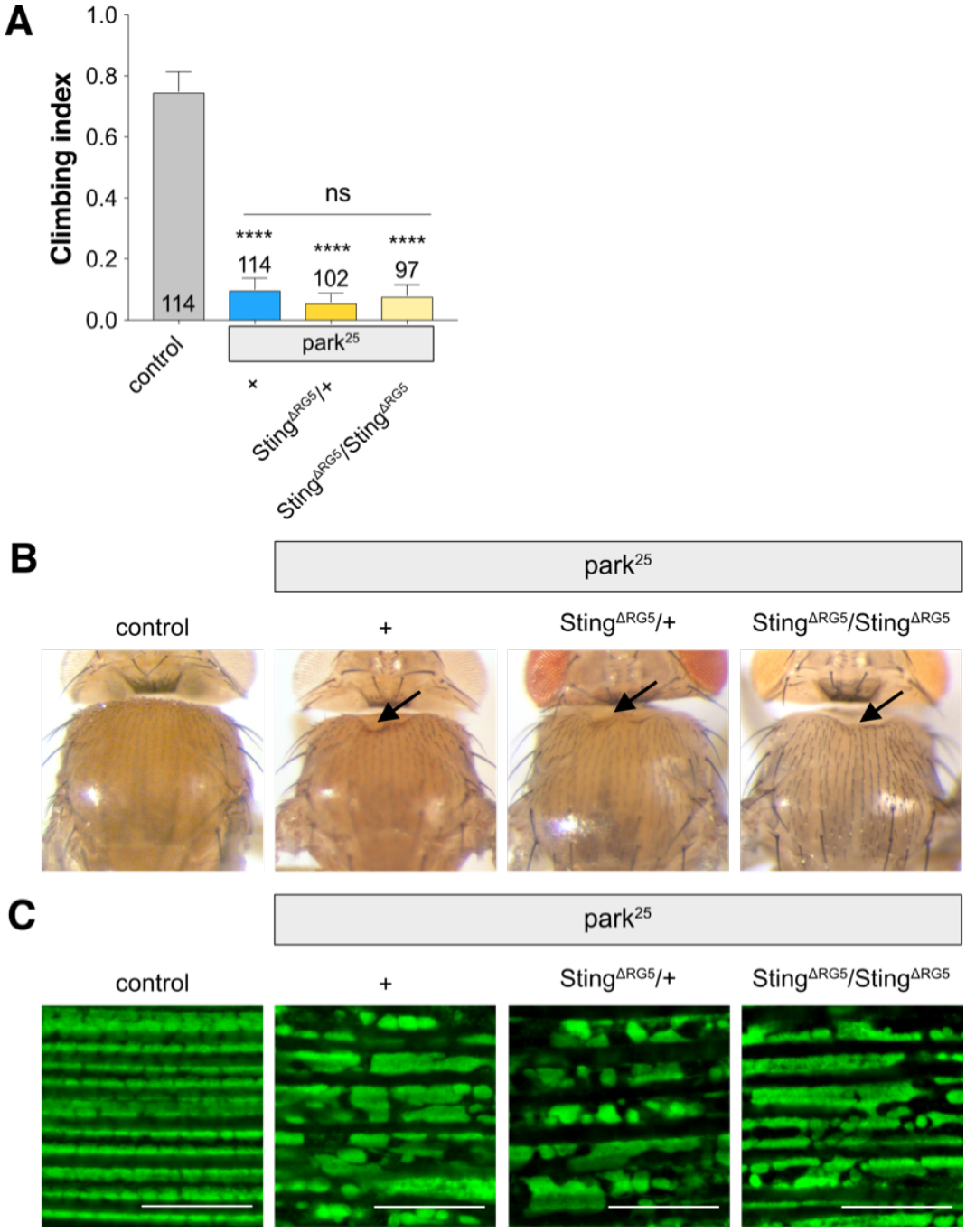

Figure 4.7. Loss of *Sting* does not rescue *park*^{25} mutant phenotypes

(A) Analysis of climbing ability, (B) thoracic indentations, and (C) mitochondrial morphology in *park*^{25} mutants combined with *Sting*$^{\Delta RG5}$. Charts show mean ± 95% CI. Number of animals analysed is shown in each bar. Statistical analysis was determined by Kruskal-Wallis non-parametric test with Dunn's post-hoc correction for multiple comparisons; **** P <0.0001 and ns = non-significant. Confocal microscopy images show flight muscle mitochondria immunostained with anti-ATP5A. Scale bar = 10 µm. Control genotypes are *w*^{1118}. Genotypes analysed are *park*^{25}/*park*^{25}, *Sting*$^{\Delta RG5}$/+; *park*^{25}/*park*^{25} and *Sting*$^{\Delta RG5}$/*Sting*$^{\Delta RG5}$; *park*^{25}/*park*^{25}.

To further interrogate whether the *Drosophila* Sting pathway acts in a similar fashion to the pathway in mice, additional experiments were performed to recapitulate the conditions used by Sliter et al (Sliter et al., 2018). To address this, loss of *Sting* was combined with a mitochondrial stressor, the mtDNA mutator, mito-APOBEC1, in addition to *parkin* loss-of-function. Mito-APOBEC1 is a powerful mutator that has been shown to introduce mutations specifically in the mtDNA. Flies expressing mito-APOBEC1 exhibit shortened lifespan and strong climbing deficits (Andreazza et al., 2019). Interestingly, neither the loss of *parkin* nor *Sting* exacerbated mito-APOBEC1 climbing defects (Figure 4.8 A). In sharp contrast to the mouse results, the combination of mito-APOBEC1 in a double mutant background, *parkin:Sting*, significantly worsened the climbing decline (Figure 4.8 A). While loss of *Sting* did not impact normal lifespan, it shortened the lifespan of mito-APOBEC1 and to a greater extend the combination of mito-APOBEC1 with *parkin* loss-of-function, consistent with the locomotor analysis (Figure 4.8 B).

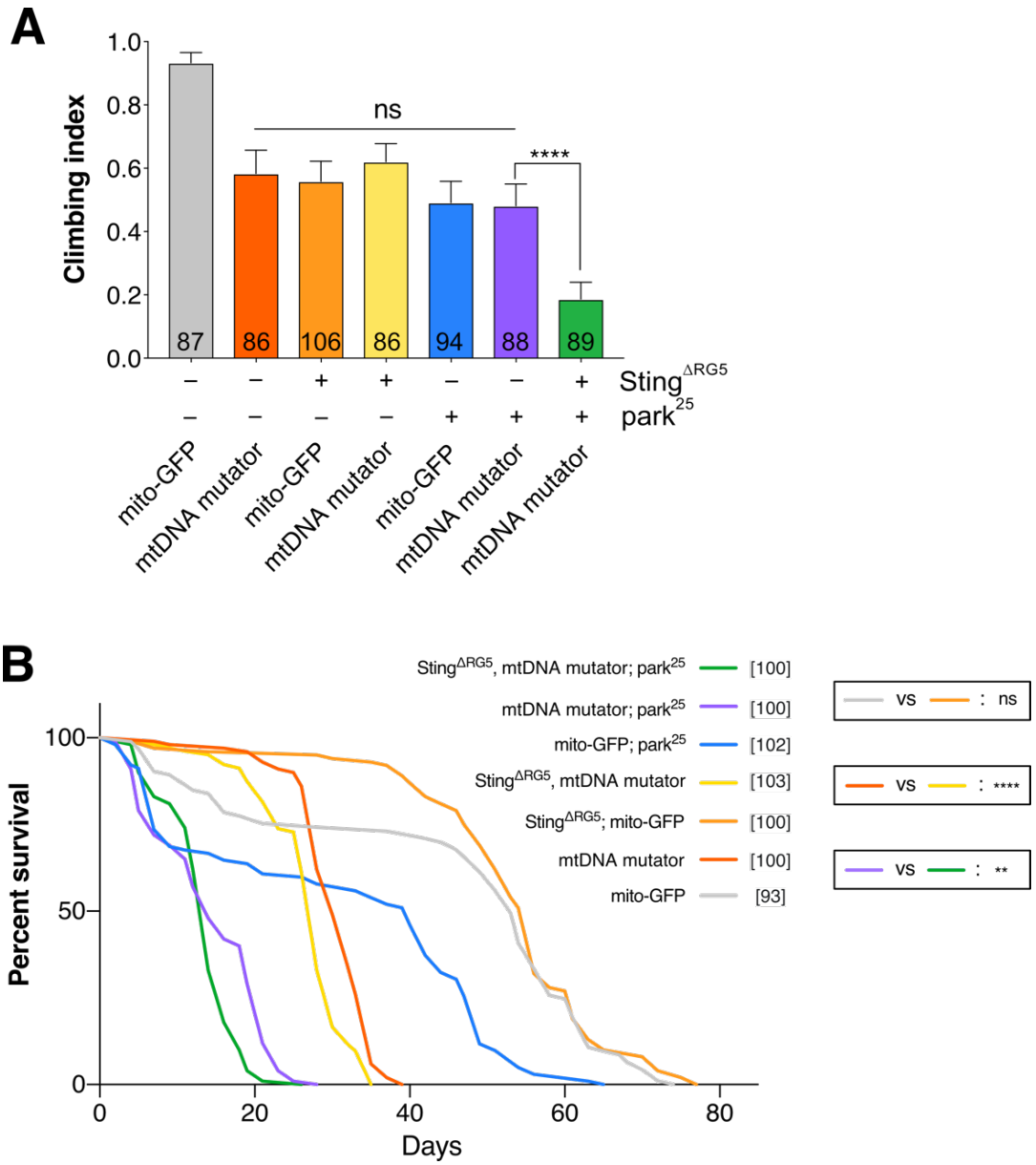

Figure 4.8. Loss of *Sting* does not ameliorate *mutator*;*parkin* combinations

Analysis of (A) climbing ability and (B) lifespan in flies combining mito-APOBEC1 expression with or without *park*^{25} and/or *Sting*$^{\Delta RG5}$. Transgene expression was driven by *da*-GAL4. UAS-mitoGFP expression was used as a control. Charts show mean ± 95% CI; number of animals analysed is shown in each bar for climbing, and beside the genotype for lifespan. For climbing, statistical significance was determined by Kruskal-Wallis test with Dunn's post hoc correction for multiple comparisons; and for lifespan, by Log-rank (Mantel Cox) test; **** P<0.0001; ** P <0.01 and ns, non-significant.

Since the loss of STING completely abrogated the *Pink1*$^{-/-}$ and *Prkn*$^{-/-}$ associated neurodegeneration and motor phenotypes provoked by additional mitochondrial stresses in mice, the lack of suppression of *Pink1/parkin* phenotypes in *Drosophila* was

surprising (Sliter et al., 2018). *Drosophila* Sting is believed to act upstream of the IMD pathway. Martin et al., have shown that Sting can activate Relish by mediating its cleavage into a short fragment Rel-49 that stays in the cytosol and a longer one, Rel-68, that translocates to the nucleus and activates the transcription of several AMPs (Martin et al., 2018; Qiu & Zhou, 2018). Therefore, the loss of the downstream transcription factor Relish (Rel), key player of the IMD pathway and homolog of NF-κB, was analysed to further examine the potential contribution of the Sting-IMD axis to the *Pink1/parkin* pathology.

To this end, *Rel*-RNAi and Rel^{E20} null mutants were subjected to behavioural assays to investigate loss of *Relish*, in a context independent of pathogenic infection. Previously established Rel^{E20} mutants have only been characterised in the context of infections. Upon *Listeria monocytogenes* infection, these null mutants display shorter lifespan due to their inability to produce AMPs and fight bacterial infections (Hedengren et al., 1999). The ubiquitous expression of two *Rel*-RNAi lines using *da*-GAL4 led to modest effect on climbing at 20 days (Figure 4.9 A and B), however, Rel^{E20} mutants displayed a stronger decrease in their locomotor abilities (Figure 4.9 C and D). Microscopy analysis of indirect flight muscles of 2-day-old Rel^{E20} mutants did not show any major disruption of their mitochondrial integrity (Figure 4.9 E). Similar to the *Sting* results, *Relish* knockdown (Figure 4.10 A) or Rel^{E20} null mutants (Figure 4.10 B) failed to modify the climbing defects observed in *Pink1* mutants. In contrast to expectation, *Relish* loss-of-function significantly enhanced *Pink1* locomotor deficits (Figure 4.10 B). Unsurprisingly, the mitochondrial organisation of these flies' flight muscles did not improve (Figure 4.10 C).

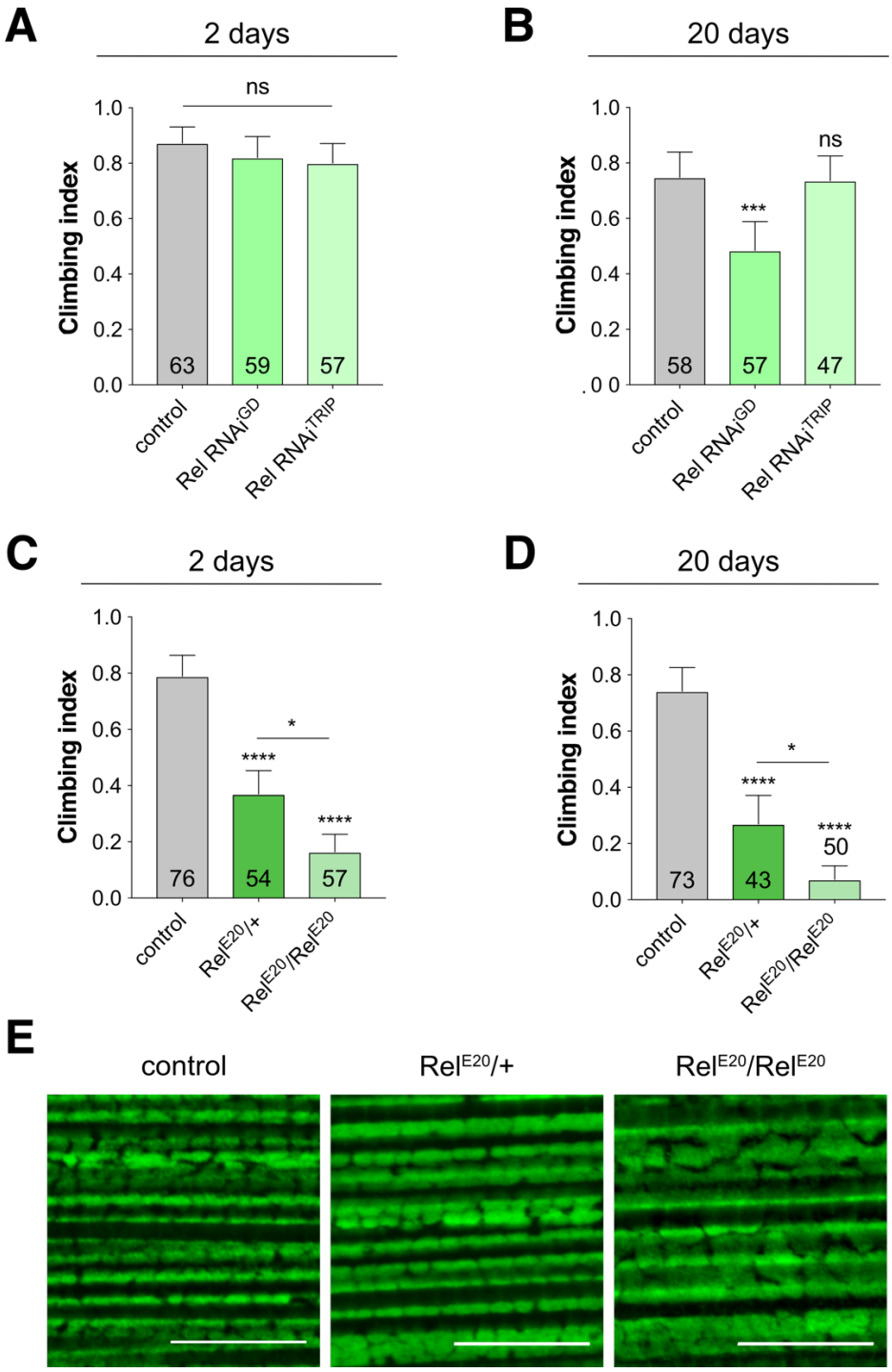

Figure 4.9. *Relish* knockdown causes mild climbing defects

Locomotor assays analysing climbing ability in (A and C) 2-day- and (B and D) 20-day-old flies of (A and B) *Relish*-RNAi expressed with *da*-GAL4 and (C and D) heterozygous and homozygous Rel^{E20} mutants. (E) Confocal microscopy analysis of mitochondria in flight muscles, immunostained with anti-ATP5A, in control (w^{1118}) and heterozygous and homozygous Rel^{E20} mutants. Charts show mean ± 95% CI. Number of animals analysed is shown in each bar. Statistical analysis was determined by Kruskal-Wallis non-parametric test with Dunn's post-hoc correction for multiple comparisons; **** $P < 0.0001$; *** $P < 0.001$; * $P < 0.05$ and ns = non-significant. Control genotypes are (A and B) *UAS-lacZ* RNAi/+; *da-GAL4/+* and (C-E) w^{1118}.

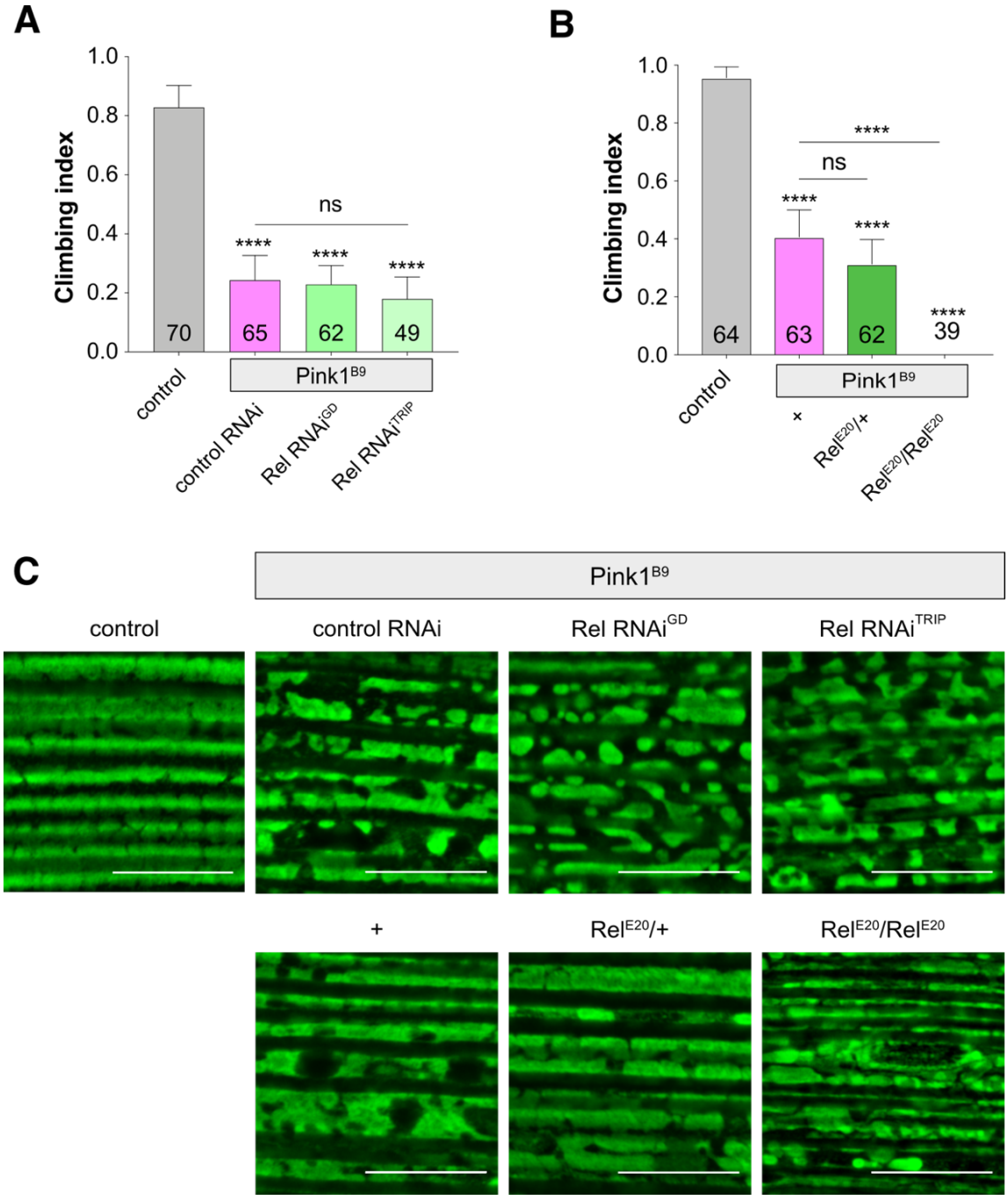

Figure 4.10. Loss of *Relish* does not modify *Pink1* mutant phenotypes

Locomotor assays analysing climbing ability in fles of (A) *Relish*-RNAi knockdown and (B) *Relish* mutant (*Rel*^{E20}) combined with *Pink1*^{B9} mutants. (C) Mitochondrial morphology in IFMs of the same genotypes. Charts show mean ± 95% CI. Number of animals analysed is shown in each bar. Statistical analysis was determined by Kruskal-Wallis non-parametric test with Dunn's post-hoc correction for multiple comparisons; **** *P* <0.0001 and ns = non-significant. Scale bar = 10 µm. Control genotypes are *UAS-lacZ* RNAi/+; *da-GAL4*/+ and *w*^{1118}. Genotypes analysed are (control RNAi) *Pink1*^{B9}/Y; *UAS-lacZ* RNAi/+; *da-GAL4*/+, *Pink1*^{B9}/Y; *UAS-Rel* RNAi^{GD}/+; *da-GAL4*/+ , *Pink1*^{B9}/Y;; *da-GAL4*/*UAS-Rel* RNAi^{TRIP}, *Pink1*^{B9}/Y, *Pink1*^{B9}/Y;; *Rel*^{E20}/+ and *Pink1*^{B9}/Y;; *Rel*^{E20}/*Rel*^{E20}.

Similar experiments were conducted in a *parkin* mutant background and led to comparable results (Figure 4.11). The climbing deficit (Figure 4.11 A) and the disrupted mitochondrial morphology observed in the flight muscles (Figure 4.11 B) of *parkin* mutant flies did not change in combination with *Rel*-RNAi expression. As *Relish* and *parkin* genes sit very close together on the third chromosome of the *Drosophila* genome, any potential recombination event between the two genes is extremely rare. Therefore, during this study, the genetic interaction between *Relish* and *parkin*, using Rel^{E20} mutant was not assessed.

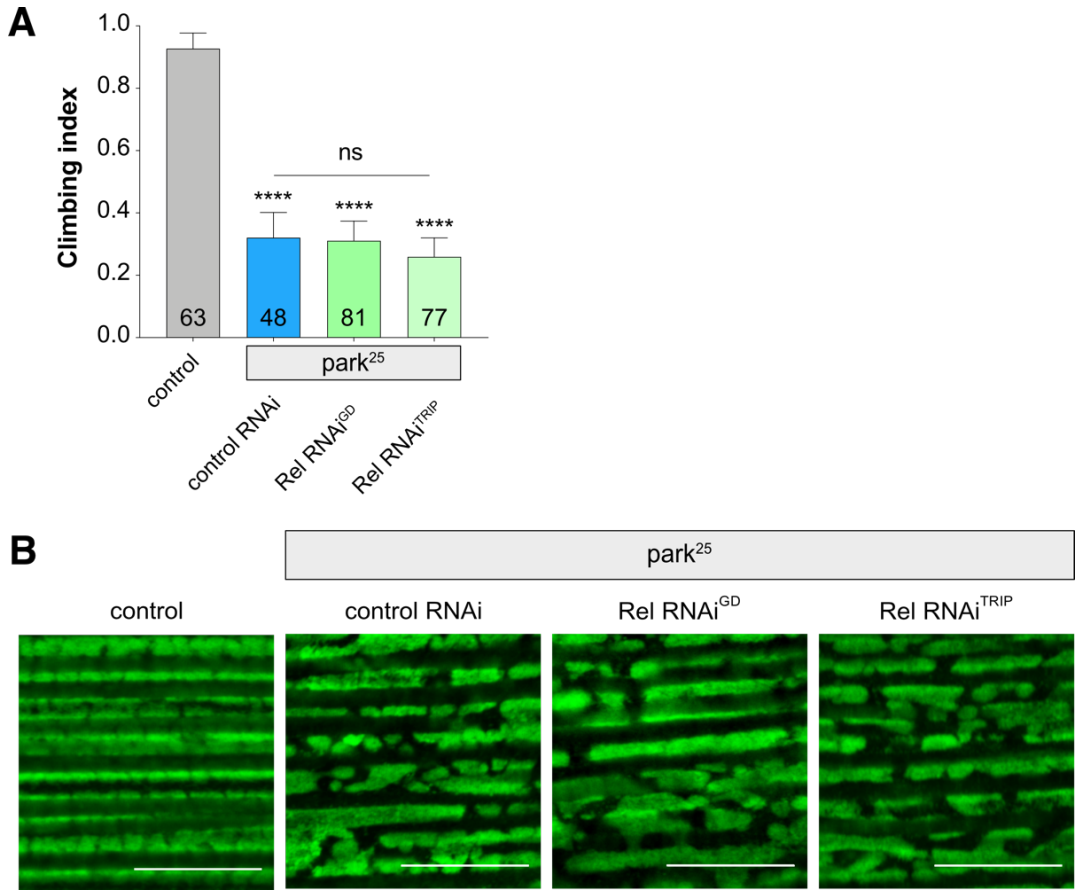

Figure 4.11. *Relish* knockdown does not modify *park*^{25} mutant phenotypes

(A) Analysis of climbing ability and (B) mitochondrial morphology in *park*^{25} mutants combined with two *Relish*-RNAi lines. Charts show mean ± 95% CI. Number of animals analysed is shown in each bar. Statistical analysis was determined by Kruskal-Wallis non-parametric test with Dunn's post-hoc correction for multiple comparisons; **** $P<0.0001$ and ns = non-significant. Confocal microscopy images show flight muscle mitochondria immunostained with anti-ATP5A. Scale bar = 10 µm. Control genotypes are *UAS-lacZ* RNAi/+; *da-GAL4*/+ for climbing and w^{1118} for microscopy. Genotypes analysed are (control RNAi) *UAS-lacZ* RNAi/+; *da-GAL4, park*^{25}/*park*^{25}, *UAS-Rel* RNAi^{GD}/+; *da-GAL4, park*^{25}/*park*^{25} and *da-GAL4, park*^{25}/*UAS-Rel* RNAi^{TRIP}, *park*^{25}.

While evidence indicate that the STING pathway plays a major role in the mammalian *Pink1/parkin* pathology, my results indicate that the Sting signalling cascade is not contributing to the *Pink1/parkin* pathological phenotypes in *Drosophila*. Although evidence from transcriptomic analysis of *Drosophila Pink1/parkin* mutants suggest an upregulation of several immune-related genes, the Sting and IMD pathways do not seem to play a role in the phenotypes observed in these mutants (Greene et al., 2005; Tufi et al., 2014). Therefore, this led to the investigation of other immune pathways in order to further uncover the implication of the innate immune system in *Pink1/parkin* mutant phenotypes.

4.3.2. Loss of key regulators of the JNK pathway does not modify *Pink1/parkin* phenotypes

The JNK pathway is a conserved signalling cascade that regulates a plethora of cellular functions ranging from morphogenesis, apoptosis and immune responses (Igaki, 2009). This signalling cascade is induced by a wide variety of intrinsic and external insults such as DNA damage, ROS and pathogen invasion in both vertebrates and invertebrates (Biteau et al., 2011). These stimuli activate a member of the JNK Kinase family which triggers a phosphorylation cascade. While vertebrates have several homologs, the JNK signalling pathway of the *Drosophila* is less complex. Flies have a single JNK, Bsk and two JNK kinases, Hep and the less studied MKK4 (Biteau et al., 2011; Igaki et al., 2002). Briefly, the *Drosophila* JNK signalling cascade is activated by a cell surface ligand, such as Eiger (Egr), the TNF homolog in fly, that binds to its receptors, Wengen and Grindelwald, the TNFR homologs. Depending on the stimuli, adaptor proteins mediate the signal to the core JNK signalling components which includes several MAPKKKs, Hep and Bsk (Biteau et al., 2011). The phosphorylation of the transcription factors, c-Jun and c-Fos, which induces various cellular responses (Figure 4.1) (Igaki, 2009).

In order to investigate whether or not the JNK pathway plays a role in the *Pink1/parkin* pathology, RNAi lines and mutants were used to induce *egr* knockdown. The egr^{3} null mutant was previously generated by Igaki et al., and several studies have confirmed the increased susceptibility of egr^{3} mutants to pathogen invasion, leading, among other consequences, to a shorter lifespan (Igaki et al., 2002; Schneider et al., 2007).

However, as for the previous mutants used in this study, loss of *egr* in a context independent of pathogenic infection has not been evaluated before. Locomotor analysis of *egr*-RNAi using *da*-GAL4 revealed a strong climbing defect at 2 days which was further enhanced at 20 days (Figure 4.12 A and B). These results were nicely complemented by similar observations in heterozygous and homozygous egr^3 null mutants (Figure 4.12 C and D).

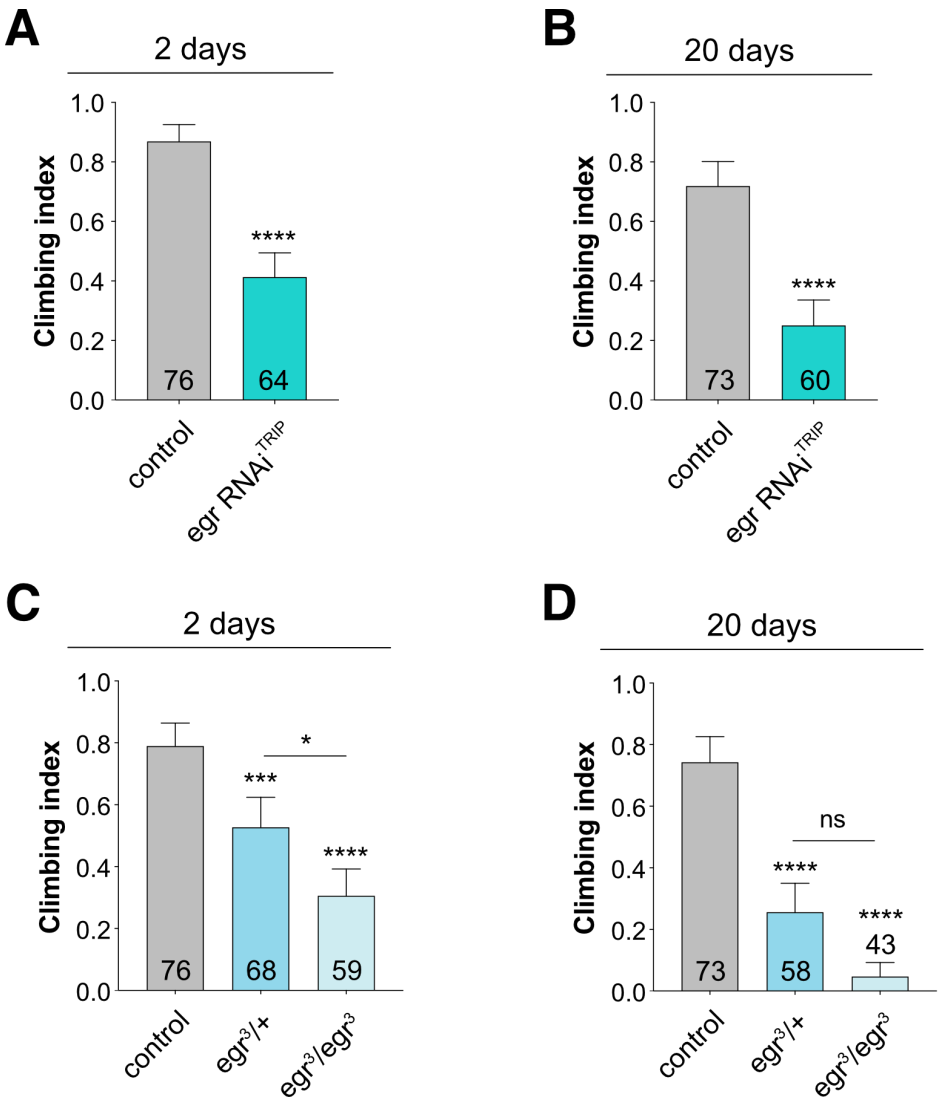

Figure 4.12. Loss of *eiger* causes strong climbing defects

Locomotor assays analysing climbing ability in (A and C) 2-day and (B and D) 20-day old flies of (A and B) *eiger*-RNAi expressed with *da*-GAL4 and (C and D) heterozygous and homozygous egr^3 mutants. Charts show mean ± 95% CI. Number of animals analysed is shown in each bar. Statistical analysis was determined by Welch's *t*-test or Kruskal-Wallis non-parametric test with Dunn's post-hoc correction for multiple comparisons; **** P <0.0001; *** P <0.001; * P<0.05 and ns = non-significant. Control genotypes are *UAS-lacZ* RNAi/+; *da-GAL4*/+ and w^{1118}.

While *egr* knockdown in a *Pink1* mutant background led to a slight rescue of the *Pink1* climbing defect at 2 days old, no change was observed in aged flies (Figure 4.13 A). Surprisingly, heterozygous or homozygous *egr*^{3} combined with *Pink1* mutant did not show any rescue of the climbing deficit; conversely, it exacerbated the phenotype (Figure 4.13 B). Finally, loss of *egr* using *egr*-RNAi (Figure 4.14 A) or *egr*^{3} mutant, in heterozygosity or homozygosity, (Figure 4.14 B) failed to improve the disrupted mitochondrial integrity observed in *Pink1* mutant IFMs.

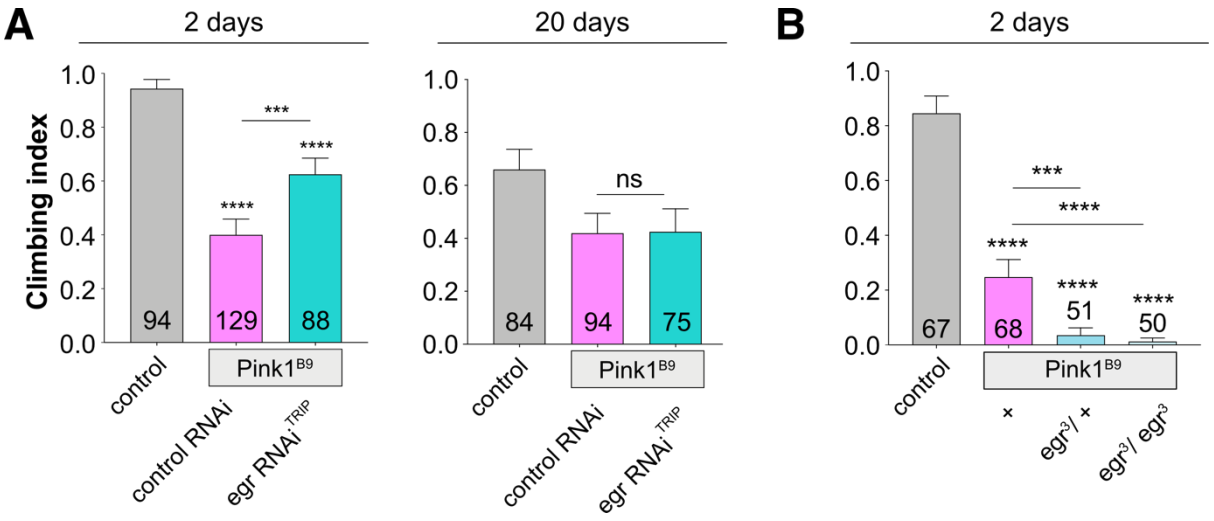

Figure 4.13. e*iger* knockdown, but not complete loss of *eiger,* rescues *Pink1* mutant climbing defects

Analysis of climbing ability in *Pink1*^{B9} mutants combined with (A) *eiger* RNAi at 2 and 20 days and (B) *egr*^{3} null mutants at 2 days. Charts show mean ± 95% CI. Number of animals analysed is shown in each bar. Statistical analysis was determined by Kruskal-Wallis non-parametric test with Dunn's post-hoc correction for multiple comparisons; **** *P* <0.0001, *** *P* <0.001; and ns = non-significant. Control genotypes are *UAS-lacZ* RNAi/+; *da-GAL4*/+ and *w*^{1118}. Genotypes analysed are (control RNAi) *Pink1*^{B9}*/Y; UAS-lacZ* RNAi/+; *da-GAL4*/+, *Pink1*^{B9}*/Y;; da-GAL4*/*UAS-egr RNAi*^{TRIP}, *Pink1*^{B9}*/Y, Pink1*^{B9}*/Y; egr*^{3}/+ and *Pink1*^{B9}*/Y; egr*^{3}*/egr*^{3}.

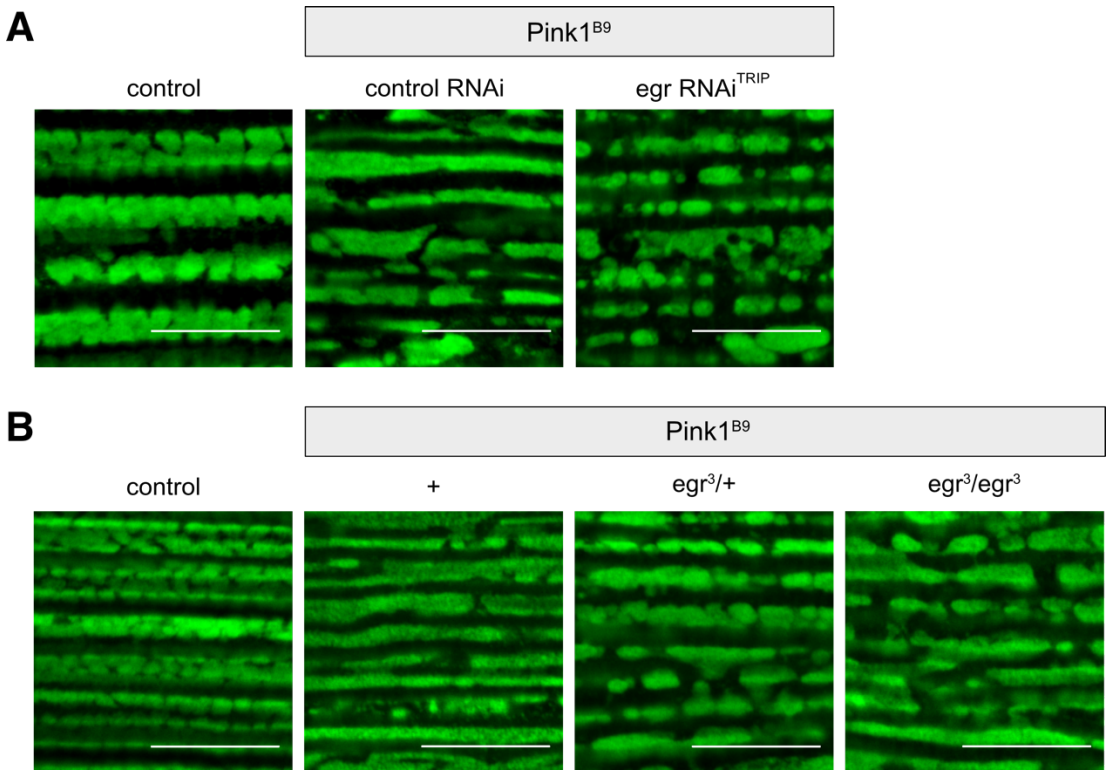

Figure 4.14. Loss of *eiger* does not rescue *Pink1*^{B9} mutant mitochondrial morphology

Confocal microscopy images show flight muscle mitochondria immunostained with anti-ATP5A in *Pink1*^{B9} mutants combined with (A) *eiger*-RNAi and (B) heterozygous and homozygous *egr*^{3} mutants. Scale bar = 10 µm. Control genotype is *w*^{1118}. Genotypes analysed are (control RNAi) *Pink1*^{B9}*/Y; UAS-lacZ* RNAi/+; *da-GAL4/+, Pink1*^{B9}*/Y;; da-GAL4*/*UAS-egr* RNAi^{TRIP}, *Pink1*^{B9}*/Y, Pink1*^{B9}*/Y; egr*^{3}/+ and *Pink1*^{B9}*/Y; egr*^{3}*/egr*^{3}.

Similar experiments were performed in a *parkin* mutant background. Consistent with the data above, loss of *egr* did not ameliorate the climbing decline (Figure 4.15 A and B) or the perturbed mitochondrial architecture characteristic of 2-day-old *parkin* mutants IFMs (Figure 4.15 C and D).

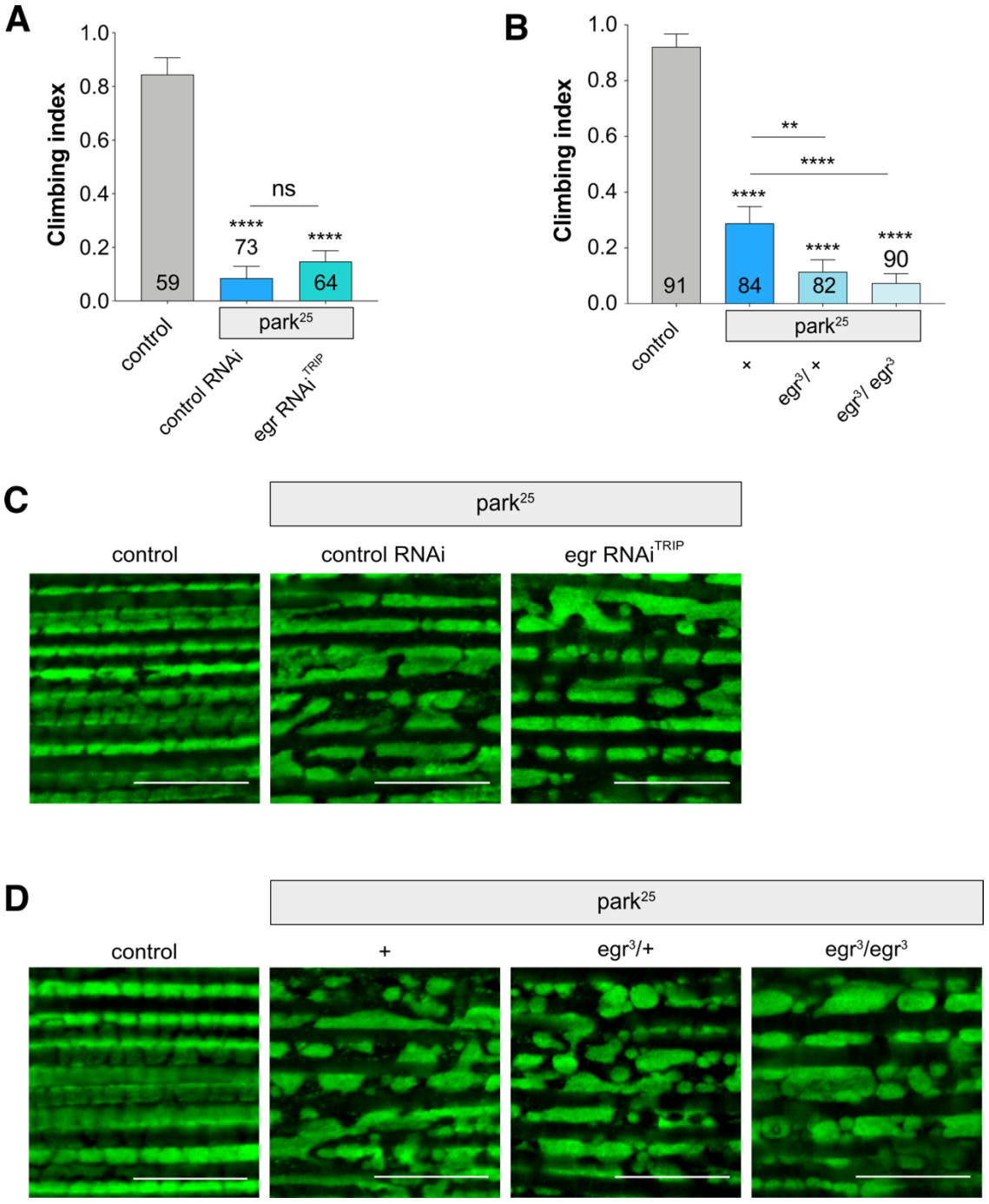

Figure 4.15. Loss of *eiger* does not rescue *park*^{25} mutant phenotypes

(A and B) Analysis of climbing ability and (C and D) mitochondrial morphology in *park*^{25} mutants combined with (A and C) *egr*-RNAi and (B and D) heterozygous and homozygous *egr*^{3} mutants. Charts show mean ± 95% CI. Number of animals analysed is shown in each bar. Statistical analysis was determined by Kruskal-Wallis non-parametric test with Dunn's post-hoc correction for multiple comparisons; **** P <0.0001, ** P <0.01; and ns = non-significant. Confocal microscopy images show flight muscle mitochondria immunostained with anti-ATP5A. Scale bar = 10 µm. *UAS-lacZ* RNAi/+; *da-GAL4*/+ and *w*^{1118}. Genotypes analysed are (control RNAi) *UAS-lacZ* RNAi/+; *da-GAL4, park*^{25}/*park*^{25}, *da-GAL4, park*^{25}/*UAS-egr* RNAi^{TRIP}, *park*^{25}, *park*^{25}/*park*^{25}, *egr*^{3}/+; *park*^{25}/*park*^{25} and *egr*^{3}/*egr*^{3}; *park*^{25}/*park*^{25}.

Loss of one of the core components of the signalling cascade, *basket*, was next analysed. Consistent with bsk^{LL} loss-of-function being homozygous lethal, expression of *bsk*-RNAi with the ubiquitous driver *da*-GAL4 was pupal lethal. Hence, subsequent experiments were performed using a weaker ubiquitous driver *armadillo* (*arm*)-GAL4 or heterozygous bsk^{LL}/+ animals. *basket* knockdown only induces mild climbing deficits at 20 days (Figure 4.16 A and B), however, this was not evident in bsk^{LL} heterozygous mutants (Figure 4.16 C and D).

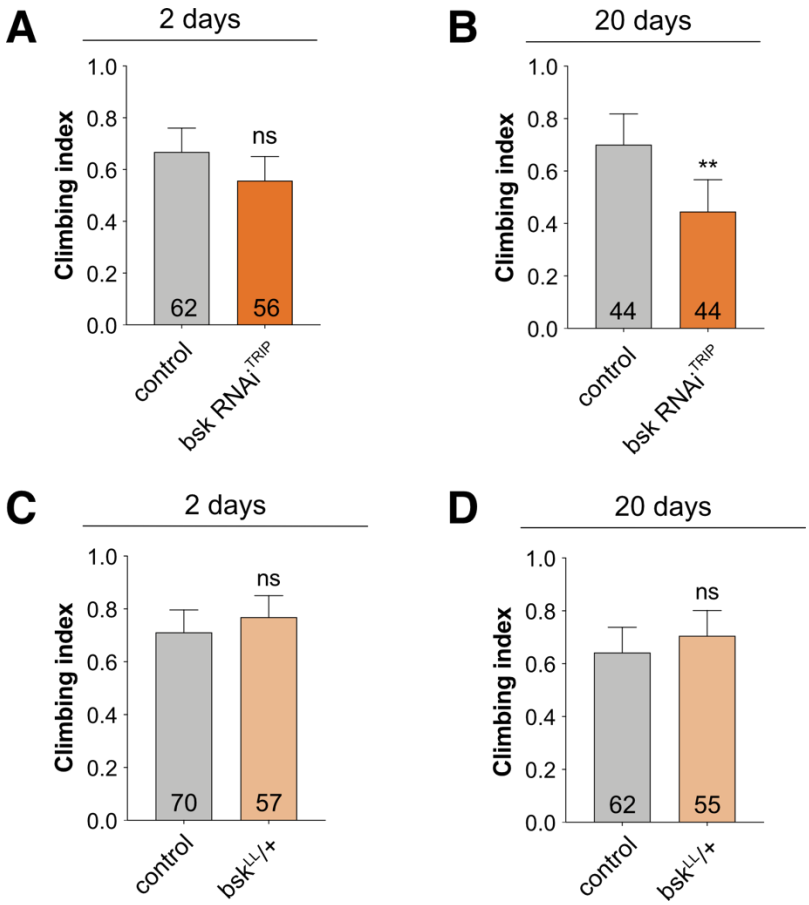

Figure 4.16. Loss of *basket* does not lead to climbing defects

Locomotor assays analysing climbing ability in (A and C) 2-day and (B and D) 20-day old flies of (A and B) *basket*-RNAi expressed with *arm*-GAL4 and (C and D) heterozygous bsk^{LL} mutants. Charts show mean ± 95% CI. Number of animals analysed is shown in each bar. Statistical analysis was determined by Welch's *t*-test; ** P <0.01 and ns = non-significant. Control genotypes are *UAS-lacZ* RNAi/+*; arm-GAL4*/+ and w^{1118}.

bsk-RNAi or heterozygous bsk^{LL} failed to improve the climbing defects observed in the *Pink1* mutants (Figure 4.17 A). Similarly, the mitochondrial integrity of the IFMs was still perturbed in *Pink1* mutants combined with *bsk*-RNAi (Figure 4.17 B). Equivalent experiments led to comparable observations in *parkin* mutants (Figure 4.17). Indeed, *bsk* knockdown using *bsk*-RNAi or bsk^{LL} heterozygous mutants did not modify the climbing deficits (Figure 4.17 A) or the disrupted mitochondrial arrangement (Figure 4.17 B) typically seen in *parkin* mutants. Altogether these results do not indicate any potential relationship between the JNK pathway and the *Pink1/parkin* pathology.

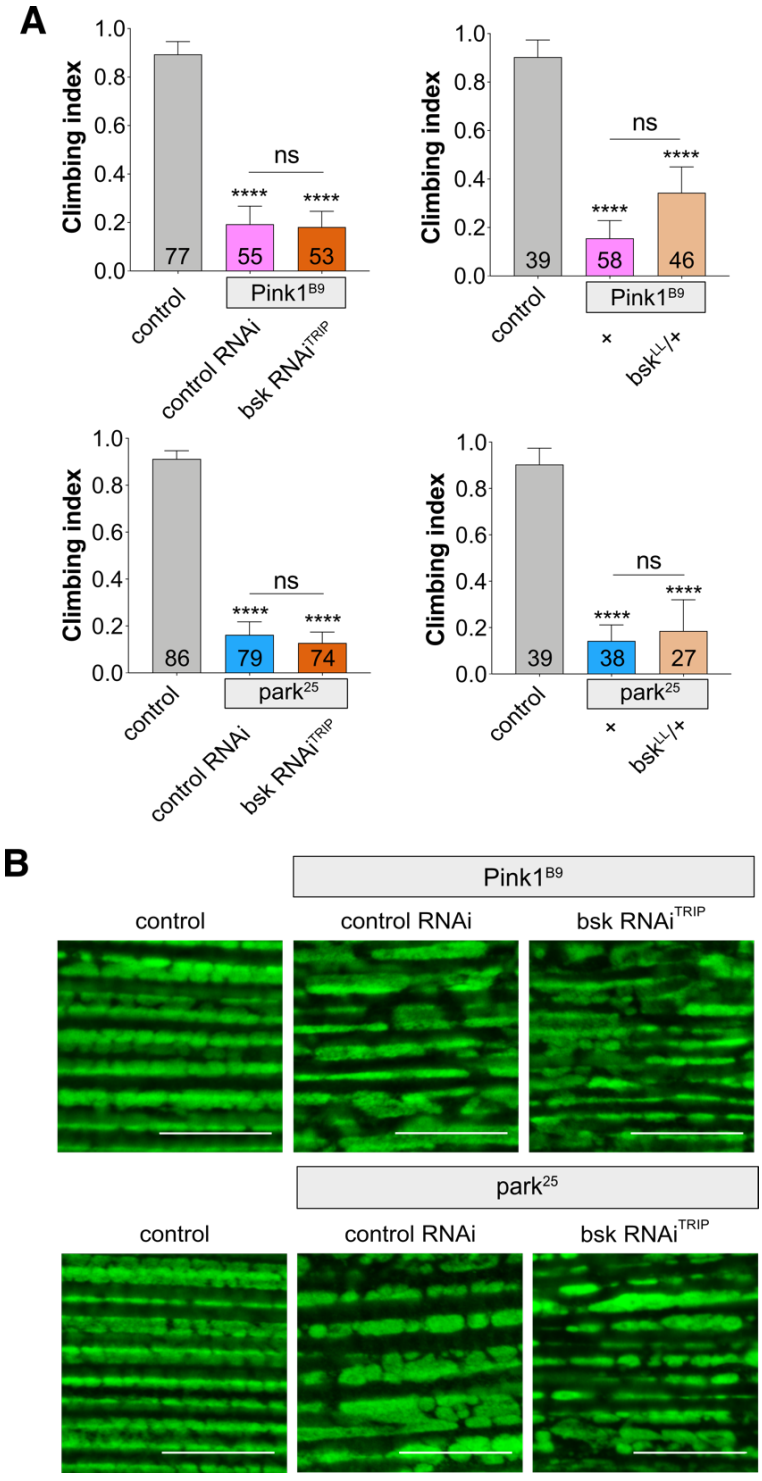

Figure 4.17. Loss of *basket* does not rescue *Pink1* or *parkin* mutant phenotypes

(A) Analysis of locomotor (climbing) ability and (B) mitochondrial morphology in *park*^{25} or *Pink1*^{B9} mutants combined with *basket* knockdown or heterozygous bsk^{LL} mutant. Charts show mean ± 95% CI. Number of animals analysed is shown in each bar. Statistical significance was measured by Kruskal-Wallis test with Dunn's post hoc correction for multiple comparisons; **** p <0.0001 and ns, non-significant. Confocal microscopy images show flight muscle mitochondria immunostained with anti-ATP5A. Scale bar = 10 µm. Control genotypes are *arm-GAL4/UAS-lacZ* RNAi and *w*^{1118}. Control RNAi is *arm-GAL4/UAS-lacZ*-RNAi in the respective mutant background.

4.3.3. Loss of key components of the p38 MAPK pathway does not modify *Pink1/parkin* phenotypes

The p38-MAPK pathway is a conserved signalling cascade activated in response to stresses, such ROS, LPS, heat-shock or DNA damage, and immune threats in both *Drosophila* and mammals. The mammalian p38 MAPKs are activated by several pro-inflammatory cytokines including IL-2 and TNF-α, which are both involved in the inflammatory response (Nebreda & Porras, 2000). Additionally, aberrant p38 signalling has been reported in many human disorders including cancer and neurodegenerative diseases (Craig et al., 2004). The *Drosophila* genome comprises three p38 kinases: p38a and p38b, the homologs of the mammalian p38α, p38β, p38δ and p38ɣ; and p38c, which is unique to the fly and and lacks the dual phosphorylation motif (TGY) (Davis et al., 2008). p38a and p38b have been shown to be involved in innate immune and stress responses (Chen et al., 2010; Vrailas-Mortimer et al., 2011). p38c has been reported to be important in wound healing as well as ROS and lipid homeostasis in the intestine (Chakrabarti et al., 2014). While both p38a and p38b are activated upon bacterial stimuli, individual mutants are not more susceptible to infection, suggesting that they are likely to exert redundant functions and compensate for each other (Chen et al., 2010). In *Drosophila*, p38a and p38b are phosphorylated and activated by the MAPKK, Licorne (lic), the fly ortholog of MKK3 (Figure 4.1) (Zhuang et al., 2006).

To investigate whether or not the p38-MAPK pathway plays a role in the *Pink1/parkin* pathology, three fly lines were used: one line combining both *p38a*-RNAi and *p38b*-RNAi; a kinase dead form of p38b ($p38b^{KD}$) and a $p38a^{1}$ loss of function allele. The $p38b^{KD}$ was established by Vrailas-Mortimer et al., and has been shown to act as a dominant-negative blocking the downstream p38-MAPK signalling cascade (Terriente-Félix et al., 2017; Vrailas-Mortimer et al., 2011). As p38a and p38b orthologs exert redundant functions, the line expressing both *p38a*-RNAi and *p38b*-RNAi was believed to maximise the interference of the pathway. The ubiquitous knockdown of *p38a* and *p38b* using *da*-GAL4 led to a strong climbing defect (Figure 4.18 A and B). This was rather surprising as evidence from the literature reported that *p38b; p38a* double mutants die at larval lethal stage, thus suggesting that flies expressing *p38a*-RNAi and *p38b*-RNAi with *da*-GAL4 only exhibit a partial knockdown of these two genes (Chen et al., 2010; Vrailas-Mortimer et al., 2011). A comparable decline was observed in flies

overexpressing *p38b*^{KD} (Figure 4.18 A and B). Finally, these results were similar to the decrease in climbing ability obtained with homozygous *p38a*^{1} null-mutant flies at 2 days (Figure 4.18 C). A significant drop of the climbing ability of homozygous *p38a*^{1} null mutants was observed at 20 days (Figure 4.18 D).

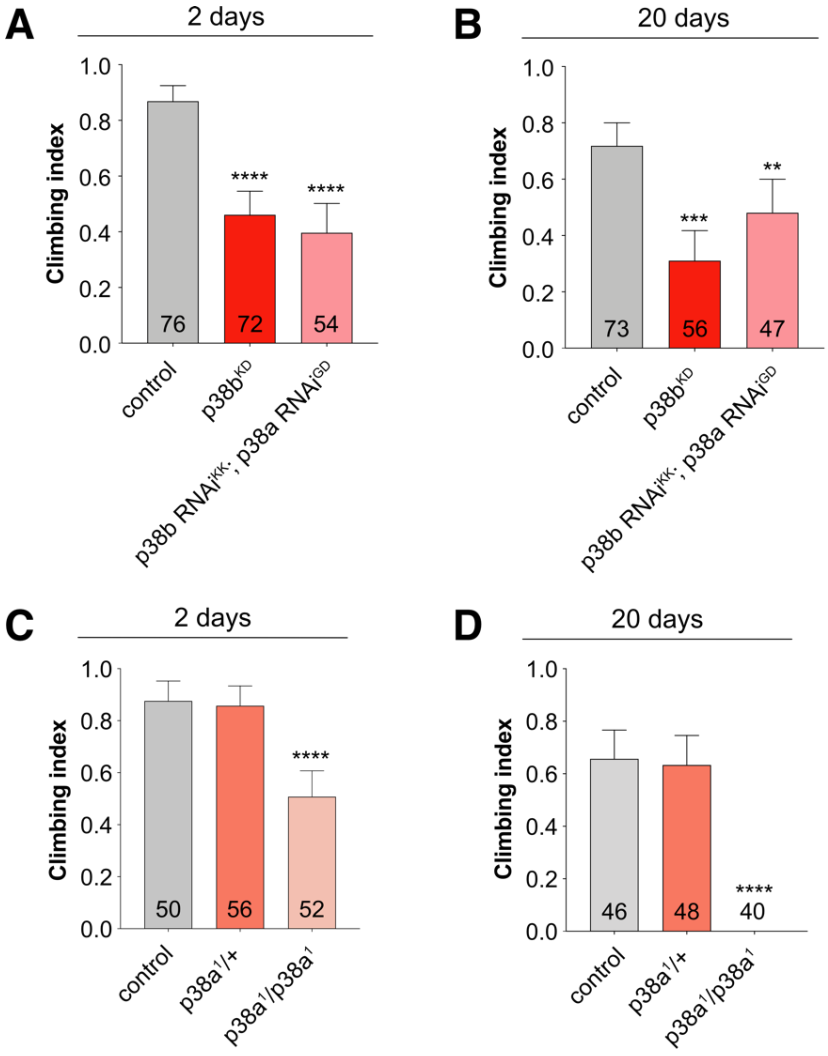

Figure 4.18. Loss of *p38a* or *p38b* results in climbing defects

Locomotor assays analysing climbing ability in (A and C) 2-day- and (B and D) 20-day-old flies of (A and B) *p38-RNAi* or *p38b*^{KD} expressed with *da*-GAL4 and (C and D) *p38a*^{1} mutants. Charts show mean ± 95% CI. Number of animals analysed is shown in each bar. Statistical analysis was determined by Kruskal-Wallis non-parametric test with Dunn's post-hoc correction for multiple comparisons; **** P<0.0001; *** P <0.001; ** P <0.01; and ns = non-significant. Control genotypes are *UAS-lacZ* RNAi/+; *da-GAL4* and *w*^{1118}.

Combination of *p38b*^{KD}, *p38a*-RNAi*; p38b*-RNAi or *p38a*^{1} with *Pink1* mutants did not lead to any change in the climbing ability (Figure 4.19 A and B) or mitochondrial integrity of IFMs (Figure 4.19 C). Interestingly, the double mutation *p38a*^{1}*; Pink1*^{B9} seemed to worsen the *Pink1*^{B9} climbing defects.

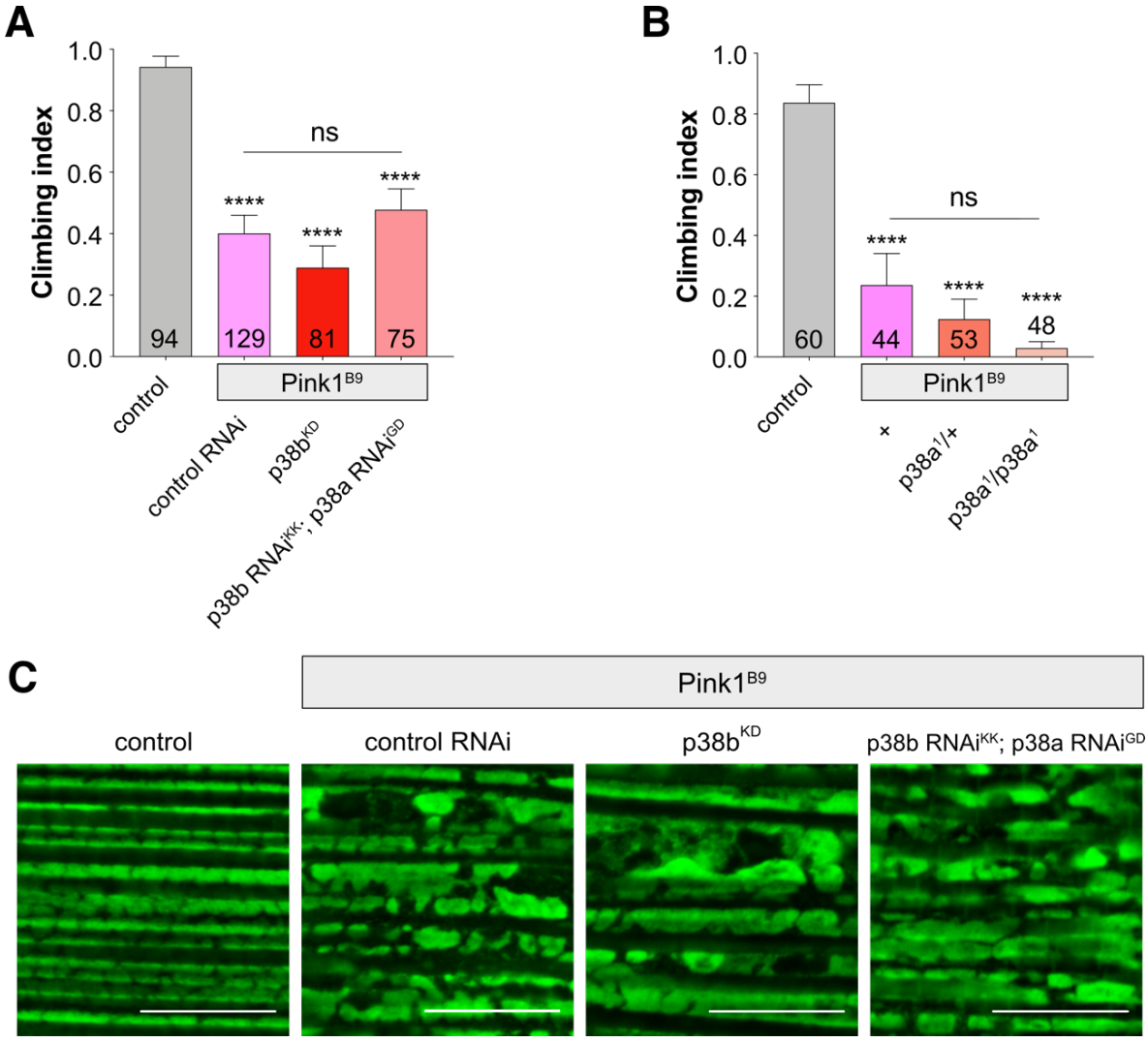

Figure 4.19. Loss of *p38a* or *p38b* does not modify *Pink1* mutant phenotypes

(A and B) Analysis of climbing ability and (C) mitochondrial morphology in *Pink1*^{B9} mutants combined with *p38*-RNAi, *p38b*^{KD} or *p38a*^{1} mutants. Charts show mean ± 95% CI. Number of animals analysed is shown in each bar. Statistical analysis was determined by Kruskal-Wallis non-parametric test with Dunn's post-hoc correction for multiple comparisons; **** P <0.0001 and ns = non-significant. Confocal microscopy images show flight muscle mitochondria immunostained with anti-ATP5A. Scale bar = 10 µm. Control genotypes are *UAS-lacZ* RNAi/+*; da-GAL4* and *w*^{1118}. Genotypes analysed are (control RNAi) *Pink1*^{B9}*/Y; UAS-lacZ* RNAi/+*; da-GAL4/+*, *Pink1*^{B9}*/Y; UAS-p38b* RNAi^{KK}/+*; p38a* RNAi^{GD}*/da-GAL4*, *Pink1*^{B9}*/Y; UAS-p38b*^{KD}*/+; da-GAL4/+*, *Pink1*^{B9}*/Y*, *Pink1*^{B9}*/Y;; p38a*^{1}*/+* and *Pink1*^{B9}*/Y;; p38a*^{1}*/p38a*^{1}.

Similar results were obtained in a *parkin* mutant background (Figure 4.20). Although expression of *p38b*^{KD} statistically seemed to improve the climbing defect of *parkin* mutants, the degree of amelioration remained quite subtle (Figure 4.20 A). However, complete loss of *p38a* did not modify the *parkin* mutant climbing defects (Figure 4.20 B). Furthermore, immunostaining and microscopy analysis of flight muscles did not reveal any improvement of the mitochondrial integrity (Figure 4.20 C).

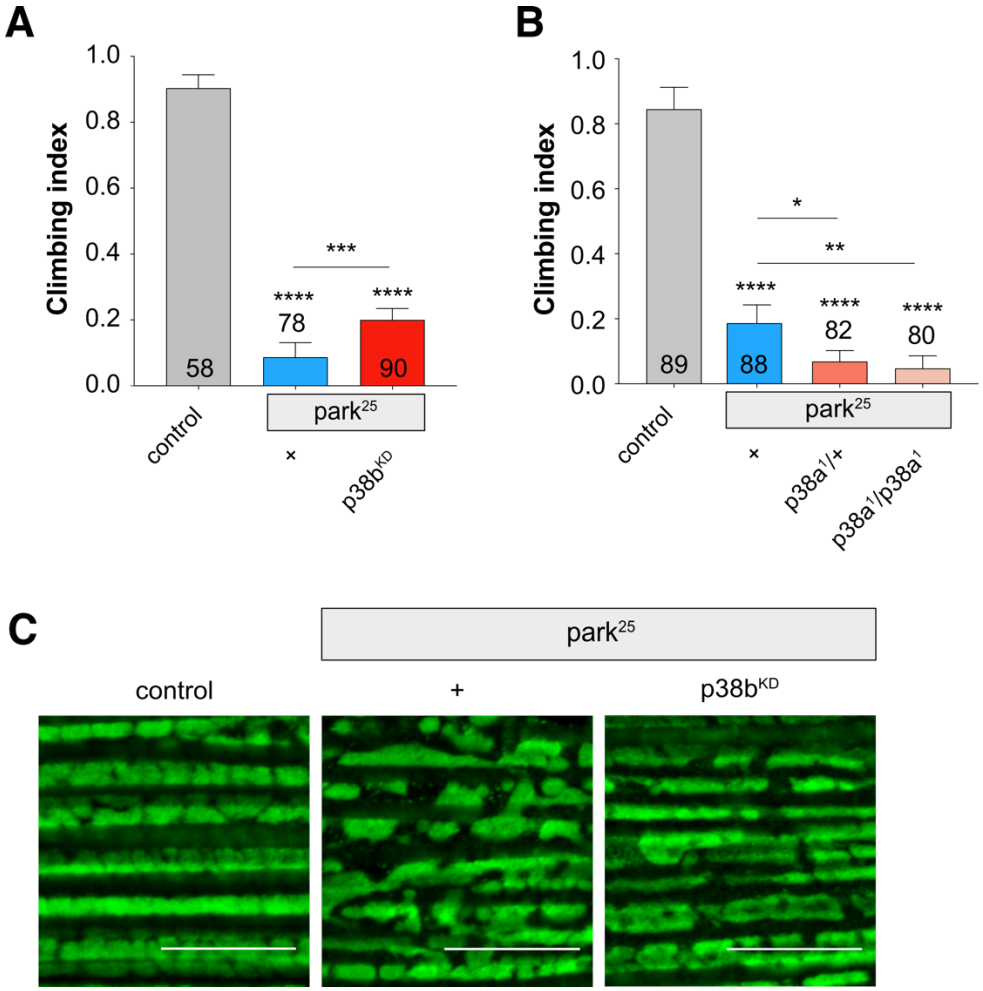

Figure 4.20. Loss of *p38a* or *p38b* does not rescue *park*^{25} mutant phenotypes

(A and B) Analysis of climbing ability and (C) mitochondrial morphology in *park*^{25} mutants combined with *p38b*^{KD} or *p38a*^{1} mutants. Charts show mean ± 95% CI. Number of animals analysed is shown in each bar. Statistical analysis was determined by Kruskal-Wallis non-parametric test with Dunn's post-hoc correction for multiple comparisons; **** P <0.0001; *** P <0.001; ** P <0.01; * P <0.05. Confocal microscopy images show flight muscle mitochondria immunostained with anti-ATP5A. Scale bar = 10 µm. Control genotypes are *UAS-LacZ* RNAi/+; *da-GAL4* and *w*^{1118}. Genotypes analysed are *UAS-LacZ* RNAi/+; *da-GAL4; park*^{25}*/park*^{25}, *UAS-p38b*^{KD}*/+; da-GAL4, park*^{25}*/park*^{25}, *p38a*^{1}, *park*^{25}*/park*^{25}, *p38a*^{1}, *park*^{25}*/ p38a*^{1}, *park*^{25} and *park*^{25}*/park*^{25}.

As knockdown of *licorne* using *da*-GAL4 driver was lethal, a weaker ubiquitous driver *arm*-GAL4, was used instead. Expression of *lic*-RNAi with *arm*-GAL4 did not lead to any climbing defect (Figure 4.21). When combined with *Pink1* or *parkin* mutants, *licorne* knockdown failed to rescue the climbing defects (Figure 4.22 A) and mitochondrial integrity of the flight muscles (Figure 4.22 B) observed in these two mutants.

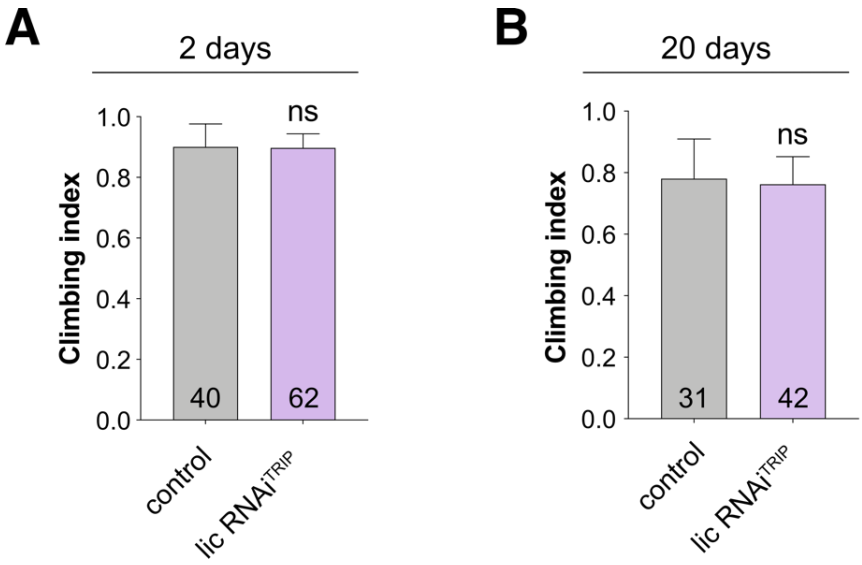

Figure 4.21. *licorne* knockdown does not lead to climbing defects

Locomotor assays analysing climbing ability in (A) 2-day- and (B) 20-day-old flies *lic-RNAi* expressed with *arm*-GAL4. Charts show mean ± 95% CI. Number of animals analysed is shown in each bar. Statistical analysis was determined Welch's *t*-test; ns = non-significant. Control genotype is *arm-GAL4/UAS-lacZ* RNAi.

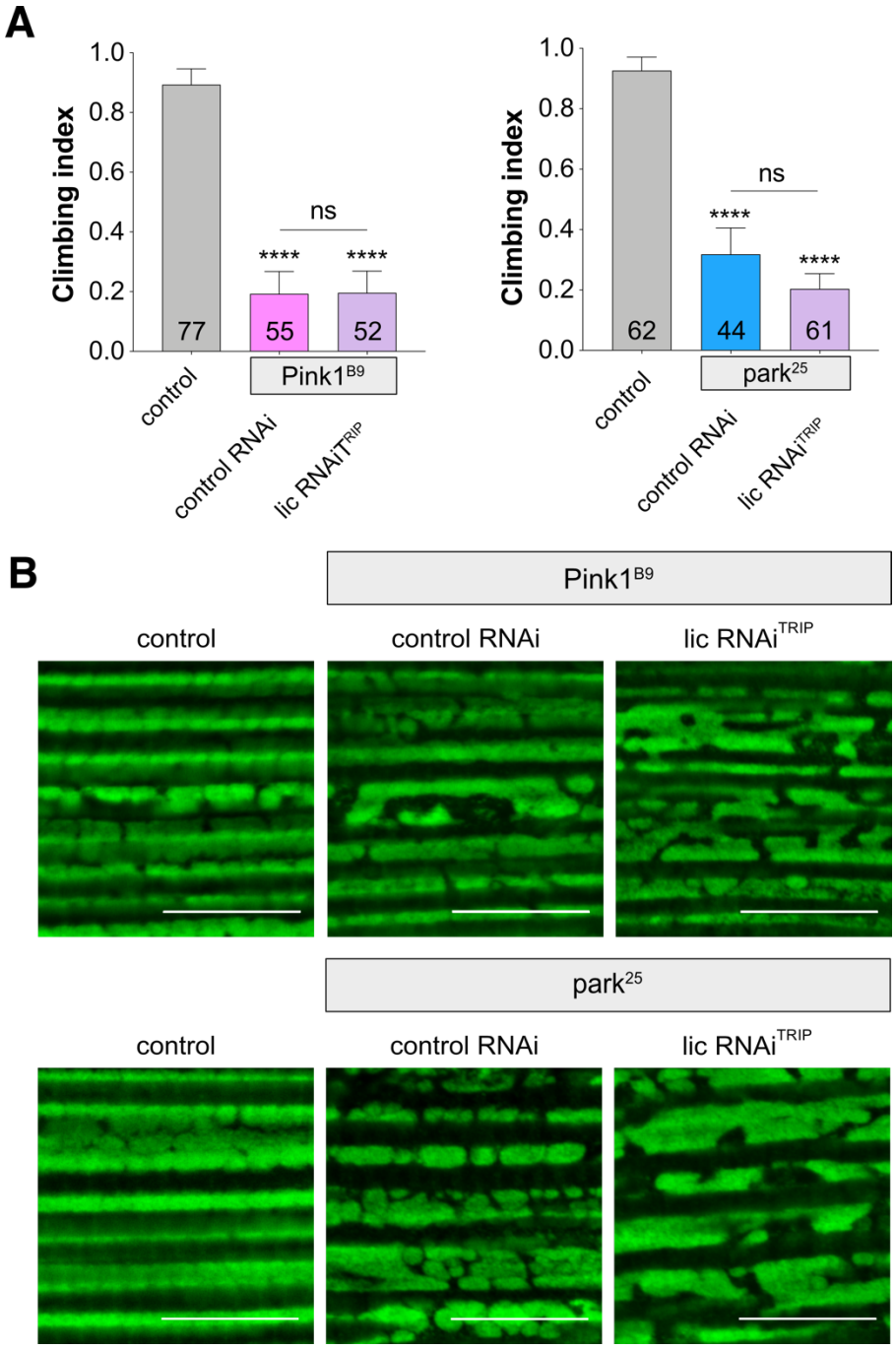

Figure 4.22. Loss of *licorne* does not rescue *Pink1* or *parkin* mutant phenotypes

(A) Analysis of locomotor (climbing) ability and (B) mitochondrial morphology in *park*^{25} or *Pink1*^{B9} mutants combined with *licorne*-RNAi. Charts show mean ± 95% CI. Number of animals analysed is shown in each bar. Statistical significance was measured by Kruskal-Wallis test with Dunn's post hoc correction for multiple comparisons; **** P <0.0001 and ns, non-significant. Confocal microscopy images show flight muscle mitochondria immunostained with anti-ATP5A. Scale bar = 10 µm. Control genotypes are *arm-GAL4/UAS-lacZ* RNAi and *w*^{1118}. Control RNAi is *arm-GAL4/UAS-lacZ*-RNAi in the respective mutant background.

Altogether, these results indicate that knockdown of the key players of the p38 MAPK signalling cascade does not seem to play a role in the *Pink1/parkin* pathology in *Drosophila*.

4.4. Discussion

Understanding how loss of PINK1/Parkin contributes to the pathogenic mechanisms that lead to the neurodegeneration observed in PD, is key to the development of new therapies. *Pink1/Prkn* KO mice do not accurately replicate the human PD pathology mainly due to the absence of phenotype. In sharp contrast to the mouse, *Drosophila* has proven to be a powerful model and provided a significant part of our current knowledge on PINK1/Parkin functions. *Drosophila Pink1/parkin* mutants exhibit extensive disruption of the IFMs resulting in locomotor deficits, apoptotic degeneration of these muscles, loss of DA neurons and a significant shorter lifespan (Greene et al., 2003; Park et al., 2006). In addition, these phenotypes are accompanied by decreased mitochondrial respiration and ATP production, indicating a functional breakdown of mitochondria (Greene et al., 2003; Park et al., 2006). As a result, genetic studies relying on suppression or enhancement of the mutant phenotypes have shed light on the key and conserved features of the PINK1/Parkin biology.

Several attempts have been made to understand the context in which *Pink1/Prkn* pathogenic mutations can give rise to a PD-like phenotype in mice. To address this, *Prkn* KO mouse was combined with the mtDNA mutator strain, a mitochondrial stressor that results in the accumulation of mtDNA mutations (Pickrell et al., 2015). Interestingly, loss of *Prkn* in combination with the mtDNA mutator leads to locomotor deficits, selective degeneration of DA neurons and decreased mitochondrial function, altogether resulting in a shorter life expectancy (Pickrell et al., 2015). These observations were further extended by Sliter et al., where the authors demonstrated that loss of *Pink1* or *Prkn* in combination with mitochondrial stressors, such as the mtDNA mutator, is accompanied by an abnormal innate immune response mediated by the cGAS-STING pathway (Sliter et al., 2018). These results are in line with several studies from the literature confirming elevated pro-inflammatory cytokines levels in post-mortem brains of PD patients (Taylor et al., 2013). This is reinforced by the fact that non-steroidal anti-inflammatory drug intake can delay PD onset, although this remains somewhat controversial (Stojkovska et al., 2015). In addition, LPS injections have been shown to induce an immune response accompanied by the loss of DA neurons and a PD-like pathology in *Prkn*$^{-/-}$ and *Pink1*$^{-/-}$ mice (Frank-Cannon et al., 2008; Matheoud et al., 2019). Altogether, these findings strongly implicate the immune

system in the development of PD pathology.

However, while the STING pathway is, to some extent, conserved in invertebrates, my results demonstrate that *Drosophila* Sting does not appear to be a key player of the Pink1/parkin biology. As it is well-established that several immune-related genes are dysregulated in *Pink1/parkin* mutant flies (Greene et al., 2005; Tufi et al., 2014), my findings were rather surprising, and it remains unclear why loss of *Sting* did not supress the strong phenotypes observed in these mutants. One possible explanation is that the abnormal immune response observed in *Pink1* and *parkin* flies is not due to the release of mtDNA in the cytosol and is therefore unrelated to the activation of the Sting pathway. The results from Sliter et al., suggest that exhaustive exercise or accumulation of mtDNA mutations increases mitophagy and this phenomenon is abrogated in *Pink1/parkin* mutants (Sliter et al., 2018). Furthermore, in the absence of PINK1/Parkin, the lack of mitophagy seems to correlate with elevated mtDNA levels in the serum of these mice (Sliter et al., 2018). These findings suggest that dysfunctional mitochondria may accumulate and potentially release mtDNA in the cytosol, subsequently activating the STING signalling cascade. However, the mechanism behind the mtDNA release occurring in *Pink1* or *Prkn* KO mice during exhaustive exercise or accumulation of mtDNA mutations still remains unclear. As *Pink1/parkin* mutant flies exhibit strong phenotypes even in the absence of mitochondrial stressors, unlike mice, it would be interesting to know if cytosolic mtDNA can be detected in these mutants, in order to draw a parallel with the mouse studies.

Loss of *Drosophila* Sting has been shown to reduce Relish cleavage, a process required for Relish activation, thus confirming that Sting acts upstream of Relish (Martin et al., 2018). This also implies that Sting is able to regulate the expression of transcription factors of the NF-κB family, in a similar fashion to the mammalian system. NF-κB is responsible for the activation of many pro-inflammatory cytokines including IL-6 and TNFα, which were both found to be upregulated in *Pink1*$^{-/-}$ and *Prkn*$^{-/-}$ mice exposed to exhaustive exercise or combined with the mtDNA mutator strain (Liu et al., 2017; Sliter et al., 2018). However, loss of *Relish* did not suppress the *Pink1/parkin* mutant phenotypes, suggesting that the whole Sting-IMD signalling cascade is not playing a role in the Pink1/parkin pathology in flies.

Although the STING pathway is quite conserved in *Drosophila*, major differences exist between vertebrates and invertebrates. Indeed, in addition to the activation of NF-κB, mammalian STING is able to recruit IRF3 through its C-terminal tail (CTT), resulting in the expression of type I IFNs (Qiu & Zhou, 2018). Interestingly, Sliter et al., observed increased levels of IFNβ, a type I IFN, in *Pink1*$^{-/-}$ and *Prkn*$^{-/-}$ mice exposed to mitochondrial stressors (Sliter et al., 2018). This is highly relevant as IRFs, and therefore IRF3, and interferon genes only arose during vertebrate evolution (Liu et al., 2018). Thus, unlike mammals, *Drosophila* Sting does not contain a CTT and is not capable of recruiting the mammalian IRF3 (Martin et al., 2018). As no homologs of *IFN* genes have been identified in insects, this suggests that the IRF3-dependent branch of the STING pathway has been acquired during evolution, which may account for the discrepancies observed in this study compare to the mouse work from Sliter et al.

None of the immune pathways tested in this chapter led to a suppression of the phenotypes observed in the *Pink1/parkin* mutant flies. These findings were surprising as several of these pathways have been implicated in ageing and many neurodegenerative disorders, including PD. The results showing that downregulation of *Relish* is not beneficial to *Pink1/parkin* mutants were probably the most surprising as upregulation of genes related to the IMD cascade, such as *Relish*, have been reported in many neurodegenerative disorders. For instance, Chinchore et al., have found that loss of *Relish* rescues the degeneration of photoreceptors in the eye in a *Drosophila* model of human retinal disorder (Chinchore et al., 2012). Similarly, Petersen et al., reported that Relish activation is responsible for the neurodegeneration occurring in a model of ataxia-telangiectasia (A-T). As such, loss of *Relish* was able to rescue the cell death and improve the lifespan of these A-T mutant flies (Petersen et al., 2013). Finally, Kounaditis et al., found that loss of several negative regulators of the IMD pathway led to increased AMPs production resulting in locomotor deficits, neurodegeneration and shorter lifespan (Kounatidis et al., 2017). This was reinforced by previous studies showing that neuronal overexpression of single AMPs was sufficient to drive neurodegeneration and downregulation of the IMD pathway, through *Relish* silencing, specifically in the brain was enough to suppress the neurodegeneration and extend lifespan (Cao et al., 2013). The rescue was even more significant when *Relish* was downregulated in glial cells (Kounatidis et al., 2017). This suggests the existence of a non-canonical IMD pathway or a tissue-specific IMD

signalling cascade that may be particularly relevant in the brain. This latter observation may explain why I did not see any effect of the loss of *Relish* in *Pink1/parkin* mutants, as my experiments mainly relied on ubiquitous downregulation of *Relish*.

Finally, increasing evidence indicates that WT mice exposed to bacterial infections or models such as LPS injections, exhibit DA neuron loss, microglia activation and elevated pro-inflammatory cytokines, suggesting that neuroinflammatory events themselves can trigger a PD-like pathology (Hunter et al., 2007, 2009). Thus, it appears that the environmental conditions in which flies and mice are kept for research purposes may give another explanation for the discrepancies we observed. Indeed, mice are kept in a rather clean environment, while flies are constantly exposed to viral and bacterial insults. The repeated exposure of external pathogens may explain why *Pink1/parkin* mutant flies exhibit strong phenotypes when mice do not. Therefore, it would be interesting to investigate if *Pink1/parkin* mutant flies develop any pathogenic phenotypes when kept in germ-free conditions.

Altogether, this work indicates that the Sting-IMD, JNK and p38-MAPK pathways do not play a role in the Pink1/parkin pathology in flies.

Chapter 5. Investigating the role of the JAK/STAT pathway in *Pink1*/*parkin* mutants

5.1. Introduction

JAK/STAT is a multi-functional, highly conserved signalling cascade. In *Drosophila*, and similarly in mammals, the JAK/STAT pathway controls several developmental steps from the embryo to the adult, such as sex determination, embryonic segmentation, cell differentiation and proliferation. Due to the implication of the pathway in important developmental processes, loss-of-function of key components of the pathway is often embryonic lethal (Binari & Perrimon, 1994; Brown et al., 2001; Yan et al., 1996). The JAK/STAT pathway also plays a pivotal role in immunity both in mammals and flies. There is increasing evidence suggesting that this signalling cascade may be dysregulated in some neurodegenerative disorders in addition to cancers or ischemia (Nicolas et al., 2013).

Although the pathway appears rather simple at first, it underlies a highly complex system. The mammalian JAK/STAT pathway is composed of more than 40 different ligands, such as cytokines, hormones and growth factors, that can bind multiple receptors, which form hetero- or homodimers when the ligand is bound (Myllymäki & Rämet, 2014). Seven STAT proteins, STAT1, STAT2, STAT3, STAT4, STAT5a and STAT5b, STAT6, and four JAK proteins, JAK1, JAK2, JAK3 and TYK2, compose the mammalian JAK/STAT cascade (Kisseleva et al., 2002). While the mammalian JAK/STAT pathway is highly complex, *Drosophila* contain the same essential components, but with much less redundancy. The *Drosophila* genome encodes for three cytokine-like proteins upd1-3 that act as ligands for the pathway (Myllymäki & Rämet, 2014). Individual *upd2* and *upd3*, but not *upd1,* null mutations are viable, and result in a much less severe phenotype than mutations of all three ligands together, indicating some redundancy between them (Bach & Perrimon, 2003). Upds bind to a single receptor Dome, which shares similarities with the mammalian class I cytokine receptors such as IL-6 receptor (Hombría et al., 2005). Additionally, *Drosophila* comprise a single JAK, named Hop and a unique STAT, Stat92E (Hou et al., 1996). The Drosophila JAK/STAT pathway highly resembles the mammalian cascade: IL-6/IL-6R/JAK1/STAT3. The activation of the pathway is detailed in Figure 5.1.

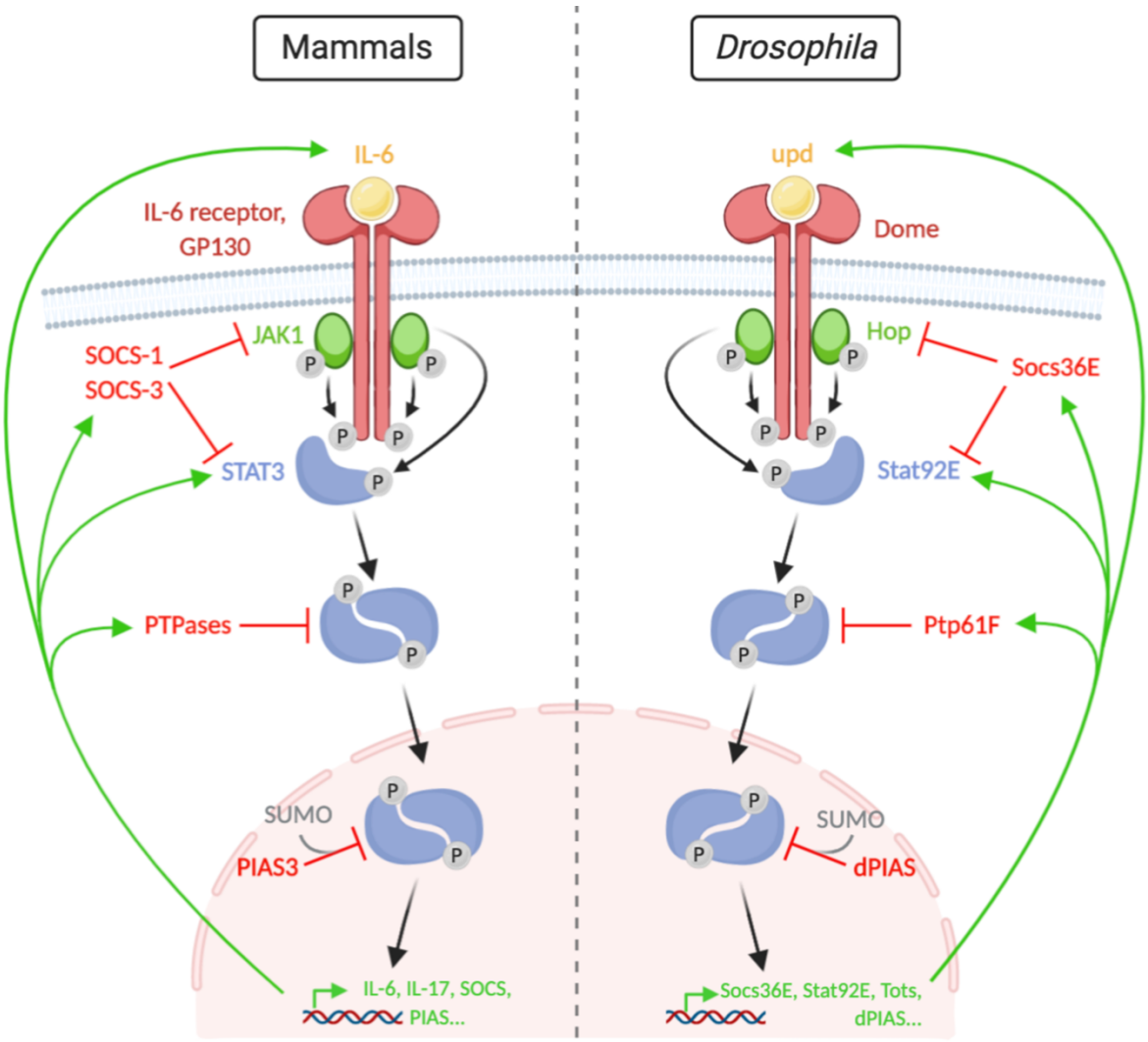

Figure 5.1 Simplified schematic representation of the JAK/STAT pathway in mammals and *Drosophila*

Binding of the upds to Dome receptor results in the Dome dimerization, which in turn brings two Hop proteins in close proximity and allows their mutual phosphorylation and subsequent activation. Activated Hop phosphorylates Dome, providing a docking site for cytosolic Stat92E. Stat92E molecules are also phosphorylated by Hop, resulting in their dissociation from the receptor and their assembly as homodimers prior to their nuclear translocation. In the nucleus, activated Stat92E triggers the transcription of several target genes. Negative regulators comprise *dPIAS* that targets activated nuclear Stat92E dimers for degradation; Socs36E that directly interacts with Hop and Stat92E to suppress their activity and Ptp61F, which targets activated Hop and possibly nuclear-localised Stat92E for deactivation. In addition, *Socs36E*, *dPIAS* and *Ptp61F* are transcriptional target genes of the pathway, that can be regulated by Stat92E activation, therefore creating a negative feedback loop. Conversely, the pathway also contains positive feedback loops, whereby high JAK/STAT activity further enhances *Stat92E* or *upds* expression.

In *Drosophila*, and particularly in the context of immune responses, JAK/STAT signalling induces the expression of immune-related genes such as the *Turandot* gene family (Ekengren & Hultmark, 2001). For instance, upon bacterial or viral insult, TotA and TotM represent an example of immune-related proteins that are produced in the fat body and accumulate in the circulating body fluid, called haemolymph (Agaisse et al., 2003; Brun et al., 2006; Dostert et al., 2005; Ekengren & Hultmark, 2001; Harsh et al., 2018; Kallio et al., 2010; Karpac et al., 2011; Lopez et al., 2018).

Tight controls of the pathway exist at various levels of the signalling cascade. Similar to the other components of the pathway, these negative regulators have been conserved during evolution and therefore also exist in *Drosophila*. The *Drosophila* genome encodes for a single PIAS gene (*dPIAS*) that has been shown to also negatively regulate the JAK/STAT pathway. dPIAS can act as an E3-ligase and promote small ubiquitin-like modifier (SUMO)ylation of activated nuclear STAT dimers, which results in their subsequent degradation (Betz et al., 2001; Hari et al., 2001; Ungureanu et al., 2003). Negative feedback also occurs through the activity of SOCS proteins, with Socs36E being the homolog of the mammalian SOCS-5 (Zeidler et al., 2000). Consistent with the role of Socs36E as a negative regulator of the JAK/STAT pathway, Socs36E was shown to directly interact with Hop and Stat92E and suppress their activity (Hou et al., 2002). Finally, Ptp61F targets activated Hop and possibly nuclear-localised Stat92E for deactivation (Baeg et al., 2005). In addition, the pathway itself can mediate the expression of these negative regulators to prevent an over-activation. *SOCS*, *PIAS* and *PTPases* are transcriptional target genes of the pathway, that can be regulated by STAT activation, therefore creating a negative feedback loop that dampens the strength of signalling and duration of the pathway activity (Arbouzova & Zeidler, 2006). In addition, alternative splicing of *Stat92E* mRNA generates an N-terminally truncated protein that acts as a dominant negative form and is able to inhibit the activity of the pathway (Bach & Perrimon, 2003). Conversely, the pathway also contains positive feedback loops, whereby high JAK/STAT activity further enhances STAT proteins or ligand expression (Arbouzova & Zeidler, 2006).

In the context of the current work, there is compelling evidence suggesting that JAK/STAT signalling may be upregulated in PD. Indeed, the two main activators of the mammalian JAK/STAT pathway, IFN-ɣ and IL-6, have been found to be elevated in PD

patients (Yan et al., 2018). Additionally, higher levels of IL-6 seem to correlate with a greater risk of developing PD (Chen et al., 2008; Sherer, 2011). Interestingly, Increased IL-6 levels were also reported in *Pink1*$^{-/-}$ and *Prkn*$^{-/-}$ mice after exhaustive exercise or when combined to the mtDNA mutator strain (Sliter et al., 2018). In rats overexpressing α-Synuclein, Qin et al., found that inhibition of JAK1/JAK2 using AZD1480 treatment, prevents the degeneration of DA neurons as well as other neuroinflammatory phenotypes, such as elevated levels of IFN-ɣ and IL-6 (Qin et al., 2016). In addition, the deficiency of IFNɣ in mice exposed to MPTP results in the maintenance of DA functional activity and the reduction of DA neuronal loss (Mount et al., 2007). In *Drosophila*, higher levels of *TotA*, *TotM* and *TotX* have been reported in flies exposed to paraquat (Ekengren & Hultmark, 2001; Maitra et al., 2019). Finally, *TotA* and *TotM* were shown to be upregulated in both *Pink1* and *parkin* mutants (Greene et al., 2005; Tufi et al., 2014). While the function of the *Tots* has not been clearly defined, they seemed to be expressed under various stress conditions, including during septic injury. However, they do not seem to have any antimicrobial properties, unlike the AMPs produced by other pathways such as the IMD or Toll pathways (Agaisse & Perrimon, 2004). Altogether, these findings suggest that reducing JAK/STAT signalling may be beneficial to attenuate the PD pathogenesis.

Drosophila gut is divided into three main parts: the foregut, midgut and hindgut that derive from the progenitor cells of the larval gut (Miguel-Aliaga et al., 2018). The larval midgut consists of absorptive enterocytes (ECs), secretory enteroendocrine cells (ee) and a population of undifferentiated progenitor cells, named adult midgut precursors (AMPs), which generates the adult intestinal stem cells (ISCs) and differentiates into EC and ee (Houtz et al., 2019; Mathur et al., 2010). AMPs are enclosed by one or more peripheral cells (PCs) that form a niche (Figure 5.2) (Houtz et al., 2019; Mathur et al., 2010). The activity of JAK/stat signalling is restricted to the PCs (Mathur et al., 2010). The adult midgut resembles the mammalian small intestine and contains multipotent ISCs that can give rise to all cell types of the midgut epithelium (Miguel-Aliaga et al., 2018; Osman et al., 2012). The adult intestinal epithelium is composed of four cell types: ISCs, ECs, ee and undifferentiated enteroblasts (EBs) (Figure 5.2) (Herrera & Bach, 2019; Jiang et al., 2009). By asymmetric division, one ISCs can produce one EB or self-renew itself by generating a new ISC (Herrera & Bach, 2019). EB can differentiate into ECs or ee (Herrera & Bach, 2019; Ohlstein & Spradling, 2006).

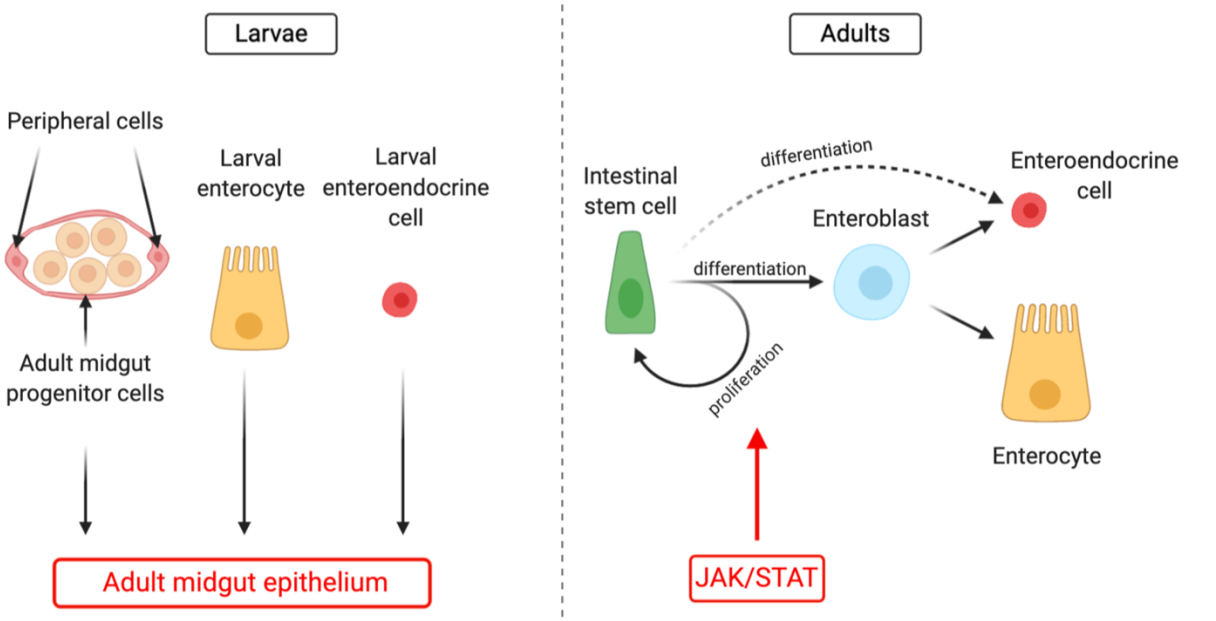

Figure 5.2. Schematic representation of the progenitor cells of the larval and adult midgut

The larval gut comprises enterocytes, enteroendocrine cells (ee) and adult midgut precursors, which generate the adult intestinal stem cells. AMPs are enclosed by one or more peripheral cells. The adult midgut is composed of ISCs that give rise to all cell types of the midgut epithelium. ISCs can differentiate into EBs or self-renew themselves by generating new ISCs. EBs differentiate into EC or ee.

Under normal conditions, the epithelium renewal through proliferation/differentiation of depends on JAK/STAT signalling (Beebe et al., 2010; Jiang et al., 2009). Bacterial ingestion or other chemical damage can modify the gut homeostasis and this seems to involve the JAK/STAT signalling cascade (Biteau et al., 2011). The first piece of evidence came from Penninger's team, and the identification of JAK/STAT activation in the gut of flies infected by *S. marcescens* (Cronin et al., 2009). In addition, the infection correlated with extensive cell death in the gut, provoking an increase in the ISCs proliferation as a compensatory mechanism (Cronin et al., 2009). The latter suggests that JAK/STAT signalling in the *Drosophila* gut acts as a pivotal component of the host defence in response to pathogen infections (Cronin et al., 2009). Interestingly, the cytokine-like *upd3* was reported to become highly expressed in intestinal EBs and ECs following bacterial infection, thus triggering the activation of the JAK/STAT signalling cascade (Buchon et al., 2009; Jiang et al., 2009). Defence to bacterial infection generates a burst of ROS in the gut in order to eliminate both invasive and dietary pathogens (Buchon et al., 2009; Iatsenko et al., 2018; Kim E. K.

et al., 2020; Lee et al., 2015; Lee et al., 2013). The release of this oxidative burst has been shown to correlate with the epithelial renewal and ISCs proliferation, together acting as a compensatory mechanism to repair the damage produced by the excess of ROS (Buchon et al., 2009; Jiang et al., 2009). In addition, the JAK/STAT cascade has also been involved in the aging process of the gut, during which the epithelium of the intestine deteriorates, due to aberrant EC differentiation and over-proliferation of ISCs. This is accompanied by intestinal dysbiosis (Biteau et al., 2010; Herrera & Bach, 2019). This alteration of the gut homeostasis results in a shorten lifespan that can be rescued by double or single *upd2*, *upd3* mutants, suggesting that the primary protective response to damage or infection mediated by JAK/STAT becomes dysregulated during aging (Herrera & Bach, 2019; Osman et al., 2012). Recently, Koehler et al., have shown that the potential mitophagy impairment occurring in *Pink1/parkin* mutant flies results in elevated levels of ROS in some intestinal cell populations, such as ISCs and EBs (Koehler et al., 2017). This is accompanied by alterations of mitochondrial structure and an incapacity of the ISCs to proliferate. Therefore, the authors hypothesised that loss of *Pink1/parkin* prevents the renewal of the intestinal epithelium and leads to a senescence state of the ISCs (Koehler et al., 2017).

5.2. Chapter aims

The aim of this chapter was to investigate the implication of the JAK/STAT signalling cascade in the *Pink1/parkin* pathology. To this end, loss of some key components of the JAK/STAT pathway was assessed in *Pink1* or *parkin* mutant backgrounds. Climbing assay and mitochondrial morphology in the IFMs were the readouts to assess for any potential genetic interactions between *Pink1/parkin* and components of the JAK/STAT pathway. After some promising genetic interactions between *Pink1* and Stat92E JAK/STAT pathway, I further assessed the involvement of other effectors of the pathway: Hop, Dome and upds; as well as TotA and TotM, two downstream targets expressed in response to viral infection and septic injury. In addition, I sought to explore other aspects of the JAK/STAT signalling. To do so, I used previously established tools to assess the levels of JAK/STAT activation in *Pink1* mutants, in particular in the midgut where JAK/STAT is known to play important roles.

5.3. Results

5.3.1. Loss of *Stat92E* partially rescues *Pink1* phenotypes

After having investigated several immune signalling cascades, a remaining pathway to analyse was the JAK/STAT pathway. To this end, preliminary work focused on one of the main components of the pathway, the transcription factor Stat92E. The previously established *Stat92E*^{06346} mutant was used. *Stat92E*^{06346} mutant has been reported to be a null and homozygous animals die during embryogenesis, so all experiments involving this mutant were performed with heterozygous animals (Henriksen et al., 2002; Hou et al., 1996). As behavioural analysis of *Stat92E* loss-of-function, has not been investigated before, *Stat92E*^{06346} mutants were subjected to climbing assay. *Stat92E*^{06346} flies display significant climbing defects at 2 days (Figure 5.3 A) that did not aggravate with age (Figure 5.3 B).

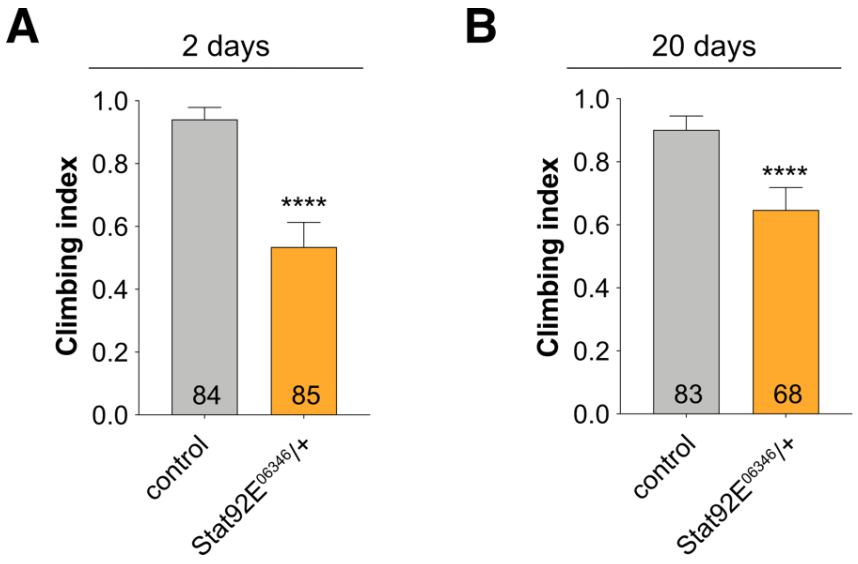

Figure 5.3. *Stat92E*^{06346} mutants exhibit climbing defects

Locomotor assays analysing climbing ability in (A) 2-day- and (B) 20-day-old flies of control and heterozygous *Stat92E*^{06346} mutants. Charts show mean ± 95% CI. Number of animals analysed is shown in each bar. Statistical analysis was determined by Welch's *t*-test; **** *P* <0.0001. Control genotype is *w*^{1118}.

Following similar experiments that were shown in the previous chapter, loss of *Stat92E* was assessed in the *Pink1* mutant background. Remarkably, *Stat92E*^{06346} partially rescued the climbing deficits observed in *Pink1*^{B9} flies at 2 days (Figure 5.4 A) and this was maintained in flies aged to 20 days (Figure 5.4 B). The fact that only a partial rescue was obtained may be explained by the climbing defects that were already present in *Stat92E*^{06346} mutants at 2 and 20 days, without adding *Pink1* loss-of-function. Therefore, there is a limitation regarding the level of rescue that can be obtained when the two mutants are combined. Loss of *Stat92E* failed to rescue the typical flight defects observed in *Pink1* mutants (Figure 5.4 C and D).

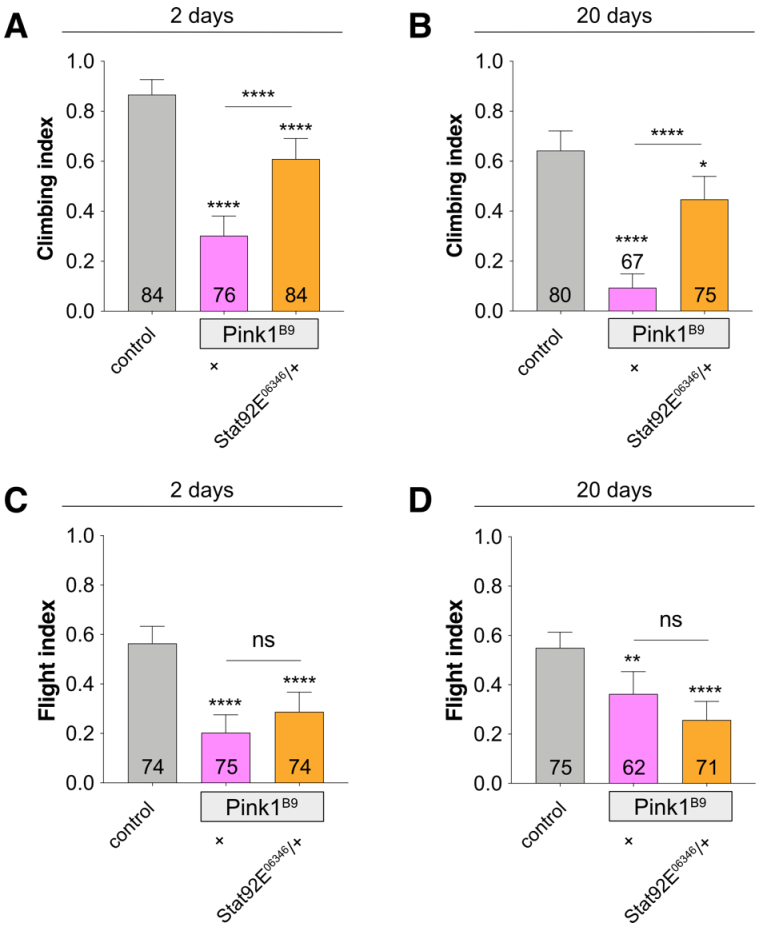

Figure 5.4. Loss of *Stat92E* with *Stat92E*^{06346} mutant partially rescues *Pink1* mutant climbing deficits

Locomotor assays analysing climbing ability in (A) 2-day- and (B) 20-day-old and flight assay in (C) 2-day- and (D) 20-day-old *Pink1*^{B9} mutant flies combined with heterozygous *Stat92E*^{06346}. Charts show mean ± 95% CI. Number of animals analysed is shown in each bar. Statistical analysis was determined by Kruskal-Wallis non-parametric test with Dunn's post-hoc correction for multiple comparisons; **** P<0.0001, ** P <0.01, *P <0.05 and ns = non-significant. Control genotype is *w*^{1118}. Genotypes analysed are *Pink1*^{B9}*/Y;;* and *Pink1*^{B9}*/Y;; Stat92E*^{06346} */+*.

Thoracic indentations are characteristic of *Drosophila Pink1/parkin* mutants and result from the muscle degeneration of the flight muscles underneath the cuticle. To address whether or not loss of *Stat92E* also rescues these thoracic indentations, images of double mutant *Pink1*^{B9}*:Stat92E*^{06346} thoraces were acquired (Figure 5.5 A). These images revealed that loss of *Stat92E* completely rescued the thoracic indentations that are characteristic of *Pink1* mutants, hence no differences were observed between the control and *Pink1*^{B9}*:Stat92E*^{06346} thoraces (Figure 5.5 A). Interestingly, in addition to rescuing the crushed thorax phenotype, immunostaining of mitochondria and confocal imaging of IFMs showed that lack of *Stat92E* also partially rescued the mitochondrial morphology (Figure 5.5 B and C). These results were consistent with the rescue of the *Pink1* mutant climbing defects.

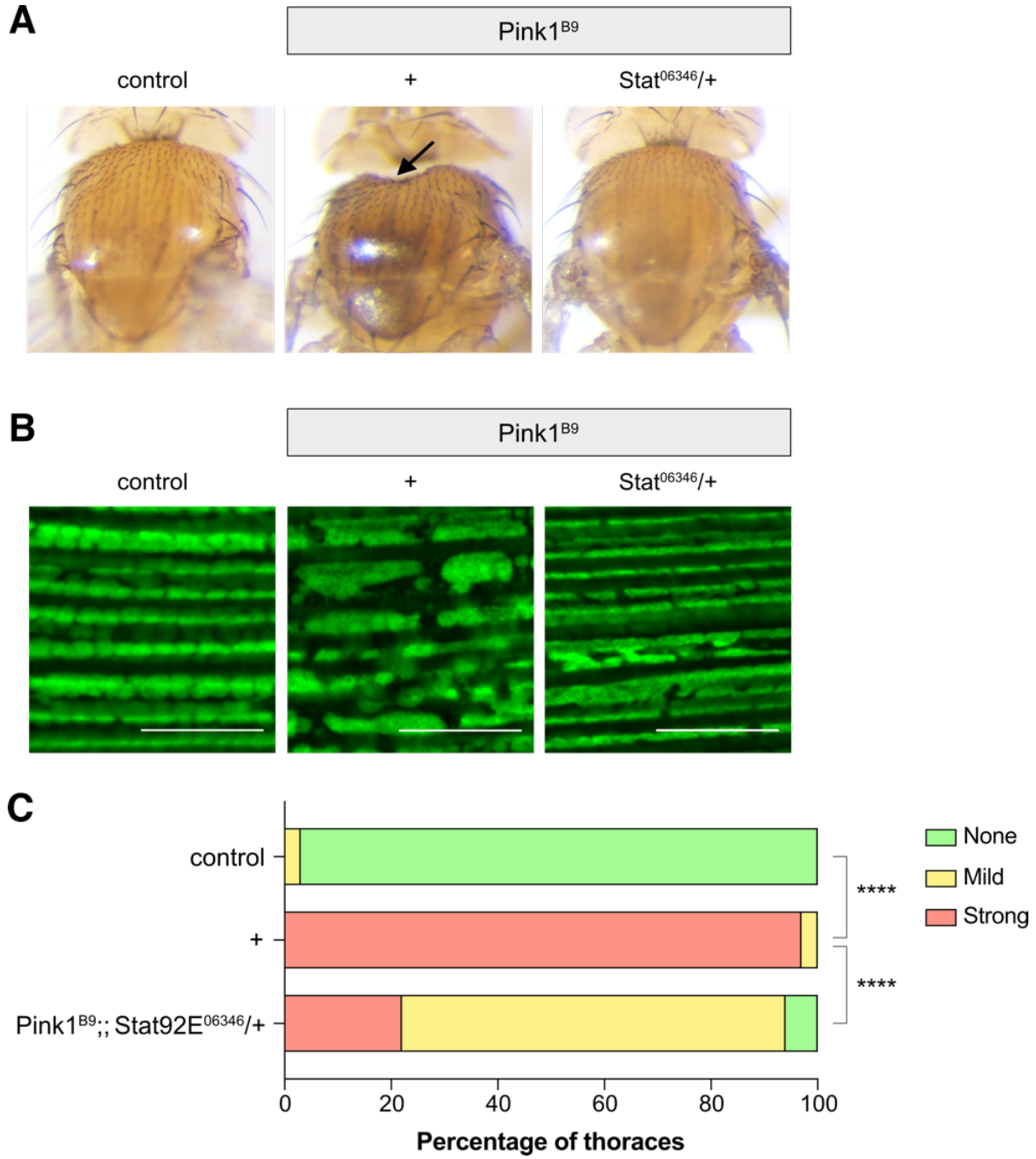

Figure 5.5. Loss of *Stat92E* with *Stat92E^{06346}* mutant partially rescues *Pink1* thoracic indentations and mitochondrial morphology of the IFMs

(A) Thoracic indentations, (B) mitochondrial morphology in *Pink1^{B9}* mutants combined with heterozygous *Stat92E^{06346}*. (C) quantification of (B) – images were scored by the disorganisation of mitochondria. Statistical analysis was determined χ^2 test. ****P <0.0001. n = 8 animals per genotype. Confocal microscopy images show flight muscle mitochondria immunostained with anti-ATP5A. Scale bar = 10 µm. Control genotype is *w^{1118}*. Genotypes analysed are *Pink1^{B9}/Y;;* and *Pink1^{B9}/Y;; Stat92E^{06346} /+*.

Finally, as *Pink1* mutants display loss of DA neurons in the PPL1 cluster, 30-day-old adult brains were dissected and stained with a TH antibody in order to count the number of DA neurons in this particular cluster. Consistent with previous work, the number of DA neurons in $Pink1^{B9}$ flies was significantly lower than control, with PPL1 clusters comprising on average 12 DA neurons compared to 14 in the control (Figure 5.6). However, the lack of *Stat92E* did not rescue the DA neuronal loss typically observed in *Pink1* mutants as on average, 12 DA neurons were present in $Pink1^{B9}$:$Stat92E^{06346}$ PPL1 clusters (Figure 5.6). Altogether these results strongly suggest that loss of *Stat92E* is beneficial to the *Pink1* pathology, although it does not rescue all the *Pink1* phenotypes.

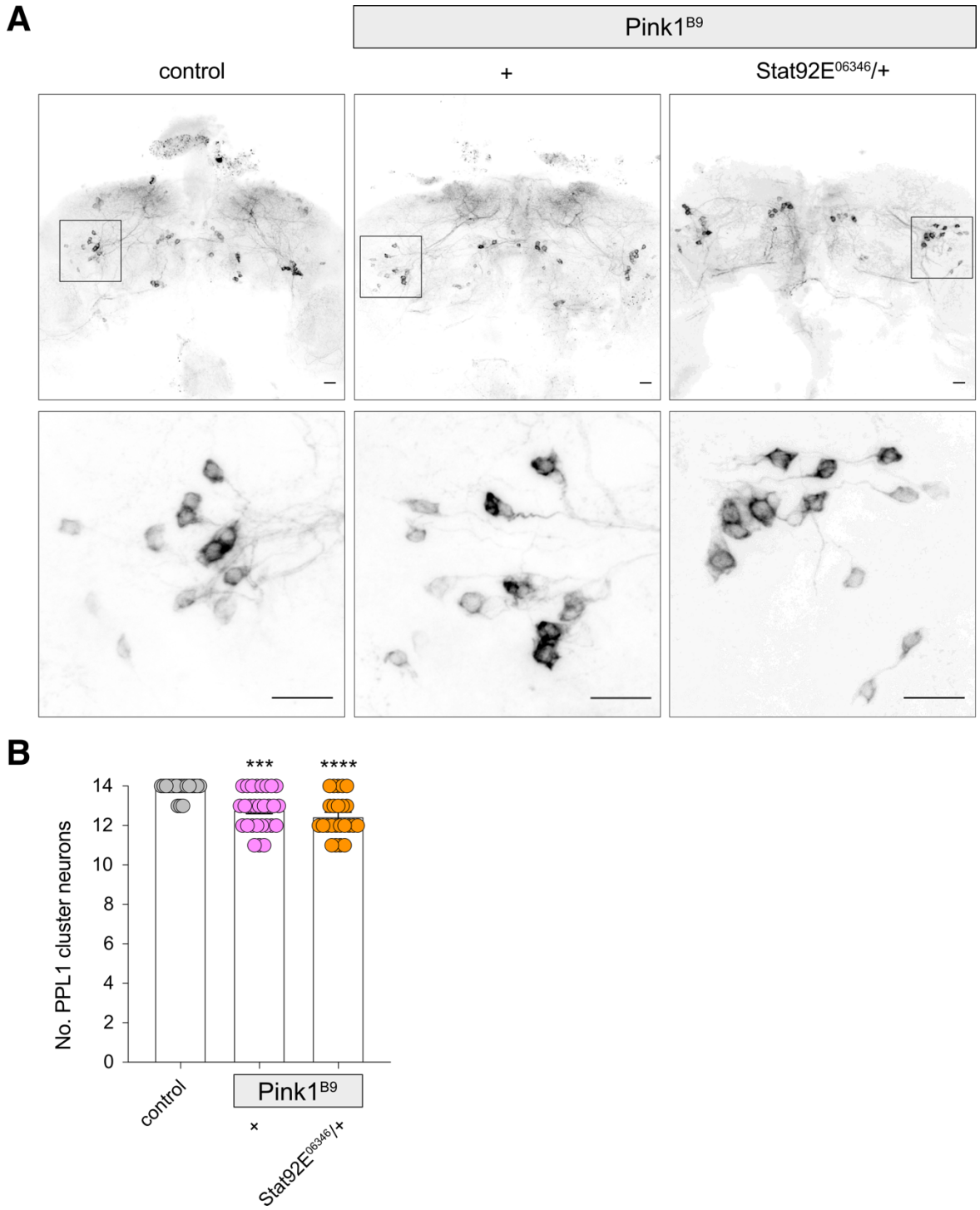

Figure 5.6. Lack of *Stat92E* with *Stat92E^{06346}* mutant does not rescue the *Pink1* DA neuronal loss

(A) Confocal microscopy images of the DA neurons of the PPL1 cluster immunostained with anti-TH in *Pink1^{B9}* mutants combined with heterozygous *Stat92E^{06346}* and (B) quantification of DA neurons shown in (A). Chart shows mean ± SEM and each point correspond to a single hemibrain. Statistical analysis was determined by one-way ANOVA with Bonferroni's post-hoc correction for multiple comparisons; **** *P* <0.0001 and *** *P* <0.001. Scale bar = 10 µm. Control genotype is *w^{1118}*. Genotypes analysed are *Pink1^{B9}/Y;;* and *Pink1^{B9}/Y;; Stat92E^{06346}* /+.

As these findings were interesting, the additional *Stat92E*^{85C9} mutant and a *Stat92E*-RNAi line were used in order to confirm these previous results. Similar to *Stat92E*^{06346}, *Stat92E*^{85C9} mutants are homozygous lethal, therefore all experiments were also performed with heterozygous flies. Behavioural analysis of the *Stat92E*^{85C9} null mutants revealed a small climbing defect at 2 days, that was surprisingly less robust than the *Stat92E*^{06346} mutants (Figure 5.7 A). However, at 20 days, a significant drop in the climbing ability of the flies was observed, slightly more severe than *Stat92E*^{06346} mutants (Figure 5.7 B). It is worth mentioning that although *Stat92E*^{06346} mutant has been classified as a null mutant, a study by Ekas et al., reported that *85C9* is a stronger allele than *06346* as *85C9* led to higher lethality rates and stronger phenotypes (Ekas et al., 2010). Thus, the stronger decrease in the climbing ability observed in *Stat92E*^{85C9} flies at 20 days, compared to *Stat92E*^{06346} flies, might be due to the strength of the *85C9* allele making the flies more susceptible to external pathogens.

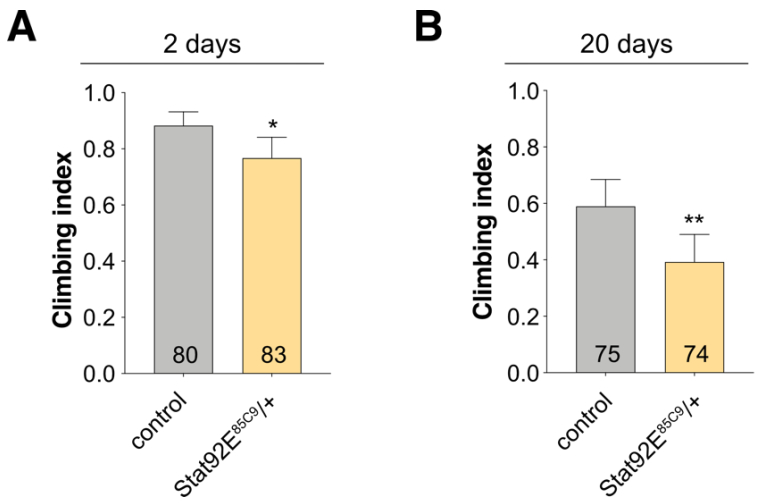

Figure 5.7. *Stat92E*^{85C9} mutants exhibit climbing defects

Locomotor assays analysing climbing ability in (A) 2-day- and (B) 20-day-old flies of control and heterozygous *Stat92E*^{85C9} mutants. Charts show mean ± 95% CI. Number of animals analysed is shown in each bar. Statistical analysis was determined by Welch's *t*-test; ** P <0.01 and *P <0.05. Control genotype is *w*^{1118}.

The combination of *Stat92E*^{85C9} with *Pink1* mutants almost completely abrogated the climbing defects of *Pink1*^{B9} flies at 2 days, however, this was less obvious at 20 days (Figure 5.8 A and B). Similar to *Stat92E*^{06346} mutants, *Stat92E*^{85C9} did not rescue the flight defects of *Pink1* mutant flies (Figure 5.8 C and D). In order to further validate

these results, *Stat92E*-RNAi was expressed with the ubiquitous driver *arm*-GAL4, as stronger expression of the transgene with *da*-GAL4 was lethal, consistent with the lethality of homozygous *Stat92E* mutants. While *Stat92E*-RNAi only mildly affected the climbing ability of the flies at 2 days (Figure 5.9 A), the expression of the transgene at 20 days resulted in a strong climbing defect, which was much stronger than what was previously observed with the two *Stat92E* mutants (Figure 5.9 B). Surprisingly, ubiquitous knockdown of *Stat92E* using the RNAi line did not rescue the *Pink1* climbing defects (Figure 5.9 C).

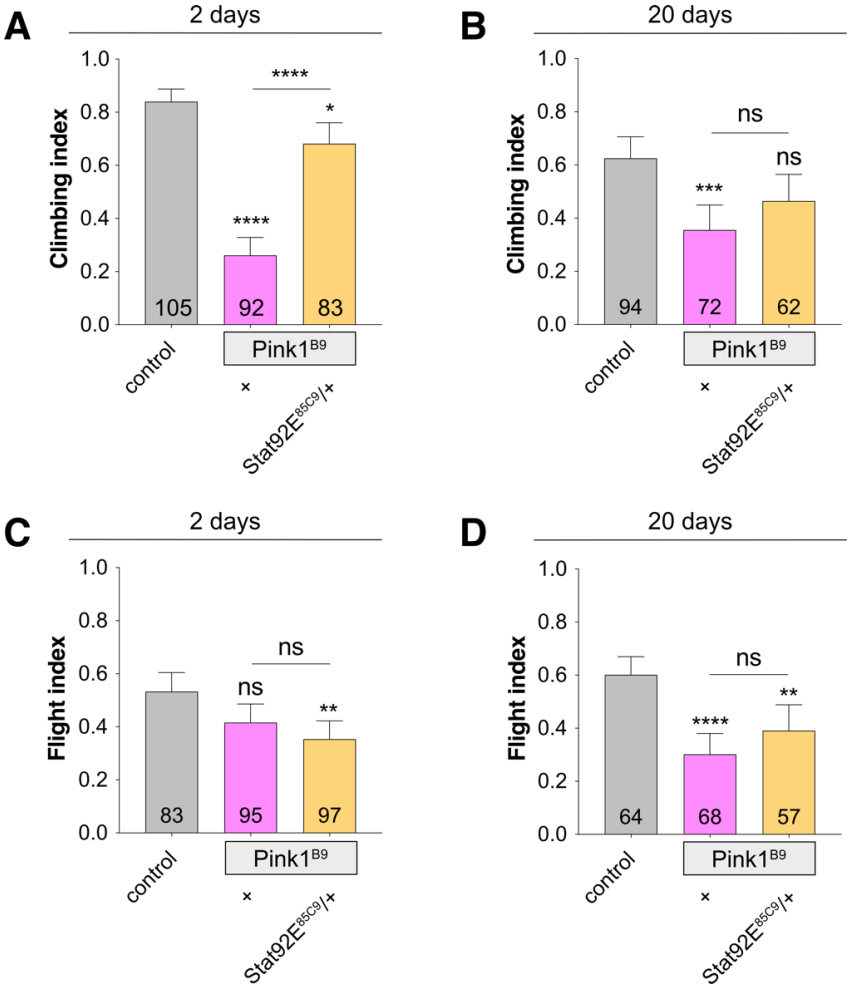

Figure 5.8. Loss of *Stat92E* with *Stat92E^{85C9}* mutant, partially rescues *Pink1* mutant climbing deficit. Locomotor assays analysing climbing ability in (A) 2-day- and (B) 20-day-old and flight assay in (C) 2-day- and (D) 20-day-old *Pink1^{B9}* mutant flies combined with heterozygous *Stat92^{85C9}*. Charts show mean ± 95% CI. Number of animals analysed is shown in each bar. Statistical analysis was determined by Kruskal-Wallis non-parametric test with Dunn's post-hoc correction for multiple comparisons; **** *P* <0.0001, *** *P* <0.001, ** *P* <0.01, **P* <0.05 and ns = non-significant. Control genotype is *w^{1118}*. Genotypes analysed are *Pink1^{B9}/Y;;* and *Pink1^{B9}/Y;; Stat92E^{85C9} /+.*

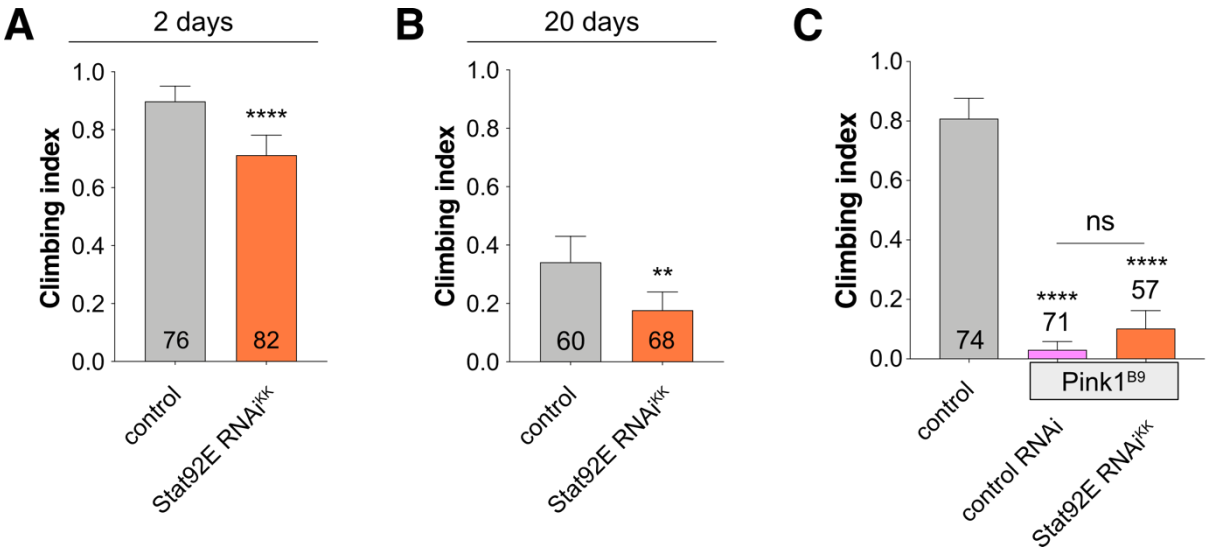

Figure 5.9. *Stat92E* knockdown causes climbing defects and does not rescue *Pink1* mutant climbing deficits

Locomotor assays analysing climbing ability in (A) 2-day- and (B) 20-day-old flies of control and *Stat92E*-RNAi line using the *arm*-GAL4 driver and (C) *Pink1*^{B9} mutants combined with *Stat92E*-RNAi line at 2 days. Charts show mean ± 95% CI. Number of animals analysed is shown in each bar. Statistical analysis was determined by Welch's *t*-test or Kruskal-Wallis non-parametric test with Dunn's post-hoc correction for multiple comparisons; **** P <0.0001; ** P <0.01 and ns = non-significant. Control genotype is *arm-GAL4/UAS-lacZ* RNAi. Genotypes analysed are (control RNAi) *Pink1*^{B9}*/Y; UAS-lacZ* RNAi*/arm-GAL4/+* and *Pink1*^{B9}*/Y; UAS-Sta92E* RNAi^{KK}*/arm-GAL4/+.*

5.3.2. Loss of *Stat92E* does not rescue *parkin* phenotypes

As Pink1 and Parkin act together in the same mitophagy pathway, loss of *Stat92E* was examined in *parkin* mutant background in order to investigate whether or not *parkin* also genetically interacts with *Stat92E*, and potentially with the JAK/STAT pathway. Interestingly, while *Stat92E* loss-of-function nicely rescued some classical phenotypes of the *Pink1* mutants, *Stat92E*^{06346} did not seem to ameliorate or worsen the *parkin* climbing deficits (Figure 5.10 A). Similarly, no changes were observed regarding the mitochondrial morphology of the IFMs double mutants *Stat92E*^{06346}*:park*^{25} (Figure 5.10 B). These data indicate that the rescue obtained by loss of *Stat92E* seems to be specific to *Pink1*.

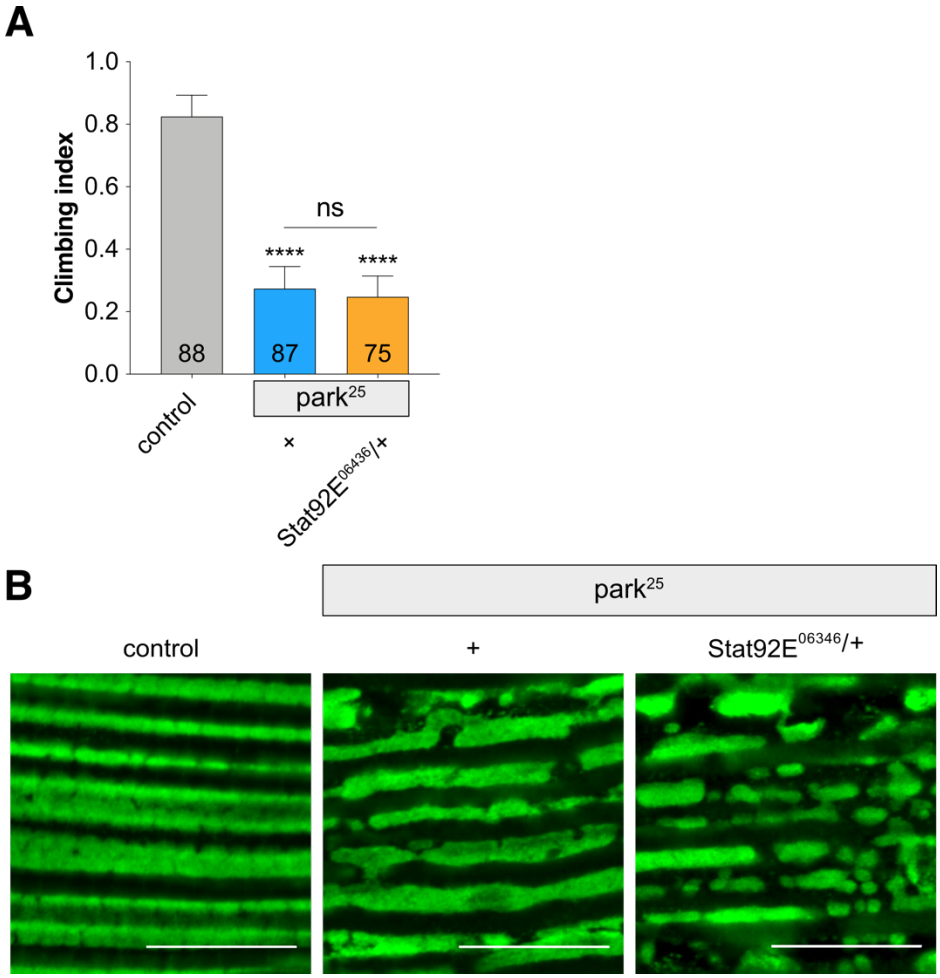

Figure 5.10. Loss of *Stat92E* with *Stat92E^{06346}* mutant does not rescue *parkin* mutant phenotypes
(A) Analysis of climbing ability and (B) mitochondrial morphology in *Pink1^{B9}* mutants combined with heterozygous *Stat92E^{06346}*. Charts show mean ± 95% CI. Number of animals analysed is shown in each bar. Statistical analysis was determined by Kruskal-Wallis non-parametric test with Dunn's post-hoc correction for multiple comparisons; **** *P* <0.0001 and ns = non-significant. Confocal microscopy images show flight muscle mitochondria immunostained with anti-ATP5A. Scale bar = 10 µm. Control genotype is *w^{1118}*. Genotypes analysed are *park^{25}/park^{25}* and *park^{25}, Stat92E^{06346} /park^{25}*.

Altogether, these results demonstrate that loss of *Stat92E* is able to rescue the climbing deficits, the thoracic indentations and the disrupted mitochondrial morphology characteristic of *Pink1* mutant flies. However, while it appears that *Stat92E* genetically interacts with *Pink1*, this seem to be specific to *Pink1* as loss of *Stat92E* does not rescue *parkin* mutant phenotypes. In addition to *Stat92E*, loss of other important players of the JAK/STAT pathway was assessed in a *Pink1* or *parkin* mutant background.

5.3.3. *upd1* knockdown does not rescue *Pink1* or *parkin* phenotypes

To address whether other components of the JAK/STAT pathway were also able to rescue *Pink1* phenotypes, I analysed whether the loss of the ligands of the pathway. In *Drosophila*, the JAK/STAT pathway can be activated by upd1-3. Strong alleles of *upd1* are lethal at the embryonic stage, similar to *hop* and *Stat92E* mutants (Agaisse et al., 2003; Harrison et al., 1998; Hombría et al., 2005). Unlike *upd1* mutants, *upd2Δ*:*upd3Δ* double mutants are homozygous viable. In the gut, *Upd3* expression is tightly regulated and has been shown to be upregulated in septic injury and when tissue repair needs to take place (Beebe et al., 2010; Buchon et al., 2009; Cronin et al., 2009; Osman et al., 2012; Zhou et al., 2013).

Consistent with the lethality of *upd1* null mutants, expression of *upd1*-RNAi with the *da*-GAL4 driver was lethal as well. Therefore, *upd1*-RNAi was expressed with the weaker ubiquitous *arm*-GAL4 driver. Expression of *upd1*-RNAi did not result in a decline in the climbing ability in young or old flies (Figure 5.11). Furthermore, *upd1*-RNAi knockdown in *Pink1* or *parkin* mutant background failed to rescue the phenotypes typically observed in these mutants, such as climbing defect (Figure 5.12 A and B) and disrupted mitochondrial morphology in IFMs (Figure 5.12 C).

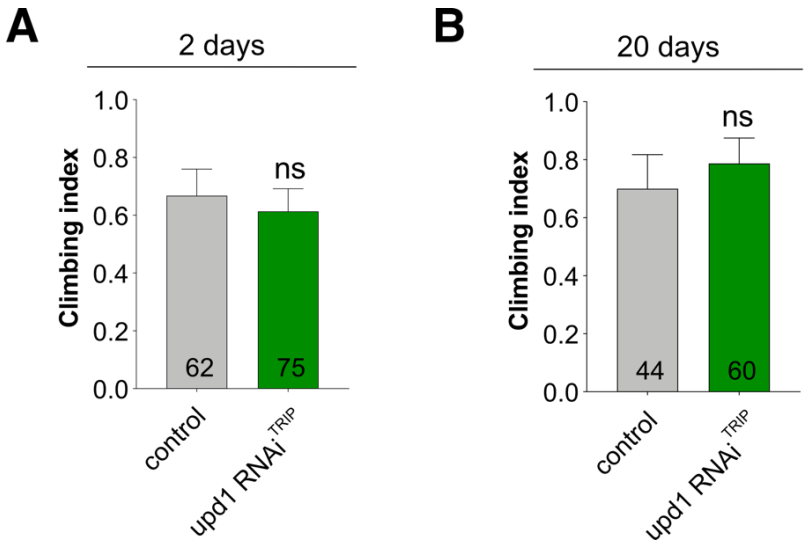

Figure 5.11. *upd1* knockdown does not result in climbing defects

Locomotor assays analysing climbing ability in (A) 2-day- and (B) 20-day-old flies of control and *upd1*-RNAi line using the *arm*-GAL4 driver. Charts show mean ± 95% CI. Number of animals analysed is shown in each bar. Statistical analysis was determined by Welch's *t*-test; ns = non-significant. Control genotype is *UAS-lacZ* RNAi*/arm-GAL4.*

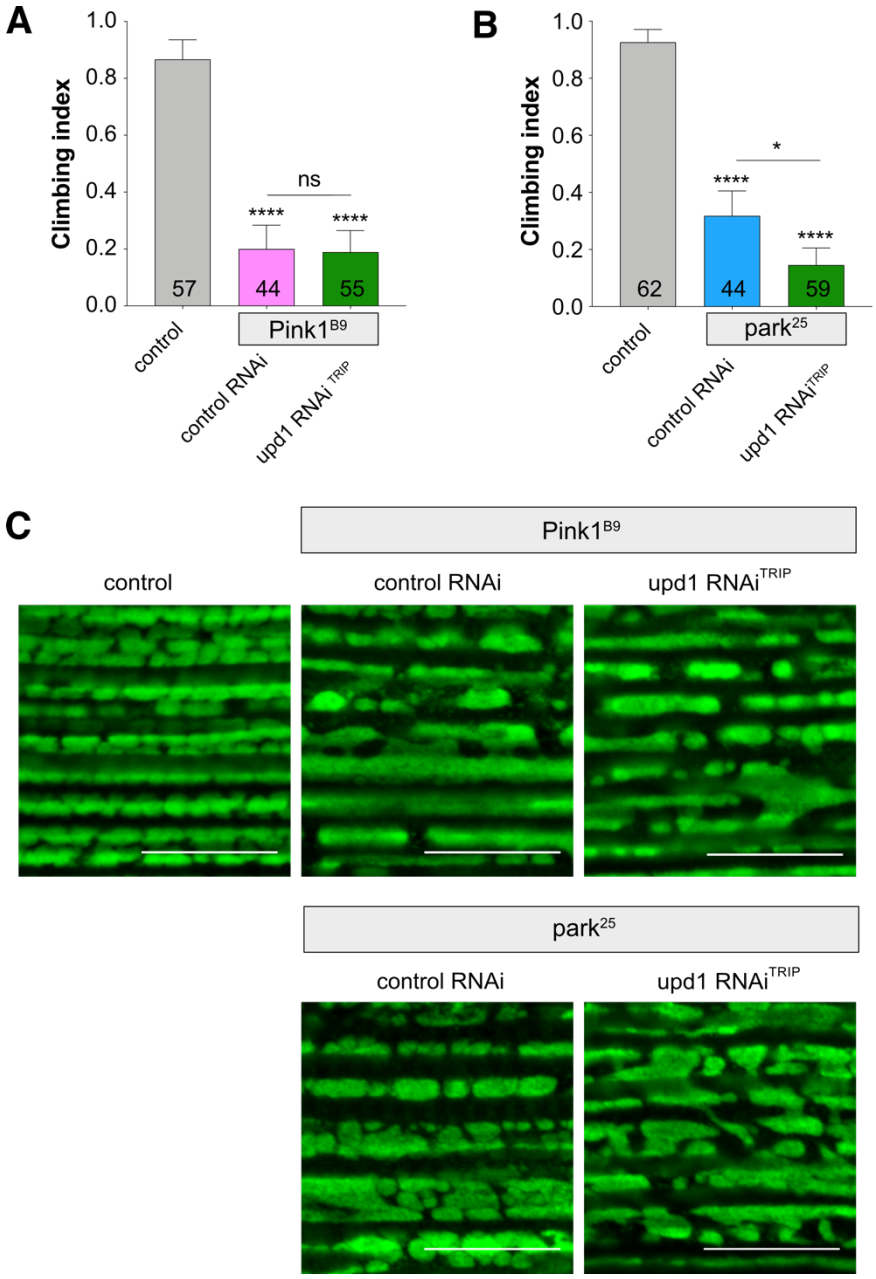

Figure 5.12. Loss of *upd1* does not rescue the *Pink1* or *parkin* mutant phenotypes

Analysis of (A) locomotor climbing ability and (B) mitochondrial morphology in *park*^{25} or *Pink1*^{B9} mutants combined with *upd1* knockdown. Charts show mean ± 95% CI. Number of animals analysed is shown in each bar. Statistical analysis was determined by Kruskal-Wallis non-parametric test with Dunn's post-hoc correction for multiple comparisons; **** P <0.0001; *P <0.05 and ns = non-significant. Confocal microscopy images show flight muscle mitochondria immunostained with anti-ATP5A. Scale bar = 10 µm. Control genotype is *arm-GAL4/UAS-lacZ* RNAi for climbing and *w*^{1118} for microscopy. Control RNAi is *arm-GAL4/UAS-lacZ* RNAi in the respective mutant background. Genotypes analysed are *Pink1*^{B9}*/Y,; Pink1*^{B9}*/Y; arm-GAL4/+; UAS-upd1* RNAi^{TRIP}/+, *park*^{25}*/park*^{25} and *arm-GAL4/+; park*^{25}*/park*^{25}*, UAS-upd1* RNAi^{TRIP}.

5.3.4. Simultaneous loss of *upd2* and *upd3* partially rescue *Pink1*, but not *parkin* phenotypes

Upd2, and more importantly *upd3*, have been shown to play a pivotal role in the activation of JAK/STAT after septic injury and to induce the production of TotA, which was found upregulated in *Pink1* and *parkin* mutants (Greene et al., 2005; Tufi et al., 2014). Therefore, in order to better understand if JAK/STAT pathway is involved in the *Pink1/parkin* pathology, previously established double mutants *upd2Δ*:*upd3Δ* were used. These mutants were generated and characterised by Osman et al., and display a shortened lifespan after bacterial infection, suggesting their inability to fight the pathogen invasion (Osman et al., 2012). The *upd2Δ* mutant lacks the entire coding region of the *upd2* gene and *upd3Δ* is deprived of the first three exons, out of four, of the *upd3* gene, suggesting that these are null mutants (Osman et al., 2012). As all upd genes are present on the X chromosome, both *upd2Δ, upd3Δ* hemizygous males and heterozygous females were tested for climbing ability (Figure 5.13). Heterozygous or hemizygous loss of *upd2* and *upd3* did not induce any climbing defects at 2 days. However, a significant decline in climbing was observed at 20 days (Figure 5.13).

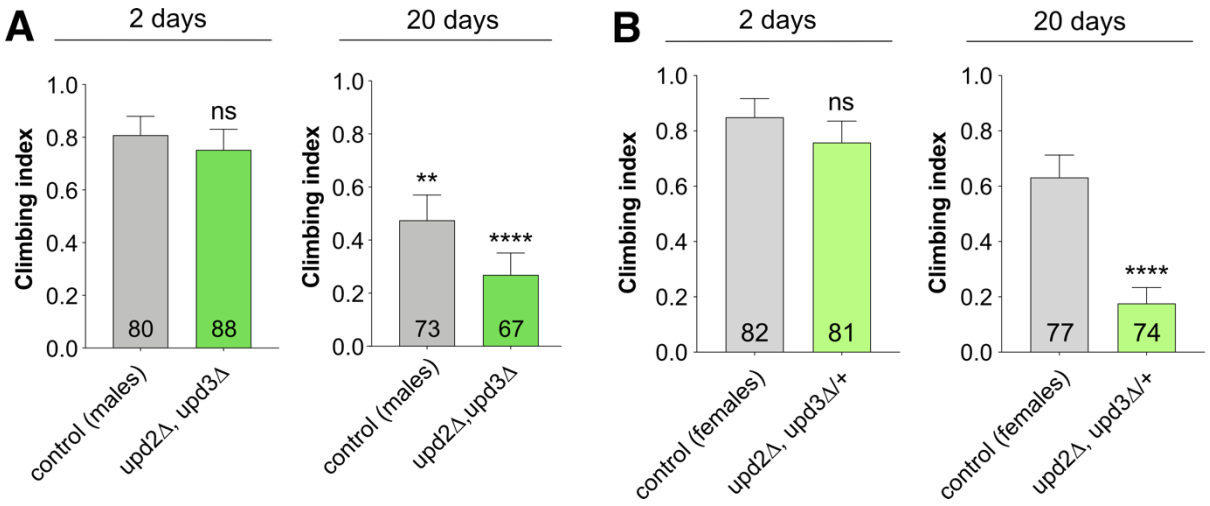

Figure 5.13. Loss of *upd2* and *upd3* causes mild climbing defects

Locomotor assays analysing climbing ability in 2-day- and 20-day-old flies of control and (A) hemizygous males and (B) heterozygous females double mutants *upd2Δ:upd3Δ*. Charts show mean ± 95% CI. Number of animals analysed is shown in each bar. Statistical analysis was determined by Welch's *t*-test; **** P <0.0001; ** P <0.01 and ns = non-significant. Control genotypes are males w^{1118} and females $w^{1118}/^{dah}$.

Interestingly, and in sharp contrast to the results from the *upd1*-RNAi, both hemizygous (Figure 5.14 A and B) and heterozygous (Figure 5.14 C and D) *upd2Δ*:*upd3Δ* mutants rescued the climbing defects of *Pink1* mutants. While the rescue was partial but appreciable at 2 days, it became less obvious in 20 days old flies (Figure 5.14 B and D). This may be explained by the strong climbing defects already present in *upd2Δ*:*upd3Δ* double mutant flies at 20 days in a WT background (Figure 5.13), thus limiting the level of rescue that can be obtained when the two mutations are combined. While behavioural assays showed a substantial rescue of the *Pink1* mutant climbing defect, this was less apparent in IFMs as confocal images revealed no change in the degree of mitochondrial disruption in this particular tissue (Figure 5.14 E).

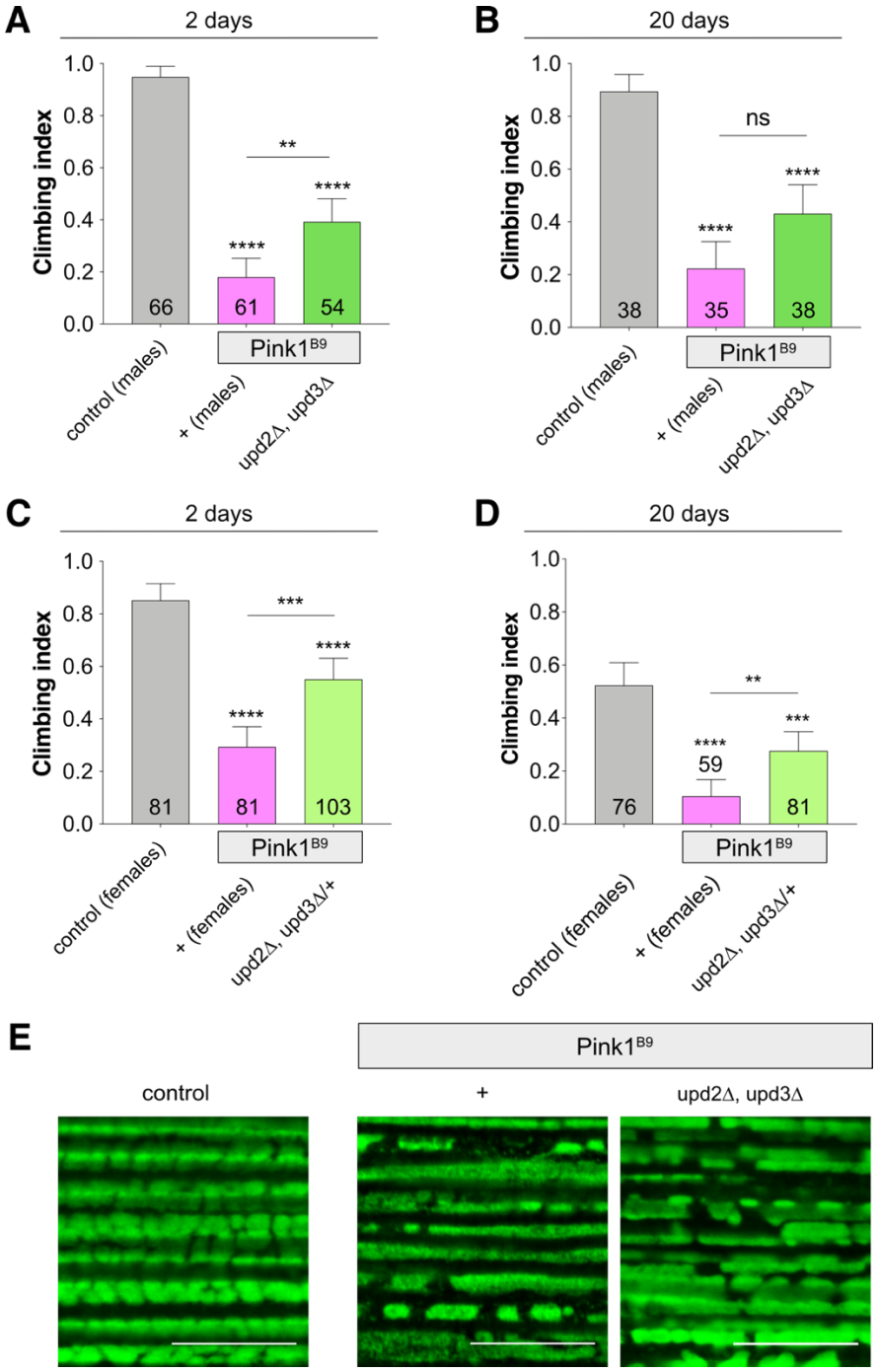

Figure 5.14. Loss of *upd2* and *upd3* partially rescues *Pink1* mutant phenotypes

(A-D) Analysis of climbing ability and (E) mitochondrial morphology in *Pink1*^{B9} mutants combined with (A, B and E) hemizygous males or (C and D) heterozygous females double mutants *upd2Δ:upd3Δ*. Charts show mean ± 95% CI. Number of animals analysed is shown in each bar. Statistical analysis was determined by Kruskal-Wallis non-parametric test with Dunn's post-hoc correction for multiple comparisons; **** P <0.0001; *** P <0.001; ** P <0.01 and ns = non-significant. Confocal microscopy images show flight muscle mitochondria immunostained with anti-ATP5A. Scale bar = 10 μm. Control genotypes are males *w*^{1118} and females *w*^{1118}/*w*^{dah} for climbing and *w*^{1118} for microscopy. Genotypes analysed are *Pink1*^{B9}, *upd2Δ, upd3Δ/Y* (males) and *Pink1*^{B9}, *upd2Δ, upd3Δ/ Pink1*^{B9} (females).

The effect of hemizygous *upd2Δ*:*upd3Δ* double mutants was assessed in a *parkin* mutant background. Similar to what was observed with *Stat92E*, the loss of *upd2* and *upd3* actually worsened the existing *parkin* climbing deficits (Figure 5.15). Due to this worsening of the *parkin* climbing defects, mitochondrial morphology was not assessed in *upd2Δ*:*upd3Δ:parkin* IFMs.

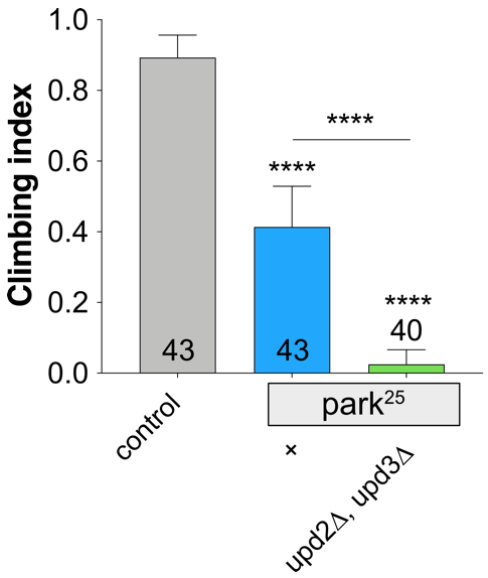

Figure 5.15. Loss of *upd2* and *upd3* does not rescue *parkin* climbing defects

Analysis of climbing ability in park^{25} mutants combined with double mutants *upd2Δ:upd3Δ*. Charts show mean ± 95% CI. Number of animals analysed is shown in each bar. Statistical analysis was determined by Kruskal-Wallis non-parametric test with Dunn's post-hoc correction for multiple comparisons; **** *P* <0.0001. Control genotypes are males *w*^{1118}. Genotypes analysed are *park*^{25}*/park*^{25} and *upd2Δ, upd3Δ/Y;; park*^{25}*/park*^{25} (males).

These last results indicate that in addition to Stat92E, two ligands of the pathway, Upd2 and Upd3, may be involved in the *Pink1* pathology.

5.3.5. Loss of *dome* is beneficial in *Pink1* mutant flies

In order to validate the implication of the JAK/STAT pathway in the *Pink1* rescue, loss of the key receptor Dome using the $dome^{G0441}$ mutant was analysed. $Dome^{G0441}$ is a strong allele previously established by Brown et al. As for the other mutants of the pathway, homozygous $dome^{G0441}$ mutants are lethal during embryonic stage (Brown et al., 2001). Because *dome* is on the X chromosome, experiments were performed using heterozygous females. Whether young or old, flies carrying the $dome^{G0441}$ mutation did not show any signs of climbing impairment (Figure 5.16 A). Consistent with the previous results obtained with the loss of *Stat92E*, *upd2* and *upd3*, a full rescue of the *Pink1* mutant climbing defect was observed in the absence of *dome* at 2 days (Figure 5.16 B). This amelioration was still appreciable in aged flies, although to a lesser extend (Figure 5.16 B).

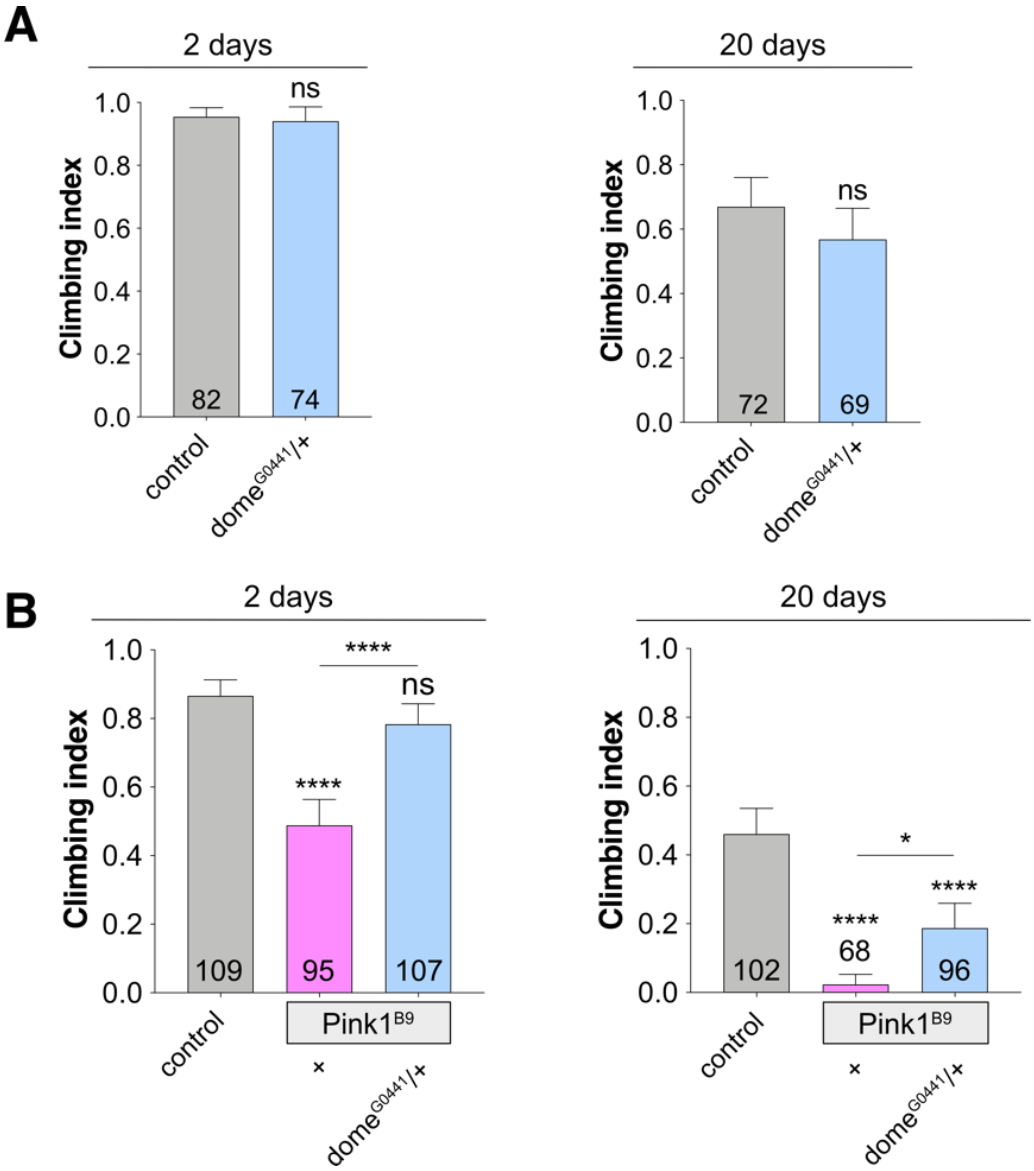

Figure 5.16. Loss of dome with *dome^{G0441}* rescues *Pink1* mutant climbing deficits

Locomotor assays analysing climbing ability at 2 and 20 days of (A) heterozygous *dome^{G0441}* and (B) *dome^{G0441}:Pink1^{B9}* females. Charts show mean ± 95% CI. Number of animals analysed is shown in each bar. Statistical analysis was determined by Welch's *t*-test or Kruskal-Wallis non-parametric test with Dunn's post-hoc correction for multiple comparisons. **** P <0.0001, *P <0.05 and ns = non-significant. Control genotype is *w^{1118}/w^{dah}* (females). Genotypes analysed are *Pink1^{B9}/Pink1^{B9}* and *Pink1^{B9}*, *dome^{G0441}/ Pink1^{B9}*.

5.3.6. Loss of *hop* rescues *Pink1* climbing phenotype

Additionally, *hop* mutants were used to confirm the implication of the JAK/STAT pathway in the *Pink1* pathology. Similar to the other components of the pathway, *hop* is on the X chromosome and hop^{2} mutation is homozygous lethal. Therefore, heterozygous hop^{2} females were tested for climbing. Consistent with the other mutants of the pathway, hop^{2} mutants did not show any decline in their climbing ability at 2 days but a significant decrease was observed at 20 days (Figure 5.17 A). The combination of the hop^{2} mutation with $Pink1^{B9}$ rescued the climbing defects of the latter, further reinforcing the implication of the JAK/STAT pathway in the *Pink1* pathology (Figure 5.17 B). However, while the *Pink1* climbing deficits were fully rescued at 2 days, it was more subtle at 20 days (Figure 5.17 B). Collectively, these results suggest that the entire JAK/STAT pathway is dysregulated in *Pink1* mutants and dampening the signalling cascade may be beneficial.

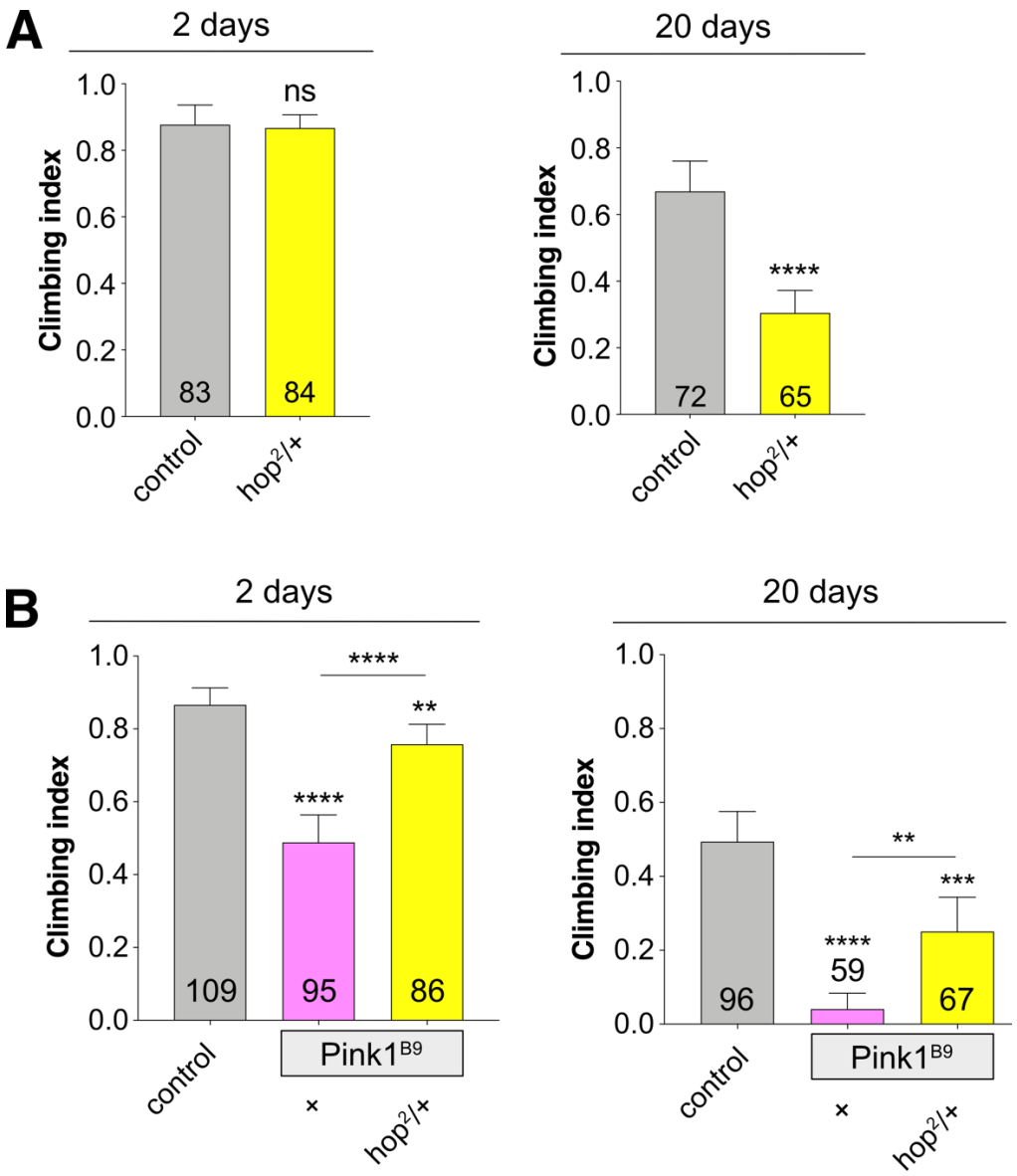

Figure 5.17. Loss of dome with *hop*^{2} rescues *Pink1* mutant climbing deficits

Locomotor assays analysing climbing ability at 2 and 20 days of (A) heterozygous *hop*^{2} and (B) *hop*^{2}*:Pink1*^{B9} females. Charts show mean ± 95% CI. Number of animals analysed is shown in each bar. Statistical analysis was determined by Welch's *t*-test or Kruskal-Wallis non-parametric test with Dunn's post-hoc correction for multiple comparisons. **** *P* <0.0001, **P* <0.05 and ns = non-significant. Control genotype is *w*^{1118}/*w*^{dah} (females). Genotypes analysed are *Pink1*^{B9}/*Pink1*^{B9} and *Pink1*^{B9}, *hop*^{2}/ *Pink1*^{B9}.

5.3.7. Loss of *TotA* and *TotM* rescue *Pink1* mutants climbing deficits

Finally, I hypothesised that if downregulating the JAK/STAT pathway is beneficial to the *Pink1* phenotype, knocking-down two downstream target genes of the pathway, such as *TotA* and *TotM*, may improve the *Pink1* mutant phenotypes. To address this, two *TotA*- and one *TotM*-RNAi lines were expressed with the ubiquitous driver *da*-GAL4 (Figure 5.18 A and B). The two *TotA*-RNAi lines only differed by their insertion sites, attP40 is inserted on the second chromosome and attP2 on the third. Unlike some of the core components of the pathway, knockdown of *TotA* or *TotM* did not result in strong climbing defects (Figure 5.18 A and B). Flies expressing the *TotA*-RNAi (attP2) displayed a slight climbing defect although this remained quite subtle (Figure 5.18 A). Interestingly, the absence of *TotA* using one RNAi-line (attP40) strongly improved the *Pink1* mutant climbing impairment (Figure 5.18 A). However, the expression of the attP2 *TotA*-RNAi line did not ameliorate the *Pink1* climbing ability. The discrepancy in the *Pink1* rescue, observed with the two *TotA*-RNAi lines might be explained by distinct efficiencies of the RNAi lines, resulting in different knockdown levels of *TotA*, which were not assessed in the present study. While the *TotM*-RNAi line increase the climbing ability of the *Pink1* mutant flies, it remained significantly lower than control flies. Together this suggests that the immune response, regulated by JAK/STAT canonical pathway, is detrimental for *Pink1* mutants.

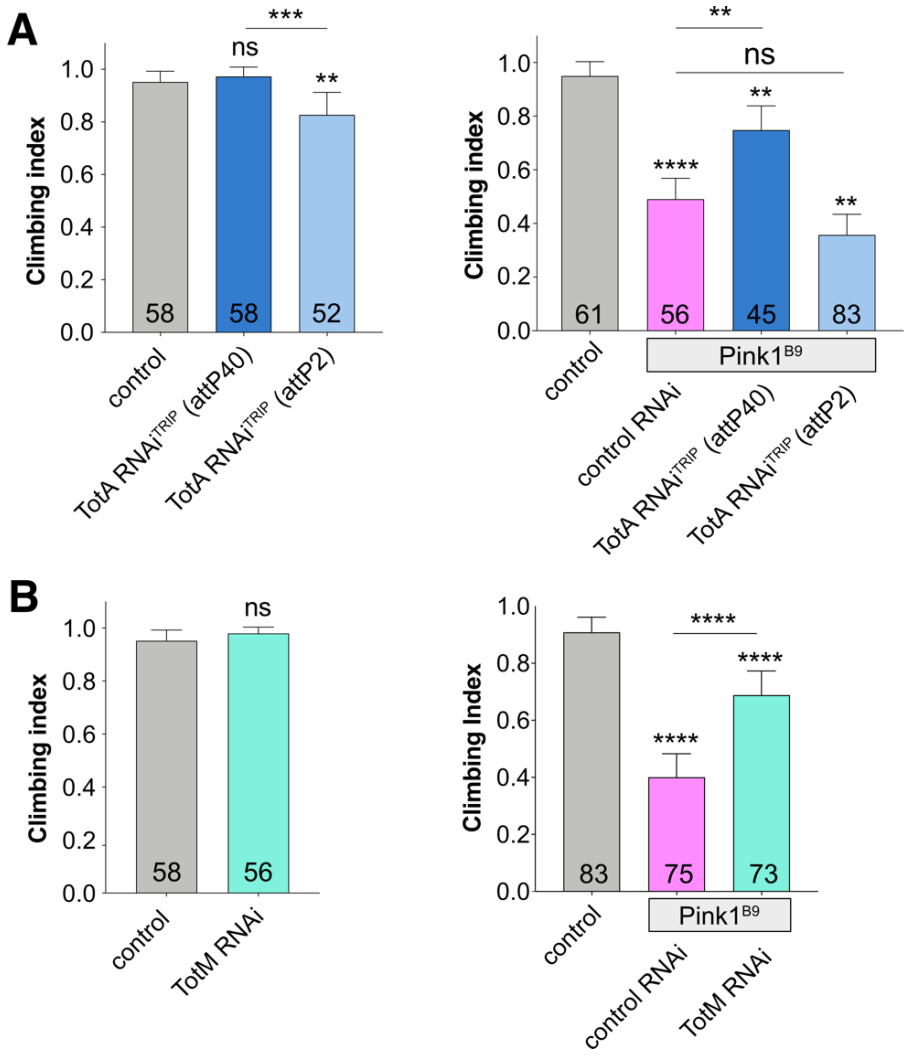

Figure 5.18. Knockdown of *TotA* or *TotM* results in mild climbing defects

Locomotor assays analysing climbing ability in 2-day old flies of (A) two *TotA* RNAi and (B) *TotM* RNAi lines using the *da*-GAL4 driver with or without *Pink1*^{B9} mutants. Charts show mean ± 95% CI. Number of animals analysed is shown in each bar. Statistical analysis was determined by Welch's *t*-test or Kruskal-Wallis non-parametric test with Dunn's post-hoc correction for multiple comparisons; **** *P* <0.0001; *** *P* <0.001; ** *P* <0.01; and ns = non-significant. Control genotypes are *w*^{1118} and *UAS-lacZ* RNAi; *da-GAL4/+*. Control RNAi is *UAS-lacZ* RNAi*/+; da-GAL4/+*. Genotypes analysed are *UAS TotA* RNAi (attP40)*/+; da-GAL4/+*, *da-GAL4*/*UAS TotA* RNAi (attP2), *UAS-TotM* RNAi*/+; da-GAL4/+,* (control RNAi) *Pink1*^{B9}*/Y; UAS-lacZ* RNAi*/+; da-GAL4/+, Pink1*^{B9}*/Y; UAS TotA* RNAi (attP40)*/+; da-GAL4/+, Pink1*^{B9}*/Y;; da-GAL4*/*UAS TotA* RNAi (attP2) and *Pink1*^{B9}*/Y; UAS TotM* RNAi */+; da-GAL4/+.*

5.3.8. The gut homeostasis seems perturbed in *Pink1* mutants

Having established the implication of the JAK/STAT in the *Pink1* pathology, and considering that the JAK/STAT pathway is a central regulator of the gut homeostasis, activation of the pathway was further investigated in the larval midgut (Herrera & Bach, 2019). To this end, the commonly used 10XStat92E-GFP reporter generated by Bach et al. was used to monitor JAK/STAT activity in the posterior midgut of *Pink1* mutant larvae (Bach et al., 2007). The 10XStat92E-GFP reporter contains 10 Stat92E binding sites of the target gene *Socs36E* that drive the expression of the GFP (Bach et al., 2007). Therefore, the reporter allows the monitoring of JAK/STAT activation using the GFP signal. One of the first observations was the general increase in the number of intestinal cells observed in the posterior midgut of *Pink1* mutant larvae, as seen by the DAPI staining (Figure 5.19 B). Looking closer at the cell populations, it also appeared that AMPs, still engulfed in PCs, were more abundant in *Pink1* mutant midguts compare to control (see red arrows Figure 5.19). Consistent with the literature, JAK/STAT activation, as detected by the 10XStat92E-GFP reporter, was appreciable in the PCs but not in AMPs or ECs of both WT and *Pink1* mutant larvae (Mathur et al., 2010; Zhang et al., 2017). However, more GFP positive cells were qualitatively observed in *Pink1* mutant larvae compare to WT, suggesting more activation of the JAK/STAT pathway in *Pink1* mutant larval guts. While these preliminary data are exciting, clearly additional experiments that would shed light on the mechanism behind JAK/STAT and *Pink1* interaction, are necessary, however, due to COVID restrictions, I was not able to pursue this further.

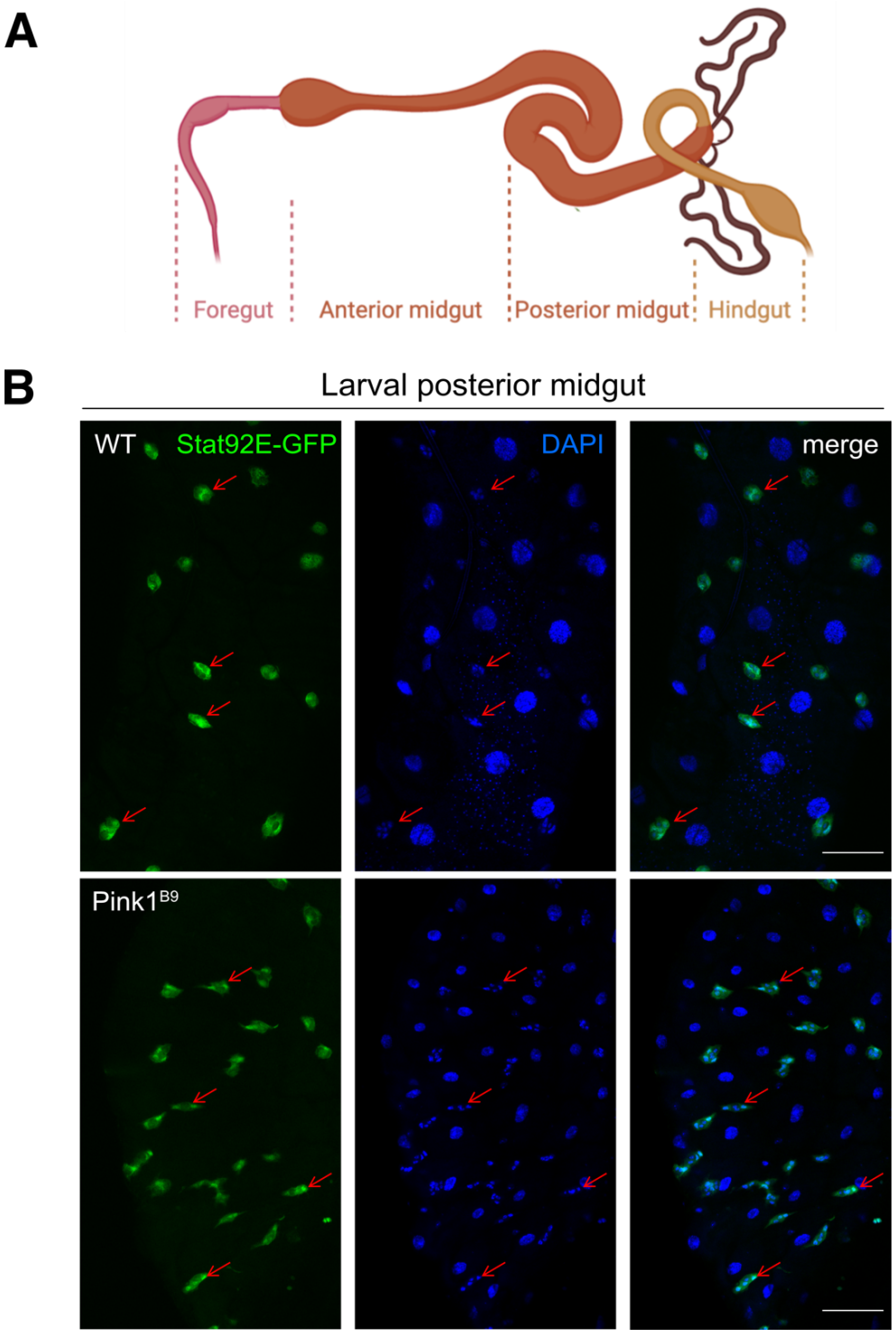

Figure 5.19. *Pink1* mutant larvae display abnormal gut homeostasis

(A) schematic representation of the larval intestinal system and (B) confocal images of larval posterior midgut in w^{1118} and $Pink1^{B9}$ mutants combined with the 10XStat92E-GFP reporter and immunostained with anti-GFP (green) and DAPI (blue). Confocal images show JAK/STAT signalling, as detected by the reporter 10XStat92E-GFP; green. PCs (red arrows) are shown wrapping AMPs (small round blue nuclei) in the WT. Scale bar = 10 μm. Genotypes analysed are *10XStat92E-GFP/+* and $Pink1^{B9}$*/Y; 10XStat92E-GFP/+*.

5.4. Discussion

Epidemiological, human post-mortem and animal studies have all confirmed the implication of the immune system in the PD pathogenesis. Several studies have reported elevated levels of a plethora of pro-inflammatory cytokines in post-mortem brains of PD patients (Taylor et al., 2013). Among these cytokines were IL-6 and IFNy, two pro-inflammatory cytokines activated by the JAK/STAT pathway (Imamura et al., 2003; Mogi et al., 2007). Additionally, several toxin-based models of PD have shown that suppressing the expression of some pro-inflammatory cytokines is beneficial. For instance, after being exposed to MPTP, mice lacking IFNy exhibit less DA neuronal loss (Mount et al., 2007). Other studies based on rotenone and paraquat treatments reported similar results. Mangano et al., showed that mice deprived of IFNy display significantly less paraquat-induced cell death (Mangano et al., 2012). While a clear correlation between PD and the immune system has been established in mammals, little has been investigated in *Drosophila* models.

In this chapter, I sought to explore the implication of the JAK/STAT pathway in the *Pink1/parkin* pathology. Interestingly, the results presented here show that the downregulation of major players of the JAK/STAT pathway is able to rescue several key phenotypes characteristic of the *Pink1* mutants. First, knockdown of *Stat92E*, the major transcription factor of the pathway and fly homolog of the mammalian STAT3, was assessed using two different *Stat92E* mutant alleles independently combined with *Pink1* mutants. Both $Stat92E^{06346}$ and $Stat92E^{85C9}$ alleles rescued the climbing defect, thoracic indentations as well as the disrupted mitochondrial morphology observed in *Pink1* mutants. It is worth mentioning that loss of *Stat92E* only partially rescued these *Pink1* phenotypes and failed to attenuate the DA neuronal death occurring in the PPL1 cluster of the *Pink1* mutants. An obvious explanation is based on the fact that heterozygous *Stat92E* mutants, especially $Stat92E^{06346}$ flies, showed significant decreased climbing abilities compare to WT at 2 days old, thus limiting the potential rescue of the *Pink1* phenotypes. To further support this, $Stat92E^{85C9}$ mutants exhibited lower climbing deficits than $Stat92E^{06346}$ mutants which resulted in a better rescue of the *Pink1* climbing defects. Surprisingly, loss of *Stat92E*, or any other components of the JAK/STAT signalling cascade, did not rescue the *parkin* mutant phenotypes, suggesting that any interaction with this pathway seems to be restricted to *Pink1* and

may be unrelated to the primary role that Pink1 and parkin play in the mitophagy process. As *Stat92E* has been shown to have additional roles independent of the canonical JAK/STAT pathway, the loss of other components of the pathway was analysed to investigate whether or not the whole JAK/STAT pathway was involved in the *Pink1* rescue. To address this, *Pink1* mutants were combined with RNAi lines and mutants for the *upd*s, the cytokine-like ligands, *hop*, JAK's homolog and *dome*, the cytokine-like receptor. While the rescue of the *Pink1* mutant phenotypes was less striking in the absence of the *upd*, *Pink1* mutants combined with either *hop* or *dome* heterozygous mutants led to almost a complete rescue of the *Pink1* climbing defects. As hop^{2} or $dome^{G0441}$ mutations do not induce any climbing defects in young flies, it would be interesting to analyse the DA neuronal loss and mitochondrial morphology in the IFMs of $Pink1^{B9}$:hop^{2} and $Pink1^{B9}$:$dome^{G0441}$ double mutants. Finally, in addition to the main components of JAK/STAT pathway, I sought to investigate the loss of downstream targets such as two genes of the Turandot family, *TotA* and *TotM*. Interestingly, loss of *TotA* completely rescued the climbing deficits observed in *Pink1* mutants. Altogether, these results strongly implicate the JAK/STAT pathway, and the immune response triggered by it, in the *Pink1* pathology, however, this seems to be independent of *parkin*. As JAK/STAT pathway plays a major role in the *Drosophila* intestinal homeostasis, I sought to examine the JAK/STAT activation in the larval midgut of *Pink1* mutants. Interestingly, the overall gut morphology and gut length seemed perturbed in the *Pink1* mutants (data not shown). Qualitative assessment of the 10XStat92E-GFP reporter showed an increased number of GFP-positive intestinal cells in the *Pink1* larval midgut, indicating a potential disruption of AMPs progenitors and their niche. While the results presented here are based on preliminary data, they clearly implicate the JAK/STAT pathology in the *Pink1* pathology. In addition, they indicate that the gut homeostasis in *Pink1* mutants is disrupted, at least at the larval stage. Clearly, there are some key areas to further investigate in order to better understand the mechanism underlying these phenotypes.

Although some mammalian pro-inflammatory cytokines that signal to JAK/STAT have been shown to be upregulated in PD, to date, there is no evidence from the literature linking dysregulated JAK/STAT signalling with the *Pink1* pathology in *Drosophila*. Therefore, rather than speculating on these early findings, I consider it more appropriate to discuss the key remaining questions to answers as well as future

experiments that could be done in order to better understand why and how the upregulation of the JAK/STAT pathway may participate in *Pink1* mutant phenotypes.

Several publications reported that loss of Mfn or Opa1 or Drp1 overexpression are able to rescue the phenotypes observed in *Pink1/parkin* mutant flies (Celardo et al., 2016; Deng et al., 2008; Liu et al., 2011; Liu et al., 2016; Park et al., 2009; Poole et al., 2008). Therefore, it is possible that the rescue of the *Pink1* mutant phenotypes obtained by modulating the JAK/STAT pathway is related to an effect on mitochondrial dynamics. Interestingly, STAT2-deficient patients exhibit elongated mitochondria due to the unphosphorylated state of Drp1 at the Ser616 residue, resulting in the inactivation of Drp1 (Shahni et al., 2015). This study links STAT2 to mitochondrial dynamics and mitochondria, and suggests a role of STAT2 in the Drp1 phosphorylation and its subsequent activation (Shahni et al., 2015). However, evidence for a potential relationship between the innate immune system and mitochondrial dynamics remains quite poor and more work is needed.

The most surprising finding is the fact that a reduction of the JAK/STAT signalling rescues *Pink1* but not *parkin* mutants. A possible explanation is that *parkin* mutants often exhibit stronger phenotypes than *Pink1* mutants, thus resulting in too severe impairments that cannot be improved in this fashion. However, the manipulation of other interactors of *parkin*, such knockdown of *UPS30*, has been shown to substantially rescue the parkin-associated phenotypes, such as muscular degeneration (Bingol et al., 2014). The differences observed between *Pink1* and *parkin* may instead be the result of divergent molecular pathways. Interestingly, Koehler et al., reported that specific depletion of *Pink1* or *parkin* in the ISC/EBs leads to disrupted mitochondrial morphology (Koehler et al., 2017). In addition, the proliferation of ISCs is impaired and this is accompanied by the expression of senescence markers (Koehler et al., 2017). Therefore, to confirm the implication of the JAK/STAT pathway and the effect on the midgut homeostasis of the midgut of *Pink1* mutants, it would be interesting to further investigate the gut morphology and progenitor cell lineages in these mutants. In addition, it will be interesting to follow the ability of adult ISCs and larval AMPs, to proliferate and differentiate into ee or ECs.

Another question that remains to be answered is why the JAK/STAT pathway is

activated in *Pink1* mutants. There are several hypotheses that can be proposed. JNK activation, in response to local tissue damage, has been shown to induce *upd2* and *upd3* expression in ECs, thus subsequently triggering the JAK/STAT signalling cascade (Jiang et al., 2009). Therefore, it is possible that the activation of another pathway, such as JNK, is responsible for the JAK/STAT signalling response observed in *Pink1* mutants. This is particularly attractive as a study from Cha et al., found that JNK signalling is highly activated in DA neurons of *parkin* mutants. In addition, the authors showed that Parkin is able to inhibit JNK signalling cascade through its E3 ligase activity (Cha et al., 2005). Thus, loss of *parkin* is responsible for the upregulation of the JNK pathway and the subsequent loss of DA neurons, although this was not demonstrated (Cha et al., 2005). Although, the results from the previous chapter did not indicate any interaction between the JNK signalling and *Pink1* or *parkin* mutants, experiments were only relying on ubiquitous depletion of JNK components, thus potential interaction between these mutants and the JNK pathways would need to be tested using a specific knockdown of JNK signalling, in the DA neurons or in midgut cells, such as ECs. Looking at the *upd1-3* transcript levels will inform on the potential upregulation of these ligands, although *upd2:upd3* double mutants showed the less robust rescue of the *Pink1* mutant. Another explanation that may account for the activation of the JAK/STAT pathway in *Pink1* mutants is the expression of a negative regulator of the pathway, such as *Socs36E*, *PTP61F* or *dPIAS*. They may be repressed in *Pink1* mutants, therefore leading to an overactivation of the signalling cascade. To address whether or not this is true, these repressors could be expressed in a *Pink1* mutant background, and flies could be subjected to climbing assay. Additionally, analysis of transcript levels by RT-qPCR could be performed in order to see if these genes are indeed downregulated in *Pink1* mutants. However, preliminary work based on the overexpression of *Socs36E* using the weak *arm*-GAL4 driver did not show any impact on the *Pink1* mutant climbing deficits (data not shown). As mentioned previously, all these genes also have important roles during development, thus our experiments may be challenged by finding the right balance between the GAL4 and the UAS, driving too much versus too little expression.

While overall these findings suggest that dysregulation of the JAK/STAT signalling is restricted to the *Pink1* pathology, it would be worth analysing mitophagy in the midgut of these mutants, perhaps using the mito-QC in specific cell populations such as ISCs,

EBs or ECs. Indeed, the study from Koehler et al., strongly indicates that ISCs heavily rely on mitophagy to maintain a healthy pool of mitochondria (Koehler et al., 2017). Interestingly, Bourke et al., have shown that following ischemia/reperfusion injury, mammalian STAT1 and STAT3, are able to interact with LC3, suggesting that STATs may play a role in the specific degradation of mitochondria through an autophagy-like mechanism (Bourke et al., 2013). To support this, the group has shown that both STAT1 and STAT3 contain conserved LIR binding motifs, although these do not seem to all be present in the *Drosophila* Stat92E (Bourke et al., 2013). The mito-QC will provide a useful tool to investigate whether loss of *Pink1* or *parkin* impact mitophagy in these specific cell types, either in normal conditions or upon mitochondrial damage such as paraquat treatment. Knockdown of other mitophagy-related proteins, such as p62/Ref(2)P or LC3/Atg8 combined with the Stat92E-GFP reporter will also provide additional information on whether or not a defect in mitophagy may be responsible for the upregulation of JAK/STAT signalling in these midgut cells.

This leads to another remaining question, can we confirm the activation of the pathway by analysing Stat92E localisation at the nucleus in *Pink1* mutants, or does Stat92E localise elsewhere, such as mitochondria? There has been increasing amount of evidence pointing towards a role of STAT3 at the mitochondria, which has even led to the term ‘mitoSTAT’. Indeed, fractionation experiments from cultured cells revealed that 5-10% of total STAT3 reside in the mitochondria, where it seems to affect complexes I and II of the respiratory chain (Wegrzyn et al., 2009). Furthermore, loss of *Stat3* correlates with significant decrease of ATP levels and reduced activity of complexes II and V, although the mechanism remains unclear (Szczepanek et al., 2012). It seems that STAT3 requires to be phosphorylated on a specific Ser residue in order to be imported in the mitochondria but also to perform its mitochondrial functions (Szczepanek et al., 2012; Tammineni et al., 2013; Wegrzyn et al., 2009). STAT3 has also been shown to play a role in reducing oxidant cellular stress. For instance, the specific depletion of *Stat3* in hematopoietic cells induces mitochondrial dysfunction which correlates with elevated ROS production and reduced hematopoietic stem cell reserves (Mantel et al., 2012). Although *Stat3* is not ‘per se’ the mammalian homolog of *Stat92E* in *Drosophila*, it would be interesting to investigate Stat92E localisation, to see whether or not a small proportion of Stat92E localises to the mitochondria, in a similar fashion to STAT3. However, while these new roles of the STATs proteins are

exciting, several studies have reported contradictory results (Meier & Larner, 2014). Indeed, considering the low abundance of STATs in the mitochondria and the difficulties of obtaining clean mitochondrial fractionations, investigating the mitochondrial targets of STATs remains a difficulty. Additionally, STATs protein levels, like Stat92E are probably varying depending on the tissue or cell type studied. These discrepancies have also been reported in studies investigating STATs localisation using fluorescent-based approaches (Meier & Larner, 2014). Therefore, care should be taken when interpreting data from these experiments.

Finally, one last important question concerns the tissue specificity of the activation of the JAK/STAT pathway. The data presented in this chapter suggest that the gut homeostasis may be affected in *Pink1* mutants. However, as these data are preliminary further work needs to be conducted to better understand which particular intestinal cell type may be compromised in these mutants. The expression of JAK/STAT repressors, such as *Socs36E* or *dPIAS*, in *Pink1* mutants, and the knockdown of *Stat92E* or *TotA/TotM*, specifically in these cell types may help us to answer the question related to the tissue specificity. Moreover, as *TotA* and *TotM* are expressed in the fat body, the depletion of these two downstream effectors specifically in the fat body of *Pink1* mutants will inform us whether the fat body is involved in this pathology.

Glial reactivity is a common characteristic of many neurodegenerative disorders. Glia cells participate in the clearance of neuronal debris, however, they can also drive inflammation through the release of pro-inflammatory cytokines and exacerbate the existing damage occurring in the CNS (Ceyzériat et al., 2016). Therefore, whether glial activation is harmful or beneficial to the CNS still remains unclear (Doherty et al., 2014). Interestingly, mammalian STAT3 has been involved in astrocyte reactivity in various models of neurodegeneration, including after MPTP exposure (O'Callaghan et al., 2014; Sriram et al., 2004). Indeed, in the absence of *Stat3* specifically in the astrocytes, mice exposed to MPTP exhibit attenuated astrocyte reactivity (O'Callaghan et al., 2014). Interestingly, the implication of STAT3 in astrocyte reactivity seems to be conserved in *Drosophila* as Stat92E has been shown to control glial reactivity upon axonal injury, suggesting that STAT3/Stat92E may be key regulators of glial reactivity (Doherty et al., 2014). Doherty et al., reported that the ability of glial cells to clean

debris of degenerating neurons is regulated by Stat92E, however their study suggests that this seems to occur through a non-canonical role of Stat92E as it is independent of Hop (Doherty et al., 2014). It is tempting to hypothesise that *Pink1* mutant phenotypes could be the result of the activation of the JAK/STAT pathway in the glial cells. Therefore, using glia-specific drivers such as *repo*-GAL4 to downregulate genes of the JAK/STAT pathway may help to elucidate if the glial cells are involved in the *Pink1* pathology. It is worth mentioning that, as almost all the components of the JAK/STAT pathway have key functions during development, as seen by their homozygous lethality, care should be taken when manipulating the expression of these various genes. Perhaps adult-restricted knockdown, using temperature sensitive drivers or GeneSwitch, may help to overcome these challenges.

Chapter 6. General discussion and future work

6.1. *In vivo* mitophagy: a controversial issue

Damage to mitochondria can have deleterious consequences on cell survival, promoting excessive ROS production that can subsequently alter protein, DNA and lipids and eventually trigger cell death by apoptosis (Nunnari & Suomalainen, 2012). Therefore, maintaining a healthy pool of mitochondria is essential and primarily occurs through MQC mechanisms, recycling either bits of the mitochondrion or the entire organelle, in case of extensive damage. While several quality controls have been investigated, my work has mainly focused on the role of PINK1 and Parkin in mitophagy *in vivo*.

Since Richard Youle's team showed the implication of PINK1/Parkin in the mitophagy process, more than 10 years ago, our knowledge about this mechanism has been growing exponentially. Due to the implication of *PINK1* and *PRKN* genes in early onset familial PD, it has been speculated that defective mitophagy could be a key mechanism leading to PD pathology. Because sporadic PD arises from a complex interaction between genes and environmental factors, the investigation of the factors driving familial PD has provided a window to understand the overall disease mechanisms. However, over the last few years, the significance of the PINK1/Parkin pathway *in vivo* has been a major source of debate. This has been challenged by the absence of robust phenotypes in *Pink1/Prkn* null mice and the concern that observations obtained from *in vitro* cultured cells and immortalised cell lines may not reflect what is happening in neurons *in vivo*. In addition, the identification of more and more PINK1/Parkin-independent regulators of mitophagy, further questioned the role of these two proteins as key mitophagy players. Most of the discoveries related to PINK1/Parkin-mitophagy arose from immortalised cultured cells often exposed to mitochondrial toxins, such as CCCP. Therefore, understanding how these models translate to more physiological conditions and neurons remained a key challenge. Cancer cells mainly rely on glycolysis for energy production, and therefore are less dependent on mitochondria than other cell types (King & Plun-Favreau, 2017). Conversely, neurons generate 95% of their ATP through OXPHOS, thus it is unlikely that these cells would switch their ATP production from OXPHOS to glycolysis (Erecinska et al., 1994). In fact, forcing cancer cells to use OXPHOS has been shown to inhibit PINK1/Parkin-mediated mitophagy following membrane depolarisation (MacVicar & Lane, 2014; Van Laar et

al., 2011). Therefore, as cancer cells are likely to have a different metabolic background than neurons, caution should be taken when interpretating these results. For a long time, studies using fibroblasts, neuroblastoma cell lines or stem cell-derived neurons and relying on endogenous Parkin, were not able to provide evidence for mitophagy, even with the use of pharmacological agents (Rakovic et al., 2013). Furthermore, although depolarising agents can be efficient in triggering Parkin translocation and subsequent mitophagy in cancer cells, primary neurons require much higher CCCP concentration and longer incubation times, further questioning how these models/conditions translate to mitophagy in neurons *in vivo* (Imaizumi et al., 2012; Rakovic et al., 2013; Van Laar et al., 2011). The difficulty to obtain evidence of PINK1/Parkin mitophagy in neurons is likely due to their low reliance on glycolysis (Rakovic et al., 2013; Sterky et al., 2011; Van Laar et al., 2011). In fact, studies on cultured neurons and mouse brains revealed that Parkin translocation to the mitochondria is rather difficult to observe and if so, not as commonly seen as in other cell lines and at slower rates following CCCP treatment. In addition, Parkin overexpression is often required to see mitophagy events (Cai et al., 2012; Ge et al., 2020; Pickrell et al., 2015; Sung et al., 2016; Van Laar et al., 2011). Therefore, there has been a need for *in vivo* models that would allow to monitor mitophagy and assess the relevance of PINK1/Parkin *in vivo*. While every model has advantages and limitations, animals offer the organismal context that is fundamentally missing in cultured cell or tissue cultured models. With the generation of mice or flies expressing different types of mitophagy reporters, the field has been rapidly moving towards more physiologically relevant *in vivo* models.

My findings suggest that mitophagy is a widespread phenomenon and contrasting with cultured cells, the use of external stimuli or depolarisation agents is not necessary to appreciate mitophagy *in vivo* in *Drosophila*. Similar observations were obtained in other *Drosophila* and mouse studies. (Cornelissen et al., 2018; McWilliams et al., 2018b; Sun et al., 2015). Additionally, I found that mitophagy rates were highly heterogeneous, further illustrating that distinct tissues may encounter variable levels of mitochondrial damage, which is reflected by different rates of mitophagy. Indeed, my data show that even though mitophagy is widespread, almost no mitophagy could be observed in adult flight muscles. Conversely, DA neurons and other neuronal cell types display high levels of mitophagy (Cornelissen et al., 2018). My results also suggest that Pink1 and

Parkin are not implicated in basal mitophagy in *Drosophila*. The fact that similar results were obtained in *Pink1*/*Prkn* mouse models suggest that an analogous scenario may also occur in humans (McWilliams et al., 2018a, 2018b). Indeed, patients carrying *PINK1* or *PRKN* mutations only start exhibiting locomotor symptoms in the third or fourth decade of their life, therefore it is likely that if *PINK1*/*PRKN* mutations were to completely block mitophagy, PD patients would display more severe phenotypes and earlier in their life. Finally, my results surprisingly show that no change in the mitophagy levels were observed in the adult IFMs of *Pink1* and *parkin* mutants. This remains a puzzling finding, especially since this tissue is highly disrupted in *Pink1*/*parkin* mutants. There are two potential explanations here. First, it is possible that the mitochondrial defects observed in the flight muscles are related to other functions of Pink1 and parkin, that do not involve mitophagy. Second, IFMs may rely on a turnover mechanism independent of Pink1/parkin, such as MDVs, which may not be detectable with the mito-QC or captured by our imaging technique. One could argue that these low levels of mitochondrial turnover are particularly important and slight changes may result in catastrophic outcomes, as seen by the *Pink1*/*parkin* mutants muscle degeneration. It is worth noting that I only qualitatively assessed mitophagy in IFMs in the absence of *Pink1/parkin*. Depending on the stimulus, MDVs have been shown to form without the requirement of PINK1/Parkin. To address this, further investigation of this particular tissue needs to be done.

These discrepancies between *in vitro* and *in vivo* observations have further fuelled the existing debate. However, the PD-phenotypes observed by combining *Pink1*/*Prkn* null mice with various stressors, such as the mtDNA mutator or bacterial infections support the idea that PINK1/Parkin may regulate evoked rather than basal mitophagy.

6.2. Potential triggers of PINK1/Parkin-mediated mitophagy

My data and work from others suggest that PINK1/Parkin do not play a role in basal mitophagy (McWilliams et al., 2018a, 2018b). While mitochondrial depolarisation has been heavily used for *in vitro* work and was thought to be the main trigger of PINK1/Parkin mitophagy, such drastic depolarisation events are unlikely to occur *in vivo*.

Aged individuals have been shown to harbour mtDNA deletions and as the onset of PD correlates with age, efforts have been put to understand the relevance of accumulation of mtDNA defects (Bender et al., 2006). In addition, PD patients also accumulate mtDNA deletions in neurons of the substantia nigra (Bender et al., 2006). It was proposed that PINK1/Parkin mitophagy may be a way to specifically degrade mitochondria with high levels of mtDNA defects such as mutations. To address the relevance of this *in vivo*, *Pink1* or *Prkn* null mice were combined with the mutator strain (Pickrell et al., 2015). Mass spectrometry analysis of the cortical brain tissues of the mutator mice revealed significantly higher levels of pSer65-Ub, reinforcing that PINK1/Parkin mitophagy may be responsible for the degradation of these dysfunctional mitochondria (Pickrell et al., 2015). While *Prkn* null mice do not develop PD-like phenotypes, *Prkn*$^{-/-}$ mice crossed with the mutator strain exhibit locomotor deficits and DA neuronal loss, that replicate the PD pathology (Pickrell et al., 2015). However, the mtDNA frequency was not increased in mutator:*Prkn*$^{-/-}$ mice suggesting that the absence of *Prkn* does not affect the removal of mitochondria carrying mtDNA mutations (Pickrell et al., 2015). MDVs could explain the finding that loss of *Prkn* modifies the mutator mouse phenotype without affecting mtDNA mutation frequency. Contradictory results were obtained by Suen et al., where Parkin overexpression was shown to eliminate mitochondria bearing COX I mutations in order to restore a pool of healthy mitochondria enriched in WT mtDNA (Suen et al., 2010). Thus, whether or not PINK1/Parkin play a role in the removal of mitochondria carrying mutated mtDNA is still an outstanding question. My data suggest that accumulation of mtDNA mutations, using the mito-APOBEC1 mutator, does not increase mitophagy levels in adult CNS and IFMs of young and aged animals. Because Pink1 or parkin overexpression in

combination with mito-APOBEC1 leads to increased mitophagy in larval CNS, it is tempting to speculate that this may be driven by Pink1/parkin. The adult lethality that arises from the combination of Pink1 overexpression and mito-APOBEC1 may be due to excessive levels of mitophagy induced by Pink1 overexpression. Thus, it may be useful to investigate how this correlates with mtDNA copy number. However, why only Pink1 overexpression, and not parkin, is lethal with the mito-APOBEC remains unclear. It would be interesting to combine *Pink1* or *parkin* mutants with mito-APOBEC1 and the mito-QC reporter to see if this results in a reduction of the mitophagy signal. Though this relationship between mtDNA mutations and PINK1/Parkin mitophagy is exciting, it is worth noting that the mutator model mainly results in the accumulation of point mutations, whereas PD patients predominantly harbour mtDNA deletions (Bender et al., 2006). Therefore, it remains unsure if the potential role of PINK1/Parkin in the elimination of mitochondria carrying point-mutated mtDNA translates to PD patients, mainly bearing mtDNA deletions.

Aging is often associated with an increase in mitochondrial damage which has led to the suggestion that aging may correlate with elevated levels of mitophagy (Balaban et al., 2005; López-Otín et al., 2013). Furthermore, increased levels of PINK1 expression have been reported with aging in mouse cortex and striatum (Barodia et al., 2019). My results validate this hypothesis and demonstrate that in some neuronal populations and IFMs, but not in DA neurons, mitophagy rates were significantly increased with age, suggesting that aging may potentially trigger mitophagy. However, my data also suggest that this turnover is not Pink1/parkin-dependent, as the absence of *Pink1* or *parkin* did not affect the mitophagy levels, at least in adult CNS. Some studies, using the mt-Keima fly and mouse models, have reported opposite findings thus raising concerns about the discrepancies observed between studies relying on different reporters (Cornelissen et al., 2018; Sun et al., 2015). Therefore, whether or not mitophagy is an age-related process remains a grey area that requires further investigation.

Unfolded mitochondrial matrix proteins has been shown to trigger PINK1/Parkin-dependent mitophagy in the absence of a reduction in the membrane potential (Burman et al., 2017; Jin & Youle, 2013; Pimenta De Castro et al., 2012). This suggests that there may be some crosstalk between the mtUPR and the PINK1/Parkin

mitophagy pathway. However, the mechanism underlying the decision of whether to repair or degrade the mitochondria bearing unfolded proteins remains to be determined. Interestingly, loss of PINK1 combined with the DA neuron specific expression of mitochondrial unfolded ornithine transcarbamylase (ΔOTC), a model that induces the accumulation of unfolded proteins in the mitochondrial matrix, results in a parkinsonian phenotype that can be reversed with L-dopa (Moisoi et al., 2014). This suggests that PINK1/Parkin may be involved in the selective removal of mitochondria bearing unfolded proteins. It could be interesting to combine the mito-QC flies with the mitochondrial stressor ΔOTC in a *Pink1* or *parkin* mutant background to see if it results in a decrease in the mitophagy levels.

Different energy metabolism backgrounds that are cell-specific, also seem to influence the mitophagy levels. For instance, myocytes lacking *PINK1* have a higher membrane potential than neurons lacking *PINK1*, and this correlates with a decrease in the mitochondrial respiration (Yao et al., 2011). However, while both cell types are able to shift to a glycolytic activity, myocytes are able to produce much more ATP than neurons, demonstrating that myocytes can compensate for their respiratory deficiency while neurons cannot (Yao et al., 2011). As mitophagy seems to be induced at a lower level when triggered in oxidative conditions, one could wonder how mitochondrial ATP production impacts on the control of mitophagy. In addition to being a source of energy, ATP exerts several functions in the cell. For instance, ATP has been shown to play a role in mitochondrial protein import (Van Der Laan et al., 2010). Thus, depletion of ATP after CCCP treatment could have several consequences that are not directly related to mitophagy; for instance, it could indirectly impede PINK1 import or degradation. Therefore, the metabolic environment in which PINK1/Parkin-mediated mitophagy is investigated may be essential to uncover the physiological relevance of this pathway. As it is likely that neurons undergo low levels of mitophagy, and due to their high dependence on the OXPHOS, neurons may be less prone to lose their mitochondria, compare to immortalised cells that mainly rely on glycolysis. Thus, in order to preserve their mitochondrial integrity as much as possible, neurons are more likely to rely on less drastic MQC such as MDVs.

Finally, using the mt-Keima, Sun et al., observed increased levels of mitophagy in mice exposed to prolonged hypoxia (Sun et al., 2015). They also reported reduced

mitophagy in mice subjected to high fat diet. Kim et al., observed increased mitophagy upon hypoxia treatment in larval wing discs, which was abolished in flies lacking *parkin* or *Pink1* (Kim et al., 2019). Similar to hypoxia exposure, rotenone treatment led to a significant increase in mitophagy signal, which was abrogated by knockdown of either *Pink1* or *parkin*. This study further illustrates the role of PINK1/Parkin pathway in mitophagy in response to mitochondrial stresses (Kim et al., 2019).

6.3. Beyond mitophagy

While mitophagy may be well suited for extensive damage, MDVs are emerging as an alternative mechanism to preserve healthy regions of the mitochondrion from elimination when the damage is restricted to local domains. MDVs are becoming more and more characterised, but the underlying mechanism has not been fully elucidated yet. PINK1/Parkin-MDVs have been shown to carry vesicles enriched with oxidised proteins thus suggesting that PINK1/Parkin regulate the formation of MDVs following oxidative or mutagenic stress (McLelland et al., 2014). This illustrates a cargo selectivity but also reinforces the idea that depending on the nature of the insult, different pathways can be activated. It is still likely that MDVs occur prior to mitophagy and in response to milder stresses. *Drosophila* work from Vincow et al., revealed that the half-lives of several ETC components, were increased in *Pink1* and *parkin* mutant flies which suggests that damaged ETC components may be selectively turned over by Pink1/parkin and this could occur through the generation of MDVs (Vincow et al., 2013). Finally, proteomic analysis in *Drosophila* identified Vps35 as a parkin substrate and genetic interaction between *vps35* and *parkin* has been reported in *Drosophila*, providing further evidence for the existence of a common pathway (Malik et al., 2015; Martinez et al., 2017). It is tempting to speculate that MDVs could occur at specific domains in the mitochondria. Mitochondrial shape and topology have been implicated as a driving force for mitophagy during starvation events (Kolitsida et al., 2019; Zhou et al., 2020). Moreover, mitochondrial matrix proteins were shown to exhibit different mitophagy rates depending on their segregation and phosphorylation status within the mitochondrion, suggesting that segregation of intramitochondrial proteins at specific subdomains may dictate the location of MDV formation (Kolitsida et al., 2019; Zhou et al., 2020). In addition, while *in vivo* work suggests that PINK1/Parkin are not involved in basal mitophagy, MDVs have been shown to occur in basal conditions in the cardiac system (Cadete et al., 2016; McLelland et al., 2014; Soubannier al., 2012a). In addition to their role in the generation of MDVs, PINK1/Parkin have been implicated in the suppression of MitAP (Matheoud et al., 2016). MitAP induces the presentation of mitochondrial antigens to MHC class I molecules on macrophages which results in the induction of autoimmune responses (Matheoud et al., 2016). PINK1/Parkin actively inhibit the recruitment of Snx9, which is required for MDV formation and MitAP (Matheoud et al., 2016). This work supports a new function of PINK1/Parkin as

repressors of the immune system.

There is some evidence that PINK1/Parkin also play a role in mitochondrial biogenesis. Mitochondrial biogenesis is governed by the peroxisome proliferator-activated receptor gamma co-activator 1 alpha (PGC-1α), a transcription factor that controls the expression of genes encoding mitochondrial proteins (Lee et al., 2017). PINK1 was reported to regulate the degradation of Parkin interacting substrate protein (PARIS), a negative regulator of PGC-1α at the transcription level (Lee et al., 2017; Shin et al., 2011; Stevens et al., 2015). Indeed, PINK1 has been shown to directly phosphorylate PARIS, thus priming the protein for Parkin ubiquitination and subsequent degradation (Lee et al., 2017). In addition, Parkin overexpression was shown to increase PGC-1α levels, mtDNA copy number and mitochondria population in cortical neurons (Zheng et al., 2017). Interestingly, mice lacking *Pink1* exhibit accumulation of PARIS which correlated with PGC-1α repression and selective degeneration of DA neurons and this was rescued by PGC-1α overexpression (Lee et al., 2017; Shin et al., 2011; Siddiqui et al., 2016). Thus, altogether these studies suggest that PINK1/Parkin are involved in the regulation of mitochondrial biogenesis and can modulate PGC-1α levels by controlling PARIS degradation, through Parkin ubiquitination. Interestingly, elevated PARIS and low PGC-1α levels were reported in the substantia nigra of PD patients with autosomal recessive and sporadic PD (Shin et al., 2011; Zheng et al., 2010).

6.4. Inflammation and PD

While a huge amount of work has been put towards the understanding of mitochondrial dysfunction in PD, clear evidence also suggests a role of inflammation in both genetic and sporadic PD. The recent implication of the cGAS/STING pathway in PD pathogenesis further reinforced the inflammatory aspect of the disease. However, several grey areas remain. First, my work suggests that a similar mechanism is not occurring in *Drosophila Pink1*/*parkin* mutants, which so far, have been better models than mice in terms of replicating the human PD pathology. While Sting performs similar functions in flies as in vertebrates, the cGAS/Sting signalling cascade is not fully conserved in *Drosophila*, which may explain the discrepancies obtained. *Drosophila* present many advantages for studying the immune system, however, it seems that for this particular aspect of inflammation, *Drosophila* are evolutionary too distant from vertebrates, which probably limited the reproducibility of the mouse findings. Sliter et al., showed that exhaustive exercise or mtDNA mutations are sufficient to induce mitophagy, but this can result in the release of mtDNA in the absence of PINK1/Parkin leading to the subsequent activation of the cGAS/STING signalling cascade and downstream inflammatory phenotypes (Sliter et al., 2018). However, the mechanism underlying the release of mtDNA when mitophagy is ineffective remains unclear. Could the mutated mtDNA be released from the mitochondria by MDVs? This could be a possibility as MDVs have been shown to carry damaged (oxidised) mitochondrial content, however, how mtDNA is released in the cytosol remains to be determined. Oxidised mtDNA has been shown to activate the NLRP3 inflammasome, suggesting that this released mtDNA can act as an inflammatory agonist (Zhong et al., 2018). While these findings are exciting, they also raise questions about how the STING-dependent inflammation triggers the DA neuronal death. Does the cGAS/STING-mediated inflammation induce microglia activation? Further work is needed in order to understand how this correlates with the neuronal death occurring in the brain. Finally, the requirement for mitochondrial stresses in addition to loss of *Pink1*/*Prkn* also raises the question on how this translates to sporadic PD.

Several studies have highlighted the potential link between the gut microbiota, inflammation and PD. However, little is known about the relationship and the mechanisms underlying this complex triad, especially in genetic animal models of PD.

Matheoud et al., reported that in the absence of *Pink1*, intestinal infections results in mitAP which generates an autoimmune response, that could cause the loss of DA neurons observed in these mice (Matheoud et al., 2019). This is consistent with the findings that peripheral infections, such as urinary tract, transiently worsen the motor symptoms in PD patients (Herrick & Tansey, 2019; Yeo et al., 2012). Matheoud et al., found that the motor deficits in these mice disappeared one year after infection, without any treatment, suggesting a transient characteristic of these symptoms (Matheoud et al., 2019). However, the authors did not investigate whether or not these mice also exhibit non-motor symptoms, such as changes in the gut microbiota, which would provide a direct implication of the digestive system in the PD pathology. While this study provides some insights on the link between inflammation and PD pathology, it also leaves some unanswered questions. First, it remains to be determined if the repeated exposure to various pathogens leads to irreversible locomotor deficits and DA neuronal loss in *Pink1*$^{-/-}$ mice, in order to draw a parallel with human PD. Second, it would be interesting to know if the upregulation of MHC class I molecules is a conserved mechanism of PD pathology, can this be also observed in sporadic PD or other genetic forms of PD? This potential immune dysfunction should be analysed in aged WT mice that do not carry any PD mutations, in order to shed light on the relevance of the Matheoud et al. findings beyond *Pink1* loss. Third, Matheoud et al., only studied *Pink1*$^{-/-}$ mice, so the study raises the question, can these observations also be appreciable in *Prkn* null mice? Systemic LPS injections in mice lacking *Prkn* were investigated some years ago by Frank-Cannon et al. and led to PD-like phenotypes, including locomotor deficits and DA neuronal loss (Frank-Cannon et al., 2008). However, the authors did not assess the involvement of immune responses, nor changes in the gut microbiome. Lastly, while Sliter et al. and Matheoud et al. findings both involve the immune system as a key driver of PD pathology, their work point towards the activation of different immune responses. Indeed, the cGAS/STING pathway is involved in innate immunity while the CD8+ T cell response belongs to the adaptive system. The activation of the immune system in PD is likely to be a combination of both innate and adaptive immune responses, however, it will be necessary to understand how these events may interact with each other and what role they may play in the PD pathology, especially since some immune responses are likely to be protective.

In addition to the implication of the gut microbiota in the PD pathology, Matheoud et al.'s work, also illustrates the involvement of the glial cells in the inflammatory aspect of the disease (Matheoud et al., 2019). Interestingly, recent work from Barodia et al., indicates that PINK1-dependent phosphorylation of Ub predominantly occurs in astrocytes, further highlighting the potential contribution of glial cells in PD pathogenesis (Barodia et al., 2019).

Finally, why *Pink1*/*parkin* mutant flies develop robust phenotypes when mice do not, still remains a key unanswered question. Matheoud et al. study raises the possibility that the environmental conditions in which flies and mice are kept for research purposes may provide an explanation. Additionally, analysing and comparing the microbiome of WT and *Pink1*/*parkin* mutants would shed light on potential difference in microbial communities of these mutants.

6.5. Relevance of genetic models of PD to sporadic PD

More effort has been put towards understanding the implication of PINK1/Parkin in the mitophagy process and how this may impact PD pathogenesis, however these genetic cases only account for a small fraction of the PD cases. The majority of PD cases are sporadic with no clear genetic etiologic. In addition, sporadic PD is believed to arise from a mixture of genetics and environmental stresses that is quite unique to individual patients making it difficult to narrow down the exact causes of the disease.

Though mitochondrial dysfunction is a clear hallmark of genetic and sporadic PD, these are not necessarily due to PINK1/Parkin or defects in MQC. Therefore, to what extend impairments in MQC processes, such as mitophagy, can have an impact on sporadic cases remains a key question to answer. Several studies have tried to address this outstanding question. Higher levels of several Parkin substrates were reported in patients of sporadic PD, suggesting that Parkin may exhibit some levels of inactivation (Fukae et al., 2009; Ge et al., 2020; Ko et al., 2005, 2010; Kurup et al., 2015; Shin et al., 2011). Additionally, Parkin has been reported to localise in LBs and to be sequestered in α-synuclein aggregates (Kawahara et al., 2008). This was shown to prevent its primary function, which is consistent with its inability to ubiquitinate its normal substrates (Fukae et al., 2009; Ge et al., 2020; Ko et al., 2005, 2010; Kurup et al., 2015). This was reinforced by elevated levels of S-nitrosylated-Parkin in LBs of brain patients with PD, resulting in the incapacity of Parkin to perform its ligase activity and the subsequent ubiquitination of its substrates (Chung et al., 2004; Lonskaya et al., 2013; Schlossmacher et al., 2002). Furthermore, PINK1 was found in 5-10% of LBs and higher PINK1 levels were reported in PD patients (Gandhi et al., 2006). Accumulation of processed forms of PINK1 were found increased in PD brains, which may suggest that the protein is not able to perform its normal function but also fails to be degraded properly (Muqit et al., 2006). While there is some evidence of PINK1/Parkin implication in sporadic PD, to what degree this contributes to the neurodegeneration observed in these patients remains unknown. Recently, Chung et al., developed a potential new therapy based on a cell-permeable Parkin protein (iCP-Parkin), which increases the solubility and intracellular delivery of Parkin (Chung et al.,

2020). Intravenous injection of iCP-Parkin was shown to cross the blood brain barrier in order to reach the neurons of the substantia nigra (Chung et al., 2020). This novel protein-based therapy was tested in 6-OHDA and α-synuclein mouse and rat models of PD. iCP-Parkin injections were able to fully rescue the locomotor deficits, DA neuronal loss and aggregation of α-synuclein (Chung et al., 2020). Interestingly, the authors showed that iCP-Parkin was able to autoactivate even in the absence of PINK1. Finally, mitophagy was increased in cultured cells treated with iCP-Parkin and exposed to CCCP, suggesting that the effect of iCP-Parkin on PD phenotypes of these mice may be due to the mitophagic role of PINK1/Parkin (Chung et al., 2020).

References

Abbas, N., Lücking, C. B., Ricard, S., Dürr, A., Bonifati, V., De Michele, G., Bouley, S., Vaughan, J. R., Gasser, T., Marconi, R., Broussolle, E., Brefel-Courbon, C., Harhangi, B. S., Oostra, B. A., Fabrizio, E., Böhme, G. A., Pradier, L., Wood, N. W., Filla, A., … Brice, A. (1999). A wide variety of mutations in the *parkin* gene are responsible for autosomal recessive parkinsonism in Europe. *Human Molecular Genetics*, *8*(4), 567–574.

Adachi-Yamada, T., Nakamura, M., Irie, K., Tomoyasu, Y., Sano, Y., Mori, E., Goto, S., Ueno, N., Nishida, Y., & Matsumoto, K. (1999). p38 Mitogen-Activated Protein Kinase Can Be Involved in Transforming Growth Factor β Superfamily Signal Transduction in *Drosophila* Wing Morphogenesis. *Molecular and Cellular Biology*, *19*(3), 2322–2329.

Agaisse, H., & Perrimon, N. (2004). The roles of JAK/STAT signaling in *Drosophila* immune responses. *Immunological Reviews*, *198*, 72–82.

Agaisse, H., Petersen, U. M., Boutros, M., Mathey-Prevot, B., & Perrimon, N. (2003). Signaling role of hemocytes in *Drosophila* JAK/STAT-dependent response to septic injury. *Developmental Cell*, *5*(3), 441–450.

Akundi, R. S., Huang, Z., Eason, J., Pandya, J. D., Zhi, L., Cass, W. A., Sullivan, P. G., & Büeler, H. (2011). Increased Mitochondrial Calcium Sensitivity and Abnormal Expression of Innate Immunity Genes Precede Dopaminergic Defects in *Pink1*-Deficient Mice. *PLoS ONE*, *6*(1), e16038.

Aldridge, J. E., Horibe, T., & Hoogenraad, N. J. (2007). Discovery of Genes Activated by the Mitochondrial Unfolded Protein Response (mtUPR) and Cognate Promoter Elements. *PLoS ONE*, *2*(9), e874.

Allen, G. F. G., Toth, R., James, J., & Ganley, I. G. (2013). Loss of iron triggers PINK1/Parkin-independent mitophagy. *EMBO Reports*, *14*(12), 1127–1135.

Altmann, R. (1890). Die Elementarorganismen Und Ihre Beziehungen Zu Den Zellen. *Leipzig: Veit & Comp.*, *145*.

Anand, R., Langer, T., & Baker, M. J. (2013). Proteolytic control of mitochondrial function and morphogenesis. *Biochimica et Biophysica Acta*, *1833*(1), 195–204.

Andreazza, S., Samstag, C. L., Sanchez-Martinez, A., Fernandez-Vizarra, E., Gomez-Duran, A., Lee, J. J., Tufi, R., Hipp, M. J., Schmidt, E. K., Nicholls, T. J., Gammage, P. A., Chinnery, P. F., Minczuk, M., Pallanck, L. J., Kennedy, S. R., & Whitworth, A. J. (2019). Mitochondrially-targeted APOBEC1 is a potent mtDNA

mutator affecting mitochondrial function and organismal fitness in *Drosophila*. *Nature Communications*, *10*(1), 1–14

Andrews, R. M., Kubacka, I., Chinnery, P. F., Lightowlers, R. N., Turnbull, D. M., & Howell, N. (1999). Reanalysis and revision of the Cambridge reference sequence for human mitochondrial DNA. *Nature Genetics*, *23*(2), 147.

Anthoney, N., Foldi, I., & Hidalgo, A. (2018). Toll and toll-like receptor signalling in development. *Development (Cambridge)*, *145*(9).

Appel-Cresswell, S., Vilarino-Guell, C., Encarnacion, M., Sherman, H., Yu, I., Shah, B., Weir, D., Thompson, C., Szu-Tu, C., Trinh, J., Aasly, J. O., Rajput, A., Rajput, A. H., Jon Stoessl, A., & Farrer, M. J. (2013). Alpha-synuclein p.H50Q, a novel pathogenic mutation for Parkinson's disease. *Movement Disorders*, *28*(6), 811–813.

Arbouzova, N. I., & Zeidler, M. P. (2006). JAK/STAT signalling in *Drosophila*: Insights into conserved regulatory and cellular functions. *Development*, *133*(14), 2605–2616.

Area-Gomez, E., Guardia-Laguarta, C., Schon, E. A., & Przedborski, S. (2019). Mitochondria, OxPhos, and neurodegeneration: cells are not just running out of gas. *Journal of Clinical Investigation, 129*(1), 34–45.

Arimoto, T., & Bing, G. (2003). Up-regulation of inducible nitric oxide synthase in the substantia nigra by lipopolysaccharide causes microglial activation and neurodegeneration. *Neurobiology of Disease*, *12*(1), 35–45.

Aryal, B., & Lee, Y. (2019). Disease model organism for Parkinson disease: *Drosophila melanogaster*. *BMB Reports, 52*(4), 250–258.

Ashrafi, G., & Schwarz, T. L. (2013). The pathways of mitophagy for quality control and clearance of mitochondria. In *Cell Death and Differentiation*, *20*(1), 31–42.

Atorino, L., Silvestri, L., Koppen, M., Cassina, L., Ballabio, A., Marconi, R., Langer, T., & Casari, G. (2003). Loss of m-AAA protease in mitochondria causes complex I deficiency and increased sensitivity to oxidative stress in hereditary spastic paraplegia. *Journal of Cell Biology*, *163*(4), 777–787.

Attardi, G., & Schatz, G. (1988). Biogenesis of mitochondria. *Annual Review of Cell Biology, 4*(1), 289–333.

Bach, E. A., Ekas, L. A., Ayala-Camargo, A., Flaherty, M. S., Lee, H., Perrimon, N., & Baeg, G. H. (2007). GFP reporters detect the activation of the *Drosophila* JAK/STAT pathway *in vivo*. *Gene Expression Patterns*, *7*(3), 323–331.

Bach, E. A., & Perrimon, N. (2003). Prime Time for the *Drosophila* JAK/STAT Pathway. *Signal Transducers and Activators of Transcription (STATs)*, 87–104.

Bader, M., Benjamin, S., Wapinski, O. L., Smith, D. M., Goldberg, A. L., & Steller, H. (2011). A conserved F box regulatory complex controls proteasome activity in *Drosophila*. *Cell*, *145*(3), 371–382.

Baeg, G.-H., Zhou, R., & Perrimon, N. (2005). Genome-wide RNAi analysis of JAK/STAT signaling components in *Drosophila*, *19*(16), 1861–1870.

Balaban, R. S., Nemoto, S., & Finkel, T. (2005). Mitochondria, Oxidants, and Aging. *Cell*, *120*(4), 483–495.

Ban, T., Ishihara, T., Kohno, H., Saita, S., Ichimura, A., Maenaka, K., Oka, T., Mihara, K., & Ishihara, N. (2017). Molecular basis of selective mitochondrial fusion by heterotypic action between OPA1 and cardiolipin. *Nature Cell Biology*, *19*(7), 856–863.

Barbot, M., & Meinecke, M. (2016). Reconstitutions of mitochondrial inner membrane remodeling. *Journal of Structural Biology*, *196*(1), 20–28.

Barcia, C., De Pablos, V., Bautista-Hernández, V., Sánchez-Bahillo, Á., Bernal, I., Fernández-Villalba, E., Martín, J., Bañón, R., Fernández-Barreiro, A., & Herrero, M. T. (2005). Increased plasma levels of TNF-α but not of IL1-β in MPTP-treated monkeys one year after the MPTP administration. *Parkinsonism and Related Disorders*, *11*(7), 435–439.

Barodia, S. K., McMeekin, L. J., Creed, R. B., Quinones, E. K., Cowell, R. M., & Goldberg, M. S. (2019). PINK1 phosphorylates ubiquitin predominantly in astrocytes. *Npj Parkinson's Disease*, *5*(1), 29.

Baughman, J. M., Perocchi, F., Girgis, H. S., Plovanich, M., Belcher-Timme, C. A., Sancak, Y., Bao, X. R., Strittmatter, L., Goldberger, O., Bogorad, R. L., Koteliansky, V., & Mootha, V. K. (2011). Integrative genomics identifies MCU as an essential component of the mitochondrial calcium uniporter. *Nature*, *476*(7360), 341–345.

Bayrhuber, M., Meins, T., Habeck, M., Becker, S., Giller, K., Villinger, S., Vonrhein, C., Griesinger, C., Zweckstetter, M., & Zeth, K. (2008). Structure of the human voltage-dependent anion channel. *Proceedings of the National Academy of Sciences of the United States of America*, *105*(40), 15370–15375.

Beebe, K., Lee, W. C., & Micchelli, C. A. (2010). JAK/STAT signaling coordinates stem cell proliferation and multilineage differentiation in the *Drosophila* intestinal stem cell lineage. *Developmental Biology*, *338*(1), 28–37.

Beilina, A., Van Der Brug, M., Ahmad, R., Kesavapany, S., Miller, D. W., Petsko, G. A., & Cookson, M. R. (2005). Mutations in PTEN-induced putative kinase 1 associated with recessive parkinsonism have differential effects on protein stability. *Proceedings of the National Academy of Sciences of the United States of America*, *102*(16), 5703–5708

Bender, A., Krishnan, K. J., Morris, C. M., Taylor, G. A., Reeve, A. K., Perry, R. H., Jaros, E., Hersheson, J. S., Betts, J., Klopstock, T., Taylor, R. W., & Turnbull, D. M. (2006). High levels of mitochondrial DNA deletions in substantia nigra neurons in aging and Parkinson disease. *Nature Genetics*, *38*(5), 515–517.

Bernstein, S. H., Venkatesh, S., Li, M., Lee, J., Lu, B., Hilchey, S. P., Morse, K. M., Metcalfe, H. M., Skalska, J., Andreeff, M., Brookes, P. S., & Suzuki, C. K. (2012). The mitochondrial ATP-dependent Lon protease: A novel target in lymphoma death mediated by the synthetic triterpenoid CDDO and its derivatives. *Blood*, *119*(14), 3321–3329.

Betarbet, R., Sherer, T. B., MacKenzie, G., Garcia-Osuna, M., Panov, A. V., & Greenamyre, J. T. (2000). Chronic systemic pesticide exposure reproduces features of Parkinson's disease. *Nature Neuroscience*, *3*(12), 1301–1306.

Betz, A., Lampen, N., Martinek, S., Young, M. W., & Darnell, J. E. (2001). A *Drosophila PIAS* homologue negatively regulates *stat92E*. *Proceedings of the National Academy of Sciences of the United States of America*, *98*(17), 9563–9568.

Bezard, E., Gross, C. E., Fournier, M. C., Dovero, S., Bloch, B., & Jaber, M. (1999). Absence of MPTP-induced neuronal death in mice lacking the dopamine transporter. *Experimental Neurology*, *155*(2), 268–273.

Binari, R., & Perrimon, N. (1994). Stripe-specific regulation of pair-rule genes by *hopscotch*, a putative Jak family tyrosine kinase in *Drosophila*. *Genes and Development*, *8*(3), 300–312.

Bindoff, L. A., Birch-Machin, M., Cartlidge, N. E. F., Parker, W. D., & Turnbull, D. M. (1989). Mitochondrial function in Parkinson's disease. *The Lancet*, *334*(8653), 49.

Bingol, B., Tea, J. S., Phu, L., Reichelt, M., Bakalarski, C. E., Song, Q., Foreman, O., Kirkpatrick, D. S., & Sheng, M. (2014). The mitochondrial deubiquitinase USP30 opposes parkin-mediated mitophagy. *Nature*, *509*(7505), 370–375.

Biteau, Benoit, Karpac, J., Hwangbo, D. S., & Jasper, H. (2011). Regulation of *Drosophila* lifespan by JNK signaling. *Experimental Gerontology*, *46*(5), 349–354.

Biteau, Benoît, Karpac, J., Supoyo, S., DeGennaro, M., Lehmann, R., & Jasper, H. (2010). Lifespan extension by preserving proliferative homeostasis in *Drosophila*. *PLoS Genetics*, *6*(10), 1–15.

Blauwendraat, C., Nalls, M. A., & Singleton, A. B. (2020). The genetic architecture of Parkinson's disease. *The Lancet Neurology*, *19*(2), 170–178.

Blesa, J., Phani, S., Jackson-Lewis, V., & Przedborski, S. (2012). Classic and new animal models of Parkinson's disease. *Journal of Biomedicine and Biotechnology*, *18*, 183–185.

Blum, D., Torch, S., Lambeng, N., Nissou, M. F., Benabid, A. L., Sadoul, R., & Verna, J. M. (2001). Molecular pathways involved in the neurotoxicity of 6-OHDA, dopamine and MPTP: Contribution to the apoptotic theory in Parkinson's disease. In *Progress in Neurobiology*, *65*(2), 135–172.

Bodner, C. R., Dobson, C. M., & Bax, A. (2009). Multiple Tight Phospholipid-Binding Modes of α-Synuclein Revealed by Solution NMR Spectroscopy. *Journal of Molecular Biology*, *390*(4), 775–790.

Boman, H. G., Nilsson, I., & Rasmuson, B. (1972). Inducible antibacterial defence system in *Drosophila*. *Nature*, *237*(5352), 232–235.

Bonifati, V., Rizzu, P., Van Baren, M. J., Schaap, O., Breedveld, G. J., Krieger, E., Dekker, M. C. J., Squitieri, F., Ibanez, P., Joosse, M., Van Dongen, J. W., Vanacore, N., Van Swieten, J. C., Brice, A., Meco, G., Van Duijn, C. M., Oostra, B. A., & Heutink, P. (2003). Mutations in the *DJ-1* gene associated with autosomal recessive early-onset parkinsonism. *Science*, *299*(5604), 256–259.

Bota, D. A., & Davies, K. J. A. (2002). Lon protease preferentially degrades oxidized mitochondrial aconitase by an ATP-stimulated mechanism. *Nature Cell Biology*,

4(9), 674–680.

Bourke, L. T., Knight, R. A., Latchman, D. S., Stephanou, A., & McCormick, J. (2013). Signal transducer and activator of transcription-1 localizes to the mitochondria and modulates mitophagy. *Jak-Stat*, *2*(4), e25666.

Braak, H., De Vos, R. A. I., Bohl, J., & Del Tredici, K. (2006). Gastric α-synuclein immunoreactive inclusions in Meissner's and Auerbach's plexuses in cases staged for Parkinson's disease-related brain pathology. *Neuroscience Letters*, *396*(1), 67–72.

Braak, H., Del Tredici, K., Rüb, U., De Vos, R. A. I., Jansen Steur, E. N. H., & Braak, E. (2003). Staging of brain pathology related to sporadic Parkinson's disease. *Neurobiology of Aging*, *24*(2), 197–211.

Braak, H., Sandmann-Keil, D., Gai, W., & Braak, E. (1999). Extensive axonal Lewy neurites in Parkinson's disease: A novel pathological feature revealed by α-synuclein immunocytochemistry. *Neuroscience Letters*, *265*(1), 67–69.

Branchi, I., D'Andrea, I., Armida, M., Cassano, T., Pèzzola, A., Potenza, R. L., Morgese, M. G., Popoli, P., & Alleva, E. (2008). Nonmotor symptoms in Parkinson's disease: Investigating early-phase onset of behavioral dysfunction in the 6-hydroxydopamine-lesioned rat model. *Journal of Neuroscience Research*, *86*(9), 2050–2061.

Braschi, E., Goyon, V., Zunino, R., Mohanty, A., Xu, L., & McBride, H. M. (2010). Vps35 mediates vesicle transport between the mitochondria and peroxisomes. *Current Biology*, *20*(14), 1310–1315.

Breitschopf, K., Haendeler, J., Malchow, P., Zeiher, A. M., & Dimmeler, S. (2000). Posttranslational Modification of Bcl-2 Facilitates Its Proteasome-Dependent Degradation: Molecular Characterization of the Involved Signaling Pathway. *Molecular and Cellular Biology*, *20*(5), 1886–1896.

Brochard, V., Combadière, B., Prigent, A., Laouar, Y., Perrin, A., Beray-Berthat, V., Bonduelle, O., Alvarez-Fischer, D., Callebert, J., Launay, J. M., Duyckaerts, C., Flavell, R. A., Hirsch, E. C., & Hunot, S. (2009). Infiltration of CD4+ lymphocytes into the brain contributes to neurodegeneration in a mouse model of Parkinson disease. *Journal of Clinical Investigation*, *119*(1), 182–192.

Brooks, A. I., Chadwick, C. A., Gelbard, H. A., Cory-Slechta, D. A., & Federoff, H. J. (1999). Paraquat elicited neurobehavioral syndrome caused by dopaminergic

neuron loss. *Brain Research*, *823*(1–2), 1–10.

Brown, S., Hu, N., & Hombría, J. C. G. (2001). Identification of the first invertebrate interleukin JAK/STAT receptor, the *Drosophila* gene *domeless*. *Current Biology*, *11*(21), 1700–1705.

Brun, S., Vidal, S., Spellman, P., Takahashi, K., Tricoire, H., & Lemaitre, B. (2006). The MAPKKK Mekk1 regulates the expression of *Turandot* stress genes in response to septic injury in *Drosophila*. *Genes to Cells*, *11*(4), 397–407.

Buchon, N., Broderick, N. A., Poidevin, M., Pradervand, S., & Lemaitre, B. (2009). *Drosophila* Intestinal Response to Bacterial Infection: Activation of Host Defense and Stem Cell Proliferation. *Cell Host & Microbe*, *5*(2), 200–211.

Burchell, V. S., Nelson, D. E., Sanchez-Martinez, A., Delgado-Camprubi, M., Ivatt, R. M., Pogson, J. H., Randle, S. J., Wray, S., Lewis, P. A., Houlden, H., Abramov, A. Y., Hardy, J., Wood, N. W., Whitworth, A. J., Laman, H., & Plun-Favreau, H. (2013). The Parkinson's disease-linked proteins Fbxo7 and Parkin interact to mediate mitophagy. *Nature Neuroscience*, *16*(9), 1257–1265.

Burdette, D. L., Monroe, K. M., Sotelo-Troha, K., Iwig, J. S., Eckert, B., Hyodo, M., Hayakawa, Y., & Vance, R. E. (2011). STING is a direct innate immune sensor of cyclic di-GMP. *Nature*, *478*(7370), 515–518.

Burman, J. L., Pickles, S., Wang, C., Sekine, S., Vargas, J. N. S., Zhang, Z., Youle, A. M., Nezich, C. L., Wu, X., Hammer, J. A., & Youle, R. J. (2017). Mitochondrial fission facilitates the selective mitophagy of protein aggregates. *Journal of Cell Biology*, *216*(10), 3231–3247.

Buzhynsky, N., Sens, P., Prima, V., Sturgis, J. N., & Scheuring, S. (2007). Rows of ATP synthase dimers in native mitochondrial inner membranes. *Biophysical Journal*, *93*(8), 2870–2876.

Cadete, V. J. J., Deschênes, S., Cuillerier, A., Brisebois, F., Sugiura, A., Vincent, A., Turnbull, D., Picard, M., McBride, H. M., & Burelle, Y. (2016). Formation of mitochondrial-derived vesicles is an active and physiologically relevant mitochondrial quality control process in the cardiac system. *Journal of Physiology*, *594*(18), 5343–5362.

Cai, Q., Zakaria, H. M., Simone, A., & Sheng, Z. H. (2012). Spatial parkin translocation and degradation of damaged mitochondria via mitophagy in live cortical neurons. *Current Biology*, *22*(6), 545–552.

Canet-Avilés, R. M., Wilson, M. A., Miller, D. W., Ahmad, R., McLendon, C., Bandyopadhyay, S., Baptista, M. J., Ringe, D., Petsko, G. A., & Cookson, M. R. (2004). The Parkinson's disease DJ-1 is neuroprotective due to cysteine-sulfinic acid-driven mitochondrial localization. *Proceedings of the National Academy of Sciences of the United States of America*, *101*(24), 9103–9108.

Cannon, J. R., Tapias, V., Na, H. M., Honick, A. S., Drolet, R. E., & Greenamyre, J. T. (2009). A highly reproducible rotenone model of Parkinson's disease. *Neurobiology of Disease*, *34*(2), 279–290.

Cao, Y., Chtarbanova, S., Petersen, A. J., & Ganetzky, B. (2013). *Dnr1* mutations cause neurodegeneration in *Drosophila* by activating the innate immune response in the brain. *Proceedings of the National Academy of Sciences of the United States of America*, *110*(19), E1752–E1760.

Cao, Y. L., Meng, S., Chen, Y., Feng, J. X., Gu, D. D., Yu, B., Li, Y. J., Yang, J. Y., Liao, S., Chan, D. C., & Gao, S. (2017). MFN1 structures reveal nucleotide-triggered dimerization critical for mitochondrial fusion. *Nature*, *542*(7641), 372–376.

Carvey, P. M., Zhao, C. H., Hendey, B., Lum, H., Trachtenberg, J., Desai, B. S., Snyder, J., Zhu, Y. G., & Ling, Z. D. (2005). 6-Hydroxydopamine-induced alterations in blood-brain barrier permeability. *European Journal of Neuroscience*, *22*(5), 1158–1168.

Casari, G., De Fusco, M., Ciarmatori, S., Zeviani, M., Mora, M., Fernandez, P., De Michele, G., Filla, A., Cocozza, S., Marconi, R., Dürr, A., Fontaine, B., & Ballabio, A. (1998). Spastic paraplegia and OXPHOS impairment caused by mutations in paraplegin, a nuclear-encoded mitochondrial metalloprotease. *Cell*, *93*(6), 973–983.

Celardo, I., Costa, A. C., Lehmann, S., Jones, C., Wood, N., Mencacci, N. E., Mallucci, G. R., Loh, S. H. Y., & Martins, L. M. (2016). Mitofusin-mediated ER stress triggers neurodegeneration in pink1/parkin models of Parkinson's disease. *Cell Death & Disease*, *7*(6), e2271–e2271.

Ceyzériat, K., Abjean, L., Carrillo-de Sauvage, M. A., Ben Haim, L., & Escartin, C. (2016). The complex STATes of astrocyte reactivity: How are they controlled by the JAK-STAT3 pathway? *Neuroscience*, *330*, 205–218.

Cha, G. H., Kim, S., Park, J., Lee, E., Kim, M., Lee, S. B., Kim, J. M., Chung, J., & Cho, K. S. (2005). Parkin negatively regulates JNK pathway in the dopaminergic

neurons of *Drosophila*. *Proceedings of the National Academy of Sciences of the United States of America*, *102*(29), 10345–10350.

Chakrabarti, S., Poidevin, M., & Lemaitre, B. (2014). The *Drosophila* MAPK p38c Regulates Oxidative Stress and Lipid Homeostasis in the Intestine. *PLoS Genetics*, *10*(9), e1004659.

Chan, P., DeLanney, L. E., Irwin, I., Langston, J. W., & Di Monte, D. (1991). Rapid ATP Loss Caused by 1-Methyl-4-Phenyl-1,2,3,6-Tetrahydropyridine in Mouse Brain. *Journal of Neurochemistry*, *57*(1), 348–351.

Chance, B., & Williams, G. R. (1955). Respiratory enzymes in oxidative phosphorylation. I. Kinetics of oxygen utilization. *The Journal of Biological Chemistry*, *217*(1), 383–393.

Chartier-Harlin, M. C., Kachergus, J., Roumier, C., Mouroux, V., Douay, X., Lincoln, S., Levecque, C., Larvor, L., Andrieux, J., Hulihan, M., Waucquier, N., Defebvre, L., Amouyel, P., Farrer, M., & Destée, A. (2004). α-synuclein locus duplication as a cause of familial Parkinson's disease. *Lancet*, *364*(9440), 1167–1169.

Chau, V., Tobias, J. W., Bachmair, A., Marriott, D., Ecker, D. J., Gonda, D. K., & Varshavsky, A. (1989). A multiubiquitin chain is confined to specific lysine in a targeted short-lived protein. *Science*, *243*(4898), 1576–1583.

Chaugule, V. K., Burchell, L., Barber, K. R., Sidhu, A., Leslie, S. J., Shaw, G. S., & Walden, H. (2011). Autoregulation of Parkin activity through its ubiquitin-like domain. *The EMBO Journal*, *30*(14), 2853–2867.

Chen, D., Gao, F., Li, B., Wang, H., Xu, Y., Zhu, C., & Wang, G. (2010). Parkin mono-ubiquitinates Bcl-2 and regulates autophagy. *Journal of Biological Chemistry*, *285*(49), 38214–38223.

Chen, G., Han, Z., Feng, D., Chen, Y., Chen, L., Wu, H., Huang, L., Zhou, C., Cai, X., Fu, C., Duan, L., Wang, X., Liu, L., Liu, X., Shen, Y., Zhu, Y., & Chen, Q. (2014). A regulatory signaling loop comprising the PGAM5 phosphatase and CK2 controls receptor-mediated mitophagy. *Molecular Cell*, *54*(3), 362–377.

Chen, H., O'Reilly, E. J., Schwarzschild, M. A., & Ascherio, A. (2008). Peripheral inflammatory biomarkers and risk of Parkinson's disease. *American Journal of Epidemiology*, *167*(1), 90–95.

Chen, J., Xie, C., Tian, L., Hong, L., Wu, X., & Han, J. (2010). Participation of the p38 pathway in *Drosophila* host defense against pathogenic bacteria and fungi. *Proceedings of the National Academy of Sciences of the United States of America*, *107*(48), 20774–20779.

Chen, Z., Liu, L., Cheng, Q., Li, Y., Wu, H., Zhang, W., Wang, Y., Sehgal, S. A., Siraj, S., Wang, X., Wang, J., Zhu, Y., & Chen, Q. (2017). Mitochondrial E3 ligase MARCH 5 regulates FUNDC 1 to fine-tune hypoxic mitophagy. *EMBO Reports*, *18*(3), 495–509.

Cheng, Z., Dai, T., He, X., Zhang, Z., Xie, F., Wang, S., Zhang, L., & Zhou, F. (2020). The interactions between cGAS-STING pathway and pathogens. In *Signal Transduction and Targeted Therapy, 5*(1), 1–15.

Chinchore, Y., Gerber, G. F., & Dolph, P. J. (2012). Alternative pathway of cell death in *Drosophila* mediated by NF-κB transcription factor Relish. *Proceedings of the National Academy of Sciences of the United States of America*, *109*(10), E605–E612.

Chinnery, P. F., & Hudson, G. (2013). Mitochondrial genetics. *British Medical Bulletin*, *106*(1), 135–159.

Chiueh, C. C., Markey, S. P., Burns, R. S., Johannessen, J. N., Pert, A., & Kopin, I. J. (1984). Neurochemical and behavioral effects of systematic and intranigral administration of N-methyl-4-phenyl-1,2,3,6-tetrahydropyridine in the rat. *European Journal of Pharmacology*, *100*(2), 189–194.

Choi, K. H., & Licht, S. (2005). Control of peptide product sizes by the energy-dependent protease ClpAP. *Biochemistry*, *44*(42), 13921–13931.

Chourasia, A. H., Tracy, K., Frankenberger, C., Boland, M. L., Sharifi, M. N., Drake, L. E., Sachleben, J. R., Asara, J. M., Locasale, J. W., Karczmar, G. S., & Macleod, K. F. (2015). Mitophagy defects arising from BNip3 loss promote mammary tumor progression to metastasis. *EMBO Reports*, *16*(9), 1145–1163.

Chu, C. T. (2019). Multiple pathways for mitophagy: A neurodegenerative conundrum for Parkinson's disease. *Neuroscience Letters*, *697*(April 2018), 66–71.

Chu, C. T., Ji, J., Dagda, R. K., Jiang, J. F., Tyurina, Y. Y., Kapralov, A. A., Tyurin, V. A., Yanamala, N., Shrivastava, I. H., Mohammadyani, D., Qiang Wang, K. Z., Zhu, J., Klein-Seetharaman, J., Balasubramanian, K., Amoscato, A. A., Borisenko, G., Huang, Z., Gusdon, A. M., Cheikhi, A., Steer, E. K., Wang, R., Baty, C., Watkins,

S., Bahar, I., Bayir, H. & Kagan, V. E. (2013). Cardiolipin externalization to the outer mitochondrial membrane acts as an elimination signal for mitophagy in neuronal cells. *Nature Cell Biology*, *15*(10), 1197–1205.

Chung, E., Choi, Y., Park, J., Nah, W., Park, J., Jung, Y., Lee, J., Lee, H., Park, S., Hwang, S., Kim, S., Lee, J., Min, D., Jo, J., Kang, S., Jung, M., Lee, P. H., Earl Ruley, H., & Jo, D. (2020). Intracellular delivery of Parkin rescues neurons from accumulation of damaged mitochondria and pathological α-synuclein. *Science Advances*, *6*(18).

Chung, K. K. K., Thomas, B., Li, X., Pletnikova, O., Troncoso, J. C., Marsh, L., Dawson, V. L., & Dawson, T. M. (2004). S-nitrosylation of Parkin regulates ubiquitination and compromises Parkin's protective function. *Science*, *304*(5675), 1328–1331.

Chung, K. K. K., Zhang, Y., Lim, K. L., Tanaka, Y., Huang, H., Gao, J., Ross, C. A., Dawson, V. L., & Dawson, T. M. (2001). Parkin ubiquitinates the α-synuclein-interacting protein, synphilin-1: Implications for Lewy-body formation in Parkinson disease. *Nature Medicine*, *7*(10), 1144–1150.

Cicchetti, F., Brownell, A. L., Williams, K., Chen, Y. I., Livni, E., & Isacson, O. (2002). Neuroinflammation of the nigrostriatal pathway during progressive 6-OHDA dopamine degeneration in rats monitored by immunohistochemistry and PET imaging. *European Journal of Neuroscience*, *15*(6), 991–998.

Clark, I. E., Dodson, M. W., Jiang, C., Cao, J. H., Huh, J. R., Seol, J. H., Yoo, S. J., Hay, B. A., & Guo, M. (2006). *Drosophila pink1* is required for mitochondrial function and interacts genetically with *parkin*. *Nature*, *441*(7097), 1162–1166.

Clark, S. (1957). Newborn mice studied with the electron mircroscope. *Biophysics and Biochemical Cytology*, *3*(3), 349–362.

Cochemé, H. M., & Murphy, M. P. (2008). Complex I is the major site of mitochondrial superoxide production by paraquat. *Journal of Biological Chemistry*, *283*(4), 1786–1798.

Cohen, M. M. J., Leboucher, G. P., Livnat-Levanon, N., Glickman, M. H., & Weissman, A. M. (2008). Ubiquitin-proteasome-dependent degradation of a mitofusin, a critical regulator of mitochondrial fusion. *Molecular Biology of the Cell*, *19*(6), 2457–2464.

Colodner, K. J., & Feany, M. B. (2010). Glial fibrillary tangles and JAK/STAT-mediated glial and neuronal cell death in a *Drosophila* model of glial tauopathy. *Journal of*

Neuroscience, *30*(48), 16102–16113.

Cornelissen, T., Vilain, S., Vints, K., Gounko, N., Verstreken, P., & Vandenberghe, W. (2018). Deficiency of parkin and PINK1 impairs age-dependent mitophagy in *Drosophila*. *eLife*, *7*, 1–14.

Corral-Debrinski, M., Horton, T., Lott, M. T., Shoffner, J. M., Beal, M. F., & Wallace, D. C. (1992). Mitochondrial DNA deletions in human brain: Regional variability and increase with advanced age. *Nature Genetics*, *2*(4), 324–329.

Corti, O. (2019). Neuronal Mitophagy: Lessons from a Pathway Linked to Parkinson's Disease. *Neurotoxicity Research*, *36*(2), 292–305.

Corti, O., Lesage, S., & Brice, A. (2011). What genetics tells us about the causes and mechanisms of Parkinson's disease. *Physiological Reviews*, *91*(4), 1161–1218.

Cortopassi, G. A., & Arnheim, N. (1990). Detection of a specific mitochondrial DNA deletion in tissues of older humans. *Nucleic Acids Research*, *18*(23), 6927–6933.

Cosson, P., Marchetti, A., Ravazzola, M., & Orci, L. (2012). Mitofusin-2 Independent Juxtaposition of Endoplasmic Reticulum and Mitochondria: An Ultrastructural Study. *PLoS ONE*, *7*(9), e46293.

Craig, C. R., Fink, J. L., Yagi, Y., Ip, Y. T., & Cagan, R. L. (2004). A *Drosophila* p38 orthologue is required for environmental stress responses. *EMBO Reports*, *5*(11), 1058–1063.

Cronin, S. J. F., Nehme, N. T., Limmer, S., Liegeois, S., Pospisilik, J. A., Schramek, D., Leibbrandt, A., De Simoes, R. M., Gruber, S., Puc, U., Ebersberger, I., Zoranovic, T., Neely, G. G., Von Haeseler, A., Ferrandon, D., & Penninger, J. M. (2009). Genome-wide RNAi screen identifies genes involved in intestinal pathogenic bacterial infection. *Science*, *325*(5938), 340–343.

Crowl, J. T., Gray, E. E., Pestal, K., Volkman, H. E., & Stetson, D. B. (2017). Intracellular nucleic acid detection in autoimmunity. In *Annual Review of Immunology*, *35*, 313–336.

Csordás, G., Várnai, P., Golenár, T., Roy, S., Purkins, G., Schneider, T. G., Balla, T., & Hajnóczky, G. (2010). Imaging Interorganelle Contacts and Local Calcium Dynamics at the ER-Mitochondrial Interface. *Molecular Cell*, *39*(1), 121–132.

Dan, X., Babbar, M., Moore, A., Wechter, N., Tian, J., Mohanty, J. G., Croteau, D. L., & Bohr, V. A. (2020). DNA damage invokes mitophagy through a pathway involving Spata18. *Nucleic Acids Research*, *48*(12), 6611–6623.

Dardiotis, E., Tsouris, Z., Mentis, A. F. A., Siokas, V., Michalopoulou, A., Sokratous, M., Dastamani, M., Bogdanos, D. P., Deretzi, G., & Kountouras, J. (2018). *H. pylori* and Parkinson's disease: Meta-analyses including clinical severity. In *Clinical Neurology and Neurosurgery*, *175*, 16–24.

Davis, G. C., Williams, A. C., Markey, S. P., Ebert, M. H., Caine, E. D., Reichert, C. M., & Kopin, I. J. (1979). Chronic parkinsonism secondary to intravenous injection of meperidine analogues. *Psychiatry Research*, *1*(3), 249–254.

Davis, M. M., Primrose, D. A., & Hodgetts, R. B. (2008). A Member of the p38 Mitogen-Activated Protein Kinase Family Is Responsible for Transcriptional Induction of Dopa decarboxylase in the Epidermis of *Drosophila melanogaster* during the Innate Immune Response. *Molecular and Cellular Biology*, *28*(15), 4883–4895.

Day, B. J., Patel, M., Calavetta, L., Chang, L. Y., & Stamler, J. S. (1999). A mechanism of paraquat toxicity involving nitric oxide synthase. *Proceedings of the National Academy of Sciences of the United States of America*, *96*(22), 12760–12765.

De Brito, O. M., & Scorrano, L. (2008). Mitofusin 2 tethers endoplasmic reticulum to mitochondria. *Nature*, *456*(7222), 605–610.

de Lau, L. M., & Breteler, M. M. (2006). Epidemiology of Parkinson's disease. *Lancet Neurology*, *5*(6), 525–535.

De Sagarra, M. R., Mayo, I., Marco, S., Rodríguez-Vilarino, S., Oliva, J., Carrascosa, J. L., & Castaño , J. G. (1999). Mitochondrial localization and oligomeric structure of HClpP, the human homologue of *E. coli* ClpP. *Journal of Molecular Biology*, *292*(4), 819–825.

De Stefani, D., Bononi, A., Romagnoli, A., Messina, A., De Pinto, V., Pinton, P., & Rizzuto, R. (2012). VDAC1 selectively transfers apoptotic Ca^{+2} signals to mitochondria. *Cell Death and Differentiation*, *19*(2), 267–273.

De Stefani, Diego, Raffaello, A., Teardo, E., Szabó, I., & Rizzuto, R. (2011). A forty-kilodalton protein of the inner membrane is the mitochondrial calcium uniporter. *Nature*, *476*(7360), 336–340.

Deas, E., Plun-Faureau, H., & Wood, N. W. (2009). PINK1 function in health and disease. In *EMBO Molecular Medicine*, *1*(3), 152–165.

Deas, E., Plun-Favreau, H., Gandhi, S., Desmond, H., Kjaer, S., Loh, S. H. Y., Renton, A. E. M., Harvey, R. J., Whitworth, A. J., Martins, L. M., Abramov, A. Y., & Wood, N. W. (2011). PINK1 cleavage at position A103 by the mitochondrial protease PARL. *Human Molecular Genetics*, *20*(5), 867–879.

Del Rey, N. L. G., Quiroga-Varela, A., Garbayo, E., Carballo-Carbajal, I., Fernández-Santiago, R., Monje, M. H. G., Trigo-Damas, I., Blanco-Prieto, M. J., & Blesa, J. (2018). Advances in parkinson's disease: 200 years later. *Frontiers in Neuroanatomy*, *12*, 113.

Delaney, J. R., Stöven, S., Uvell, H., Anderson, K. V., Engström, Y., & Mlodzik, M. (2006). Cooperative control of *Drosophila* immune responses by the JNK and NF-κB signaling pathways. *EMBO Journal*, *25*(13), 3068–3077.

Demontis, F., & Perrimon, N. (2010). FOXO/4E-BP signaling in *Drosophila* muscles regulates organism-wide proteostasis during aging. *Cell*, *143*(5), 813–825.

Demontis, F., Piccirillo, R., Goldberg, A. L., & Perrimon, N. (2013). Mechanisms of skeletal muscle aging: Insights from *Drosophila* and mammalian models. *DMM Disease Models and Mechanisms*, *6*(6), 1339–1352.

Deng, H., Dodson, M. W., Huang, H., & Guo, M. (2008). The Parkinson's disease genes *pink1* and *parkin* promote mitochondrial fission and/or inhibit fusion in *Drosophila*. *Proceedings of the National Academy of Sciences*, *105*(38), 14503–14508.

Dennis, E. A., & Kennedy, E. P. (1972). Intracellular sites of lipid synthesis and the biogenesis of mitochondria. *Journal of Lipid Research*, *13*(2), 263–267.

Denton, R. M. (2009). Regulation of mitochondrial dehydrogenases by calcium ions. *Biochimica et Biophysica Acta, 1787*(11), 1309–1316.

Detmer, S. A., & Chan, D. C. (2007). Functions and dysfunctions of mitochondrial dynamics. *Nature Reviews Molecular Cell Biology*, *8*(11), 870–879.

Devos, D., Lebouvier, T., Lardeux, B., Biraud, M., Rouaud, T., Pouclet, H., Coron, E., Bruley des Varannes, S., Naveilhan, P., Nguyen, J. M., Neunlist, M., & Derkinderen, P. (2013). Colonic inflammation in Parkinson's disease.

Neurobiology of Disease, *50*(1), 42–48.

Di Rita, A., D'Acunzo, P., Simula, L., Campello, S., Strappazzon, F., & Cecconi, F. (2018a). AMBRA1-mediated mitophagy counteracts oxidative stress and apoptosis induced by neurotoxicity in human neuroblastoma SH-SY5Y cells. *Frontiers in Cellular Neuroscience*, *12*(April), 1–11.

Di Rita, A., Peschiaroli, A., D'Acunzo, P., Strobbe, D., Hu, Z., Gruber, J., Nygaard, M., Lambrughi, M., Melino, G., Papaleo, E., Dengjel, J., El Alaoui, S., Campanella, M., Dötsch, V., Rogov, V. V., Strappazzon, F., & Cecconi, F. (2018b). HUWE1 E3 ligase promotes PINK1/PARKIN-independent mitophagy by regulating AMBRA1 activation via IKKα. *Nature Communications*, *9*(1).

Dickson, D. W. (2012). Parkinson's disease and parkinsonism: Neuropathology. *Cold Spring Harbor Perspectives in Medicine*, *2*(8), 1–15.

Doherty, J., Sheehan, A. E., Bradshaw, R., Fox, A. N., Lu, T. Y., & Freeman, M. R. (2014). PI3K Signaling and Stat92E Converge to Modulate Glial Responsiveness to Axonal Injury. *PLoS Biology*, *12*(11), e1001985.

Dostert, C., Jouanguy, E., Irving, P., Troxler, L., Galiana-Arnoux, D., Hetru, C., Hoffmann, J. A., & Imler, J.-L. (2005). The Jak-STAT signaling pathway is required but not sufficient for the antiviral response of *Drosophila*. *Nature Immunology*, *6*(9), 946–953.

Edenharter, O., Schneuwly, S., & Navarro, J. A. (2018). Mitofusin-dependent ER stress triggers glial dysfunction and nervous system degeneration in a *Drosophila* model of Friedreich's ataxia. *Frontiers in Molecular Neuroscience*, *11*, 38.

Edwards, L. L., Quigley, E. M. M., & Pfeiffer, R. F. (1992). Gastrointestinal dysfunction in parkinson's disease: Frequency and pathophysiology. *Neurology*, *42*(4), 726–732.

Ekas, L. A., Cardozo, T. J., Flaherty, M. S., McMillan, E. A., Gonsalves, F. C., & Bach, E. A. (2010). Characterization of a dominant-active STAT that promotes tumorigenesis in *Drosophila*. *Developmental Biology*, *344*(2), 621–636.

Ekengren, S., & Hultmark, D. (2001). A family of *Turandot*-related genes in the humoral stress response of *Drosophila*. *Biochemical and Biophysical Research Communications*, *284*(4), 998–1003.

Erecinska, M., Nelson, D., Yudkoff, M., & Silver, I. A. (1994). Energetics of the nerve terminal in relation to central nervous system function. *Biochemical Society Transactions*, *22*(4), 959–965.

Ernster, L., & Schatz, G. (1981). Mitochondria : A Historical Review. *The Journal Of Cell Biology*, *91*(December).

Esteban-Martínez, L., Sierra-Filardi, E., McGreal, R. S., Salazar-Roa, M., Mariño, G., Seco, E., Durand, S., Enot, D., Graña, O., Malumbres, M., Cvekl, A., Cuervo, A. M., Kroemer, G., & Boya, P. (2017). Programmed mitophagy is essential for the glycolytic switch during cell differentiation. *The EMBO Journal*, *36*(12), 1688–1706.

Fabre, E., Monserrat, J., Herrero, A., Barja, G., & Leret, M. L. (1999). Effect of MPTP on brain mitochondrial H_2O_2 and ATP production and on dopamine and DOPAC in the striatum. *Journal of Physiology and Biochemistry*, *55*(4), 325–332.

Fang, E. F., Hou, Y., Palikaras, K., Adriaanse, B. A., Kerr, J. S., Yang, B., Lautrup, S., Hasan-Olive, M. M., Caponio, D., Dan, X., Rocktäschel, P., Croteau, D. L., Akbari, M., Greig, N. H., Fladby, T., Nilsen, H., Cader, M. Z., Mattson, M. P., Tavernarakis, N., & Bohr, V. A. (2019). Mitophagy inhibits amyloid-β and tau pathology and reverses cognitive deficits in models of Alzheimer's disease. *Nature Neuroscience*, *22*(3), 401–412.

Faull, R. L. M., & Laverty, R. (1969). Changes in dopamine levels in the corpus striatum following lesions in the substantia nigra. *Experimental Neurology*, *23*(3), 332–340.

Ferguson, S. M., & De Camilli, P. (2012). Dynamin, a membrane-remodelling GTPase. *Nature Reviews Molecular Cell Biology*, *13*(2), 75–88.

Fernagut, P. O., Hutson, C. B., Fleming, S. M., Tetreaut, N. A., Salcedo, J., Masliah, E., & Chesselet, M. F. (2007). Behavioral and histopathological consequences of paraquat intoxication in mice: Effects of α-synuclein over-expression. *Synapse*, *61*(12), 991–1001.

Ferree, A. W., Trudeau, K., Zik, E., Benador, I. Y., Twig, G., Gottlieb, R. A., & Shirihai, O. S. (2013). MitoTimer probe reveals the impact of autophagy, fusion, and motility on subcellular distribution of young and old mitochondrial protein and on relative mitochondrial protein age. *Autophagy*, *9*(11), 1887–1896.

Filadi, R., Greotti, E., Turacchio, G., Luini, A., Pozzan, T., & Pizzo, P. (2015). Mitofusin 2 ablation increases endoplasmic reticulum-mitochondria coupling. *Proceedings*

of the National Academy of Sciences of the United States of America, *112*(17), E2174–E2181.

Fischer, F., Hamann, A., & Osiewacz, H. D. (2012). Mitochondrial quality control : an integrated network of pathways. *Trends in Biochemical Sciences*, *37*(7), 284–292.

Fischer, F., Langer, J. D., & Osiewacz, H. D. (2015). Identification of potential mitochondrial CLPXP protease interactors and substrates suggests its central role in energy metabolism. *Scientific Reports*, *5*(December), 1–13.

Fleming, S. M., Zhu, C., Fernagut, P. O., Mehta, A., DiCarlo, C. D., Seaman, R. L., & Chesselet, M. F. (2004). Behavioral and immunohistochemical effects of chronic intravenous and subcutaneous infusions of varying doses of rotenone. *Experimental Neurology*, *187*(2), 418–429.

Flemming, A. (2017). Insect Immunity: Mechanism of adaptive immunity found in the fruitfly. *Nature Reviews Immunology*, *17*(5), 278–279.

Frank-Cannon, T. C., Tran, T., Ruhn, K. A., Martinez, T. N., Hong, J., Marvin, M., Hartley, M., Trevino, I., O'Brien, D. E., Casey, B., Goldberg, M. S., & Tansey, M. G. (2008). Parkin Deficiency Increases Vulnerability to Inflammation-Related Nigral Degeneration. *Journal of Neuroscience*, *28*(43), 10825–10834.

Fredriksson, A., & Archer, T. (1994). MPTP-induced behavioural and biochemical deficits: A parametric analysis. *Journal of Neural Transmission - Parkinson's Disease and Dementia Section*, *7*(2), 123–132.

Frey, T. G., & Mannella, C. A. (2000). The internal structure of mitochondria. *Trends in Biochemical Sciences*, *25*(7), 319–324.

Friedman, J. R., Lackner, L. L., West, M., DiBenedetto, J. R., Nunnari, J., & Voeltz, G. K. (2011). ER tubules mark sites of mitochondrial division. *Science*, *334*(6054), 358–362.

Fröhlich, C., Grabiger, S., Schwefel, D., Faelber, K., Rosenbaum, E., Mears, J., Rocks, O., & Daumke, O. (2013). Structural insights into oligomerization and mitochondrial remodelling of dynamin 1-like protein. *EMBO Journal*, *32*(9), 1280–1292.

Fujiwara, H., Hasegawa, M., Dohmae, N., Kawashima, A., Masliah, E., Goldberg, M. S., Shen, J., Takio, K., & Iwatsubo, T. (2002). α-synuclein is phosphorylated in

synucleinopathy lesions. *Nature Cell Biology*, *4*(2), 160–164.

Fukae, J., Sato, S., Shiba, K., Sato, K. ichi, Mori, H., Sharp, P. A., Mizuno, Y., & Hattori, N. (2009). Programmed cell death-2 isoform1 is ubiquitinated by Parkin and increased in the substantia nigra of patients with autosomal recessive Parkinson's disease. *FEBS Letters*, *583*(3), 521–525.

Gammage, P. A., & Frezza, C. (2019). Mitochondrial DNA: The overlooked oncogenome? *BMC Biology*, *17*(1), 1–10.

Gandhi, S., Muqit, M. M. K., Stanyer, L., Healy, D. G., Abou-Sleiman, P. M., Hargreaves, I., Heales, S., Ganguly, M., Parsons, L., Lees, A. J., Latchman, D. S., Holton, J. L., Wood, N. W., & Revesz, T. (2006). PINK1 protein in normal human brain and Parkinson's disease. *Brain*, *129*(7), 1720–1731.

Gandre-Babbe, S., & Van Der Bliek, A. M. (2008). The novel tail-anchored membrane protein Mff controls mitochondrial and peroxisomal fission in mammalian cells. *Molecular Biology of the Cell*, *19*(6), 2402–2412.

Gao, H. M., Jiang, J., Wilson, B., Zhang, W., Hong, J. S., & Liu, B. (2002). Microglial activation-mediated delayed and progressive degeneration of rat nigral dopaminergic neurons: Relevance to Parkinson's disease. *Journal of Neurochemistry*, *81*(6), 1285–1297.

Gao, H. M., Hong, J. S., Zhang, W., & Liu, B. (2003a). Synergistic dopaminergic neurotoxicity of the pesticide rotenone and inflammogen lipopolysaccharide: Relevance to the etiology of Parkinson's disease. *Journal of Neuroscience*, *23*(4), 1228–1236.

Gao, H. M., Liu, B., & Hong, J. S. (2003b). Critical role for microglial NADPH oxidase in rotenone-induced degeneration of dopaminergic neurons. *Journal of Neuroscience*, *23*(15), 6181–6187.

Gao, H. M., Liu, B., Zhang, W., & Hong, J. S. (2003c). Synergistic dopaminergic neurotoxicity of MPTP and inflammogen lipopolysaccharide: relevance to the etiology of Parkinson's disease. *The FASEB Journal*, *17*(13), 1–25.

Ge, P., Dawson, V. L., & Dawson, T. M. (2020). PINK1 and Parkin mitochondrial quality control: A source of regional vulnerability in Parkinson's disease. *Molecular Neurodegeneration*, *15*(1), 1–18.

Gelpi, E., Navarro-Otano, J., Tolosa, E., Gaig, C., Compta, Y., Rey, M. J., Martí, M. J., Hernández, I., Valldeoriola, F., Reñé, R., & Ribalta, T. (2014). Multiple organ involvement by alpha-synuclein pathology in lewy body disorders. *Movement Disorders*, *29*(8), 1010–1018.

Ghosh, A., Roy, A., Liu, X., Kordower, J. H., Mufson, E. J., Hartley, D. M., Ghosh, S., Mosley, R. L., Gendelman, H. E., & Pahan, K. (2007). Selective inhibition of NF-κB activation prevents dopaminergic neuronal loss in a mouse model of Parkinson's disease. *Proceedings of the National Academy of Sciences of the United States of America*, *104*(47), 18754–18759.

Giacomello, M., Drago, I., Bortolozzi, M., Scorzeto, M., Gianelle, A., Pizzo, P., & Pozzan, T. (2010). Ca^{2+} Hot Spots on the Mitochondrial Surface Are Generated by Ca^{2+} Mobilization from Stores, but Not by Activation of Store-Operated Ca^{2+} Channels. *Molecular Cell*, *38*(2), 280–290.

Giasson, B. I., Murray, I. V. J., Trojanowski, J. Q., & Lee, V. M. Y. (2001). A Hydrophobic Stretch of 12 Amino Acid Residues in the Middle of α-Synuclein Is Essential for Filament Assembly. *Journal of Biological Chemistry*, *276*(4), 2380–2386.

Gilkerson, R. W., Schon, E. A., Hernandez, E., & Davidson, M. M. (2008). Mitochondrial nucleoids maintain genetic autonomy but allow for functional complementation. *Journal of Cell Biology*, *181*(7), 1117–1128.

Gilks, W. P., Abou-Sleiman, P. M., Gandhi, S., Jain, S., Singleton, A., Lees, A. J., Shaw, K., Bhatia, K. P., Bonifati, V., Quinn, N. P., Lynch, J., Healy, D. G., Holton, J. L., Revesz, T., & Wood, N. W. (2005). A common *LRRK2* mutation in idiopathic Parkinson's disease. *Lancet*, *365*(9457), 415–416.

Gispert, S., Ricciardi, F., Kurz, A., Azizov, M., Hoepken, H.-H., Becker, D., Voos, W., Leuner, K., Müller, W. E., Kudin, A. P., Kunz, W. S., Zimmermann, A., Roeper, J., Wenzel, D., Jendrach, M., García-Arencíbia, M., Fernández-Ruiz, J., Huber, L., Rohrer, H., Barrera, M., Reichert, A. S., Rüb, U., Chen, A., Nussbaum, R. L., & Auburger, G. (2009). Parkinson Phenotype in Aged *PINK1*-Deficient Mice Is Accompanied by Progressive Mitochondrial Dysfunction in Absence of Neurodegeneration. *PLoS ONE*, *4*(6), e5777.

Gladkova, C., Maslen, S. L., Skehel, J. M., & Komander, D. (2018). Mechanism of parkin activation by PINK1. *Nature*, *559*(7714), 410–414.

Glise, B., Bourbon, H., & Noselli, S. (1995). hemipterous encodes a novel *Drosophila*

MAP kinase kinase, required for epithelial cell sheet movement. *Cell*, *83*(3), 451–461.

Gloeckner, C. J., Kinkl, N., Schumacher, A., Braun, R. J., O'Neill, E., Meitinger, T., Kolch, W., Prokisch, H., & Ueffing, M. (2006). The Parkinson disease causing *LRRK2* mutation I2020T is associated with increased kinase activity. *Human Molecular Genetics*, *15*(2), 223–232.

Gold, K. S., & Brückner, K. (2015). Macrophages and cellular immunity in *Drosophila melanogaster*. *Seminars in Immunology*, *27*(6), 357–368.

Gold, V. A. M., Ieva, R., Walter, A., Pfanner, N., Van Der Laan, M., & Kühlbrandt, W. (2014). Visualizing active membrane protein complexes by electron cryotomography. *Nature Communications*, *5*(1), 1–9.

Gorell, J. M., Johnson, C. C., Rybicki, B. A., Peterson, E. L., & Richardson, R. J. (1998). The risk of Parkinson's disease with exposure to pesticides, farming, well water, and rural living. *Neurology*, *50*(5), 1346–1350.

Goto, A., Okado, K., Martins, N., Cai, H., Barbier, V., Lamiable, O., Troxler, L., Santiago, E., Kuhn, L., Paik, D., Silverman, N., Holleufer, A., Hartmann, R., Liu, J., Peng, T., Hoffmann, J. A., Meignin, C., Daeffler, L., & Imler, J. L. (2018). The Kinase IKKβ Regulates a STING- and NF-κB-Dependent Antiviral Response Pathway in Drosophila. *Immunity*, *49*(2), 225-234.

Gottlieb, R. A., & Stotland, A. (2015). MitoTimer: a novel protein for monitoring mitochondrial turnover in the heart. *Journal of Molecular Medicine*, *93*(3), 271–278.

Gray, M. W. (2012). Mitochondrial evolution. *Cold Spring Harbor Perspectives in Biology*, *4*(9), 1–16.

Grazioli, S., & Pugin, J. (2018). Mitochondrial damage-associated molecular patterns: From inflammatory signaling to human diseases. *Frontiers in Immunology*, *9*(MAY).

Greene, A. W., Grenier, K., Aguileta, M. A., Muise, S., Farazifard, R., Haque, M. E., McBride, H. M., Park, D. S., & Fon, E. A. (2012). Mitochondrial processing peptidase regulates PINK1 processing, import and Parkin recruitment. *EMBO Reports*, *13*(4), 378–385.

Greene, J. C., Whitworth, A. J., Kuo, I., Andrews, L. A., Feany, M. B., & Pallanck, L. J. (2003). Mitochondrial pathology and apoptotic muscle degeneration in *Drosophila parkin* mutants. *Proceedings of the National Academy of Sciences*, *100*(7), 4078–4083.

Greene, Jessica C., Whitworth, A. J., Andrews, L. A., Parker, T. J., & Pallanck, L. J. (2005). Genetic and genomic studies of *Drosophila parkin* mutants implicate oxidative stress and innate immune responses in pathogenesis. *Human Molecular Genetics*, *14*(6), 799–811.

Gross, O., Thomas, C. J., Guarda, G., & Tschopp, J. (2011). The inflammasome: An integrated view. *Immunological Reviews*, *243*(1), 136–151.

Grünewald, A., Kumar, K. R., & Sue, C. M. (2019). New insights into the complex role of mitochondria in Parkinson's disease. *Progress in Neurobiology*, *177*(September 2018), 73–93.

Guha, S., López-Maury, L., Shaw, M., Bähler, J., Norbury, C. J., & Agashe, V. R. (2011). Transcriptional and cellular responses to defective mitochondrial proteolysis in fission yeast. *Journal of Molecular Biology*, *408*(2), 222–237.

Han, S. J., Choi, K. Y., Brey, P. T., & Lee, W. J. (1998). Molecular cloning and characterization of a *Drosophila* p38 mitogen-activated protein kinase. *Journal of Biological Chemistry*, *273*(1), 369–374.

Han, Z. S., Enslen, H., Hu, X., Meng, X., Wu, I.-H., Barrett, T., Davis, R. J., & Ip, Y. T. (1998a. A Conserved p38 Mitogen-Activated Protein Kinase Pathway Regulates *Drosophila* Immunity Gene Expression. *Molecular and Cellular Biology*, *18*(6), 3527–3539.

Hanna, R. A., Quinsay, M. N., Orogo, A. M., Giang, K., Rikka, S., & Gustafsson, Å. B. (2012). Microtubule-associated protein 1 light chain 3 (LC3) interacts with Bnip3 protein to selectively remove endoplasmic reticulum and mitochondria via autophagy. *Journal of Biological Chemistry*, *287*(23), 19094–19104.

Hanson, M. A., & Lemaitre, B. (2020). New insights on *Drosophila* antimicrobial peptide function in host defense and beyond. *Current Opinion in Immunology*, *62*, 22–30.

Hari, K. L., Cook, K. R., & Karpen, G. H. (2001). The *Drosophila Su(var)2-10* locus regulates chromosome structure and function and encodes a member of the PIAS protein family. *Genes and Development*, *15*(11), 1334–1348.

Harms, A. S., Delic, V., Thome, A. D., Bryant, N., Liu, Z., Chandra, S., Jurkuvenaite, A., & West, A. B. (2017). α-Synuclein fibrils recruit peripheral immune cells in the rat brain prior to neurodegeneration. *Acta Neuropathologica Communications*, *5*(85), 1–16.

Harrison, D. A., McCoon, P. E., Binari, R., Gilman, M., & Perrimon, N. (1998). *Drosophila* unpaired encodes a secreted protein that activates the JAK signaling pathway. *Genes & Development*, *12*(20), 3252–3263.

Harsh, S., Ozakman, Y., Kitchen, S. M., Paquin-Proulx, D., Nixon, D. F., & Eleftherianos, I. (2018). Dicer-2 Regulates Resistance and Maintains Homeostasis against Zika Virus Infection in *Drosophila*. *The Journal of Immunology*, *201*(10), 3058–3072.

Hayakawa, T., Matsuzawa, A., Noguchi, T., Takeda, K., & Ichijo, H. (2006). The ASK1–MAP kinase pathways in immune and stress responses. *Microbes and Infection*, *8*(4), 1098–1107.

Haynes, C. M., & Ron, D. (2010). The mitochondrial UPR - Protecting organelle protein homeostasis. *Journal of Cell Science*, *123*(22), 3849–3855.

Hedengren, M., Åsling, B., Dushay, M. S., Ando, I., Ekengren, S., Wihlborg, M., & Hultmark, D. (1999). *Relish*, a central factor in the control of humoral but not cellular immunity in *Drosophila*. *Molecular Cell*, *4*(5), 827–837.

Henriksen, M. A., Betz, A., Fuccillo, M. V, & Darnell, J. E. (2002). Negative regulation of STAT92E by an N-terminally truncated STAT protein derived from an alternative promoter site. *Genes and Development*, *16*(18), 2379–2389.

Heo, J. M., Ordureau, A., Paulo, J. A., Rinehart, J., & Harper, J. W. (2015). The PINK1-PARKIN Mitochondrial Ubiquitylation Pathway Drives a Program of OPTN/NDP52 Recruitment and TBK1 Activation to Promote Mitophagy. *Molecular Cell*, *60*(1), 7–20.

Herrera, S. C., & Bach, E. A. (2019). JAK/STAT signaling in stem cells and regeneration: from *Drosophila* to vertebrates. *Development*, *146*(2), 1–13.

Herrick, M. K., & Tansey, M. G. (2019). Infection triggers symptoms similar to those of Parkinson's disease in mice lacking PINK1 protein. *Nature*, *571*(7766), 481–482.

Hertzman, C., Wiens, M., Bowering, D., Snow, B., & Calne, D. (1990). Parkinson's

disease: A case-control study of occupational and environmental risk factors. *American Journal of Industrial Medicine*, *17*(3), 349–355.

Hisata, J. (2002). Final supplemental environmental impact statement. Lake and stream rehabilitation: rotenone use and health risks *(Washington Department of Fish and Wildlife).*

Hoffmann, J. A. (2003). The immune response of *Drosophila*. *Nature*, *426*(6962), 33–38.

Hombría, J. C. G., Brown, S., Häder, S., & Zeidler, M. P. (2005). Characterisation of Upd2, a *Drosophila* JAK/STAT pathway ligand. *Developmental Biology*, *288*(2), 420–433.

Hoppins, S., Edlich, F., Cleland, M. M., Banerjee, S., McCaffery, J. M., Youle, R. J., & Nunnari, J. (2011). The Soluble Form of Bax Regulates Mitochondrial Fusion via MFN2 Homotypic Complexes. *Molecular Cell*, *41*(2), 150–160.

Hoppins, S., & Nunnari, J. (2009). The molecular mechanism of mitochondrial fusion. *Biochimica et Biophysica Acta*, *1793*(1), 20–26.

Horibe, T., & Hoogenraad, N. J. (2007). The *Chop* gene contains an element for the positive regulation of the mitochondrial unfolded protein response. *PLoS ONE*, *2*(9).

Hou, S. X., Zheng, Z., Chen, X., & Perrimon, N. (2002). The JAK/STAT pathway in model organisms: Emerging roles in cell movement. *Developmental Cell*, *3*(6), 765–778.

Hou, X. S., Melnick, M. B., & Perrimon, N. (1996). *marelle* acts downstream of the *Drosophila* HOP/JAK kinase and encodes a protein similar to the mammalian STATs. *Cell*, *84*(3), 411–419.

Houtkooper, R. H., Mouchiroud, L., Ryu, D., Moullan, N., Katsyuba, E., Knott, G., Williams, R. W., & Auwerx, J. (2013). Mitonuclear protein imbalance as a conserved longevity mechanism. *Nature*, *497*(7450), 451–457.

Houtz, P., Bonfini, A., Bing, X., & Buchon, N. (2019). Recruitment of Adult Precursor Cells Underlies Limited Repair of the Infected Larval Midgut in *Drosophila*. *Cell Host and Microbe*, *26*(3), 412-425.

Hristova, V. A., Beasley, S. A., Rylett, R. J., & Shaw, G. S. (2009). Identification of a novel Zn^{2+} -binding domain in the autosomal recessive juvenile Parkinson-related E3 ligase parkin. *Journal of Biological Chemistry*, *284*(22), 14978–14986.

Hunter, R. L., Cheng, B., Choi, D. Y., Liu, M., Liu, S., Cass, W. A., & Bing, G. (2009). Intrastriatal lipopolysaccharide injection induces Parkinsonism in C57/B6 mice. *Journal of Neuroscience Research*, *87*(8), 1913–1921.

Hunter, R. L., Dragicevic, N., Seifert, K., Choi, D. Y., Liu, M., Kim, H. C., Cass, W. A., Sullivan, P. G., & Bing, G. (2007). Inflammation induces mitochondrial dysfunction and dopaminergic neurodegeneration in the nigrostriatal system. *Journal of Neurochemistry*, *100*(5), 1375–1386.

Iatsenko, I., Boquete, J. P., & Lemaitre, B. (2018). Microbiota-Derived Lactate Activates Production of Reactive Oxygen Species by the Intestinal NADPH Oxidase Nox and Shortens *Drosophila* Lifespan. *Immunity*, *49*(5), 929-942.

Ibáñez, P., Bonnet, A. M., Débarges, B., Lohmann, E., Tison, F., Pollak, P., Agid, Y., Dürr, A., & Brice, P. A. (2004). Causal relation between α-synuclein gene duplication and familial Parkinson's disease. *Lancet*, *364*(9440), 1169–1171.

Ibáñez, Pablo, Lesage, S., Lohmann, E., Thobois, S., De Michele, G., Borg, M., Agid, Y., Dürr, A., & Brice, A. (2006). Mutational analysis of the *PINK1* gene in early-onset parkinsonism in Europe and North Africa. *Brain*, *129*(3), 686–694.

Igaki, T. (2009). Correcting developmental errors by apoptosis: Lessons from *Drosophila* JNK signaling. *Apoptosis*, *14*(8), 1021–1028.

Igaki, T., Kanda, H., Yamamoto-Goto, Y., Kanuka, H., Kuranaga, E., Aigaki, T., & Miura, M. (2002). Eiger, a TNF superfamily ligand that triggers the *Drosophila* JNK pathway. *EMBO Journal*, *21*(12), 3009–3018.

Igarashi, R., Yamashita, S., Yamashita, T., Inoue, K., Fukuda, T., Fukuchi, T., & Kanki, T. (2020). Gemcitabine induces Parkin-independent mitophagy through mitochondrial-resident E3 ligase MUL1-mediated stabilization of PINK1. *Scientific Reports*, *10*(1), 1465.

Imaizumi, Y., Okada, Y., Akamatsu, W., Koike, M., Kuzumaki, N., Hayakawa, H., Nihira, T., Kobayashi, T., Ohyama, M., Sato, S., Takanashi, M., Funayama, M., Hirayama, A., Soga, T., Hishiki, T., Suematsu, M., Yagi, T., Ito, D., Kosakai, A., Mizushima, N., Amagai, M., Uchiyama, Y., Mochizuki, H., Hattori, N. & Okano, H. (2012). Mitochondrial dysfunction associated with increased oxidative stress and

α-synuclein accumulation in PARK2 iPSC-derived neurons and postmortem brain tissue. *Molecular Brain*, *5*(1).

Imamura, K., Hishikawa, N., Sawada, M., Nagatsu, T., Yoshida, M., & Hashizume, Y. (2003). Distribution of major histocompatibility complex class II-positive microglia and cytokine profile of Parkinson's disease brains. *Acta Neuropathologica*, *106*(6), 518–526.

Inden, M., Kitamura, Y., Abe, M., Tamaki, A., Takata, K., & Taniguchi, T. (2011). Parkinsonian rotenone mouse model: Reevaluation of long-term administration of rotenone in C57BL/6 mice. *Biological and Pharmaceutical Bulletin*, *34*(1), 92–96.

Ingerman, E., Perkins, E. M., Marino, M., Mears, J. A., McCaffery, J. M., Hinshaw, J. E., & Nunnari, J. (2005). Dnm1 forms spirals that are structurally tailored to fit mitochondria. *Journal of Cell Biology*, *170*(7), 1021–1027.

Inoue, H., Tateno, M., Fujimura-Kamada, K., Takaesu, G., Adachi-Yamada, T., Ninomiya-Tsuji, J., Irie, K., Nishida, Y., & Matsumoto, K. (2001). A *Drosophila* MAPKKK, D-MEKK1, mediates stress responses through activation of p38 MAPK. *EMBO Journal*, *20*(19), 5421–5430.

Ip, Y. T., & Davis, R. J. (1998). Signal transduction by the c-Jun N-terminal kinase (JNK) - From inflammation to development. *Current Opinion in Cell Biology*, *10*(2), 205–219.

Ishihara, N., Nomura, M., Jofuku, A., Kato, H., Suzuki, S. O., Masuda, K., Otera, H., Nakanishi, Y., Nonaka, I., Goto, Y. I., Taguchi, N., Morinaga, H., Maeda, M., Takayanagi, R., Yokota, S., & Mihara, K. (2009). Mitochondrial fission factor Drp1 is essential for embryonic development and synapse formation in mice. *Nature Cell Biology*, *11*(8), 958–966.

Ishikawa, H., & Barber, G. N. (2008). STING is an endoplasmic reticulum adaptor that facilitates innate immune signalling. *Nature*, *455*(7213), 674–678.

Itsara, L. S., Kennedy, S. R., Fox, E. J., Yu, S., Hewitt, J. J., Sanchez-Contreras, M., Cardozo-Pelaez, F., & Pallanck, L. J. (2014). Oxidative Stress Is Not a Major Contributor to Somatic Mitochondrial DNA Mutations. *PLoS Genetics*, *10*(2), e1003974.

Jackson-Lewis, V., Blesa, J., & Przedborski, S. (2012). Animal models of Parkinson's disease. *Parkinsonism and Related Disorders*, *18*, S183–S185.

Jagmag, S. A., Tripathi, N., Shukla, S. D., Maiti, S., & Khurana, S. (2016). Evaluation of models of Parkinson's disease. *Frontiers in Neuroscience*, *9*(JAN), 1–13.

Javitch, J. A., D'Amato, R. J., Strittmatter, S. M., & Snyder, S. H. (1985). Parkinsonism-inducing neurotoxin, N-methyl-4-phenyl-1,2,3,6-tetrahydropyridine: Uptake of the metabolite N-methyl-4-phenylpyridine by dopamine neurons explains selective toxicity. *Proceedings of the National Academy of Sciences of the United States of America*, *82*(7), 2173–2177.

Jeon, B. S., Jackson-Lewis, V., & Burke, R. E. (1995). 6-Hydroxydopamine Lesion of the Rat Substantia Nigra: Time Course and Morphology of Cell Death. *Neurodegeneration*, *4*(2), 131–137.

Jiang, H., Patel, P. H., Kohlmaier, A., Grenley, M. O., McEwen, D. G., & Edgar, B. A. (2009). Cytokine/Jak/Stat Signaling Mediates Regeneration and Homeostasis in the *Drosophila* Midgut. *Cell*, *137*(7), 1343–1355.

Jin, S. M., Lazarou, M., Wang, C., Kane, L. A., Narendra, D. P., & Youle, R. J. (2010). Mitochondrial membrane potential regulates PINK1 import and proteolytic destabilization by PARL. *Journal of Cell Biology*, *191*(5), 933–942.

Jin, S. M., & Youle, R. J. (2013). The accumulation of misfolded proteins in the mitochondrial matrix is sensed by PINK1 to induce PARK2/Parkin-mediated mitophagy of polarized mitochondria. *Autophagy*, *9*(11), 1750–1757.

Johnson, M. E., Stecher, B., Labrie, V., Brundin, L., & Brundin, P. (2019). Triggers, Facilitators, and Aggravators: Redefining Parkinson's Disease Pathogenesis. *Trends in Neurosciences*, *42*(1), 4–13.

Joo, H. S., Fu, C. I., & Otto, M. (2016). Bacterial strategies of resistance to antimicrobial peptides. Philosophical Transactions of the Royal Society B: Biological Sciences, 371(1695).

Jung, J. H., Bae, S., Lee, J. Y., Woo, S. R., Cha, H. J., Yoon, Y., Suh, K. S., Lee, S. J., Park, I. C., Jin, Y. W., Lee, K. H., An, S., & Lee, J. H. (2011). E3 ubiquitin ligase Hades negatively regulates the exonuclear function of p53. *Cell Death and Differentiation*, *18*(12), 1865–1875.

Kallio, J., Myllymäki, H., Grönholm, J., Armstrong, M., Vanha-Aho, L., Mäkinen, L., Silvennoinen, O., Valanne, S., & Rämet, M. (2010). Eye transformer is a negative regulator of *Drosophila* JAK/STAT signaling. *The FASEB Journal*, *24*(11), 4467–4479.

Kamel, F., Tanner, C. M., Umbach, D. M., Hoppin, J. A., Alavanja, M. C. R., Blair, A., Comyns, K., Goldman, S. M., Korell, M., Langston, J. W., Ross, G. W., & Sandler, D. P. (2007). Pesticide exposure and self-reported Parkinson's disease in the agricultural health study. *American Journal of Epidemiology*, *165*(4), 364–374.

Kamp, F., Exner, N., Lutz, A. K., Wender, N., Hegermann, J., Brunner, B., Nuscher, B., Bartels, T., Giese, A., Beyer, K., Eimer, S., Winklhofer, K. F., & Haass, C. (2010). Inhibition of mitochondrial fusion by α-synuclein is rescued by PINK1, Parkin and DJ-1. *The EMBO Journal*, *29*(20), 3571–3589.

Kandul, N. P., Zhang, T., Hay, B. A., & Guo, M. (2016). Selective removal of deletion-bearing mitochondrial DNA in heteroplasmic Drosophila. *Nature Communications*, *7*(1), 13100.

Kane, L. A., Lazarou, M., Fogel, A. I., Li, Y., Yamano, K., Sarraf, S. A., Banerjee, S., & Youle, R. J. (2014). PINK1 phosphorylates ubiquitin to activate parkin E3 ubiquitin ligase activity. *Journal of Cell Biology*, *205*(2), 143–153.

Kaneko, T., Yano, T., Aggarwal, K., Lim, J. H., Ueda, K., Oshima, Y., Peach, C., Erturk-Hasdemir, D., Goldman, W. E., Oh, B. H., Kurata, S., & Silverman, N. (2006). PGRP-LC and PGRP-LE have essential yet distinct functions in the *Drosophila* immune response to monomeric DAP-type peptidoglycan. *Nature Immunology*, *7*(7), 715–723.

Kang, P. J., Ostermann, J., Shilling, J., Neupert, W., Craig, E. A., & Pfanner, N. (1990). Requirement for hsp70 in the mitochondrial matrix for translocation and folding of precursor proteins. *Nature*, *348*(6297), 137–143.

Karbowski, M., & Youle, R. J. (2011). Regulating mitochondrial outer membrane proteins by ubiquitination and proteasomal degradation. *Current Opinion in Cell Biology*, *23*(4), 476–482.

Karin, M., & Clevers, H. (2016). Reparative inflammation takes charge of tissue regeneration. *Nature, 529*(7586), 307–315.

Karpac, J., Younger, A., & Jasper, H. (2011). Dynamic coordination of innate immune signaling and insulin signaling regulates systemic responses to localized DNA damage. *Developmental Cell*, *20*(6), 841–854.

Kasap, M., Akpinar, G., Sazci, A., Idrisoglu, H. A., & Vahaboğlu, H. (2009). Evidence for the presence of full-length PARK2 mRNA and Parkin protein in human blood. *Neuroscience Letters*, *460*(3), 196–200.

Katayama, H., Hama, H., Nagasawa, K., Kurokawa, H., Sugiyama, M., Ando, R., Funata, M., Yoshida, N., Homma, M., Nishimura, T., Takahashi, M., Ishida, Y., Hioki, H., Tsujihata, Y., & Miyawaki, A. (2020). Visualizing and Modulating Mitophagy for Therapeutic Studies of Neurodegeneration. *Cell*, *181*(5), 1176-1187.

Katayama, H., Kogure, T., Mizushima, N., Yoshimori, T., & Miyawaki, A. (2011). A sensitive and quantitative technique for detecting autophagic events based on lysosomal delivery. *Chemistry and Biology*, *18*(8), 1042–1052.

Kato, H., Lu, Q., Rapaport, D., & Kozjak-Pavlovic, V. (2013). Tom70 Is Essential for PINK1 Import into Mitochondria. *PLoS ONE*, *8*(3), 1–6.

Kawahara, K., Hashimoto, M., Bar-On, P., Ho, G. J., Crews, L., Mizuno, H., Rockenstein, E., Imam, S. Z., & Masliah, E. (2008). α-Synuclein aggregates interfere with parkin solubility and distribution: Role in the pathogenesis of parkinson disease. *Journal of Biological Chemistry*, *283*(11), 6979–6987.

Kawajiri, S., Saiki, S., Sato, S., & Hattori, N. (2011). Genetic mutations and functions of PINK1. *Trends in Pharmacological Sciences*, *32*(10), 573–580.

Kazak, L., Reyes, A., & Holt, I. J. (2012). Minimizing the damage: Repair pathways keep mitochondrial DNA intact. *Nature Reviews Molecular Cell Biology*, *13*(10), 659–671.

Kazlauskaite, A., Kondapalli, C., Gourlay, R., Campbell, D. G., Ritorto, M. S., Hofmann, K., Alessi, D. R., Knebel, A., Trost, M., & Muqit, M. M. K. (2014). Parkin is activated by PINK1-dependent phosphorylation of ubiquitin at Ser65. *The Biochemical Journal*, *460*(1), 127–139.

Kazlauskaite, A., Martínez-Torres, R. J., Wilkie, S., Kumar, A., Peltier, J., Johnson, C., Zhang, J., Hope, A. G., Peggie, M., Trost, M., Mf, D., Aalten, V., Alessi, D. R., Prescott, A. R., Knebel, A., Walden, H., & Muqit, M. M. K. (2015). Binding to serine 65-phosphorylated ubiquitin primes Parkin for optimal PINK1-dependent phosphorylation and activation. *EMBO Reports*, *16*(8), 1–16.

Kazlauskaite, A., & Muqit, M. M. K. (2015). PINK1 and Parkin - Mitochondrial interplay between phosphorylation and ubiquitylation in Parkinson's disease. *FEBS Journal*, *282*(2), 215–223.

Keeney, P. M., Xie, J., Capaldi, R. A., & Bennett, J. P. (2006). Parkinson's disease brain mitochondrial complex I has oxidatively damaged subunits and is

functionally impaired and misassembled. *Journal of Neuroscience*, *26*(19), 5256–5264.

Kennedy, S. R., Salk, J. J., Schmitt, M. W., & Loeb, L. A. (2013). Ultra-Sensitive Sequencing Reveals an Age-Related Increase in Somatic Mitochondrial Mutations That Are Inconsistent with Oxidative Damage. *PLoS Genetics*, *9*(9), e1003794.

Khan, N. L., Jain, S., Lynch, J. M., Pavese, N., Abou-Sleiman, P., Holton, J. L., Healy, D. G., Gilks, W. P., Sweeney, M. G., Ganguly, M., Gibbons, V., Gandhi, S., Vaughan, J., Eunson, L. H., Katzenschlager, R., Gayton, J., Lennox, G., Revesz, T., Nicholl, D., Bhatia, K. P., Quinn, N., Brooks, D., Lees, A. J., Davis, M. B., Piccini, P., Singleton, A. B. & Wood, N. W. (2005). Mutations in the gene *LRRK2* encoding dardarin (*PARK8*) cause familial Parkinson's disease: Clinical, pathological, olfactory and functional imaging and genetic data. *Brain*, *128*(12), 2786–2796.

Kiely, A. P., Asi, Y. T., Kara, E., Limousin, P., Ling, H., Lewis, P., Proukakis, C., Quinn, N., Lees, A. J., Hardy, J., Revesz, T., Houlden, H., & Holton, J. L. (2013). α-synucleinopathy associated with G51D *SNCA* mutation: A link between Parkinson's disease and multiple system atrophy? *Acta Neuropathologica*, *125*(5), 753–769.

Kim, E. K., Lee, K. A., Hyeon, D. Y., Kyung, M., Jun, K. Y., Seo, S. H., Hwang, D., Kwon, Y., & Lee, W. J. (2020). Bacterial Nucleoside Catabolism Controls Quorum Sensing and Commensal-to-Pathogen Transition in the *Drosophila* Gut. *Cell Host and Microbe*, *27*(3), 345-357.

Kim, Y. Y., Um, J. H., Yoon, J. H., Kim, H., Lee, D. Y., Lee, Y. J., Jee, H. J., Kim, Y. M., Jang, J. S., Jang, Y. G., Chung, J., Park, H. T., Finkel, T., Koh, H., & Yun, J. (2019). Assessment of mitophagy in mt-Keima Drosophila revealed an essential role of the PINK1-Parkin pathway in mitophagy induction in vivo. *FASEB Journal*, *33*(9), 9742–9751.

King, L., & Plun-Favreau, H. (2017). Chapter 5 - Mitophagy. *Parkinson's Disease*.

Kirisako, T., Kamei, K., Murata, S., Kato, M., Fukumoto, H., Kanie, M., Sano, S., Tokunaga, F., Tanaka, K., & Iwai, K. (2006). A ubiquitin ligase complex assembles linear polyubiquitin chains. *EMBO Journal*, *25*(20), 4877–4887.

Kisseleva, T., Bhattacharya, S., Braunstein, J., & Schindler, C. W. (2002). Signaling through the JAK/STAT pathway, recent advances and future challenges. *Gene*, *285*(1–2), 1–24.

Kiššová, I., Deffieu, M. M., Phen Manon, S., & Camougrand, N. (2004). Uth1p Is Involved in the Autophagic Degradation of Mitochondria. *The Journal of Biological Chemistry*, *279*(37), 39068–39074.

Kitada, T., Asakawa, S., Hattori, N., Matsumine, H., Yamamura, Y., Minoshima, S., Yokochi, M., Mizuno, Y., & Shimizu, N. (1998). Mutations in the *parkin* gene cause autosomal recessive juvenile parkinsonism. *Nature*, *392*(6676), 605–608.

Klein, C., Lohmann-Hedrich, K., Rogaeva, E., Schlossmacher, M. G., & Lang, A. E. (2007). Deciphering the role of heterozygous mutations in genes associated with parkinsonism. *Lancet Neurology*, *6*(7), 652–662.

Kleino, A., & Silverman, N. (2014). The *Drosophila* IMD pathway in the activation of the humoral immune response. *Developmental & Comparative Immunology*, *42*(1), 25–35.

Ko, H. S., Lee, Y., Shin, J. H., Karuppagounder, S. S., Gadad, B. S., Koleske, A. J., Pletnikova, O., Troncoso, J. C., Dawson, V. L., & Dawson, T. M. (2010). Phosphorylation by the c-Abl protein tyrosine kinase inhibits parkin's ubiquitination and protective function. *Proceedings of the National Academy of Sciences of the United States of America*, *107*(38), 16691–16696.

Ko, H. S., Von Coelln, R., Sriram, S. R., Kim, S. W., Chung, K. K. K., Pletnikova, O., Troncoso, J., Johnson, B., Saffary, R., Goh, E. L., Song, H., Park, B. J., Kim, M. J., Kim, S., Dawson, V. L., & Dawson, T. M. (2005). Accumulation of the authentic parkin substrate aminoacyl-tRNA synthetase cofactor, p38/JTV-1, leads to catecholaminergic cell death. *Journal of Neuroscience*, *25*(35), 7968–7978.

Koch, A., Thiemann, M., Grabenbauer, M., Yoon, Y., McNiven, M. A., & Schrader, M. (2003). Dynamin-like protein 1 is involved in peroxisomal fission. *Journal of Biological Chemistry*, *278*(10), 8597–8605.

Koehler, C. L., Perkins, G. A., Ellisman, M. H., & Jones, D. L. (2017). Pink1 and Parkin regulate *Drosophila* intestinal stem cell proliferation during stress and aging. *Journal of Cell Biology*, *216*(8), 2315–2327.

Kolitsida, P., Zhou, J., Rackiewicz, M., Nolic, V., Dengjel, J., & Abeliovich, H. (2019). Phosphorylation of mitochondrial matrix proteins regulates their selective mitophagic degradation. *Proceedings of the National Academy of Sciences of the United States of America*, *116*(41), 20517–20527.

Kondapalli, C., Kazlauskaite, A., Zhang, N., Woodroof, H. I., Campbell, D. G., Gourlay,

R., Burchell, L., Walden, H., Macartney, T. J., Deak, M., Knebel, A., Alessi, D. R., & Muqit, M. M. K. (2012). PINK1 is activated by mitochondrial membrane potential depolarization and stimulates Parkin E3 ligase activity by phosphorylating Serine 65. *Open Biology*, *2*(5), 1–17.

Kopin, I. J., & Markey, S. P. (1988). MPTP Toxicity: Implications for Research in Parkinson's Disease. *Annual Review of Neuroscience*, *11*(1), 81–96.

Koppen, M., & Langer, T. (2007). Protein degradation within mitochondria: Versatile activities of AAA proteases and other peptidases. *Critical Reviews in Biochemistry and Molecular Biology*, *42*(3), 221–242.

Koros, C., Simitsi, A., & Stefanis, L. (2017). Chapter 8 - Genetics of Parkinson's Disease: Genotype–Phenotype Correlation. *International Review of Neurobiology.*

Kounatidis, I., Chtarbanova, S., Cao, Y., Hayne, M., Jayanth, D., Ganetzky, B., & Ligoxygakis, P. (2017). NF-κB Immunity in the Brain Determines Fly Lifespan in Healthy Aging and Age-Related Neurodegeneration. *Cell Reports*, *19*(4), 836–848.

Kraytsberg, Y., Kudryavtseva, E., McKee, A. C., Geula, C., Kowall, N. W., & Khrapko, K. (2006). Mitochondrial DNA deletions are abundant and cause functional impairment in aged human substantia nigra neurons. *Nature Genetics*, *38*(5), 518–520.

Krüger, R., Kuhn, W., Müller, T., Woitalla, D., Graeber, M., Kösel, S., Przuntek, H., Epplen, J. T., Schöls, L., & Riess, O. (1998). Ala30Pro mutation in the gene encoding α-synuclein in Parkinson's disease. *Nature Genetics*, *18*(2), 106–108.

Kühlbrandt, W. (2015). Structure and function of mitochondrial membrane protein complexes. *BMC Biology*, *13*(1), 1–11.

Kujoth, G. C., Hiona, A., Pugh, T. D., Someya, S., Panzer, K., Wohlgemuth, S. E., Hofer, T., Seo, A. Y., Sullivan, R., Jobling, W. A., Morrow, J. D., Remmen, H. Van, Sedivy, J. M., Yamasoba, T., Tanokura, M., Weindruch, R., Leeuwenburgh, C., & Prolla, T. A. (2005). Mitochondrial DNA Mutations, Oxidative Stress, and Apoptosis in Mammalian Aging. *Science*, *309*(5733), 481–485.

Kundu, M., Lindsten, T., Yang, C. Y., Wu, J., Zhao, F., Zhang, J., Selak, M. A., Ney, P. A., & Thompson, C. B. (2008). Ulk1 plays a critical role in the autophagic clearance of mitochondria and ribosomes during reticulocyte maturation. *Blood*, *112*(4),

1493–1502.

Kuroda, Y., Mitsui, T., Kunishige, M., Shono, M., Akaike, M., Azuma, H., & Matsumoto, T. (2006). Parkin enhances mitochondrial biogenesis in proliferating cells. *Human Molecular Genetics*, *15*(6), 883–895.

Kurup, P. K., Xu, J., Videira, R. A., Ononenyi, C., Baltazar, G., Lombroso, P. J., & Nairn, A. C. (2015). STEP61 is a substrate of the E3 ligase parkin and is upregulated in Parkinson's disease. *Proceedings of the National Academy of Sciences of the United States of America*, *112*(4), 1202–1207.

Kyriakis, J. M., & Avruch, J. (1996). Protein kinase cascades activated by stress and inflammatory cytokines. *BioEssays*, *18*(7), 567–577.

Laker, R. C., Xu, P., Ryall, K. A., Sujkowski, A., Kenwood, B. M., Chain, K. H., Zhang, M., Royal, M. A., Hoehn, K. L., Driscoll, M., Adler, P. N., Wessells, R. J., Saucerman, J. J., & Yan, Z. (2014). A novel mitoTimer reporter gene for mitochondrial content, structure, stress, and damage *in vivo*. *Journal of Biological Chemistry*, *289*(17), 12005–12015.

Lane, N., & Martin, W. (2010). The energetics of genome complexity. *Nature*, *467*(7318), 929–934.

Lang, A. E., & Lozano, A. M. (1998a). Parkinson's disease. First of two parts. *New England Journal of Medicine*, *339*(15), 1044–1053.

Lang, A. E., & Lozano, A. M. (1998b). Parkinson's disease. Second of two parts. *New England Journal of Medicine*, *339*(16), 1130–1143.

Langer, T. (2000). AAA proteases: Cellular machines for degrading membrane proteins. *Trends in Biochemical Sciences*, *25*(5), 247–251.

Langston, J. W., Forno, L. S., Tetrud, J., Reeves, A. G., Kaplan, J. A., & Karluk, D. (1999). Evidence of active nerve cell degeneration in the substantia nigra of humans years after 1-methyl-4-phenyl-1,2,3,6-tetrahydropyridine exposure. *Annals of Neurology*, *46*(4), 598–605.

Langston, J. W. (2006). The Parkinson's complex: Parkinsonism is just the tip of the Iceberg. *Annals of Neurology*, *59*(4), 591–596.

Langston, J. W., Langston, E. B., & Irwin, I. (1984). MPTP-induced parkinsonism in

human and non-human primates–clinical and experimental aspects. *Acta Neurologica Scandinavica. Supplementum*, *100*, 49–54.

Langston, J. W., Ballard, P., Tetrud, J. W., & Irwin, I. (1983). Chronic parkinsonism in humans due to a product of meperidine-analog synthesis. *Science*, *219*(4587), 979–980.

Lapointe, N., St-Hilaire, M., Martinoli, M., Blanchet, J., Gould, P., Rouillard, C., & Cicchetti, F. (2004). Rotenone induces non-specific central nervous system and systemic toxicity. *The FASEB Journal*, *18*(6), 717–719.

Lazarou, M., Jin, S. M., Kane, L. A., & Youle, R. J. (2012). Role of PINK1 Binding to the TOM Complex and Alternate Intracellular Membranes in Recruitment and Activation of the E3 Ligase Parkin. *Developmental Cell*, *22*(2), 320–333.

Lazarou, M., Sliter, D. A., Kane, L. A., Sarraf, S. A., Wang, C., Burman, J. L., Sideris, D. P., Fogel, A. I., & Youle, R. J. (2015). The ubiquitin kinase PINK1 recruits autophagy receptors to induce mitophagy. *Nature*, *524*(7565), 309–314.

Lee, J. E., Westrate, L. M., Wu, H., Page, C., & Voeltz, G. K. (2016). Multiple dynamin family members collaborate to drive mitochondrial division. *Nature*, *540*(7631), 139–143.

Lee, J. J., Sanchez-Martinez, A., Zarate, A. M., Benincá, C., Mayor, U., Clague, M. J., & Whitworth, A. J. (2018). Basal mitophagy is widespread in *Drosophila* but minimally affected by loss of *Pink1* or *parkin*. *Journal of Cell Biology*, *217*(5), 1613–1622.

Lee, K. A., Kim, B., Bhin, J., Kim, D. H., You, H., Kim, E. K., Kim, S. H., Ryu, J. H., Hwang, D., & Lee, W. J. (2015). Bacterial Uracil Modulates *Drosophila* DUOX-Dependent Gut Immunity via Hedgehog-Induced Signaling Endosomes. *Cell Host & Microbe*, *17*(2), 191–204.

Lee, K. A., Kim, S. H., Kim, E. K., Ha, E. M., You, H., Kim, B., Kim, M. J., Kwon, Y., Ryu, J. H., & Lee, W. J. (2013). Bacterial-derived uracil as a modulator of mucosal immunity and gut-microbe homeostasis in *Drosophila*. *Cell*, *153*(4), 797–811.

Lee, Y., Stevens, D. A., Kang, S. U., Jiang, H., Lee, Y. Il, Ko, H. S., Scarffe, L. A., Umanah, G. E., Kang, H., Ham, S., Kam, T. I., Allen, K., Brahmachari, S., Kim, J. W., Neifert, S., Yun, S. P., Fiesel, F. C., Springer, W., Dawson, V. L., Shin, J. H. and Dawson, T. M. (2017). PINK1 Primes Parkin-Mediated Ubiquitination of PARIS in Dopaminergic Neuronal Survival. *Cell Reports*, *18*(4), 918–932.

Lees, A. J., Hardy, J., & Revesz, T. (2009). Parkinson's disease. *The Lancet*, *373*(9680), 2055–2066.

Lemaitre, B., & Hoffmann, J. (2007). The Host Defense of *Drosophila melanogaster*. *Annual Review of Immunology*, *25*(1), 697–743.

Lemaitre, B., Reichhart, J. M., & Hoffmann, J. A. (1997). *Drosophila* host defense: Differential induction of antimicrobial peptide genes after infection by various classes of microorganisms. *Proceedings of the National Academy of Sciences of the United States of America*, *94*(26), 14614–14619.

Lemasters, J. J. (2005). Selective mitochondrial autophagy, or mitophagy, as a targeted defense against oxidative stress, mitochondrial dysfunction, and aging. *Rejuvenation Research, 8*(1), 3–5.

Leonhard, K., Herrmann, J. M., Stuart, R. A., Mannhaupt, G., Neupert, W., & Langer, T. (1996). AAA proteases with catalytic sites on opposite membrane surfaces comprise a proteolytic system for the ATP-dependent degradation of inner membrane proteins in mitochondria. *The EMBO Journal*, *15*(16), 4218–4229.

Leonhard, Klaus, Guiard, B., Pellecchia, G., Tzagoloff, A., Neupert, W., & Langer, T. (2000). Membrane protein degradation by AAA proteases in mitochondria: Extraction of substrates from either membrane surface. *Molecular Cell*, *5*(4), 629–638.

Letts, J. A., Fiedorczuk, K., & Sazanov, L. A. (2016). The architecture of respiratory supercomplexes. *Nature*, *537*(7622), 644–648.

Li, J., Qi, W., Chen, G., Feng, D., Liu, J., Ma, B., Zhou, C., Mu, C., Zhang, W., Chen, Q., & Zhu, Y. (2015). Mitochondrial outer-membrane E3 ligase MUL1 ubiquitinates ULK1 and regulates selenite-induced mitophagy. *Autophagy*, *11*(8), 1216–1229.

Li, X. D., Wu, J., Gao, D., Wang, H., Sun, L., & Chen, Z. J. (2013). Pivotal roles of cGAS-cGAMP signaling in antiviral defense and immune adjuvant effects. *Science*, *341*(6152), 1390–1394.

Li, X., Sundquist, J., & Sundquist, K. (2012). Subsequent risks of Parkinson disease in patients with autoimmune and related disorders: A nationwide epidemiological study from Sweden. *Neurodegenerative Diseases*, *10*(1–4), 277–284.

Lill, C. M., & Klein, C. (2017). Chapter 1 – The Neurogenetics of Parkinson's Disease

and Putative Links to Other. *Parkinson's Disease*.

Lin, C. H., Chen, C. C., Chiang, H. L., Liou, J. M., Chang, C. M., Lu, T. P., Chuang, E. Y., Tai, Y. C., Cheng, C., Lin, H. Y., & Wu, M. S. (2019). Altered gut microbiota and inflammatory cytokine responses in patients with Parkinson's disease. *Journal of Neuroinflammation*, *16*(1), 1–9.

Lin, W., & Kang, U. J. (2008). Characterization of PINK1 processing, stability, and subcellular localization. *Journal of Neurochemistry*, *106*(1), 464–474.

Lin, Y. F., Schulz, A. M., Pellegrino, M. W., Lu, Y., Shaham, S., & Haynes, C. M. (2016). Maintenance and propagation of a deleterious mitochondrial genome by the mitochondrial unfolded protein response. *Nature*, *533*(7603), 416–419.

Liu, L., Feng, D., Chen, G., Chen, M., Zheng, Q., Song, P., Ma, Q., Zhu, C., Wang, R., Qi, W., Huang, L., Xue, P., Li, B., Wang, X., Jin, H., Wang, J., Yang, F., Liu, P., Zhu, Y., Sui, S. and Chen, Q. (2012). Mitochondrial outer-membrane protein FUNDC1 mediates hypoxia-induced mitophagy in mammalian cells. *Nature Cell Biology*, *14*(2), 177–185.

Liu, T., Zhang, L., Joo, D., & Sun, S. C. (2017). NF-κB signaling in inflammation. *Signal Transduction and Targeted Therapy*, *2*(1), e17023.

Liu, W., Acin-Perez, R., Geghman, K. D., Manfredi, G., Lu, B., & Li, C. (2011). Pink1 regulates the oxidative phosphorylation machinery via mitochondrial fission. *Proceedings of the National Academy of Sciences*, *108*(31), 12920–12924.

Liu, Y., Lin, J., Zhang, M., Chen, K., Yang, S., Wang, Q., Yang, H., Xie, S., Zhou, Y., Zhang, X., Chen, F., & Yang, Y. (2016). PINK1 is required for timely cell-type specific mitochondrial clearance during Drosophila midgut metamorphosis. *Developmental Biology*, *16*.

Liu, Y., Gordesky-Gold, B., Leney-Greene, M., Weinbren, N. L., Tudor, M., & Cherry, S. (2018). Inflammation-Induced, STING-Dependent Autophagy Restricts Zika Virus Infection in the *Drosophila* Brain. *Cell Host and Microbe*, *24*(1), 57-68.

Liu, Zhan, Huang, Y., Cao, B. B., Qiu, Y. H., & Peng, Y. P. (2017). Th17 Cells Induce Dopaminergic Neuronal Death via LFA-1/ICAM-1 Interaction in a Mouse Model of Parkinson's Disease. *Molecular Neurobiology*, *54*(10), 7762–7776.

Liu, Z., Hazan-Halevy, I., Harris, D. M., Li, P., Ferrajoli, A., Faderl, S., Keating, M. J.,

& Estrov, Z. (2011). STAT-3 activates NF-kB in chronic lymphocytic leukemia cells. *Molecular Cancer Research*, *9*(4), 507–515.

Lonskaya, I., Hebron, M. L., Algarzae, N. K., Desforges, N., & Moussa, C. E. H. (2013). Decreased parkin solubility is associated with impairment of autophagy in the nigrostriatum of sporadic Parkinson's disease. *Neuroscience*, *232*, 90–105.

López-Otín, C., Blasco, M. A., Partridge, L., Serrano, M., & Kroemer, G. (2013). The hallmarks of aging. *Cell*, *153*(6), 1194–1217.

Lopez, W., M. Page, A., J. Carlson, D., L. Ericson, B., F. Cserhati, M., Guda, C., & A. Carlson, K. (2018). Analysis of immune-related genes during Nora virus infection of *Drosophila melanogaster* using next generation sequencing. *AIMS Microbiology*, *4*(1), 123–139.

Losón, O. C., Song, Z., Chen, H., & Chan, D. C. (2013). Fis1, Mff, MiD49, and MiD51 mediate Drp1 recruitment in mitochondrial fission. *Molecular Biology of the Cell*, *24*(5), 659–667.

Lücking, C. B., Dürr, A., Bonifati, V., Vaughan, J., De Michele, G., Gasser, T., Harhangi, B. S., Meco, G., Denèfle, P., Wood, N. W., Agid, Y., Nicholl, D., Breteler, M. M. B., Oostra, B. A., De Mari, M., Marconi, R., Filla, A., Bonnet, A.-M., Broussolle, E., Pollak, P., Rascol, O., Rosier, M., Arnould, A. & Brice, A. (2000). Association between Early-Onset Parkinson's Disease and Mutations in the *Parkin* Gene. *New England Journal of Medicine*, *342*(21), 1560–1567.

Luthman, J., Fredriksson, A., Sundström, E., Jonsson, G., & Archer, T. (1989). Selective lesion of central dopamine or noradrenaline neuron systems in the neonatal rat: motor behavior and monoamine alterations at adult stage. *Behavioural Brain Research*, *33*(3), 267–277.

MacVicar, T. D. B., & Lane, J. D. (2014). Impaired OMA1-dependent cleavage of OPA1 and reduced DRP1 fission activity combine to prevent mitophagy in cells that are dependent on oxidative phosphorylation. *Journal of Cell Science*, *127*(10), 2313–2325.

Main, B. S., Zhang, M., Brody, K. M., Kirby, F. J., Crack, P. J., & Taylor, J. M. (2017). Type-I interferons mediate the neuroinflammatory response and neurotoxicity induced by rotenone. *Journal of Neurochemistry*, *141*(1), 75–85.

Maitra, U., Scaglione, M. N., Chtarbanova, S., & O'Donnell, J. M. (2019). Innate immune responses to paraquat exposure in a *Drosophila* model of Parkinson's

disease. *Scientific Reports*, *9*(1), 1–17.

Malik, B. R., Godena, V. K., & Whitworth, A. J. (2015). *VPS35* pathogenic mutations confer no dominant toxicity but partial loss of function in *Drosophila* and genetically interact with *parkin*. *Human Molecular Genetics*, *24*(21), 6106–6117.

Manfruelli, P., Reichhart, J. M., Steward, R., Hoffmann, J. A., & Lemaitre, B. (1999). A mosaic analysis in *Drosophila* fat body cells of the control of antimicrobial peptide genes by the Rel proteins Dorsal and DIF. *EMBO Journal*, *18*(12), 3380–3391.

Mangano, E. N., Litteljohn, D., So, R., Nelson, E., Peters, S., Bethune, C., Bobyn, J., & Hayley, S. (2012). Interferon-γ plays a role in paraquat-induced neurodegeneration involving oxidative and proinflammatory pathways. *Neurobiology of Aging*, *33*(7), 1411–1426.

Manning-Bog, A. B., McCormack, A. L., Li, J., Uversky, V. N., Fink, A. L., & Di Monte, D. A. (2002). The herbicide paraquat causes up-regulation and aggregation of α-synuclein in mice: Paraquat and α-synuclein. *Journal of Biological Chemistry*, *277*(3), 1641–1644.

Mantel, C., Messina-Graham, S., Moh, A., Cooper, S., Hangoc, G., Fu, X. Y., & Broxmeyer, H. E. (2012). Mouse hematopoietic cell-targeted STAT3 deletion: Stem/progenitor cell defects, mitochondrial dysfunction, ROS overproduction, and a rapid aging-like phenotype. *Blood*, *120*(13), 2589–2599.

Manzanillo, P. S., Ayres, J. S., Watson, R. O., Collins, A. C., Souza, G., Rae, C. S., Schneider, D. S., Nakamura, K., Shiloh, M. U., & Cox, J. S. (2013). The ubiquitin ligase parkin mediates resistance to intracellular pathogens. *Nature*, *501*(7468), 512–516.

Margineantu, D. H., Emerson, C. B., Diaz, D., & Hockenbery, D. M. (2007). Hsp90 inhibition decreases mitochondrial protein turnover. PLoS ONE, 2(10), e1066.

Maria Fimia, G., Stoykova, A., Romagnoli, A., Giunta, L., Di Bartolomeo, S., Nardacci, R., Corazzari, M., Fuoco, C., Ucar, A., Schwartz, P., Gruss, P., Piacentini, M., Chowdhury, K., & Cecconi, F. (2007). Ambra1 regulates autophagy and development of the nervous system. *Nature*, *447*(7148), 1121–1125.

Marks, A. R. (1997). Intracellular calcium-release channels: Regulators of cell life and death. *American Journal of Physiology - Heart and Circulatory Physiology*, *272*(2 Pt 2), 597–605.

Martin, M., Hiroyasu, A., Guzman, R. M., Roberts, S. A., & Goodman, A. G. (2018). Analysis of *Drosophila* STING Reveals an Evolutionarily Conserved Antimicrobial Function. *Cell Reports*, *23*(12), 3537-3550.

Martinez, A., Lectez, B., Ramirez, J., Popp, O., Sutherland, J. D., Urbé, S., Dittmar, G., Clague, M. J., & Mayor, U. (2017). Quantitative proteomic analysis of Parkin substrates in *Drosophila* neurons. *Molecular Neurodegeneration*, *12*(1), 1–19.

Martinon, F., Burns, K., & Tschopp, J. (2002). The Inflammasome: A molecular platform triggering activation of inflammatory caspases and processing of proIL-β. *Molecular Cell*, *10*(2), 417–426.

Matheoud, D., Cannon, T., Voisin, A., Penttinen, A. M., Ramet, L., Fahmy, A. M., Ducrot, C., Laplante, A., Bourque, M. J., Zhu, L., Cayrol, R., Le Campion, A., McBride, H. M., Gruenheid, S., Trudeau, L. E., & Desjardins, M. (2019). Intestinal infection triggers Parkinson's disease-like symptoms in *Pink1*$^{-/-}$ mice. *Nature*, *571*(7766), 565–569.

Matheoud, D., Sugiura, A., Bellemare-Pelletier, A., Laplante, A., Rondeau, C., Chemali, M., Fazel, A., Bergeron, J. J., Trudeau, L. E., Burelle, Y., Gagnon, E., McBride, H. M., & Desjardins, M. (2016). Parkinson's Disease-Related Proteins PINK1 and Parkin Repress Mitochondrial Antigen Presentation. *Cell*, *166*(2), 314–327.

Mathur, D., Bost, A., Driver, L., & Ohlstein, B. (2010). A transient niche regulates the specification of *Drosophila* intestinal stem cells. *Science*, *327*(5962), 210–213.

Matsuda, N., Kitami, T., Suzuki, T., Mizuno, Y., Hattori, N., & Tanaka, K. (2006). Diverse effects of pathogenic mutations of Parkin that catalyze multiple monoubiquitylation *in vitro*. *Journal of Biological Chemistry*, *281*(6), 3204–3209.

Matsuda, N., Sato, S., Shiba, K., Okatsu, K., Saisho, K., Gautier, C. A., Sou, Y., Saiki, S., Kawajiri, S., Sato, F., Kimura, M., Komatsu, M., Hattori, N., & Tanaka, K. (2010). PINK1 stabilized by mitochondrial depolarization recruits Parkin to damaged mitochondria and activates latent Parkin for mitophagy. *The Journal Of Cell Biology*, *189*(2), 211–221.

Matsushima, M., Fujiwara, T., Takahashi, E. I., Minaguchi, T., Eguchi, Y., Tsujimoto, Y., Suzumori, K., & Nakamura, Y. (1998). Isolation, mapping, and functional analysis of a novel human cDNA (*BNIP3L*) encoding a protein homologous to human NIP3. *Genes Chromosomes and Cancer*, *21*(3), 230–235.

Mattila, P. M., Rinne, J. O., Helenius, H., Dickson, D. W., & Röyttä, M. (2000). α-synuclein-immunoreactive cortical Lewy bodies are associated with cognitive impairment in Parkinson's disease. *Acta Neuropathologica*, *100*(3), 285–290.

McCormack, A. L., Thiruchelvam, M., Manning-Bog, A. B., Thiffault, C., Langston, J. W., Cory-Slechta, D. A., & Di Monte, D. A. (2002). Environmental risk factors and Parkinson's disease: Selective degeneration of nigral dopaminergic neurons caused by the herbicide paraquat. *Neurobiology of Disease*, *10*(2), 119–127.

McCoy, M. K., Martinez, T. N., Ruhn, K. A., Szymkowski, D. E., Smith, C. G., Botterman, B. R., Tansey, K. E., & Tansey, M. G. (2006). Blocking soluble tumor necrosis factor signaling with dominant-negative tumor necrosis factor inhibitor attenuates loss of dopaminergic neurons in models of Parkinson's disease. *Journal of Neuroscience*, *26*(37), 9365–9375.

McGee, D. J., Lu, X. H., & Disbrow, E. A. (2018). Stomaching the possibility of a pathogenic role for *Helicobacter pylori* in Parkinson's disease. *Journal of Parkinson's Disease*, *8*(3), 367–374.

McGeer, P. L., Itagaki, S., Boyes, B. E., & McGeer, E. G. (1988). Reactive microglia are positive for HLA-DR in the: Substantia nigra of Parkinson's and Alzheimer's disease brains. *Neurology*, *38*(8), 1285–1291.

McLelland, G. L., Goiran, T., Yi, W., Dorval, G., Chen, C. X., Lauinger, N. D., Krahn, A. I., Valimehr, S., Rakovic, A., Rouiller, I., Durcan, T. M., Trempe, J. F., & Fon, E. A. (2018). Mfn2 ubiquitination by PINK1/parkin gates the p97-dependent release of ER from mitochondria to drive mitophagy. *eLife*, *7*, 1–35.

McLelland, G. L., Lee, S. A., McBride, H. M., & Fon, E. A. (2016). Syntaxin-17 delivers PINK1/parkin-dependent mitochondrial vesicles to the endolysosomal system. *Journal of Cell Biology*, *214*(3), 275–291.

McLelland, G. L., Soubannier, V., Chen, C. X., Mcbride, H. M., & Fon, E. A. (2014). Parkin and PINK 1 function in a vesicular trafficking pathway regulating mitochondrial quality control. *The EMBO Journal*, *33*(4), 282–295.

McWilliams, T. G., Barini, E., Pohjolan-Pirhonen, R., Brooks, S. P., Singh, F., Burel, S., Balk, K., Kumar, A., Montava-Garriga, L., Prescott, A. R., Hassoun, S. M., Mouton-Liger, F., Ball, G., Hills, R., Knebel, A., Ulusoy, A., Di Monte, D. A., Tamjar, J., Antico, O., Fears, K., Smith, L., Brambilla, R., Palin, E., Valori, M., Eerola-Rautio, J., Tienari, P., Corti, O., Dunnett, S. B., Ganley, I. G., Suomalainen, A. & Muqit, M. M. K. (2018a). Phosphorylation of Parkin at serine 65 is essential for its

activation *in vivo*. *Open Biology*, *8*(11), 180108.

McWilliams, T. G., Prescott, A. R., Montava-Garriga, L., Ball, G., Singh, F., Barini, E., Muqit, M. M. K., Brooks, S. P., & Ganley, I. G. (2018b). Basal Mitophagy Occurs Independently of PINK1 in Mouse Tissues of High Metabolic Demand. *Cell Metabolism*, *27*(2), 439-449.

McWilliams, T. G., & Muqit, M. M. (2017). PINK1 and Parkin: emerging themes in mitochondrial homeostasis. *Current Opinion in Cell Biology*, *45*, 83–91.

McWilliams, T. G., Prescott, A. R., Allen, G. F. G., Tamjar, J., Munson, M. J., Thomson, C., Muqit, M. M. K., & Ganley, I. G. (2016). Mito-QC illuminates mitophagy and mitochondrial architecture *in vivo*. *Journal of Cell Biology*, *214*(3), 333–345.

Mears, J. A., Lackner, L. L., Fang, S., Ingerman, E., Nunnari, J., & Hinshaw, J. E. (2011). Conformational changes in Dnm1 support a contractile mechanism for mitochondrial fission. *Nature Structural and Molecular Biology*, *18*(1), 20–27.

Meier, J. A., & Larner, A. C. (2014). Toward a new STATe: The role of STATs in mitochondrial function. *Seminars in Immunology*, *26*(1), 20–28.

Meissner, C., Lorenz, H., Weihofen, A., Selkoe, D. J., & Lemberg, M. K. (2011). The mitochondrial intramembrane protease PARL cleaves human Pink1 to regulate Pink1 trafficking. *Journal of Neurochemistry*, *117*(5), 856–867.

Melser, S., Chatelain, E. H., Lavie, J., Mahfouf, W., Jose, C., Obre, E., Goorden, S., Priault, M., Elgersma, Y., Rezvani, H. R., Rossignol, R., & Bénard, G. (2013). Rheb regulates mitophagy induced by mitochondrial energetic status. *Cell Metabolism*, *17*(5), 719–730.

Meng, X., Khanuja, B. S., & Ip, Y. T. (1999). Toll receptor-mediated *Drosophila* immune response requires Dif, an NF- κB factor. *Genes and Development*, *13*(7), 792–797.

Miguel-Aliaga, I., Jasper, H., & Lemaitre, B. (2018). Anatomy and Physiology of the Digestive Tract of *Drosophila melanogaster*. *Genetics*, *210*(2), 357–396.

Miller, D. W., Hague, S. M., Clarimon, J., Baptista, M., Gwinn-Hardy, K., Cookson, M. R., & Singleton, A. B. (2004). α-synuclein in blood and brain from familial Parkinson disease with *SNCA* locus triplication. *Neurology*, *62*(10), 1835–1838.

Mishra, P., & Chan, D. C. (2014). Mitochondrial dynamics and inheritance during cell division, development and disease. *Nature Reviews Molecular Cell Biology*, *15*(10), 634–646.

Mitchell, P. (1966). Chemiosmotic coupling in oxidative and photosynthetic phosphorylation. *Biological reviews of the Cambridge Philosophical Society*, *41*(3), 445–502.

Mitchell, Peter. (1961). Coupling of phosphorylation to electron and hydrogen transfer by a chemi-osmotic type of mechanism. *Nature*, *191*(4784), 144–148.

Mogi, M., Kondo, T., Mizuno, Y., & Nagatsu, T. (2007). p53 protein, interferon-γ, and NF-κB levels are elevated in the parkinsonian brain. *Neuroscience Letters*, *414*(1), 94–97.

Mogi, M., Togari, A., Tanaka, K. I., Ogawa, N., Ichinose, H., & Nagatsu, T. (1999). Increase in level of tumor necrosis factor (TNF)-α in 6- hydroxydopamine-lesioned striatum in rats without influence of systemic L- DOPA on the TNF-α induction. *Neuroscience Letters*, *268*(2), 101–104.

Moisoi, N., Fedele, V., Edwards, J., & Martins, L. M. (2014). Loss of *PINK1* enhances neurodegeneration in a mouse model of Parkinson's disease triggered by mitochondrial stress. *Neuropharmacology*, *77*, 350–357.

Molina, A. J. A., Wikstrom, J. D., Stiles, L., Las, G., Mohamed, H., Elorza, A., Walzer, G., Twig, G., Katz, S., Corkey, B. E., & Shirihai, O. S. (2009). Mitochondrial networking protects β-cells from nutrient-induced apoptosis. *Diabetes*, *58*(10), 2303–2315.

Montava-Garriga, L., & Ganley, I. G. (2020). Outstanding Questions in Mitophagy: What We Do and Do Not Know. *Journal of Molecular Biology*, *432*(1), 206–230.

Mount, M. P., Lira, A., Grimes, D., Smith, P. D., Faucher, S., Slack, R., Anisman, H., Hayley, S., & Park, D. S. (2007). Involvement of interferon-γ in microglial-mediated loss of dopaminergic neurons. *Journal of Neuroscience*, *27*(12), 3328–3337.

Mouton-Liger, F., Rosazza, T., Sepulveda-Diaz, J., Ieang, A., Hassoun, S. M., Claire, E., Mangone, G., Brice, A., Michel, P. P., Corvol, J. C., & Corti, O. (2018). Parkin deficiency modulates NLRP3 inflammasome activation by attenuating an A20-dependent negative feedback loop. *Glia*, *66*(8), 1736–1751.

Muenter, M. D., Forno, L. S., Hornykiewicz, O., Kish, S. J., Maraganore, D. M., Caselli, R. J., Okazaki, H., Howard, F. M., Snow, B. J., & Calne, D. B. (1998). Hereditary form of parkinsonism-dementia. *Annals of Neurology*, *43*(6), 768–781.

Muqit, M. M. K., Abou-Sleiman, P. M., Saurin, A. T., Harvey, K., Gandhi, S., Deas, E., Eaton, S., Payne Smith, M. D., Venner, K., Matilla, A., Healy, D. G., Gilks, W. P., Lees, A. J., Holton, J., Revesz, T., Parker, P. J., Harvey, R. J., Wood, N. W., & Latchman, D. S. (2006). Altered cleavage and localization of PINK1 to aggresomes in thepresence of proteasomal stress. *Journal of Neurochemistry*, *98*(1), 156–169.

Murley, A., Lackner, L. L., Osman, C., West, M., Voeltz, G. K., Walter, P., & Nunnari, J. (2013). ER-associated mitochondrial division links the distribution of mitochondria and mitochondrial DNA in yeast. *eLife*, *2013*(2).

Murphy, M. P. (2009). How mitochondria produce reactive oxygen species. *Biochemical Journal*, *417*(1), 1–13.

Murphy, M. P. (2018). Newly made mitochondrial DNA drives inflammation. *Nature*, *560*(7717), 176–177.

Myers, A. L., Harris, C. M., Choe, K. M., & Brennan, C. A. (2018). Inflammatory production of reactive oxygen species by *Drosophila* hemocytes activates cellular immune defenses. *Biochemical and Biophysical Research Communications*, *505*(3), 726–732.

Myllymäki, H., & Rämet, M. (2014). JAK/STAT Pathway in *Drosophila* Immunity. *Scandinavian Journal of Immunology*, *79*(6), 377–385.

Myllymäki, Henna, Valanne, S., & Rämet, M. (2014). The *Drosophila* Imd Signaling Pathway . *The Journal of Immunology*, *192*(8), 3455–3462.

Nagashima, S., Tábara, L.-C., Tilokani, L., Paupe, V., Anand, H., Pogson, J. H., Zunino, R., McBride, H. M., & Prudent, J. (2020). Golgi-derived PI(4)P-containing vesicles drive late steps of mitochondrial division. *Science*, *367*(6484), 1366–1371.

Nagata, S. (2018). Apoptosis and clearance of apoptotic cells. *Annual Review of Immunology*, *36*(1), 489–517.

Nakahira, K., Haspel, J. A., Rathinam, V. A. K., Lee, S. J., Dolinay, T., Lam, H. C.,

Englert, J. A., Rabinovitch, M., Cernadas, M., Kim, H. P., Fitzgerald, K. A., Ryter, S. W., & Choi, A. M. K. (2011). Autophagy proteins regulate innate immune responses by inhibiting the release of mitochondrial DNA mediated by the NALP3 inflammasome. *Nature Immunology*, *12*(3), 222–230.

Nakahira, K., Hisata, S., & Choi, A. M. K. (2015). The Roles of Mitochondrial Damage-Associated Molecular Patterns in Diseases. *Antioxidants and Redox Signaling*, *23*(17), 1329–1350.

Nalls, M. A., Plagnol, V., Hernandez, D. G., Sharma, M., Sheerin, U. M., Saad, M., Simón-Sánchez, J., Schulte, C., Lesage, S., Sveinbjörnsdóttir, S., Stefánsson, K., Martinez, M., Hardy, J., Heutink, P., Brice, A., Gasser, T., Singleton, A. B., & Wood, N. W. (2011). Imputation of sequence variants for identification of genetic risks for Parkinson's disease: A meta-analysis of genome-wide association studies. *The Lancet*, *377*(9766), 641–649.

Narendra, D. P., Jin, S. M., Tanaka, A., Suen, D., Gautier, C. A., Shen, J., Cookson, M. R., & Youle, R. J. (2010). PINK1 Is Selectively Stabilized on Impaired Mitochondria to Activate Parkin. *PLoS Biology*, *8*(1).

Narendra, D., Tanaka, A., Suen, D., & Youle, R. J. (2008). Parkin is recruited selectively to impaired mitochondria and promotes their autophagy. *The Journal Of Cell Biology*, *183*(5), 795–803.

Nautiyal, M., Sweatt, A. J., MacKenzie, J. A., Mark Payne, R., Szucs, S., Matalon, R., Wallin, R., & Hutson, S. M. (2010). Neuronal localization of the mitochondrial protein NIPSNAP1 in rat nervous system. *European Journal of Neuroscience*, *32*(4), 560–569.

Nebreda, A. R., & Porras, A. (2000). p38 MAP kinases: beyond the stress response. *Trends in Biochemical Sciences*, *25*(6), 257–260.

Nerius, M., Doblhammer, G., & Tamgüney, G. (2019). GI infections are associated with an increased risk of Parkinson's disease. *Gut*, *69*(6), 1154–1156.

Neuspiel, M., Schauss, A. C., Braschi, E., Zunino, R., Rippstein, P., Rachubinski, R. A., Andrade-Navarro, M. A., & McBride, H. M. (2008). Cargo-Selected Transport from the Mitochondria to Peroxisomes Is Mediated by Vesicular Carriers. *Current Biology*, *18*(2), 102–108.

Newman, L. E., & Shadel, G. S. (2018). Pink1/Parkin link inflammation, mitochondrial stress, and neurodegeneration. *Journal of Cell Biology*, *217*(10), 3327–3329.

Ngo, J. K., & Davies, K. J. A. (2009). Mitochondrial Lon protease is a human stress protein. *Free Radical Biology and Medicine*, *46*(8), 1042–1048.

Nguyen, Thanh N., Padman, B. S., & Lazarou, M. (2016). Deciphering the Molecular Signals of PINK1/Parkin Mitophagy. *Trends in Cell Biology*, *26*(10), 733–744.

Nguyen, Thanh Ngoc, Padman, B. S., Usher, J., Oorschot, V., Ramm, G., & Lazarou, M. (2016). Atg8 family LC3/GABARAP proteins are crucial for autophagosome–lysosome fusion but not autophagosome formation during PINK1/Parkin mitophagy and starvation. *Journal of Cell Biology*, *215*(6), 857–874.

Ni, H. M., Williams, J. A., & Ding, W. X. (2015). Mitochondrial dynamics and mitochondrial quality control. *Redox Biology*, *4*, 6–13.

Nicolas, C. S., Amici, M., Bortolotto, Z. A., Doherty, A., Csaba, Z., Fafouri, A., Dournaud, P., Gressens, P., Collingridge, G. L., & Peineau, S. (2013). The role of JAK-STAT signaling within the CNS. *Jak-Stat*, *2*(1), e22925.

Nolden, M., Ehses, S., Koppen, M., Bernacchia, A., Rugarli, E. I., & Langer, T. (2005). The m-AAA protease defective in hereditary spastic paraplegia controls ribosome assembly in mitochondria. *Cell*, *123*(2), 277–289.

Nunnari, J., & Suomalainen, A. (2012). Mitochondria: In Sickness and in Health. *Cell*, *148*(6), 1145–1159.

Nunomura, A., Perry, G., Aliev, G., Hirai, K., Takeda, A., Balraj, E. K., Jones, P. K., Ghanbari, H., Wataya, T., Shimohama, S., Chiba, S., Atwood, C. S., Petersen, R. B., & Smith, M. A. (2001). Oxidative damage is the earliest event in Alzheimer disease. *Journal of Neuropathology and Experimental Neurology*, *60*(8), 759–767.

Nuytemans, K., Theuns, J., Cruts, M., & Van Broeckhoven, C. (2010). Genetic etiology of Parkinson disease associated with mutations in the *SNCA, PARK2, PINK1, PARK7*, and *LRRK2* genes: A mutation update. *Human Mutation*, *31*(7), 763–780).

O'Callaghan, J. P., Kelly, K. A., VanGilder, R. L., Sofroniew, M. V., & Miller, D. B. (2014). Early activation of STAT3 regulates reactive astrogliosis induced by diverse forms of neurotoxicity. *PLoS ONE*, *9*(7).

Ogawa, N., Hirose, Y., Ohara, S., Ono, T., & Watanabe, Y. (1985). A simple quantitative bradykinesia test in MPTP-treated mice. *Research Communications*

in Chemical Pathology and Pharmacology, *50*(3), 435–441.

Ohlstein, B., & Spradling, A. (2006). The adult *Drosophila* posterior midgut is maintained by pluripotent stem cells. *Nature*, *439*(7075), 470–474.

Okatsu, K., Koyano, F., Kimura, M., Kosako, H., Saeki, Y., Tanaka, K., & Matsuda, N. (2015). Phosphorylated ubiquitin chain is the genuine Parkin receptor. *The Journal Of Cell Biology*, *209*(1), 111–128.

Okatsu, K., Oka, T., Iguchi, M., Imamura, K., Kosako, H., Tani, N., Kimura, M., Go, E., Koyano, F., Funayama, M., Shiba-Fukushima, K., Sato, S., Shimizu, H., Fukunaga, Y., Taniguchi, H., Komatsu, M., Hattori, N., Mihara, K., Tanaka, K., & Matsuda, N. (2012). PINK1 autophosphorylation upon membrane potential dissipation is essential for Parkin recruitment to damaged mitochondria. *Nature Communications*, *3*(1016), 1–7.

Ordureau, A., Sarraf, S. A., Duda, D. M., Heo, J. M., Jedrychowski, M. P., Sviderskiy, V. O., Olszewski, J. L., Koerber, J. T., Xie, T., Beausoleil, S. A., Wells, J. A., Gygi, S. P., Schulman, B. A., & Harper, J. W. (2014). Quantitative proteomics reveal a feedforward mechanism for mitochondrial PARKIN translocation and ubiquitin chain synthesis. *Molecular Cell*, *56*(3), 360–375.

Osellame, L. D., Singh, A. P., Stroud, D. A., Palmer, C. S., Stojanovski, D., Ramachandran, R., & Ryan, M. T. (2016). Cooperative and independent roles of the Drp1 adaptors Mff, MiD49 and MiD51 in mitochondrial fission. *Journal of Cell Science*, *129*(11), 2170–2181.

Osman, C., Voelker, D. R., & Langer, T. (2011). Making heads or tails of phospholipids in mitochondria. *Journal of Cell Biology*, *192*(1), 7–16.

Osman, D., Buchon, N., Chakrabarti, S., Huang, Y. T., Su, W. C., Poidevin, M., Tsai, Y. C., & Lemaitre, B. (2012). Autocrine and paracrine unpaired signaling regulate intestinal stem cell maintenance and division. *Journal of Cell Science*, *125*(24), 5944–5949.

Ostermann, J., Voos, W., Kang, P. J., Craig, E. A., Neupert, W., & Pfanner, N. (1990). Precursor proteins in transit through mitochondrial contact sites interact with hsp70 in the matrix. *FEBS Letters*, *277*(1–2), 281–284.

Otera, H., Miyata, N., Kuge, O., & Mihara, K. (2016). Drp1-dependent mitochondrial fission via MiD49/51 is essential for apoptotic cristae remodeling. *Journal of Cell Biology*, *212*(5), 531–544.

Padman, B. S., Bach, M., Lucarelli, G., Prescott, M., & Ramm, G. (2013). The protonophore CCCP interferes with lysosomal degradation of autophagic cargo in yeast and mammalian cells. *Autophagy*, *9*(11), 1862–1875.

Pagliarini, D. J., & Rutter, J. (2013). Hallmarks of a new era in mitochondrial biochemistry. *Genes and Development*, *27*(24), 2615–2627.

Paisán-Ruíz, C., Jain, S., Evans, E. W., Gilks, W. P., Simón, J., Van Der Brug, M., De Munain, A. L., Aparicio, S., Gil, A. M., Khan, N., Johnson, J., Martinez, J. R., Nicholl, D., Carrera, I. M., Peňa, A. S., De Silva, R., Lees, A., Martí-Massó, J. F., Pérez-Tur, J., Wood, N. W & Singleton, A. B. (2004). Cloning of the gene containing mutations that cause *PARK8*-linked Parkinson's disease. *Neuron*, *44*(4), 595–600.

Palikaras, K., Lionaki, E., & Tavernarakis, N. (2018). Mechanisms of mitophagy in cellular homeostasis, physiology and pathology. *Nature Cell Biology*, *20*(9), 1013–1022.

Palmer, C. S., Osellame, L. D., Laine, D., Koutsopoulos, O. S., Frazier, A. E., & Ryan, M. T. (2011). MiD49 and MiD51, new components of the mitochondrial fission machinery. *EMBO Reports*, *12*(6), 565–573.

Paludan, S. R., & Bowie, A. G. (2013). Immune Sensing of DNA. *Immunity*, *38*(5), 870–880.

Pan-Montojo, F., Anichtchik, O., Dening, Y., Knels, L., Pursche, S., Jung, R., Jackson, S., Gille, G., Spillantini, M. G., Reichmann, H., & Funk, R. H. W. (2010a). Progression of Parkinson's disease pathology is reproduced by intragastric administration of rotenone in mice. *PLoS ONE*, *5*(1).

Pan-Montojo, F. J., & Funk, R. H. W. (2010b). Oral administration of rotenone using a gavage and image analysis of alpha-synuclein inclusions in the enteric nervous system. *Journal of Visualized Experiments*, *44,* 2123.

Park, J., Lee, S. B., Lee, S., Kim, Y., Song, S., Kim, S., Bae, E., Kim, J., Shong, M., Kim, J., & Chung, J. (2006). Mitochondrial dysfunction in *Drosophila PINK1* mutants is complemented by *parkin*. *Nature*, *441*(7097), 1157–1161.

Park, J., Lee, G., & Chung, J. (2009). The PINK1–Parkin pathway is involved in the regulation of mitochondrial remodeling process. *Biochemical and Biophysical Research Communications*, *378*(3), 518–523.

Parker, W. D., Boyson, S. J., & Parks, J. K. (1989). Abnormalities of the electron transport chain in idiopathic parkinson's disease. *Annals of Neurology*, *26*(6), 719–723.

Paupe, V., & Prudent, J. (2018). New insights into the role of mitochondrial calcium homeostasis in cell migration. *Biochemical and Biophysical Research Communications*, *500*(1), 75–86.

Pearson, G., Robinson, F., Beers Gibson, T., Xu, B., Karandikar, M., Berman, K., & Cobb, M. H. (2001). Mitogen-Activated Protein (MAP) Kinase Pathways: Regulation and Physiological Functions. *Endocrine Reviews*, *22*(2), 153–183.

Pebay-Peyroula, E., Dahout-Gonzalez, C., Kahn, R., Trézéguet, V., Lauquin, G. J. M., & Brandolin, G. (2003). Structure of mitochondrial ADP/ATP carrier in complex with carboxyatractyloside. *Nature*, *426*(6962), 39–44.

Pellegrino, M. W., Nargund, A. M., & Haynes, C. M. (2013). Signaling the mitochondrial unfolded protein response. *Biochimica et Biophysica Acta - Molecular Cell Research*, *1833*(2), 410–416.

Perez-Pardo, P., Dodiya, H. B., Engen, P. A., Forsyth, C. B., Huschens, A. M., Shaikh, M., Voigt, R. M., Naqib, A., Green, S. J., Kordower, J. H., Shannon, K. M., Garssen, J., Kraneveld, A. D., & Keshavarzian, A. (2018). Role of TLR4 in the gut-brain axis in Parkinson's disease: A translational study from men to mice. *Gut*, *68*(5), 829–843.

Perez, F. A., & Palmiter, R. D. (2005). Parkin-deficient mice are not a robust model of parkinsonism. *Proceedings of the National Academy of Sciences of the United States of America*, *102*(6), 2174–2179.

Perier, C., & Vila, M. (2012). Mitochondrial biology and Parkinson's disease. *Cold Spring Harbor Perspectives in Medicine*, *2*(2), 1–19.

Perkins, G. A., & Frey, T. G. (2000). Recent structural insight into mitochondria gained by microscopy. *Micron*, *31*(1), 97–111.

Perkins, G., Renken, C., Martone, M. E., Young, S. J., Ellisman, M., & Frey, T. (1997). Electron tomography of neuronal mitochondria: Three-dimensional structure and organization of cristae and membrane contacts. *Journal of Structural Biology*, *119*(3), 260–272.

Petersen, A. J., Katzenberger, R. J., & Wassarman, D. A. (2013). The innate immune response transcription factor relish is necessary for neurodegeneration in a *Drosophila* model of Ataxia-Telangiectasia. *Genetics*, *194*(1), 133–142.

Petersen, A. J., Rimkus, S. A., & Wassarman, D. A. (2012). ATM kinase inhibition in glial cells activates the innate immune response and causes neurodegeneration in *Drosophila*. *Proceedings of the National Academy of Sciences of the United States of America*, *109*(11), E656–E664.

Pétrilli, V., Papin, S., Dostert, C., Mayor, A., Martinon, F., & Tschopp, J. (2007). Activation of the NALP3 inflammasome is triggered by low intracellular potassium concentration. *Cell Death and Differentiation*, *14*(9), 1583–1589.

Pham, L. N., Dionne, M. S., Shirasu-Hiza, M., & Schneider, D. S. (2007). A Specific Primed Immune Response in *Drosophila* Is Dependent on Phagocytes. *PLoS Pathogens*, *3*(3).

Phillips, M. J., & Voeltz, G. K. (2016). Structure and function of ER membrane contact sites with other organelles. *Nature Reviews Molecular Cell Biology*, *17*(2), 69–82.

Pickles, S., Vigié, P., & Youle, R. J. (2018). Mitophagy and Quality Control Mechanisms in Mitochondrial Maintenance. *Current Biology*, *28*(4), 170–185.

Pickrell, A. M., Huang, C. H., Kennedy, S. R., Ordureau, A., Sideris, D. P., Hoekstra, J. G., Harper, J. W., & Youle, R. J. (2015). Endogenous Parkin Preserves Dopaminergic Substantia Nigral Neurons following Mitochondrial DNA Mutagenic Stress. *Neuron*, *87*(2), 371–382.

Pickrell, A. M., & Youle, R. J. (2015). The roles of PINK1, Parkin, and mitochondrial fidelity in parkinson's disease. *Neuron*, *85*(2), 257–273.

Pimenta De Castro, I., Costa, A. C., Lam, D., Tufi, R., Fedele, V., Moisoi, N., Dinsdale, D., Deas, E., Loh, S. H. Y., & Martins, L. M. (2012). Genetic analysis of mitochondrial protein misfolding in *Drosophila melanogaster*. *Cell Death and Differentiation*, *19*(8), 1308–1316.

Poewe, W., Antonini, A., Zijlmans, J. C., Burkhard, P. R., & Vingerhoets, F. (2010). Levodopa in the treatment of Parkinson's disease: an old drug still going strong. *Clinical Interventions in Aging*, *5*, 229–238.

Polymeropoulos, M. H., Lavedan, C., Leroy, E., Ide, S. E., Dehejia, A., Dutra, A., Pike,

B., Root, H., Rubenstein, J., Boyer, R., Stenroos, E. S., Chandrasekharappa, S., Athanassiadou, A., Papapetropoulos, T., Johnson, W. G., Lazzarini, A. M., Duvoisin, R. C., Di Iorio, G., Golbe, L. I., & Nussbaum, R. L. (1997). Mutation in the *α-synuclein* gene identified in families with Parkinson's disease. *Science*, *276*(5321), 2045–2047.

Pridgeon, J. W., Olzmann, J. A., Chin, L.-S., & Li, L. (2007). PINK1 Protects against Oxidative Stress by Phosphorylating Mitochondrial Chaperone TRAP1. *PLoS Biology*, *5*(7), e172.

Princely Abudu, Y., Pankiv, S., Mathai, B. J., Håkon Lystad, A., Bindesbøll, C., Brenne, H. B., Yoke Wui Ng, M., Thiede, B., Yamamoto, A., Mutugi Nthiga, T., Lamark, T., Esguerra, C. V., Johansen, T., & Simonsen, A. (2019). NIPSNAP1 and NIPSNAP2 Act as "Eat Me" Signals for Mitophagy. *Developmental Cell*, *49*(4), 509–525.

Proukakis, C., Dudzik, C. G., Brier, T., MacKay, D. S., Cooper, J. M., Millhauser, G. L., Houlden, H., & Schapira, A. H. (2013). A novel α-synuclein missense mutation in Parkinson disease. *Neurology*, *80*(11), 1062–1064.

Przedbroski, S., Leviver, M., Jiang, H., Ferreira, M., Jackson-Lewis, V., Donaldson, D., & Togasaki, D. M. (1995). Dose-dependent lesions of the dopaminergic nigrostriatal pathway induced by instrastriatal injection of 6-hydroxydopamine. *Neuroscience*, *67*(3), 631–647.

Prudent, J., Zunino, R., Sugiura, A., Mattie, S., Shore, G. C., & McBride, H. M. (2015). MAPL SUMOylation of Drp1 Stabilizes an ER/Mitochondrial Platform Required for Cell Death. *Molecular Cell*, *59*(6), 941–955.

Qi, Y., Yan, L., Yu, C., Guo, X., Zhou, X., Hu, X., Huang, X., Rao, Z., Lou, Z., & Hu, J. (2016). Structures of human mitofusin 1 provide insight into mitochondrial tethering. *Journal of Cell Biology*, *215*(5), 621–629.

Qin, H., Buckley, J. A., Li, X., Liu, Y., Fox, T. H., Meares, G. P., Yu, H., Yan, Z., Harms, A. S., Li, Y., Standaert, D. G., & Benveniste, E. N. (2016). Inhibition of the JAK/STAT pathway protects against α-synuclein-induced neuroinflammation and dopaminergic neurodegeneration. *Journal of Neuroscience*, *36*(18), 5144–5159.

Qin, X. Y., Zhang, S. P., Cao, C., Loh, Y. P., & Cheng, Y. (2016). Aberrations in peripheral inflammatory cytokine levels in Parkinson disease: A systematic review and meta-analysis. *JAMA Neurology*, *73*(11), 1316–1324.

Qiu, Y., & Zhou, X. (2018). STING: From Mammals to Insects. *Cell Host and Microbe*,

24(1), 5–7.

Quirós, P. M., Ramsay, A. J., Sala, D., Fernández-Vizarra, E., Rodríguez, F., Peinado, J. R., Fernández-García, M. S., Vega, J. A., Enríquez, J. A., Zorzano, A., & López-Otín, C. (2012). Loss of mitochondrial protease OMA1 alters processing of the GTPase OPA1 and causes obesity and defective thermogenesis in mice. *EMBO Journal*, *31*(9), 2117–2133.

Raj, T., Rothamel, K., Mostafavi, S., Ye, C., Lee, M. N., Replogle, J. M., Feng, T., Lee, M., Asinovski, N., Frohlich, I., Imboywa, S., Von Korff, A., Okada, Y., Patsopoulos, N. A., Davis, S., McCabe, C., Paik, H. Il, Srivastava, G. P., Raychaudhuri, S., Hafler, D. A., Koller, D., Regev, A., Hacohen, N., Mathis, D., Benoist, C., Stranger, B. E., & De Jager, P. L. (2014). Polarization of the effects of autoimmune and neurodegenerative risk alleles in leukocytes. *Science*, *344*(6183), 519–523.

Rakovic, A., Shurkewitsch, K., Seibler, P., Grünewald, A., Zanon, A., Hagenah, J., Krainc, D., & Klein, C. (2013). Phosphatase and tensin homolog (PTEN)-induced Putative Kinase 1 (PINK1)-dependent ubiquitination of endogenous parkin attenuates mitophagy: Study in human primary fibroblasts and induced pluripotent stem cell-derived neurons. *Journal of Biological Chemistry*, *288*(4), 2223–2237.

Rambold, A. S., Kostelecky, B., Elia, N., & Lippincott-Schwartz, J. (2011). Tubular network formation protects mitochondria from autophagosomal degradation during nutrient starvation. *Proceedings of the National Academy of Sciences of the United States of America*, *108*(25), 10190–10195.

Ramsay, R. R., Dadgar, J., Trevor, A., & Singer, T. P. (1986a). Energy-driven uptake of N-methyl-4-phenylpyridine by brain mitochondria mediates the neurotoxicity of MPTP. *Life Sciences*, *39*(7), 581–588.

Ramsay, R. R., Salach, J. I., Dadgar, J., & Singer, T. P. (1986b). Inhibition of mitochondrial NADH dehydrogenase by pyridine derivatives and its possible relation to experimental and idiopathic parkinsonism. *Biochemical and Biophysical Research Communications*, *135*(1), 269–275.

Rawlings, J. S., Rosler, K. M., & Harrison, D. A. (2004). The JAK/STAT signaling pathway. *Journal of Cell Science*, *117*(8), 1281–1283.

Reddy, P. H., McWeeney, S., Park, B. S., Manczak, M., Gutala, R. V., Partovi, D., Jung, Y., Yau, V., Searles, R., Mori, M., & Quinn, J. (2004). Gene expression profiles of transcripts in amyloid precursor protein transgenic mice: Up-regulation of mitochondrial metabolism and apoptotic genes is an early cellular change in

Alzheimer's disease. *Human Molecular Genetics*, *13*(12), 1225–1240.

Riesgo-Escovar, J. R., Jenni, M., Fritz, A., & Hafen, E. (1996). The *Drosophila* Jun-N-terminal kinase is required for cell morphogenesis but not for DJun-dependent cell fate specification in the eye. *Genes & Development*, *10*(21), 2759–2768.

Ritz, B. R., Manthripragada, A. D., Costello, S., Lincoln, S. J., Farrer, M. J., Cockburn, M., & Bronstein, J. (2009). Dopamine transporter genetic variants and pesticides in Parkinson's disease. *Environmental Health Perspectives*, *117*(6), 964–969.

Rizzuto, R., Brini, M., Murgia, M., & Pozzan, T. (1993). Microdomains with high Ca^{2+} close to IP3-sensitive channels that are sensed by neighboring mitochondria. *Science*, *262*(5134), 744–747.

Rizzuto, R., De Stefani, D., Raffaello, A., & Mammucari, C. (2012). Mitochondria as sensors and regulators of calcium signalling. *Nature Reviews Molecular Cell Biology*, *13*(9), 566–578.

Roberts, R. F., & Fon, E. A. (2016). Presenting mitochondrial antigens: PINK1, Parkin and MDVs steal the show. *Cell Research*, *26*(11), 1180–1181.

Roberts, R. F., Tang, M. Y., Fon, E. A., & Durcan, T. M. (2016). Defending the mitochondria: The pathways of mitophagy and mitochondrial-derived vesicles. *International Journal of Biochemistry and Cell Biology*, *79*, 427–436.

Robin, E. D., & Wong, R. (1988). Mitochondrial DNA molecules and virtual number of mitochondria per cell in mammalian cells. *Journal of Cellular Physiology*, *136*(3), 507–513.

Robinson, A. J., Overy, C., & Kunji, E. R. S. (2008). The mechanism of transport by mitochondrial carriers based on analysis of symmetry. *Proceedings of the National Academy of Sciences of the United States of America*, *105*(46), 17766–17771.

Rock, F. L., Hardiman, G., Timans, J. C., Kastelein, R. A., & Bazan, J. F. (1998). A family of human receptors structurally related to *Drosophila* Toll. *Proceedings of the National Academy of Sciences of the United States of America*, *95*(2), 588–593.

Rodger, C. E., McWilliams, T. G., & Ganley, I. G. (2018). Mammalian mitophagy – from *in vitro* molecules to *in vivo* models. *FEBS Journal*, *285*(7), 1185–1202.

Roger, A. J., Muñoz-Gómez, S. A., & Kamikawa, R. (2017). The Origin and Diversification of Mitochondria. *Current Biology*, *27*(21), R1177–R1192.

Rogov, V. V., Suzuki, H., Marinković, M., Lang, V., Kato, R., Kawasaki, M., Buljubašić, M., Šprung, M., Rogova, N., Wakatsuki, S., Hamacher-Brady, A., Dötsch, V., Dikic, I., Brady, N. R., & Novak, I. (2017). Phosphorylation of the mitochondrial autophagy receptor Nix enhances its interaction with LC3 proteins. *Scientific Reports*, *7*(1), 1–12.

Rojansky, R., Cha, M. Y., & Chan, D. C. (2016). Elimination of paternal mitochondria in mouse embryos occurs through autophagic degradation dependent on PARKIN and MUL1. *eLife*, *5,* e17896.

Ron, D., & Walter, P. (2007). Signal integration in the endoplasmic reticulum unfolded protein response. *Nature Reviews Molecular Cell Biology*, *8*(7), 519–529.

Rosado, C., Mijaljica, D., Hatzinisiriou, I., Prescott, M., & Devenish, R. J. (2008). Rosella: A fluorescent pH-biosensor for reporting vacuolar turnover of cytosol and organelles in yeast. *Autophagy*, *4*(2), 205–213.

Saitoh, T., Fujita, N., Jang, M. H., Uematsu, S., Yang, B. G., Satoh, T., Omori, H., Noda, T., Yamamoto, N., Komatsu, M., Tanaka, K., Kawai, T., Tsujimura, T., Takeuchi, O., Yoshimori, T., & Akira, S. (2008). Loss of the autophagy protein Atg16L1 enhances endotoxin-induced IL-1β production. *Nature*, *456*(7219), 264–268.

Sampson, T. R., Debelius, J. W., Thron, T., Janssen, S., Shastri, G. G., Ilhan, Z. E., Challis, C., Schretter, C. E., Rocha, S., Gradinaru, V., Chesselet, M. F., Keshavarzian, A., Shannon, K. M., Krajmalnik-Brown, R., Wittung-Stafshede, P., Knight, R., & Mazmanian, S. K. (2016). Gut Microbiota Regulate Motor Deficits and Neuroinflammation in a Model of Parkinson's Disease. *Cell*, *167*(6), 1469-1480.e12.

Sandoval, H., Thiagarajan, P., Dasgupta, S. K., Schumacher, A., Prchal, J. T., Chen, M., & Wang, J. (2008). Essential role for Nix in autophagic maturation of erythroid cells. *Nature*, *454*(7201), 232–235.

Saner, A., & Thoenen, H. (1971). Model experiments on the molecular mechanism of action of 6-hydroxydopamine. *Molecular Pharmacology*, *7*(2), 147–154.

Santagata, S., Bhattacharyya, D., Wang, F. H., Singha, N., Hodtsev, A., & Spanopoulou, E. (1999). Molecular cloning and characterization of a mouse

homolog of bacterial ClpX, a novel mammalian class II member of the Hsp100/Clp chaperone family. *Journal of Biological Chemistry*, *274*(23), 16311–16319.

Sauer, H., & Oertel, W. H. (1994). Progressive degeneration of nigrostriatal dopamine neurons following intrastriatal terminal lesions with 6-hydroxydopamine: A combined retrograde tracing and immunocytochemical study in the rat. *Neuroscience*, *59*(2), 401–415.

Sazanov, L. A. (2015). A giant molecular proton pump: Structure and mechanism of respiratory complex I. *Nature Reviews Molecular Cell Biology*, *16*(6), 375–388.

Scalzo, P., Kümmer, A., Cardoso, F., & Teixeira, A. L. (2010). Serum levels of interleukin-6 are elevated in patients with Parkinson's disease and correlate with physical performance. *Neuroscience Letters*, *468*(1), 56–58.

Schapira, A. H. V., Cooper, J. M., Dexter, D., Jenner, P., Clark, J. B., & Marsden, C. D. (1989). Mitochondrial complex I deficiency in Parkinson's disease. *The Lancet*, *333*(8649), 1269.

Schapira, Anthony H., & Jenner, P. (2011). Etiology and pathogenesis of Parkinson's disease. *Movement Disorders*, *26*(6), 1049–1055.

Schapira, A. H. V., Cooper, J. M., Dexter, D., Clark, J. B., Jenner, P., & Marsden, C. D. (1990). Mitochondrial Complex I Deficiency in Parkinson's Disease. *Journal of Neurochemistry*, *54*(3), 823–827.

Schiavi, A., Maglioni, S., Palikaras, K., Shaik, A., Strappazzon, F., Brinkmann, V., Torgovnick, A., Castelein, N., De Henau, S., Braeckman, B. P., Cecconi, F., Tavernarakis, N., & Ventura, N. (2015). Iron-Starvation-Induced Mitophagy Mediates Lifespan Extension upon Mitochondrial Stress in *C. elegans*. *Current Biology*, *25*(14), 1810–1822.

Schlossmacher, M. G., Frosch, M. P., Gai, W. P., Medina, M., Sharma, N., Forno, L., Ochiishi, T., Shimura, H., Sharon, R., Hattori, N., Langston, J. W., Mizuno, Y., Hyman, B. T., Selkoe, D. J., & Kosik, K. S. (2002). Parkin localizes to the Lewy bodies of Parkinson disease and dementia with Lewy bodies. *American Journal of Pathology*, *160*(5), 1655–1667.

Schneider, D. S., Ayres, J. S., Brandt, S. M., Costa, A., Dionne, M. S., Gordon, M. D., Mabery, E. M., Moule, M. G., Pham, L. N., & Shirasu-Hiza, M. M. (2007). *Drosophila eiger* Mutants Are Sensitive to Extracellular Pathogens. *PLoS Pathogens*, *3*(3), e41.

Schweers, R. L., Zhang, J., Randall, M. S., Loyd, M. R., Li, W., Dorsey, F. C., Kundu, M., Opferman, J. T., Cleveland, J. L., Miller, J. L., & Ney, P. A. (2007). NIX is required for programmed mitochondrial clearance during reticulocyte maturation. *Proceedings of the National Academy of Sciences of the United States of America*, *104*(49), 19500–19505.

Scorrano, L., Oakes, S. A., Opferman, J. T., Cheng, E. H., Sorcinelli, M. D., Pozzan, T., & Korsmeyer, S. J. (2003). BAX and BAK regulation of endoplasmic reticulum Ca^{2+}: A control point for apoptosis. *Science*, *300*(5616), 135–139.

Sebastián, D., Hernández-Alvarez, M. I., Segalés, J., Sorianello, E., Muñoz, J. P., Sala, D., Waget, A., Liesa, M., Paz, J. C., Gopalacharyulu, P., Orešič, M., Pich, S., Burcelin, R., Palacín, M., & Zorzano, A. (2012). Mitofusin 2 (Mfn2) links mitochondrial and endoplasmic reticulum function with insulin signaling and is essential for normal glucose homeostasis. *Proceedings of the National Academy of Sciences of the United States of America*, *109*(14), 5523–5528.

Seisenbacher, G., Hafen, E., & Stocker, H. (2011). MK2-dependent p38b signalling protects *Drosophila* hindgut enterocytes against JNK-induced apoptosis under chronic stress. *PLoS Genetics*, *7*(8), e1002168.

Senoh, S., Witkop, B., Creveling, C. R., & Udenfriend, S. (1959). 2,4,5-Trihydroxyphenethylamine, a new metabolite of 3,4-dihydroxyphenethylamine. *Journal of the American Chemical Society*, *81*(7), 1768–1769.

Shahni, R., Cale, C. M., Anderson, G., Osellame, L. D., Hambleton, S., Jacques, T. S., Wedatilake, Y., Taanman, J.-W., Chan, E., Qasim, W., Plagnol, V., Chalasani, A., Duchen, M. R., Gilmour, K. C., & Rahman, S. (2015). Signal transducer and activator of transcription 2 deficiency is a novel disorder of mitochondrial fission.

Sharma, N., & Nehru, B. (2015). Characterization of the lipopolysaccharide induced model of Parkinson's disease: Role of oxidative stress and neuroinflammation. Neurochemistry International, 87, 92–105.

Shen, Z., Huang, J., Wei, H., Niu, H., Li, B., Li, R., & Liu, G. (2020). Validation of an *in vivo* electrochemical immunosensing platform for simultaneous detection of multiple cytokines in Parkinson's disease mice model. *Bioelectrochemistry*, *134*, 107532.

Sherer, T. B. (2011). Biomarkers for parkinson's disease. *Science Translational Medicine*, *3*(79), 79ps14.

Sherer, T. B., Betarbet, R., Testa, C. M., Seo, B. B., Richardson, J. R., Kim, J. H., Miller, G. W., Yagi, T., Matsuno-Yagi, A., & Greenamyre, J. T. (2003). Mechanism of Toxicity in Rotenone Models of Parkinson's Disease. *Journal of Neuroscience*, *23*(34), 10756–10764.

Shiba-Fukushima, K., Imai, Y., Yoshida, S., Ishihama, Y., Kanao, T., Sato, S., & Hattori, N. (2012). PINK1-mediated phosphorylation of the Parkin ubiquitin-like domain primes mitochondrial translocation of Parkin and regulates mitophagy. *Scientific Reports*, *2*, 1002.

Shimada, K., Crother, T. R., Karlin, J., Dagvadorj, J., Chiba, N., Chen, S., Ramanujan, V. K., Wolf, A. J., Vergnes, L., Ojcius, D. M., Rentsendorj, A., Vargas, M., Guerrero, C., Wang, Y., Fitzgerald, K. A., Underhill, D. M., Town, T., & Arditi, M. (2012). Oxidized Mitochondrial DNA Activates the NLRP3 Inflammasome during Apoptosis. *Immunity*, *36*(3), 401–414.

Shimura, H., Hattori, N., Kubo, S. I., Mizuno, Y., Asakawa, S., Minoshima, S., Shimizu, N., Iwai, K., Chiba, T., Tanaka, K., & Suzuki, T. (2000). Familial Parkinson disease gene product, parkin, is a ubiquitin-protein ligase. *Nature Genetics*, *25*(3), 302–305.

Shin, J. H., Ko, H. S., Kang, H., Lee, Y. Il, Lee, Y. Il, Pletinkova, O., Troconso, J. C., Dawson, V. L., & Dawson, T. M. (2011). PARIS (ZNF746) repression of PGC-1α contributes to neurodegeneration in parkinson's disease. *Cell*, *144*(5), 689–702.

Shires, S. E., Kitsis, R. N., & Gustafsson, Å. B. (2017). Beyond Mitophagy: The Diversity and Complexity of Parkin Function. *Circulation Research*, *120*(8), 1234–1236.

Siddiqui, A., Rane, A., Rajagopalan, S., Chinta, S. J., & Andersen, J. K. (2016). Detrimental effects of oxidative losses in parkin activity in a model of sporadic Parkinson's disease are attenuated by restoration of PGC1α. *Neurobiology of Disease*, *93*, 115–120.

Silvestri, L., Caputo, V., Bellacchio, E., Atorino, L., Dallapiccola, B., Valente, E. M., & Casari, G. (2005). Mitochondrial import and enzymatic activity of *PINK1* mutants associated to recessive parkinsonism. *Human Molecular Genetics*, *14*(22), 3477–3492.

Singleton, A. B., Farrer, M., Johnson, J., Singleton, A., Hague, S., Kachergus, J., Hulihan, M., Peuralinna, T., Dutra, A., Nussbaum, R., Lincoln, S., Crawley, A., Hanson, M., Maraganore, D., Adler, C., Cookson, M. R., Muenter, M., Baptista,

M., Miller, D., Blancato, J., Hardy, J., & Gwinn-Hardy, K. (2003). *α-Synuclein* Locus Triplication Causes Parkinson's Disease. *Science*, *302*(5646), 841.

Sliter, D. A., Martinez, J., Hao, L., Chen, X., Sun, N., Fischer, T. D., Burman, J. L., Li, Y., Cai, H., Borsche, M., Klein, C., Youle, R. J., Zhang, Z., & Derek, P. (2018). Parkin and PINK1 mitigate STING-induced inflammation. *Nature*, *561*, 258–262.

Sluss, H. K., Han, Z., Barrett, T., Davis, R. J., & Ip, Y. T. (1996). A JNK signal transduction pathway that mediates morphogenesis and an immune response in *Drosophila*. *Genes and Development*, *10*(21), 2745–2758.

Smirnova, E., Griparic, L., Shurland, D. L., & Van der Bliek, A. M. (2001). Dynamin-related protein Drp1 is required for mitochondrial division in mammalian cells. *Molecular Biology of the Cell*, *12*(8), 2245–2256.

Snyder, S. H., & D'amato, R. J. (1985). Neurology: Predicting Parkinson's disease. *Nature*, *317*(6034), 198–199.

Sommer, A., Maxreiter, F., Krach, F., Fadler, T., Grosch, J., Maroni, M., Graef, D., Eberhardt, E., Riemenschneider, M. J., Yeo, G. W., Kohl, Z., Xiang, W., Gage, F. H., Winkler, J., Prots, I., & Winner, B. (2018). Th17 Lymphocytes Induce Neuronal Cell Death in a Human iPSC-Based Model of Parkinson's Disease. *Cell Stem Cell*, *23*(1), 123-131.

Song, L., McMackin, M., Nguyen, A., & Cortopassi, G. (2017). Parkin deficiency accelerates consequences of mitochondrial DNA deletions and Parkinsonism. *Neurobiology of Disease*, *100*, 30–38.

Song, Z., Ghochani, M., McCaffery, J. M., Frey, T. G., & Chan, D. C. (2009). Mitofusins and OPA1 mediate sequential steps in mitochondrial membrane fusion. *Molecular Biology of the Cell*, *20*(15), 3525–3532.

Soubannier, V., McLelland, G.-L., Zunino, R., Braschi, E., Rippstein, P., Fon, E. A., & Mcbride, H. M. (2012). A Vesicular Transport Pathway Shuttles Cargo from Mitochondria to Lysosomes. *Current Biology*, *22*(2), 135–141.

Soubannier, V., Rippstein, P., Kaufman, B. A., Shoubridge, E. A., & McBride, H. M. (2012). Reconstitution of Mitochondria Derived Vesicle Formation Demonstrates Selective Enrichment of Oxidized Cargo. *PLoS ONE*, *7*(12).

Sowter, H. M., Ratcliffe, P. J., Watson, P., Greenberg, A. H., & Harris, A. L. (2001).

HIF-1-dependent regulation of hypoxic induction of the cell death factors BNIP3 and NIX in human tumors. *Cancer Research*, *61*(18), 6669–6673.

Spillantini, M. G., Schmidt, M. L., Lee, V. M. Y., Trojanowski, J. Q., Jakes, R., & Goedert, M. (1997). Alpha-synuclein in Lewy bodies. In *Nature*, *388*(6645), 839–840)

Sriram, K., Benkovic, S. A., Hebert, M. A., Miller, D. B., & O'Callaghan, J. P. (2004). Induction of gp130-related cytokines and activation of JAK2/STAT3 pathway in astrocytes precedes up-regulation of glial fibrillary acidic protein in the 1-methyl-4-phenyl-1,2,3,6-tetrahydropyridine model of neurodegeneration: Key signaling pathway for astrogliosis *in vivo*?. *Journal of Biological Chemistry*, *279*(19), 19936–19947.

Sriram, K., Matheson, J. M., Benkovic, S. A., Miller, D. B., Luster, M. I., & O'Callaghan, J. P. (2002). Mice deficient in TNF receptors are protected against dopaminergic neurotoxicity: Implications for Parkinson's disease. *The FASEB Journal*, *16*(11), 1474–1476.

Stec, W., Vidal, O., & Zeidler, M. P. (2013). *Drosophila* SOCS36E negatively regulates JAK/STAT pathway signaling via two separable mechanisms. *Molecular Biology of the Cell*, *24*(18), 3000–3009.

Stefanis, L. (2012). α-Synuclein in Parkinson's Disease. *Cold Spring Harbor Perspectives in Medicine*, *2*(2), 1–23.

Sterky, F. H., Lee, S., Wibom, R., Olson, L., & Larsson, N.-G. (2011). Impaired mitochondrial transport and Parkin-independent degeneration of respiratory chain-deficient dopamine neurons *in vivo*. *Proceedings of the National Academy of Sciences of the United States of America*, *108*(31), 12937–12942.

Stevens, D. a., Lee, Y., Kang, H. C., Lee, B. D., Lee, Y.-I., Bower, A., Jiang, H., Kang, S.-U., Andrabi, S. a., Dawson, V. L., Shin, J.-H., & Dawson, T. M. (2015). Parkin loss leads to PARIS-dependent declines in mitochondrial mass and respiration. *Proceedings of the National Academy of Sciences*, *112*(37), 11696–11701.

Stojkovska, I., Wagner, B. M., & Morrison, B. E. (2015). Parkinson's disease and enhanced inflammatory response. *Experimental Biology and Medicine*, *240*(11), 1387–1395.

Stokes, B. A., Yadav, S., Shokal, U., Smith, L. C., & Eleftherianos, I. (2015). Bacterial and fungal pattern recognition receptors in homologous innate signaling pathways

of insects and mammals. *Frontiers in Microbiology*, *6*(JAN).

Strappazzon, F., Nazio, F., Corrado, M., Cianfanelli, V., Romagnoli, A., Fimia, G. M., Campello, S., Nardacci, R., Piacentini, M., Campanella, M., & Cecconi, F. (2015). AMBRA1 is able to induce mitophagy via LC3 binding, regardless of PARKIN and p62/SQSTM1. *Cell Death and Differentiation*, *22*(3), 419–432.

Suen, D. F., Narendra, D. P., Tanaka, A., Manfredi, G., & Youle, R. J. (2010). Parkin overexpression selects against a deleterious mtDNA mutation in heteroplasmic cybrid cells. *Proceedings of the National Academy of Sciences of the United States of America*, *107*(26), 11835–11840.

Sugiura, A., McLelland, G.-L., Fon, E. A., & Mcbride, H. M. (2014). A new pathway for mitochondrial quality control : mitochondrial-derived vesicles. *The EMBO Journal*, *33*(19), 2142–2156.

Sulzer, D., & Surmeier, D. J. (2013). Neuronal vulnerability, pathogenesis, and Parkinson's disease. *Movement Disorders*, *28*(6), 715–724.

Sun, Lijun, Wu, J., Du, F., Chen, X., & Chen, Z. J. (2013). Cyclic GMP-AMP synthase is a cytosolic DNA sensor that activates the type I interferon pathway. *Science*, *339*(6121), 786–791.

Sun, L., Shen, R., Agnihotri, S. K., Chen, Y., Huang, Z., & Büeler, H. (2018). Lack of PINK1 alters glia innate immune responses and enhances inflammation-induced, nitric oxide-mediated neuron death. *Scientific Reports*, *8*(1), 1–16.

Sun, M. F., & Shen, Y. Q. (2018). Dysbiosis of gut microbiota and microbial metabolites in Parkinson's Disease. *Ageing Research Reviews*, *45*(April), 53–61.

Sun, N., Malide, D., Liu, J., Rovira, I. I., Combs, C. A., & Finkel, T. (2017). A fluorescence-based imaging method to measure *in vitro* and *in vivo* mitophagy using mt-Keima. *Nature Protocols*, *12*(8), 1576–1587.

Sun, N., Yun, J., Liu, J., Malide, D., Liu, C., Rovira, I. I., Holmström, K. M., Fergusson, M. M., Yoo, Y. H., Combs, C. A., & Finkel, T. (2015). Measuring *In Vivo* Mitophagy. *Molecular Cell*, *60*(4), 685–696.

Sun, Y., Zhang, D., Li, C., Huang, J., Li, W., Qiu, Y., Mao, A., Zhou, M., & Xue, L. (2019). Lic regulates JNK-mediated cell death in *Drosophila*. *Cell Proliferation*, *52*(3), 1–12.

Sung, H., Tandarich, L. C., Nguyen, K., & Hollenbeck, P. J. (2016). Compartmentalized regulation of Parkin-mediated mitochondrial quality control in the *Drosophila* nervous system *in vivo*. *Journal of Neuroscience*, *36*(28), 7375–7391.

Suzanne, M., Irie, K., Glise, B., Agnès, F., Mori, E., Matsumoto, K., & Noselli, S. (1999). The *Drosophila* p38 MAPK pathway is required during oogenesis for egg asymmetric development. *Genes and Development*, *13*(11), 1464–1474.

Suzuki, C. K., Suda, K., Wang, N., & Schatz, G. (1994). Requirement for the yeast gene LON in intramitochondrial proteolysis and maintenance of respiration. *Science*, *264*(5156), 273–276.

Svenning, S., & Johansen, T. (2013). Selective autophagy. *Essays in Biochemistry*, *55*(1), 79–92.

Szczepanek, K., Lesnefsky, E. J., & Larner, A. C. (2012). Multi-tasking: Nuclear transcription factors with novel roles in the mitochondria. *Trends in Cell Biology*, *22*(8), 429–437.

Szendroedi, J., Phielix, E., & Roden, M. (2012). The role of mitochondria in insulin resistance and type 2 diabetes mellitus. *Nature Reviews Endocrinology*, *8*(2), 92–103)

Tadaiesky, M. T., Dombrowski, P. A., Figueiredo, C. P., Cargnin-Ferreira, E., Da Cunha, C., & Takahashi, R. N. (2008). Emotional, cognitive and neurochemical alterations in a premotor stage model of Parkinson's disease. *Neuroscience*, *156*(4), 830–840.

Tafesh-Edwards, G., & Eleftherianos, I. (2020). JNK signaling in *Drosophila* immunity and homeostasis. *Immunology Letters*, *226*(April), 7–11.

Taira, T., Saito, Y., Niki, T., Iguchi-Ariga, S. M. M., Takahashi, K., & Ariga, H. (2004). DJ-1 has a role in antioxidative stress to prevent cell death. *EMBO Reports*, *5*(2), 213–218.

Takeuchi, H., Yanagida, T., Inden, M., Takata, K., Kitamura, Y., Yamakawa, K., Sewada, H., Izumi, Y., Yamamoto, N., Kihara, T., Uemura, K., Inoue, H., Taniguchi, T., Akaike, A., Takahashi, R., & Shimohama, S. (2009). Nicotinic receptor stimulation protects nigral dopaminergic neurons in rotenone-induced Parkinson's disease models. *Journal of Neuroscience Research*, *87*(2), 576–585.

Tammineni, P., Anugula, C., Mohammed, F., Anjaneyulu, M., Larner, A. C., & Sepuri, N. B. V. (2013). The import of the transcription factor STAT3 into mitochondria depends on GRIM-19, a component of the electron transport chain. *Journal of Biological Chemistry*, *288*(7), 4723–4732.

Tan, E. K., Chao, Y. X., West, A., Chan, L. L., Poewe, W., & Jankovic, J. (2020). Parkinson disease and the immune system – associations, mechanisms and therapeutics. *Nature Reviews Neurology*, *16*(6), 303–318.

Tan, L., Schedl, P., Song, H. J., Garza, D., & Konsolaki, M. (2008). The Toll→NFκB signaling pathway mediates the neuropathological effects of the human Alzheimer's Aβ42 polypeptide in *Drosophila*. *PLoS ONE*, *3*(12).

Tanaka, A., Cleland, M. M., Xu, S., Narendra, D. P., Suen, D. F., Karbowski, M., & Youle, R. J. (2010). Proteasome and p97 mediate mitophagy and degradation of mitofusins induced by Parkin. *Journal of Cell Biology*, *191*(7), 1367–1380.

Tanji, T., Hu, X., Weber, A. N. R., & Ip, Y. T. (2007). Toll and IMD Pathways Synergistically Activate an Innate Immune Response in *Drosophila melanogaster*. *Molecular and Cellular Biology*, *27*(12), 4578–4588.

Tanner, C. M. (1992). Epidemiology of Parkinson's disease. *Neurologic Clinics*, *10*(2), 317–329.

Tanner, Caroline M., Kamel, F., Ross, G. W., Hoppin, J. A., Goldman, S. M., Korell, M., Marras, C., Bhudhikanok, G. S., Kasten, M., Chade, A. R., Comyns, K., Richards, M. B., Meng, C., Priestley, B., Fernandez, H. H., Cambi, F., Umbach, D. M., Blair, A., Sandler, D. P., & Langston, J. W. (2011). Rotenone, Paraquat, and Parkinson's Disease. *Environmental Health Perspectives*, *119*(6), 866–872.

Tassetto, M., Kunitomi, M., & Andino, R. (2017). Circulating Immune Cells Mediate a Systemic RNAi-Based Adaptive Antiviral Response in *Drosophila*. *Cell*, *169*(2), 314-325.

Taylor, E. B., & Rutter, J. (2011). Mitochondrial quality control by the ubiquitin–proteasome system. *Biochemical Society Transactions*, *39*(5), 1509–1513.

Taylor, J. M., Main, B. S., & Crack, P. J. (2013). Neuroinflammation and oxidative stress: co-conspirators in the pathology of Parkinson's disease. *Neurochemistry International*, *62*(5), 803–819.

Tepass, U., Fessler, L. I., Aziz, A., & Hartenstein, V. (1994). Embryonic origin of hemocytes and their relationship to cell death in *Drosophila*. *Development*, *120*(7), 1829–1837.

Terriente-Félix, A., Pérez, L., Bray, S. J., Nebreda, A. R., & Milán, M. (2017). A *Drosophila* model of myeloproliferative neoplasm reveals a feedforward loop in the JAK pathway mediated by p38 MAPK signalling. *DMM Disease Models and Mechanisms*, *10*(4), 399–407.

Terskikh, A., Fradkov, A., Ermakova, G., Zaraisky, A., Tan, P., Kajava, A. V., Zhao, X., Lukyanov, S., Matz, M., Kim, S., Weissman, I., & Siebert, P. (2000). 'Fluorescent timer': Protein that changes color with time. *Science*, *290*(5496), 1585–1588.

Thiruchelvam, M., McCormack, A., Richfield, E. K., Baggs, R. B., Tank, A. W., Di Monte, D. A., & Cory-Slechta, D. A. (2003). Age-related irreversible progressive nigrostriatal dopaminergic neurotoxicity in the paraquat and maneb model of the Parkinson's disease phenotype. *European Journal of Neuroscience*, *18*(3), 589–600.

Thompson, W. E., Ramalho-Santos, J., & Sutovsky, P. (2003). Ubiquitination of prohibitin in mammalian sperm mitochondria: Possible roles in the regulation of mitochondrial inheritance and sperm quality control. *Biology of Reproduction*, *69*(1), 254–260.

Thrower, J. S., Hoffman, L., Rechsteiner, M., & Pickart, C. M. (2000). Recognition of the polyubiquitin proteolytic signal. *EMBO Journal*, *19*(1), 94–102.

Tieu, K. (2011). A guide to neurotoxic animal models of Parkinson's disease. *Cold Spring Harbor Perspectives in Medicine*, *1*(1), a009316.

Tilokani, L., Nagashima, S., Paupe, V., & Prudent, J. (2018). Mitochondrial dynamics: Overview of molecular mechanisms. *Essays in Biochemistry*, *62*(3), 341–360.

Trempe, J. -F., Sauve, V., Grenier, K., Seirafi, M., Tang, M. Y., Menade, M., Al-Abdul-Wahid, S., Krett, J., Wong, K., Kozlov, G., Nagar, B., Fon, E. A., & Gehring, K. (2013). Structure of Parkin Reveals Mechanisms for Ubiquitin Ligase Activation. *Science*, *340*(6139), 1451–1455.

Trempe, J. -F., Fon, E. A., Lynn Montie, H., Ann Johansen, J., & Liu, Y. (2013). Structure and function of Parkin, PINK1, and DJ-1, the three musketeers of neuroprotection. *Frontiers in neurology*, *4*(38).

Trinh, J., & Farrer, M. (2013). Advances in the genetics of Parkinson disease. *Nature Reviews Neurology*, *9*(8), 445–454.

Tufi, R., Gandhi, S., De Castro, I. P., Lehmann, S., Angelova, P. R., Dinsdale, D., Deas, E., Plun-Favreau, H., Nicotera, P., Abramov, A. Y., Willis, A. E., Mallucci, G. R., Loh, S. H. Y., & Martins, L. M. (2014). Enhancing nucleotide metabolism protects against mitochondrial dysfunction and neurodegeneration in a *PINK1* model of Parkinson's disease. *Nature Cell Biology*, *16*(2), 157–166.

Twig, G., Hyde, B., & Shirihai, O. S. (2008). Mitochondrial fusion, fission and autophagy as a quality control axis: The bioenergetic view. *Biochimica et Biophysica Acta*, *1777*(9), 1092–1097.

Ungerstedt, U. (1968). 6-hydroxy-dopamine induced degeneration of central monoamine neurons. *European Journal of Pharmacology*, *5*(1), 107–110.

Ungureanu, D., Vanhatupa, S., Kotaja, N., Yang, J., Aittomäki, S., Jänne, O. A., Palvimo, J. J., & Silvennoinen, O. (2003). PIAS proteins promote SUMO-1 conjugation to STAT1. *Blood*, *102*(9), 3311–3313.

Valanne, S., Wang, J.-H., & Rämet, M. (2011). The *Drosophila* Toll Signaling Pathway. *The Journal of Immunology*, *186*(2), 649–656.

Valente, E. M., Brancati, F., Caputo, V., Graham, E. A., Davis, M. B., Ferraris, A., Breteler, M. M. B., Gasser, T., Bonifati, V., Bentivoglio, A. R., De Michele, G., Dürr, A., Cortelli, P., Filla, A., Meco, G., Oostra, B. A., Brice, A., Albanese, A., Dallapiccola, B., & Wood, N. W. (2002). *PARK6* is a common cause of familial parkinsonism. *Neurological Sciences*, *23*(SUPPL. 2), 117–118.

Valente, Eriza Maria, Abou-Sleiman, P. M., Caputo, V., Muqit, M. M. K., Harvey, K., Gispert, S., Ali, Z., Del Turco, D., Bentivoglio, A. R., Healy, D. G., Albanese, A., Nussbaum, R., González-Maldonado, R., Deller, T., Salvi, S., Cortelli, P., Gilks, W. P., Latchman, D. S., Harvey, R. J., Dallapiccola, B., Auburger, G., & Wood, N. W. (2004). Hereditary early-onset Parkinson's disease caused by mutations in *PINK1*. *Science*, *304*(5674), 1158–1160.

Van De Warrenburg, B. P. C., Lammens, M., Lücking, C. B., Denèfle, P., Wesseling, P., Booij, J., Praamstra, P., Quinn, N., Brice, A., & Horstink, M. W. I. M. (2001). Clinical and pathologic abnormalities in a family with parkinsonism and *parkin* gene mutations. *Neurology*, *56*(4), 555–557.

Van Der Laan, M., Hutu, D. P., & Rehling, P. (2010). On the mechanism of preprotein

import by the mitochondrial presequence translocase. *Biochimica et Biophysica Acta (BBA) - Molecular Cell Research*, *1803*(6), 732–739.

Van Dyck, L., Pearce, D. A., & Sherman, F. (1994). *PIM1* encodes a mitochondrial ATP-dependent protease that is required for mitochondrial function in the yeast *Saccharomyces cerevisiae*. *Journal of Biological Chemistry*, *269*(1), 238–242.

Van Humbeeck, C., Cornelissen, T., Hofkens, H., Mandemakers, W., Gevaert, K., de Strooper, B., & Vandenberghe, W. (2011). Parkin interacts with ambra1 to induce mitophagy. *Journal of Neuroscience*, *31*(28), 10249–10261.

Van Laar, V. S., Arnold, B., Cassady, S. J., Chu, C. T., Burton, E. A., & Berman, S. B. (2011). Bioenergetics of neurons inhibit the translocation response of Parkin following rapid mitochondrial depolarization. *Human Molecular Genetics*, *20*(5), 927–940.

Veeriah, S., Taylor, B. S., Meng, S., Fang, F., Yilmaz, E., Vivanco, I., Janakiraman, M., Schultz, N., Hanrahan, A. J., Pao, W., Ladanyi, M., Sander, C., Heguy, A., Holland, E. C., Paty, P. B., Mischel, P. S., Liau, L., Cloughesy, T. F., Mellinghoff, I. K., Solit, D. B., & Chan, T. A. (2010). Somatic mutations of the Parkinson's disease-associated gene *PARK2* in glioblastoma and other human malignancies. *Nature Genetics*, *42*(1), 77–82.

Villa, E., Marchetti, S., & Ricci, J. E. (2018). No Parkin Zone: Mitophagy without Parkin. *Trends in Cell Biology*, *28*(11), 882–895.

Villa, E., Proïcs, E., Rubio-Patiño, C., Obba, S., Zunino, B., Bossowski, J. P., Rozier, R. M., Chiche, J., Mondragón, L., Riley, J. S., Marchetti, S., Verhoeyen, E., Tait, S. W. G., & Ricci, J. E. (2017). Parkin-Independent Mitophagy Controls Chemotherapeutic Response in Cancer Cells. *Cell Reports*, *20*(12), 2846–2859.

Villarán, R. F., Espinosa-Oliva, A. M., Sarmiento, M., De Pablos, R. M., Argüelles, S., Delgado-Cortés, M. J., Sobrino, V., Van Rooijen, N., Venero, J. L., Herrera, A. J., Cano, J., & MacHado, A. (2010). Ulcerative colitis exacerbates lipopolysaccharide-induced damage to the nigral dopaminergic system: Potential risk factor in Parkinson's disease. *Journal of Neurochemistry*, *114*(6), 1687–1700.

Vincow, E. S., Merrihew, G., Thomas, R. E., Shulman, N. J., Beyer, R. P., MacCoss, M. J., & Pallanck, L. J. (2013). The PINK1-Parkin pathway promotes both mitophagy and selective respiratory chain turnover *in vivo*. *Proceedings of the National Academy of Sciences*, *110*(16), 6400–6405.

Vrailas-Mortimer, A., del Rivero, T., Mukherjee, S., Nag, S., Gaitanidis, A., Kadas, D., Consoulas, C., Duttaroy, A., & Sanyal, S. (2011). A Muscle-Specific p38 MAPK/Mef2/MnSOD Pathway Regulates Stress, Motor Function, and Life Span in *Drosophila*. *Developmental Cell*, *21*(4), 783–795.

Wakabayashi, K., Takahashi, H., Takeda, S., Ohama, E., & Ikuta, F. (1988). Parkinson's disease: the presence of Lewy bodies in Auerbach's and Meissner's plexuses. *Acta Neuropathologica*, *76*(3), 217–221.

Wallace, D. C. (2005). A Mitochondrial Paradigm of Metabolic and Degenerative Diseases , Aging , and Cancer : A Dawn for Evolutionary Medicine. *Annual review of genetics, 39*(2005), 359–407.

Wallace, D. C. (2012). Mitochondria and cancer. *Nature Reviews Cancer*, *12*(10), 685–698).

Wang, C., & Youle, R. J. (2009). The Role of Mitochondria in Apoptosis. *Annual Review of Genetics*, *43*(1), 95–118.

Wang, Y., Nartiss, Y., Steipe, B., McQuibban, G. A., & Kim, P. K. (2012). ROS-induced mitochondrial depolarization initiates PARK2/PARKIN-dependent mitochondrial degradation by autophagy. *Autophagy*, *8*(10), 1462–1476.

Watt, I. N., Montgomery, M. G., Runswick, M. J., Leslie, A. G. W., & Walker, J. E. (2010). Bioenergetic cost of making an adenosine triphosphate molecule in animal mitochondria. *Proceedings of the National Academy of Sciences of the United States of America*, *107*(39), 16823–16827.

Wauer, T., & Komander, D. (2013). Structure of the human Parkin ligase domain in an autoinhibited state. *EMBO Journal*, *32*(15), 2099–2112.

Wauer, T., Simicek, M., Schubert, A., & Komander, D. (2015). Mechanism of phospho-ubiquitin-induced PARKIN activation. *Nature*, *524*(7565), 370–374.

Weber, A. N. R., Tauszig-Delamasure, S., Hoffmann, J. A., Lelièvre, E., Gascan, H., Ray, K. P., Morse, M. A., Imler, J. L., & Gay, N. J. (2003). Binding of the *Drosophila* cytokine Spätzle to Toll is direct and establishes signaling. *Nature Immunology*, *4*(8), 794–800.

Wegrzyn, J., Potla, R., Chwae, Y. J., Sepuri, N. B. V., Zhang, Q., Koeck, T., Derecka, M., Szczepanek, K., Szelag, M., Gornicka, A., Moh, A., Moghaddas, S., Chen, Q.,

Bobbili, S., Cichy, J., Dulak, J., Baker, D. P., Wolfman, A., Stuehr, D., Hassan, M. O., Fu, X. Y., Avadhani, N., Drake, J. I., Fawcett, P., Lesnefsky, E. J., & Larner, A. C. (2009). Function of mitochondrial Stat3 in cellular respiration. *Science*, *323*(5915), 793–797.

Wei, Y., Chiang, W. C., Sumpter, R., Mishra, P., & Levine, B. (2017). Prohibitin 2 Is an Inner Mitochondrial Membrane Mitophagy Receptor. *Cell*, *168*(1–2), 224-238.

West, A. B., Moore, D. J., Biskup, S., Bugayenko, A., Smith, W. W., Ross, C. A., Dawson, V. L., & Dawson, T. M. (2005). Parkinson's disease-associated mutations in *leucine-rich repeat kinase 2* augment kinase activity. *Proceedings of the National Academy of Sciences of the United States of America*, *102*(46), 16842–16847.

West, A. P., Khoury-Hanold, W., Staron, M., Tal, M. C., Pineda, C. M., Lang, S. M., Bestwick, M., Duguay, B. A., Raimundo, N., MacDuff, D. A., Kaech, S. M., Smiley, J. R., Means, R. E., Iwasaki, A., & Shadel, G. S. (2015). Mitochondrial DNA stress primes the antiviral innate immune response. *Nature*, *520*(7548), 553–557.

Whiteley, A. T., Eaglesham, J. B., de Oliveira Mann, C. C., Morehouse, B. R., Lowey, B., Nieminen, E. A., Danilchanka, O., King, D. S., Lee, A. S. Y., Mekalanos, J. J., & Kranzusch, P. J. (2019). Bacterial cGAS-like enzymes synthesize diverse nucleotide signals. *Nature*, *567*(7747), 194–199.

Wilkins, H. M., Koppel, S. J., Weidling, I. W., Roy, N., Ryan, L. N., Stanford, J. A., & Swerdlow, R. H. (2016). Extracellular Mitochondria and Mitochondrial Components Act as Damage-Associated Molecular Pattern Molecules in the Mouse Brain. *Journal of Neuroimmune Pharmacology*, *11*(4), 622–628.

Witoelar, A., Jansen, I. E., Wang, Y., Desikan, R. S., Gibbs, J. R., Blauwendraat, C., Thompson, W. K., Hernandez, D. G., Djurovic, S., Schork, A. J., Bettella, F., Ellinghaus, D., Franke, A., Lie, B. A., McEvoy, L. K., Karlsen, T. H., Lesage, S., Morris, H. R., Brice, A., … Weale, M. (2017). Genome-wide pleiotropy between Parkinson disease and autoimmune diseases. *JAMA Neurology*, *74*(7), 780–792.

Wong, Y. C., & Holzbaur, E. L. F. (2014). Optineurin is an autophagy receptor for damaged mitochondria in parkin-mediated mitophagy that is disrupted by an ALS-linked mutation. *Proceedings of the National Academy of Sciences of the United States of America*, *111*(42), E4439–E4448.

Wood-Kaczmar, A., Gandhi, S., & Wood, N. W. (2006). Understanding the molecular causes of Parkinson's disease. *Trends in Molecular Medicine*, *12*(11), 521–528.

Woodroof, H. I., Pogson, J. H., Begley, M., Cantley, L. C., Deak, M., Campbell, D. G., Van Aalten, D. M. F., Whitworth, A. J., Alessi, D. R., & Muqit, M. M. K. (2011). Discovery of catalytically active orthologues of the Parkinson's disease kinase PINK1: Analysis of substrate specificity and impact of mutations. *Open Biology*, *1*(NOVEMBER).

Wrighton, P., Shwartz, A., Heo, J.-M., Quenzer, E., LaBella, K., Harper, J. W., & Goessling, W. (2020). Live imaging defines the dynamics and molecular basis of *in vivo* mitophagy. *BioRxiv*,

Wu, W., Tian, W., Hu, Z., Chen, G., Huang, L., Li, W., Zhang, X., Xue, P., Zhou, C., Liu, L., Zhu, Y., Zhang, X., Li, L., Zhang, L., Sui, S., Zhao, B., & Feng, D. (2014). ULK1 translocates to mitochondria and phosphorylates FUNDC1 to regulate mitophagy. *EMBO Reports*, *15*(5), 566–575.

Wu, X., Wu, F.-H., Wang, X., Wang, L., Siedow, J. N., Zhang, W., & Pei, Z.-M. (2014). Molecular evolutionary and structural analysis of the cytosolic DNA sensor cGAS and STING. *Nucleic Acids Research*, *42*(13), 8243–8257.

Xiao, T. S., & Fitzgerald, K. A. (2013). The cGAS-STING Pathway for DNA Sensing. *Molecular Cell*, *51*(2), 135–139.

Xu, S., Peng, G., Wang, Y., Fang, S., & Karbowski, M. (2011). The AAA-ATPase p97 is essential for outer mitochondrial membrane protein turnover. *Molecular Biology of the Cell*, *22*(3), 291–300.

Yamano, K., Matsuda, N., & Tanaka, K. (2016). The ubiquitin signal and autophagy: an orchestrated dance leading to mitochondrial degradation. *EMBO Reports*, *17*(3), 300–316.

Yamano, K., Queliconi, B. B., Koyano, F., Saeki, Y., Hirokawa, T., Tanaka, K., & Matsuda, N. (2015). Site-specific interaction mapping of phosphorylated ubiquitin to uncover Parkin activation. *Journal of Biological Chemistry*, *290*(42), 25199–25211.

Yan, C., Gong, L., Chen, L., Xu, M., Abou-Hamdan, H., Tang, M., Désaubry, L., & Song, Z. (2019). PHB2 (prohibitin 2) promotes PINK1-PRKN/Parkin-dependent mitophagy by the PARL-PGAM5-PINK1 axis. *Autophagy*, *16*(2), 419–434.

Yan, R., Small, S., Desplan, C., Dearolf, C. R., & Darnell, J. E. (1996). Identification of a *Stat* gene that functions in *Drosophila* development. *Cell*, *84*(3), 421–430.

Yan, Z., Gibson, S. A., Buckley, J. A., Qin, H., & Benveniste, E. N. (2018). Role of the JAK/STAT signaling pathway in regulation of innate immunity in neuroinflammatory diseases. *Clinical Immunology*, *189*, 4–13.

Yang, J., Liao, X., Agarwal, M. K., Barnes, L., Auron, P. E., & Stark, G. R. (2007). Unphosphorylated STAT3 accumulates in response to IL-6 and activates transcription by binding to NFκB. *Genes and Development*, *21*(11), 1396–1408.

Yao, Z., Gandhi, S., Burchell, V. S., Plun-Favreau, H., Wood, N. W., & Abramov, A. Y. (2011). Cell metabolism affects selective vulnerability in PINK1-associated Parkinson's disease. *Journal of Cell Science*, *124*(24), 4194–4202.

Yeo, L., Singh, R., Gundeti, M., Barua, J. M., & Masood, J. (2012). Urinary tract dysfunction in Parkinson's disease: A review. *International Urology and Nephrology*, *44*(2), 415–424).

Yokota, T., Sugawara, K., Ito, K., Takahashi, R., Ariga, H., & Mizusawa, H. (2003). Down regulation of DJ-1 enhances cell death by oxidative stress, ER stress, and proteasome inhibition. *Biochemical and Biophysical Research Communications*, *312*(4), 1342–1348.

Yoneda, T., Benedetti, C., Urano, F., Clark, S. G., Harding, H. P., & Ron, D. (2004). Compartment-specific perturbation of protein handling activates genes encoding mitochondrial chaperones. *Journal of Cell Science*, *117*(18), 4055–4066.

Yoshida, K., Yamaguchi, T., Natsume, T., Kufe, D., & Miki, Y. (2005). JNK phosphorylation of 14-3-3 proteins regulates nuclear targeting of c-Abl in the apoptotic response to DNA damage. *Nature Cell Biology*, *7*(3), 278–285.

Youle, R. J., & Narendra, D. P. (2011). Mechanisms of mitophagy. *Nat Rev Mol Cell Biol*, *12*(1), 9–14.

Yun, J., Puri, R., Yang, H., Lizzio, M. A., Wu, C., Sheng, Z.-H., & Guo, M. (2014). MUL1 acts in parallel to the PINK1/parkin pathway in regulating mitofusin and compensates for loss of PINK1/parkin. *eLife*, *3*, 1–26.

Zarranz, J. J., Alegre, J., Gómez-Esteban, J. C., Lezcano, E., Ros, R., Ampuero, I., Vidal, L., Hoenicka, J., Rodriguez, O., Atarés, B., Llorens, V., Gomez Tortosa, E., Del Ser, T., Muñoz, D. G., & De Yebenes, J. G. (2004). The New Mutation, E46K, of α-Synuclein Causes Parkinson and Lewy Body Dementia. *Annals of Neurology*, *55*(2), 164–173.

Zeidler, M. P., Bach, E. A., & Perrimon, N. (2000). The roles of the *Drosophila* JAK/STAT pathway. *Oncogene*, *19*(21), 2598–2606.

Zeke, A., Misheva, M., Reményi, A., & Bogoyevitch, M. A. (2016). JNK Signaling: Regulation and Functions Based on Complex Protein-Protein Partnerships. *Microbiology and Molecular Biology Reviews*, *80*(3), 793–835.

Zhang, L., Turner, B., Ribbeck, K., & Ten Hagen, K. G. (2017). Loss of the mucosal barrier alters the progenitor cell niche via Janus kinase/signal transducer and activator of transcription (JAK/STAT) signaling. *Journal of Biological Chemistry*, *292*(52), 21231–21242.

Zhao, C., Ling, Z., Newman, M. B., Bhatia, A., & Carvey, P. M. (2007). TNF-α knockout and minocycline treatment attenuates blood-brain barrier leakage in MPTP-treated mice. *Neurobiology of Disease*, *26*(1), 36–46.

Zhao, Q., Wang, J., Levichkin, I. V., Stasinopoulos, S., Ryan, M. T., & Hoogenraad, N. J. (2002). A mitochondrial specific stress response in mammalian cells. *EMBO Journal*, *21*(17), 4411–4419.

Zheng, B., Liao, Z., Locascio, J. J., Lesniak, K. A., Roderick, S. S., Watt, M. L., Eklund, A. C., Zhang-James, Y., Kim, P. D., Hauser, M. A., Grünblatt, E., Moran, L. B., Mandel, S. A., Riederer, P., Miller, R. M., Federoff, H. J., Wüllner, U., Papapetropoulos, S., Youdim, M. B., Cantuti-Castelvetri, I., Young, A. B., Vance, J. M., Davis, R. L., Hedreen, J. C., Adler, C. H., Beach, T. G,, Graeber, M. B., Middleton, F. A, Rochet, J. C., & Scherzer, C. R. (2010). PGC-1α, a potential therapeutic target for early intervention in Parkinson's disease. *Science Translational Medicine*, *2*(52), 52ra73.

Zheng, L., Bernard-Marissal, N., Moullan, N., D'Amico, D., Auwerx, J., Moore, D. J., Knott, G., Aebischer, P., & Schneider, B. L. (2017). Parkin functionally interacts with PGC-1α to preserve mitochondria and protect dopaminergic neurons. *Human Molecular Genetics*, *26*(3), 582–598.

Zhong, Z., Liang, S., Sanchez-Lopez, E., He, F., Shalapour, S., Lin, X. jia, Wong, J., Ding, S., Seki, E., Schnabl, B., Hevener, A. L., Greenberg, H. B., Kisseleva, T., & Karin, M. (2018). New mitochondrial DNA synthesis enables NLRP3 inflammasome activation. *Nature*, *560*(7717), 198–203.

Zhong, Z., Umemura, A., Sanchez-Lopez, E., Liang, S., Shalapour, S., Wong, J., He, F., Boassa, D., Perkins, G., Ali, S. R., McGeough, M. D., Ellisman, M. H., Seki, E., Gustafsson, A. B., Hoffman, H. M., Diaz-Meco, M. T., Moscat, J., & Karin, M.

(2016). NF-κB Restricts Inflammasome Activation via Elimination of Damaged Mitochondria. *Cell*, *164*(5), 896–910.

Zhou, C., Huang, Y., Shao, Y., May, J., Prou, D., Perier, C., Dauer, W., Schon, E. A., & Przedborski, S. (2008). The kinase domain of mitochondrial PINK1 faces the cytoplasm. *Proceedings of the National Academy of Sciences of the United States of America*, *105*(33), 12022–12027.

Zhou, R., Yazdi, A. S., Menu, P., & Tschopp, J. (2011). A role for mitochondria in NLRP3 inflammasome activation. *Nature*, *469*(7329), 221–226.

Zhou, Y., Long, Q., Wu, H., Li, W., Qi, J., Wu, Y., Xiang, G., Tang, H., Yang, L., Chen, K., Li, L., Bao, F., Li, H., Wang, Y., Li, M., & Liu, X. (2020). Topology-dependent, bifurcated mitochondrial quality control under starvation. *Autophagy*, *16*(3), 562–574.

Zhu, C., Vourc'h, P., Fernagut, P. O., Fleming, S. M., Lacan, S., Dicarlo, C. D., Seaman, R. L., & Chesselet, M. F. (2004). Variable effects of chronic subcutaneous administration of rotenone on striatal histology. *Journal of Comparative Neurology*, *478*(4), 418–426.

Zhu, Y., Wang, M., Lin, H., Huang, C., Shi, X., & Luo, J. (2002). Epidermal growth factor up-regulates the transcription of mouse Lon homology ATP-dependent protease through extracellular signal-regulated protein kinase- and phosphatidylinositol-3-kinase-dependent pathways. *Experimental Cell Research*, *280*(1), 97–106.

Zhuang, Z. H., Zhou, Y., Yu, M. C., Silverman, N., & Ge, B. X. (2006). Regulation of *Drosophila* p38 activation by specific MAP2 kinase and MAP3 kinase in response to different stimuli. *Cellular Signalling*, *18*(4), 441–448.

Zimprich, A., Benet-Pagès, A., Struhal, W., Graf, E., Eck, S. H., Offman, M. N., Haubenberger, D., Spielberger, S., Schulte, E. C., Lichtner, P., Rossle, S. C., Klopp, N., Wolf, E., Seppi, K., Pirker, W., Presslauer, S., Mollenhauer, B., Katzenschlager, R., Foki, T., Hotzy, C., Reinthaler, E., Harutyunyan, A., Kralovics, R., Peters, A., Zimprich, F., Brücke, T., Poewe, W., Auff, E., Trenkwalder, C., Rost, B., Ransmayr, G., Winkelmann, J., Meitinger, T., & Strom, T. M. (2011). A mutation in *VPS35*, encoding a subunit of the retromer complex, causes late-onset parkinson disease. *American Journal of Human Genetics*, *89*(1), 168–175.

Zimprich, A., Biskup, S., Leitner, P., Lichtner, P., Farrer, M., Lincoln, S., Kachergus, J., Hulihan, M., Uitti, R. J., Calne, D. B., Stoessl, A. J., Pfeiffer, R. F., Patenge, N.,

Carbajal, I. C., Vieregge, P., Asmus, F., Müller-Myhsok, B., Dickson, D. W., Meitinger, T., Strom, T. M., Wszolek, Z. K., & Gasser, T. (2004). Mutations in *LRRK2* cause autosomal-dominant parkinsonism with pleomorphic pathology. *Neuron*, *44*(4), 601–607.

Ziviani, E., Tao, R. N., & Whitworth, A. J. (2010). Drosophila Parkin requires PINK1 for mitochondrial translocation and ubiquitinates Mitofusin. *Proceedings of the National Academy of Sciences*, *107*(11), 5018–5023.

Zong, W. X., Li, C., Hatzivassiliou, G., Lindsten, T., Yu, Q. C., Yuan, J., & Thompson, C. B. (2003). Bax and Bak can localize to the endoplasmic reticulum to initiate apoptosis. Journal of Cell Biology, 162(1), 59–69.

Publications arising from this work

Lee, J. J., Sanchez-Martinez, A., Zarate, A. M., Benincá, C., Mayor, U., Clague, M. J., & Whitworth, A. J. (2018). Basal mitophagy is widespread in *Drosophila* but minimally affected by loss of *Pink1* or *parkin*. *Journal of Cell Biology*, *217*(5), 1613–1622.

Lee, J. J., Andreazza, S. & Whitworth, A. J. (2020) The STING pathway does not contribute to behavioural or mitochondrial phenotypes in *Drosophila Pink1/parkin* or mtDNA mutator models. *Scientific Reports, 10*(1), 2693.